

Postinjury Neuroplasticity in Central Neural Networks

Guest Editors: Bae Hwan Lee, Tae-Hong Lim, Young Wook Yoon, Midori A. Yenari, and Yong Jeong





Postinjury Neuroplasticity in Central Neural Networks

Postinjury Neuroplasticity in Central Neural Networks

Guest Editors: Bae Hwan Lee, Tae-Hong Lim,
Young Wook Yoon, Midori A. Yenari, and Yong Jeong



Copyright © 2015 Hindawi Publishing Corporation. All rights reserved.

This is a special issue published in “Neural Plasticity.” All articles are open access articles distributed under the Creative Commons Attribution License, which permits unrestricted use, distribution, and reproduction in any medium, provided the original work is properly cited.

Editorial Board

Shimon Amir, Canada
Michel Baudry, USA
Michael S. Beattie, USA
Clive R. Bramham, Norway
Anna K. Braun, Germany
Sumantra Chattarji, India
Rajnish Chaturvedi, India
Vincenzo De Paola, UK
Zygmunt Galdzicki, USA
Preston E. Garraghty, USA
Paul E. Gold, USA

Anthony J. Hannan, Australia
George W. Huntley, USA
Alexandre H. Kihara, Brazil
Jeansok J. Kim, USA
Eric Klann, USA
Malgorzata Kossut, Poland
Stuart C. Mangel, USA
Aage R. Møller, USA
Diane K. O'Dowd, USA
Martin Oudega, USA
Maurizio Popoli, Italy

Bruno Poucet, France
Timothy Schallert, USA
Menahem Segal, Israel
Panagiotis Smirniotis, USA
Naweed I. Syed, Canada
Christian Wozny, UK
Chun-Fang Wu, USA
Long-Jun Wu, USA
James M. Wyss, USA
Lin Xu, China

Contents

Postinjury Neuroplasticity in Central Neural Networks, Bae Hwan Lee, Tae-Hong Lim, Young Wook Yoon, Midori A. Yenari, and Yong Jeong
Volume 2015, Article ID 857085, 2 pages

Acute Putrescine Supplementation with Schwann Cell Implantation Improves Sensory and Serotonergic Axon Growth and Functional Recovery in Spinal Cord Injured Rats, J. Bryan Iorgulescu, Samik P. Patel, Jack Louro, Christian M. Andrade, Andre R. Sanchez, and Damien D. Pearce
Volume 2015, Article ID 186385, 11 pages

Clinical Trial of Human Fetal Brain-Derived Neural Stem/Progenitor Cell Transplantation in Patients with Traumatic Cervical Spinal Cord Injury, Ji Cheol Shin, Keung Nyun Kim, Jeehyun Yoo, Il-Sun Kim, Seokhwan Yun, Hyejin Lee, Kwangsoo Jung, Kyujin Hwang, Miri Kim, Il-Shin Lee, Jeong Eun Shin, and Kook In Park
Volume 2015, Article ID 630932, 22 pages

The Effects of Exercise on Cognitive Recovery after Acquired Brain Injury in Animal Models: A Systematic Review, Elise Wogensen, Hana Malá, and Jesper Mogensen
Volume 2015, Article ID 830871, 22 pages

Spinal Cord Hemisection Facilitates Aromatic L-Amino Acid Decarboxylase Cells to Produce Serotonin in the Subchronic but Not the Chronic Phase, Bushra Azam, Jacob Wienecke, Dennis Bo Jensen, Aleena Azam, and Mengliang Zhang
Volume 2015, Article ID 549671, 10 pages

Contralateral Metabolic Activation Related to Plastic Changes in the Spinal Cord after Peripheral Nerve Injury in Rats, Ran Won and Bae Hwan Lee
Volume 2015, Article ID 438319, 6 pages


Cortical Excitability Measured with nTMS and MEG during Stroke Recovery, Jyrki P. Mäkelä, Pantelis Lioumis, Kristina Laaksonen, Nina Forss, Turgut Tatlisumak, Markku Kaste, and Satu Mustanoja
Volume 2015, Article ID 309546, 8 pages

Plasticity-Related PKM ζ Signaling in the Insular Cortex Is Involved in the Modulation of Neuropathic Pain after Nerve Injury, Jeongsoo Han, Minjee Kwon, Myeounghoon Cha, Motomasa Tanioka, Seong-Karp Hong, Sun Joon Bai, and Bae Hwan Lee
Volume 2015, Article ID 601767, 10 pages

Reactive Oxygen Species Donors Increase the Responsiveness of Dorsal Horn Neurons and Induce Mechanical Hyperalgesia in Rats, Hee Young Kim, Inhyung Lee, Sang Woo Chun, and Hee Kee Kim
Volume 2015, Article ID 293423, 10 pages

Modulation of Spinal GABAergic Inhibition and Mechanical Hypersensitivity following Chronic Compression of Dorsal Root Ganglion in the Rat, Moon Chul Lee, Taick Sang Nam, Se Jung Jung, Young S. Gwak, and Joong Woo Leem
Volume 2015, Article ID 924728, 12 pages

PKA Inhibitor H89 (N-[2-p-bromocinnamylamino-ethyl]- 5-isoquinolinesulfonamide) Attenuates Synaptic Dysfunction and Neuronal Cell Death following Ischemic Injury, Juhyun Song, So Yeong Cheon, Won Taek Lee, Kyung Ah Park, and Jong Eun Lee
Volume 2015, Article ID 374520, 13 pages



Statins Promote Long-Term Recovery after Ischemic Stroke by Reconnecting Noradrenergic Neuronal Circuitry, Kyoung Joo Cho, So Young Cheon, and Gyung Whan Kim
Volume 2015, Article ID 585783, 10 pages

Editorial

Postinjury Neuroplasticity in Central Neural Networks

Bae Hwan Lee,¹ Tae-Hong Lim,² Young Wook Yoon,³ Midori A. Yenari,⁴ and Yong Jeong⁵

¹*Department of Physiology, Brain Korea 21 PLUS Project for Medical Science, Yonsei University College of Medicine, Seoul 120-752, Republic of Korea*

²*Department of Biomedical Engineering, Seamans Center for the Engineering Arts and Sciences, College of Engineering, University of Iowa, Iowa City, IA 52242, USA*

³*Department of Physiology, Korea University College of Medicine, Seoul 136-705, Republic of Korea*

⁴*Department of Neurology, University of California, San Francisco, and San Francisco Veterans Affairs Medical Center, San Francisco, CA 94121, USA*

⁵*Department of Bio and Brain Engineering, Korea Advanced Institute of Science and Technology, Daejeon 305-701, Republic of Korea*

Correspondence should be addressed to Bae Hwan Lee; bhlee@yuhs.ac

Received 26 July 2015; Accepted 26 July 2015

Copyright © 2015 Bae Hwan Lee et al. This is an open access article distributed under the Creative Commons Attribution License, which permits unrestricted use, distribution, and reproduction in any medium, provided the original work is properly cited.

Traumatic insult, ischemia, or degenerative disorder can damage neuronal cell bodies, axons, or synapses in the complex circuitry of the central nervous system (CNS). Peripheral as well as central injuries induce tremendous changes at the molecular, cellular, and system levels in the spinal cord and brain, which lead to devastating losses of functions including sensory, motor, and higher-order functions. Symptoms related to functional deficits depend on the site and extent of injury. Functional deficits caused by neural injury reflect the disruption of the intricate central neural circuits.

After injury, neuronal death or dysfunction occurs in affected areas. Sometimes, however, certain changes may occur in the adjacent and/or remote areas of the nervous system. The CNS possesses plasticity to respond to injury of either the peripheral nerves, the spinal cord, or the brain. Due to neural plasticity, lost functions may be restored. The plastic changes are often maladaptive as shown in neuropathic pain and are exacerbated hypersensitivity.

Although the regeneration capacity of central neurons is limited, extensive changes can occur in the CNS circuitry after injury, reflecting neuroplasticity. Neuroplasticity can modify the functions of the CNS including the brain and spinal cord, thereby providing opportunities for improving the limited ability of the CNS to recover from functional deficits. Axonal sprouting of survived neurons, new synapse

formation, and factors produced by neurons and glia help reestablish the neural networks and functions. For example, at the cellular level, axonal sprouting, and dendritic arborization appear in injured areas. Peri-injury area and the repaired area of the injured tissue are getting attention for processes through which functional recovery occurs. In these areas, growth-promoting factors and growth-inhibitory proteins are released after injury. Genes which are related to survival, repair, and plasticity are also activated following injury. Enhanced electrical and chemical activities are expected to promote axonal sprouting, contributing to functional recovery. Indeed, axonal outgrowth after injury may be dependent on activities of neural circuits. Otherwise, silent synapses, pathways, or circuits may be activated.

Changes in the central neural circuits which are related to injured neurons play a crucial role not only in functional deficits but also in functional recovery. Furthermore, a variety of strategies including external interventions to manipulate neuroplasticity may be beneficial to improve functional recovery.

In this special issue, we focus on postinjury neural plasticity in central neural networks. Papers covering a wide spectrum of studies related to neural injury are included. The scientific reports updated results of both basic experimental studies in animals and clinical studies in humans.

The original research articles as well as a review cover the field of neuroplastic changes in the CNS after injury and functional recovery.

Behavioral hypersensitivity may be related to biochemical alterations in the spinal cord. H. Y. Kim et al. show that elevated reactive oxygen species (ROS) in the spinal cord sensitized dorsal horn neurons and produced hyperalgesia in normal rats. M. C. Lee et al. report the relationship between the alteration of spinal GABAergic inhibition and mechanical hypersensitivity following unilateral chronic compression of dorsal root ganglion in rats.

Peripheral nerve injury can induce plastic changes in the spinal cord and the brain. In this regard, using an animal model of peripheral nerve injury, R. Won and B. H. Lee show that contralateral metabolic activation to nerve injury is related to behavioral crossed-withdrawal reflex in rats. Furthermore, J. Han et al. report that PKM zeta signaling in the insular cortex of the brain is involved in the modulation of neuropathic pain.

In relation to spinal cord injury, B. Azam et al. report experimental data suggesting that plastic changes of the 5-HT system mediated by aromatic L-amino acid decarboxylase cells might happen primarily in the subchronic phase and its function could be compensated by plastic changes of other modulation systems in longer chronic phase.

Stem cell therapy may be helpful to improve functional recovery after spinal cord injury. Experimentally, J. B. Iorgulescu et al. show that the combination of putrescine with Schwann cells improves functional recovery in rats with spinal cord injury. Clinically, J. C. Shin et al. report that the transplantation of human neural stem/progenitor cells (hNSPCs) into the injured cervical spinal cord is safe and provides modest neurological benefit up to 1 year after transplants.

Brain injury is much more dynamic and multifactorial compared to peripheral or spinal injury. In relation to functional recovery after brain injury, K. J. Cho et al. report that statins may affect not only the outcome of stroke by the recovery of noradrenergic (NA) neuronal circuitry but also the NA circuit's function after transient focal cerebral ischemia in mice. J. Song et al. provide experimental data suggesting that PKA inhibitor H89 may contribute to functional recovery after ischemic stroke by regulating neuronal death and proteins related to synaptic plasticity in mice. Clinically, J. P. Mäkelä et al. report covarying excitability measured with navigated transcranial magnetic stimulation and magnetoencephalography in the lesioned and nonlesioned hemispheres of stroke patients. As a systematic review, E. Wogensen et al. present a topic related to the effects of exercise on cognitive recovery after acquired brain injury in animal models.

This special issue compiles the state-of-the-art studies on central neuroplasticity after neural injury. We hope that this special issue will contribute to a better understanding of underlying mechanisms of neuroplasticity following neural injury and to development of novel neuromodulation strategies for functional recovery after injury.

Acknowledgments

We would like to express our sincere gratitude to all authors and reviewers for their contribution.

*Bae Hwan Lee
Tae-Hong Lim
Young Wook Yoon
Midori A. Yenari
Yong Jeong*

Research Article

Acute Putrescine Supplementation with Schwann Cell Implantation Improves Sensory and Serotonergic Axon Growth and Functional Recovery in Spinal Cord Injured Rats

J. Bryan Iorgulescu,^{1,2} Samik P. Patel,¹ Jack Louro,^{1,3} Christian M. Andrade,^{1,4}
Andre R. Sanchez,¹ and Damien D. Pearse^{1,5,6,7}

¹The Miami Project to Cure Paralysis, University of Miami Miller School of Medicine, Miami, FL 33136, USA

²Weill Cornell Medical College, New York, NY 10021, USA

³Department of Anesthesiology, Columbia University Medical Center, New York, NY 10032, USA

⁴Department of Internal Medicine, University of South Florida Morsani College of Medicine, Tampa, FL 33612, USA

⁵Department of Neurological Surgery, University of Miami Miller School of Medicine, Miami, FL 33136, USA

⁶The Neuroscience Program, University of Miami Miller School of Medicine, Miami, FL 33136, USA

⁷Interdisciplinary Stem Cell Institute, University of Miami Miller School of Medicine, Miami, FL 33136, USA

Correspondence should be addressed to Damien D. Pearse; dpearse@med.miami.edu

Received 11 March 2015; Revised 25 June 2015; Accepted 2 July 2015

Academic Editor: Bae Hwan Lee

Copyright © 2015 J. Bryan Iorgulescu et al. This is an open access article distributed under the Creative Commons Attribution License, which permits unrestricted use, distribution, and reproduction in any medium, provided the original work is properly cited.

Schwann cell (SC) transplantation exhibits significant potential for spinal cord injury (SCI) repair and its use as a therapeutic modality has now progressed to clinical trials for subacute and chronic human SCI. Although SC implants provide a receptive environment for axonal regrowth and support functional recovery in a number of experimental SCI models, axonal regeneration is largely limited to local systems and the behavioral improvements are modest without additional combinatory approaches. In the current study we investigated whether the concurrent delivery of the polyamine putrescine, started either 30 min or 1 week after SCI, could enhance the efficacy of SCs when implanted subacutely (1 week after injury) into the contused rat spinal cord. Polyamines are ubiquitous organic cations that play an important role in the regulation of the cell cycle, cell division, cytoskeletal organization, and cell differentiation. We show that the combination of putrescine with SCs provides a significant increase in implant size, an enhancement in axonal (sensory and serotonergic) sparing and/or growth, and improved open field locomotion after SCI, as compared to SC implantation alone. These findings demonstrate that polyamine supplementation can augment the effectiveness of SCs when used as a therapeutic approach for subacute SCI repair.

1. Introduction

To date no treatment can completely reverse the clinical outcomes associated with spinal cord injury (SCI). Tissue injury following SCI occurs in two phases: the first involves the primary mechanical injury itself, whereas the second is progressive, mediated over the course of days to weeks after SCI by a variety of cytotoxic factors present within the injury environment. Host cellular efforts to restrict progressive tissue injury, including glial reactivity, extracellular

matrix deposition, and scar formation around the lesion site, subsequently give rise to a nonpermissive environment for axon regeneration and the endogenous recovery of function [1]. This extrinsic antagonism of neurorepair is compounded by a reduction in the intrinsic growth capacity of adult central neurons [2]. Finding novel therapeutics that combat secondary injury, overcome the growth-inhibiting environment of the lesion site, and/or enhance the intrinsic capacity of neurons to regenerate is imperative for restoring function after SCI. Strategies combining cellular with pharmacological,

molecular, or biomaterial approaches have shown the most promise in overcoming these obstacles to attain meaningful anatomical and functional repair [3].

One encouraging adjunctive strategy for both surmounting the growth-inhibitory environment of the lesion and stimulating intrinsic regeneration has been the elevation of cyclic adenosine monophosphate (cyclic AMP), a second messenger molecule [4]. Sustained elevation of cyclic AMP has been shown to facilitate the extension of neurites across inhibitory substrates such as myelin and myelin-associated glycoprotein, to promote neuroprotection by elevating anti-apoptotic proteins, and to suppress immune cell activation and ensuing inflammation [4]. The primary target of the cyclic AMP pathway is the DNA-bound, constitutive transcription factor CREB, which upon phosphorylation by the cyclic AMP-activated protein kinase A (PKA) initiates the expression of numerous genes, including those that encode certain neuropeptides, neurotrophins, and arginase 1 (a crucial enzyme in the synthesis of polyamines; Figure 1) [5]. Downstream products of arginase 1, including the polyamine putrescine, have been shown to mediate several of cyclic AMP's effects on neurite outgrowth [6]. Supplementing glial-derived neurotrophic factor gene delivery with the substrate of arginase 1, L-arginine, demonstrated significant reductions in contusion size in traumatic brain injury models, although without improvement in cognitive function [7]. In paradigms of SCI, augmenting peripheral nerve grafts with acidic fibroblast growth factor supplementation increased *arginase 1* expression and polyamine synthesis and was associated with favorable M2 macrophage responses and axonal regeneration [8, 9]. Additionally, human mesenchymal stromal cell implants that overexpressed a key enzyme in the synthesis of polyamines, arginine decarboxylase, resulted in improved locomotor recovery and reduced scar formation following SCI [10]. Based upon our previous studies demonstrating the ability of cyclic AMP elevation to improve the effectiveness of SC implants after SCI and the growing evidence that polyamine synthesis may mediate several of cyclic AMP's downstream effects on axon regeneration [3, 4, 6], we investigated whether the supplementation of SC implants with putrescine, given either within 30 minutes or following a 1-week delay after contusive SCI, could improve SC implant-host integration, axon growth support, and locomotor recovery in an experimental contusive SCI paradigm.

2. Materials and Methods

2.1. Schwann Cells. SCs were obtained from the sciatic nerves of adult female Fischer rats (Harlan Co., Indianapolis, IN) as previously described [11, 12]. SCs were grown to confluence and thrice passaged onto new dishes. Following previous methods, SC purity for implantation was measured to be between 95% and 98%, according to p75 immunoreactivity [13].

2.2. Animals. Adult female Fischer rats (Harlan Co., $N = 34$; 180–200 g) were housed according to the guidelines recommended by the NIH and the Guide for the Care and Use of

Animals. All animal procedures were approved by the Institutional Animal Care and Use Committee of the University of Miami. Prior to surgery, rats were anesthetized (70 mg/kg ketamine, 5 mg/kg xylazine) by intraperitoneal injection.

2.3. Moderate Thoracic Contusion Injury. The MASCIS weight drop device was used to induce a moderate thoracic (T9) contusion injury [14]. A laminectomy was performed at the T8 thoracic vertebra prior to injury in order to expose the dorsal surface of the underlying spinal cord (T9) without perturbing the dura mater. The exposed spinal cord was then subjected to a moderate injury by dropping a 10 g rod from a height of 12.5 mm. Contusion impact height, velocity, and compression distance were monitored for all animals. Those which had height or velocity errors exceeding 6% or a compression distance that was not within a range of 1.25–1.75 mm were immediately excluded [3, 15]. According to these injury parameter criteria no animals required exclusion from the study. Following injury, the muscles were sutured in layers and the skin was closed with metal wound clips. Animals were allowed to recover in warmed cages with easy access to food and water. Gentamicin (5 mg/kg; Abbott Laboratories, North Chicago, IL) was intramuscularly administered immediately after the surgery and repeated daily for 7 days. The analgesic buprenorphine (0.03 mg/kg; Reckitt Benckiser, Richmond, VA) was delivered subcutaneously following surgery and then daily for 2 days, accompanied by postoperative treatment as described previously [16].

2.4. Subcutaneous Minipump Delivery of Putrescine. Prior to SCI induction, animals were randomly assigned into one of the following three treatment groups: (i) SC implant with 0.9% physiological saline (vehicle) control ($n = 11$), (ii) SC implant with acute putrescine (administered within 30 minutes of injury, $n = 14$), and (iii) SC implant with delayed putrescine (administered 1 week after injury at time of implantation, $n = 9$). Putrescine (100 mM) was delivered at a rate of 0.5 μ L/hr using two sequentially implanted subcutaneous Alzet minipumps (model 2001; Durect Corp., Cupertino, CA) for a 2-week administration period; emptied pumps were replaced after 1 week [17]. Figure 2 presents a timeline of the methodology.

2.5. Schwann Cell Implantation. Before implantation, SCs were trypsinized, harvested, counted, resuspended in DMEM/F12 media as aliquots and placed on ice prior to surgery. One week after injury the rats were anesthetized with 2% halothane and the injured spinal cord was reexposed. Rats then received fluid implants of SCs as described elsewhere [3]. Cells were implanted within 2 hours of preparation. For implantation, all animals received 2×10^6 SCs in 6 μ L of DMEM-F12 media into the epicenter of the contused area, injected at the midline to a depth of 1 mm. Injections were performed at a rate of 2 μ L/min using a 10 μ L siliconized Hamilton syringe with a pulled, beveled glass pipette tip (120 μ m diameter), which was held in a micromanipulator with an attached microinjector (World Precision Instruments, Sarasota, FL). The injection pipette

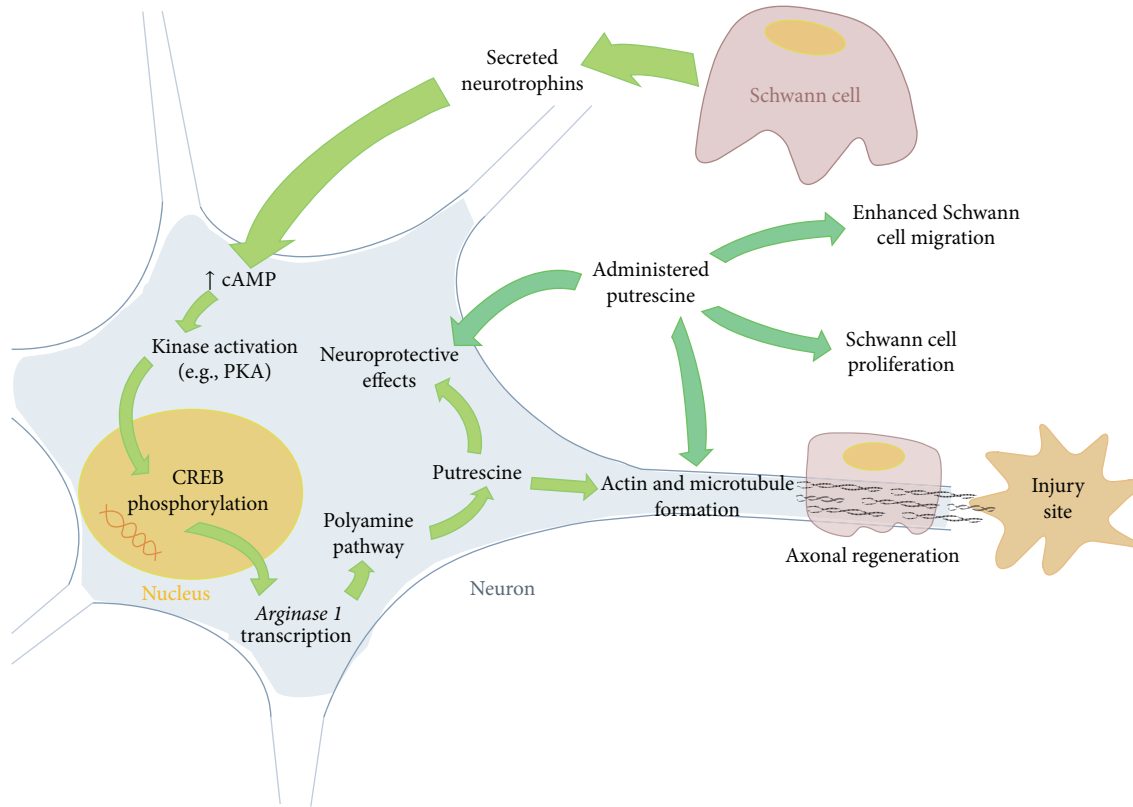


FIGURE 1: The role of putrescine in neuron and Schwann cell responses. This figure summarizes the previously reported functions of polyamines in neurons and Schwann cells within the wider literature from *in vitro* and *in vivo* studies and how these mechanisms could elicit the observed responses in the current study. Neurotrophins and growth factors secreted by implanted Schwann can elevate intrinsic cyclic AMP levels within neurons. Cyclic AMP is an important second messenger whose main effectors are downstream protein kinase signaling cascades (e.g., PKA) that result in the phosphorylation and activation of the constitutive transcription factor CREB. Bound to the nuclear DNA, CREB is known to enhance the expression of a number of genes that include *arginase 1*, which encodes the first enzyme of the polyamine pathway to generate endogenous putrescine. Putrescine produces a number of neuroprotective effects by scavenging free radicals and suppressing excitotoxicity. Putrescine also promotes the reorganization of actin and microtubules, allowing axons to grow. Administered putrescine is known to be taken up by both the neuron, bolstering the effects of the endogenous polyamines, and SCs, encouraging their migration and proliferation *in vitro*. We hypothesize that SC implants and administered putrescine work in concert to augment each other's ability to promote neuropreservation and neuroregeneration following SCI.

was held in place for an additional 3 min postinjection to minimize leakage upon withdrawal. One animal was excluded from the study due to a malfunction of the microinjector during cell transplantation. Following the injection, the muscle layers and the skin were closed separately and animals received postoperative care as described above.

2.6. Histology. Rats were euthanized at 10 weeks after injury (9 weeks after implantation; 100 mg/kg ketamine, 10 mg/kg xylazine) and transcardially perfused with 4% paraformaldehyde (PFA, 0.1M, pH 7.4). The tissue was then dissected and sectioned with a freezing microtome for immunohistochemical analysis according to previous procedures [3]. Spinal cords (2 cm) encompassing the injury epicenter were sectioned sagittally at 40 μ m into five series free-floating.

2.7. Immunohistochemistry. As previously described, every fifth sagittal section was immunochemically stained for

subsequent fluorescent microscopic analysis using a double labeling procedure involving monoclonal and polyclonal antibodies [15]. These antibodies were raised against the low-affinity neurotrophin receptor (p75^{NTR}; 1:5,000; Abcam, Cambridge, MA), serotonin (5HT; 1:5,000; Immunostar, Hudson, WI), or calcitonin gene related peptide (CGRP; 1:1,000; Peninsula Laboratories, San Carlos, CA) for identifying the implanted SCs or delineating the growth of specific descending or ascending axonal populations, respectively, within the p75⁺ SC implants. Sections were then washed and incubated with corresponding fluorescent secondary antibodies (Alexa 488- or Alexa 594-conjugated goat anti-rabbit or anti-mouse antibodies, 1:200; Molecular Probes, Eugene, OR). Sections were mounted onto Snowcoat X-tra slides (Surgipath, Richmond, IL) and cover-slipped with Vectashield mounting medium (Vector Laboratories, Burlingame, CA) containing the nuclear dye Hoechst for storage at 4°C.

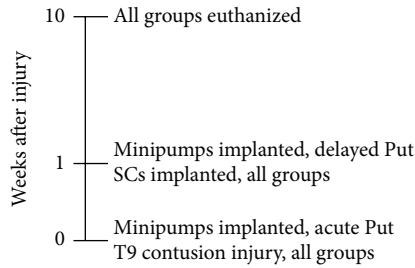


FIGURE 2: Methodology timeline: all groups received a T9 contusion injury at the 0-week time point. The Acute Put + SC group also received the putrescine-administering minipumps within 30 minutes of injury. At 1 week after injury all groups received SC. Also at 1 week after injury the Delayed Put + SC group received the putrescine-administering minipumps. All groups were euthanized and prepared for tissue processing at 10 weeks after injury.

2.8. Stereological Quantification of Implant Area. In one series of sections, the average area of p75-positive cellular immunoreactivity was quantified across three sections containing the center of the SC implant. Expression of p75 permits delineation of the implant and identification of the implant-host cord interface. For this analysis, stained sections were visualized and quantitatively assessed using an unbiased method employing computer-assisted fluorescence microscopy and Neurolucida software (version 4.5; MicroBrightField Bioscience, Williston, VT). The p75⁺ area for each of the three sections that comprised the center of the SC implant was traced under a 20x objective, quantified using Neurolucida, and then the SC implant area calculated for each animal as the average p75⁺ area across the three sections [18].

2.9. Determination of 5HT and CGRP Fiber Growth. Quantification of 5-hydroxytryptophan (5HT) labeled axon growth along the rostral-caudal axis of the spinal cord at distances of 1000, 500, 100, and 0 μm rostral to the center of the implant (as identified using p75 immunoreactivity) was performed on the second series of sections using 63x objective under oil immersion. Calcitonin gene related peptide (CGRP) labeled axons were quantified similarly, but at 1000, 500, 100, and 0 μm caudal to the center of the implant. The average number of fibers per section was obtained by counting those immunostained axons that crossed imaginary lines perpendicular to the rostral-caudal axis at the 1000, 500, 100, and 0 μm intervals from the center of the implant [19]. The total number of axons counted for a given animal was summated across the sections analyzed (~10–12 sections per animal) and then divided by the number of sections to determine the number of fibers per section (f/s) at each distance [4].

2.10. Behavioral Testing. The open field BBB locomotor test developed by Basso et al. was employed to assess weekly gross locomotor performance after SCI for 10 weeks [20]. In addition, a subscore analysis of the BBB that allows for evaluation of hind limb positioning and placement as well as balance and tail use on a 0–13 point scale was also used

as described previously by our group [3]. Lastly, deficits in descending motor control were examined by counting footfall errors on an irregularly spaced horizontal grid walk at the end of the study, prior to animal perfusion [4]. All behavioral tests were conducted by two individuals blinded to the animal's treatment.

2.11. Statistical Analysis. A one-way ANOVA and subsequent Bonferroni post hoc test were used to compare counts of immunostained axons among groups. For analysis of weekly functional recovery patterns following implantation (BBB and BBB subscore), a mixed factorial (repeated measures) ANOVA followed by the Tukey-Kramer posttest was employed. Differences were acknowledged to be statistically significant at $p < 0.05^{*,\#}$, $< 0.01^{**,\#\#}$, and $< 0.001^{***,\#\#\#}$, compared to the SC only control or the other temporal treatment group, as indicated. All errors are given as standard errors of the mean.

3. Results

3.1. SC Implant Size Increased with Delayed Putrescine Supplementation. Statistical comparison of SC implant size among control and treatment cohorts showed a significant effect of treatment ($F_{2,31} = 5.784$, $p < 0.05$). Compared to the implant size in the SC only group ($1.23 \pm 0.07 \text{ mm}^2$), those animals receiving putrescine administration beginning at the time of implantation exhibited 1.8-fold increase in implant area ($2.24 \pm 0.34 \text{ mm}^2$; $t_{33} = 3.391$, $p < 0.01$; Figures 3(a), 3(c), and 3(d)) as identified using p75 immunocytochemistry (a marker highly expressed on SCs) [13]. In contrast, putrescine administration beginning at the time of injury was without effect ($1.56 \pm 0.19 \text{ mm}^2$, $p < 0.05$).

3.2. Putrescine Improves Serotonergic Fiber Growth into the SC Implant. Serotonergic axons descending from the reticular formation and raphe nuclei of the brainstem were identified penetrating the SC implant using immunostaining for 5HT (Figures 4(a)–4(c); white arrows). For all animal groups there were few serotonergic axons that were able to penetrate beyond the center of the SC implant and no treatment effect was observed at this location ($F_{2,31} = 1.414$, $p > 0.05$; Figure 3(c)). However, statistical comparison of 5HT axon numbers within the rostral part of the SC implant showed a significant treatment effect ($F_{2,31} = 4.104$, $p < 0.05$ at 1000 μm , $F_{2,31} = 6.200$, $p < 0.01$ at 500 μm , and $F_{2,31} = 41.15$, $p < 0.001$ at 100 μm from the center of the implant). Acute putrescine supplementation significantly increased the number of serotonergic fibers within the proximal SC implant compared to the vehicle control: an average of 20 ± 1.2 5HT⁺ fibers per section (f/s) at 500 μm ($t_{33} = 4.829$, $p < 0.01$) and 9 ± 0.6 f/s at 100 μm ($t_{33} = 12.82$, $p < 0.001$) was quantified rostral to the center of the SC implant, while in vehicle controls 13 ± 1.8 5HT⁺ f/s and 2 ± 0.4 f/s, respectively, were observed at these distances (Figures 4(a)–4(b)). In addition, many more 5HT⁺ axons were observed crossing the host-SC implant interface in acute putrescine treated animals (Figures 4(a)–4(b); white arrows). Delayed

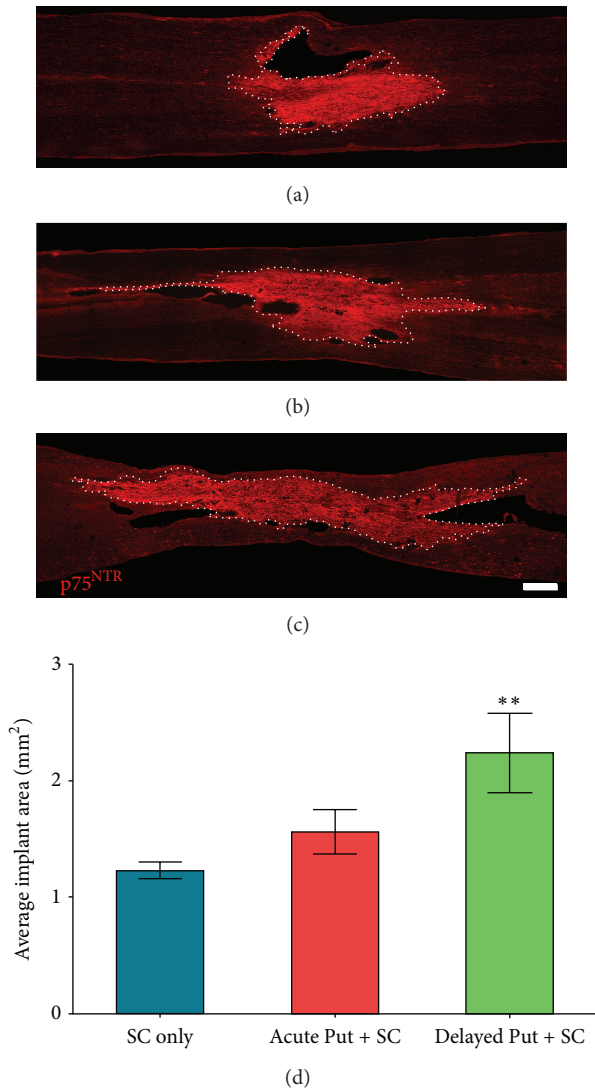


FIGURE 3: Delayed putrescine supplementation significantly increases SC implant size. To determine the effect of putrescine on the size of the implant, immunostaining for p75^{NTR} was performed and the area of immunoreactivity quantified. Images from representative animals show the extent of p75^{NTR} immunoreactivity among the different SC implant groups: (a) vehicle control, (b) immediate putrescine, and (c) delayed putrescine. Scale bar = 500 μm. Dotted white lines indicate the extent of the SC implant. Stereological quantification of the implant area shows an increase in size when putrescine is administered in a delayed fashion, but not acutely, as compared to the SC with vehicle control (d). Statistical significance indicated at ** $p < 0.01$ compared to SCs with vehicle control group.

putrescine supplementation produced a significant increase in 5HT⁺ axon numbers only at 100 μm rostral to the center of the SC implant (5.6 ± 0.8 f/s, $t_{33} = 6.011$, $p < 0.001$).

3.3. Putrescine Supplementation Improves Sensory Fiber Growth into the SC Implant.

Small diameter sensory axons

originating from dorsal root ganglia that were immunoreactive for CGRP were quantified within the SC implant (Figures 5(a)–5(c); white arrows). Statistical comparison of CGRP⁺ axon numbers among groups showed a significant treatment effect at both 100 μm caudal to ($F_{2,31} = 35.17$, $p < 0.001$) and within the center of the SC implant ($F_{2,31} = 16.16$, $p < 0.001$). At 100 μm caudal to the center of the SC implant, acute and delayed putrescine supplementation resulted in 2.3-fold (19 ± 1.0 f/s, $t_{33} = 11.86$, $p < 0.001$) and 1.7-fold (14 ± 0.8 f/s, $t_{33} = 5.941$, $p < 0.001$) increases in CGRP⁺ axon numbers, respectively, compared to the vehicle control (8.3 ± 0.77 f/s). In addition, acute putrescine administration (11 ± 1.2 f/s) significantly increased CGRP⁺ axon ingrowth within the center of the SC implant compared to the vehicle control (2.8 ± 0.4 f/s, $t_{33} = 9.491$, $p < 0.001$, a 3.9-fold increase). Acute putrescine was also significantly more effective in promoting CGRP⁺ axon growth than delayed delivery at both 100 μm caudal to (14 ± 0.8 f/s, $t_{33} = 4.935$, $p < 0.01$, a 1.4-fold increase) and within the center of the SC implant (5.3 ± 0.7 f/s, $t_{33} = 6.257$, $p < 0.001$, a 2.1-fold increase).

3.4. Putrescine Supplementation Improves Locomotor Recovery.

Locomotor performance and functional recovery following SCI, SC implantation, and putrescine treatment were assessed using the BBB score, BBB subscore, and the irregularly spaced grid walk test. Statistical comparison of BBB scores among groups showed a significant treatment effect both at endpoint ($F_{2,31} = 4.303$, $p < 0.05$) and at various time points after implantation ($F_{2,31} = 8.520$, $p < 0.01$ at week 3; $F_{2,31} = 4.771$, $p < 0.05$ at week 5; Figure 6(a)). Compared to the SC implant, vehicle controls (11.3 ± 0.3 , 10 weeks after SCI), open field locomotor performance was significantly greater at endpoint in both the acute (12.1 ± 0.1 , $t_{33} = 4.079$, $p < 0.05$) and delayed (11.9 ± 0.3 , $t_{33} = 3.929$, $p < 0.05$) putrescine with SC implant treatment groups. Statistical comparison of BBB subscores among groups showed a significant effect of treatment at all weeks after implantation ($F_{2,31} = 4.320$, $p < 0.05$, 10 weeks after SCI; Figure 6(b)). Compared to SC implant, vehicle controls (3.0 ± 0.3 , 10 weeks post-SCI), hind paw placement and tail positioning were significantly superior in both acute (6.6 ± 1.1 , $t_{33} = 3.631$, $p < 0.05$) and delayed (7.0 ± 1.4 , $t_{33} = 3.574$, $p < 0.05$) putrescine with SC implant treatment groups. Statistical comparison of the number of footfall errors on the grid walk among groups showed a significant effect of treatment ($F_{2,31} = 16.76$, $p < 0.001$; Figure 6(c)). Acute putrescine administration with SC implantation resulted in significantly better hind paw placement performance as evidenced by a lower number of footfalls on the grid walk (5.9 ± 0.2 footfalls) compared to both delayed administration (7.3 ± 0.2 footfalls, $t_{33} = 3.832$, $p < 0.01$) and the SC implant, vehicle controls (7.8 ± 0.4 footfalls, $t_{33} = 5.538$, $p < 0.001$).

4. Discussion

Bridging the hostile environment of the injured spinal cord with implanted SCs has been shown to be an effective foundation approach for a number of combinatorial repair

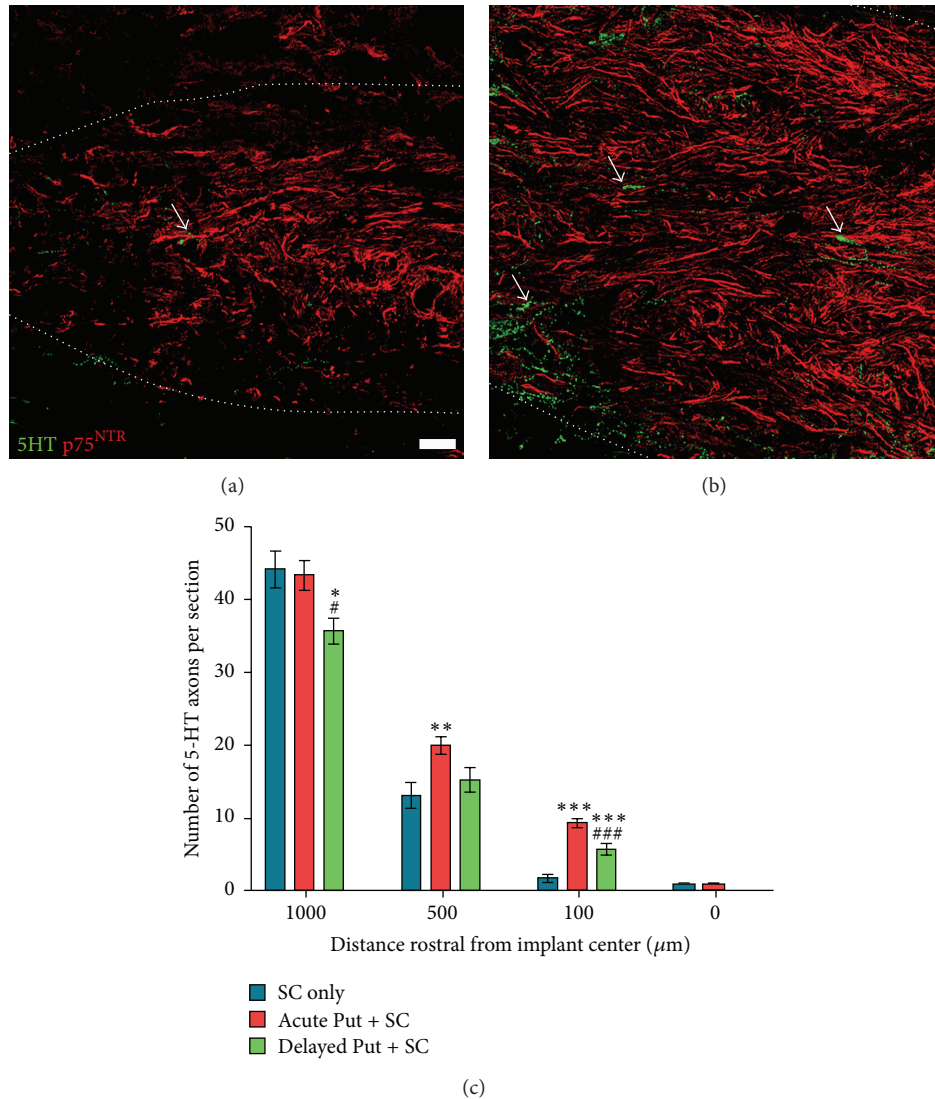


FIGURE 4: Putrescine supplementation enhances serotonergic axon numbers within the SC implant. Immunofluorescence staining for serotonergic axons (green, representative examples indicated by white arrows) shows many more axons within the rostral part of the SC implant (identified by p75 labeling, red) following (b) acute putrescine delivery compared to (a) when vehicle is given. Scale bar = 20 μm. Dotted white lines indicate the extent of the SC implant. (c) Stereological analysis shows a significant increase in 5-HT⁺ axon numbers with putrescine; the greatest effects are seen further from the center of the SC implant (i.e., closer to rostral host cord SC implant interface) and with acute administration. Statistical significance indicated at * $p < 0.05$, ** $p < 0.01$, and *** $p < 0.001$ compared to the vehicle control group and # $p < 0.05$ and ### $p < 0.001$ compared to acute putrescine treatment.

strategies in a diverse array of experimental SCI models [3, 4, 19]. In addition to ensheathing and myelinating axons, SCs provide growth-promoting neurotrophins, which may limit tissue loss and encourage axons to overcome the growth-inhibitory injury milieu. Importantly, SCs can be safely harvested from a patient's own peripheral nerve and autologously implanted back into his spinal cord, a major advantage to their use in the clinical setting [4]. However, SC implants by themselves cannot entice significant numbers of axons to exit the injury site, are unable to support robust growth of most supraspinal axon populations except under specific conditions, and provide only modest improvements in functional outcome [13, 15, 21]. In order

to mediate significant anatomical repair and/or functional improvements, SC implants must be augmented with various pharmacological, molecular, or biomaterial approaches that overcome intrinsic or extrinsic inhibitors of axon growth, such as neurotrophin supplementation, chondroitinase ABC, polysialic acid, matrix suspension, or cyclic AMP elevation [4, 19, 22].

In the current study we have demonstrated that the administration of the initial polyamine, putrescine, when combined with SC implants, significantly improved the size of the implant ~2-fold and thus potentially the number of surviving, implanted SCs. In addition, acute putrescine administration enhanced the sprouting and/or sparing of

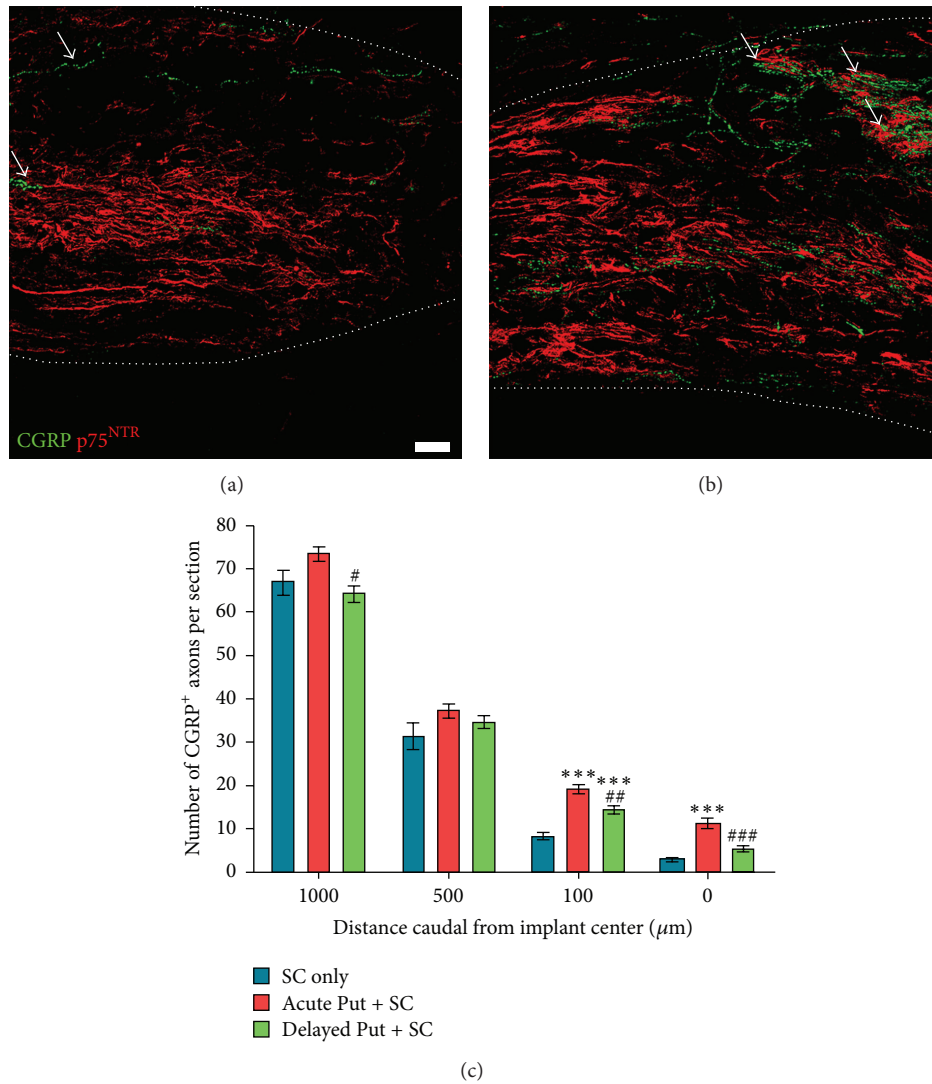


FIGURE 5: Putrescine administration increases peptidergic axon numbers within the SC implant. Immunofluorescence staining for peptidergic axons with CGRP (green, representative examples indicated by white arrows) shows that many more axons are present within SC implants (p75 labeling, red) following (b) acute putrescine delivery compared to (a) when vehicle is given. Scale bar = 20 μm . Dotted white lines indicate the extent of the SC implant. (c) Stereological analysis revealed a significant increase in CGRP⁺ axon numbers with putrescine: the greatest effects are observed within the SC implants with acute putrescine administration. Statistical significance indicated at *** $p < 0.001$ compared to the vehicle control group and # $p < 0.05$, ## $p < 0.01$, and ### $p < 0.001$ compared to acute putrescine treatment.

both descending serotonergic and ascending peptidergic axons within the implant/lesion site by up to 400%. Delaying the administration of putrescine mirrored the effects of the acute model, but generally with a reduced effectiveness. The improvements in implant size and axon growth support following putrescine administration were accompanied by enhanced functional recovery, including significant gains in open field locomotor ability and hind paw placement compared to animals receiving SC implants alone.

We have previously shown the therapeutic potential of combining SC implantation with cyclic AMP elevation [4]. Elevated levels of cyclic AMP are critical in facilitating the growth of axons over inhibitory substrates, such as myelin *in vitro* [2], and across the growth-retarding milieu

of the injured spinal cord [3]. The upregulation of *arginase 1*, a downstream effector of cyclic AMP that synthesizes the precursor for polyamines, has similarly been shown to enhance axonal regeneration, whereas blocking ornithine decarboxylase, the rate limiting enzyme which decarboxylates the product of arginase 1 into putrescine, attenuates the ability of dibutyl cyclic AMP and brain-derived neurotrophic factor to overcome growth antagonism by myelin-associated inhibitors [6–10]. The polyamine putrescine can further be converted into the polyamines spermidine and spermine; however the reverse reactions release toxic aldehyde byproducts, making putrescine the polyamine of choice for experimental or clinical application of polyamines [23, 24]. In addition to its axon growth-promoting abilities,

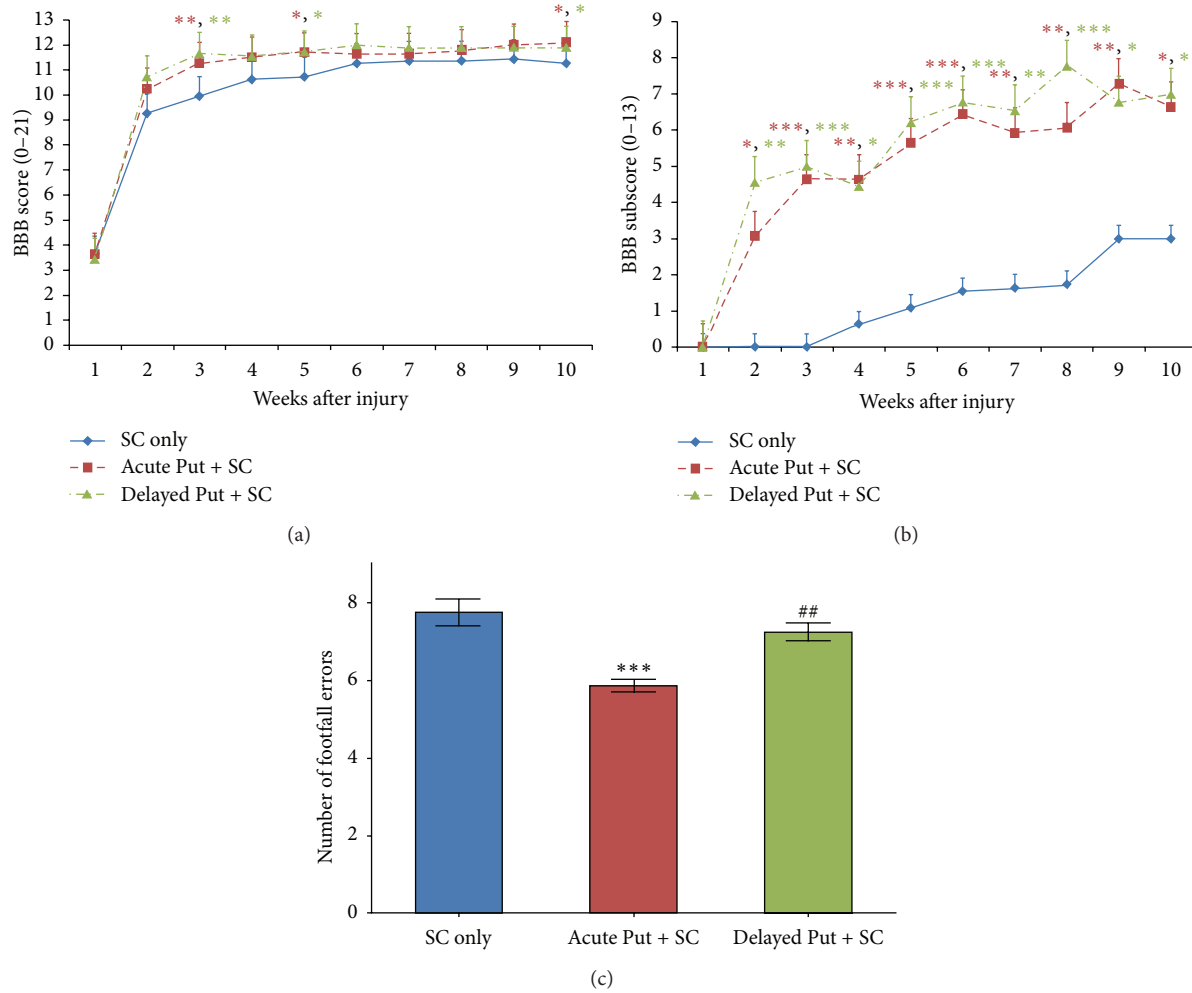


FIGURE 6: Putrescine supplementation enhances the functional outcomes obtained with SC implants. Assessment of open field locomotor performance with the (a) BBB score and subsequent (b) BBB subscore analysis shows that animals receiving either acute or delayed putrescine have improved walking behavior over SC implanted, vehicle controls. Improvements in foot and tail positioning, as measured by the BBB subscore, exhibit a more acute and stable pattern of recovery. (c) Recording the number of footfalls that occur while traversing a horizontal grid walk test also showed an improvement in hind paw positioning when acute putrescine was administered (red) compared to vehicle only controls (blue). Delayed putrescine (green) was without effect. Statistical significance indicated at * $p < 0.05$, ** $p < 0.01$, and *** $p < 0.001$ compared to the vehicle control group or ## $p < 0.01$ compared to acute putrescine.

putrescine has also been shown to act as a neuroprotectant, preventing neuronal cell death following ischemia or trauma, likely through its antioxidant and free radical scavenging actions [25, 26]. In addition, polyamines are thought to be incorporated into the eIF5A factor, which has been reported to mediate the neurotrophic and neuroprotective effects of nerve growth factor [27]. Taken together, these studies evidence the therapeutic benefit of using polyamines to enhance the functionality of cellular implants after SCI.

In the current study, SC implants were visualized immunohistochemically using an antibody against p75, the low-affinity nerve growth factor receptor highly expressed in SCs both in culture and following spinal cord implantation. The p75 receptor has been used previously to identify SC implants *in vivo* [4]. We show that delayed, but not acute, supplementation of SC implants with putrescine resulted

in an 80% increase in the size of the implant. From the overlap in administration time between the acute and delayed paradigms and the absence of an effect with acute putrescine, it is unlikely that the observed enhancement in implant size is due to a direct stimulation of SC survival or proliferation by putrescine but instead requires the presence of additional host-supplied factors. As both endogenous SC in-migration and axonal ingrowth occur with a 1–3-week delay after SCI, the later delivery of putrescine may enhance endogenous SC in-migration and/or work in concert with signals from in-growing axons to stimulate proliferation of implanted SCs [3, 28]. Following traumatic SCI, endogenous SCs have been shown to dedifferentiate in the spinal nerve roots, migrate into the injury site, proliferate, and significantly upregulate p75 expression [28, 29]. Migration and proliferation of endogenous SCs occur between 1 and

3 weeks following injury, which temporally corresponds with our delayed putrescine supplementation paradigm. In addition, axon presence is one of the strongest signals for inducing SC mitogenesis and proliferation, and there may be insufficient growth of axons within the implant/lesion site during the first week after SCI to stimulate SC proliferation acutely. Therefore, implanted SC proliferation and an ensuing increase in implant size may be best benefited by the combination of putrescine and axonal growth signals during the delayed administration period. Whether an increased area of p75 immunoreactivity denotes an enhanced proliferation of implanted SCs or an enhanced proliferation and/or migration of endogenous SCs into the lesion is difficult to determine unequivocally without cell tracking methods. However, depletion of polyamines in a variety of cell types has been shown to impair cell migration by reorganizing the F-actin of lamellipodia, impeding microtubule reformation, and preventing the accumulation of β -actin and α -tubulin mRNA [30–32]. Thus putrescine could enhance the migratory ability of endogenous SCs. On the other hand, SCs are largely mitotically quiescent under normal physiological conditions, proliferating only during development, Wallerian degeneration, or a demyelinating condition or insult. The enhanced proliferative capacity of SCs during Wallerian degeneration has been closely associated with an elevation of ornithine decarboxylase activity, suggesting that putrescine supplementation may promote the proliferation of either endogenous or exogenous SCs within the lesion [33, 34]. Amplified activity of ornithine decarboxylase and polyamines and the eIF5A translation factor derived from polyamines have all been shown to upregulate proliferation of a number of cell types [35, 36]. Further investigations are needed to ascertain the exact mechanism by which p75 and SC implant size are enhanced following SCI, implantation, and delayed supplementation of putrescine.

In addition to mediating cell migration and proliferation, putrescine and other downstream polyamines have also been shown to promote cell survival. Deficiencies in putrescine levels cause swelling of the endoplasmic reticulum and Golgi bodies, as well as the disappearance of stress fibers, all of which are hallmarks associated with necrosis [37]. Intracellular polyamines can alter ion transport, either blocking K^+ channels to prevent neuron excitotoxicity or promoting Ca^{2+} influxes [38, 39]. Polyamine-induced ion influxes have been shown to be required to induce the release of 5HT synaptosomes, which may help restore serotonergic axon functionality after SCI [40]. SC implants, when used in combinatory approaches, were previously shown to improve the regeneration of serotonergic fibers following SCI [4]. Here we observed that supplementing SC implants with putrescine significantly increased the number of serotonergic fibers proximal to the center of the implant/lesion, an effect strengthened by administering the putrescine acutely. Serotonergic axon projections within the spinal cord are believed to be important for the recovery of locomotion following injury [41]. While it is difficult to determine whether the increase in the numbers of serotonergic fibers is due to the regeneration of axotomized axons, collateral

sprouting from existing serotonergic fibers, or sparing of axons, an enhanced presence of serotonergic axons following putrescine administration may provide important stimulatory effects for improved locomotor functioning [42]. Future use of a complete spinal cord transection paradigm with SC grafting [12] would provide a means for identifying whether such 5HT axon growth is due to regeneration, sprouting, or sparing and, when combined with neuroanatomical tracing, whether the serotonergic axons are from supraspinal or intraspinal neurons.

The growth of primary sensory afferents, immunoreactive for CGRP, which have terminations in the superficial lamina of the spinal cord and are associated with transmission of pain, also benefitted from the delivery of putrescine, with enhanced axon numbers within the center of the SC implant. CGRP-positive neurons have also been implicated in the modulation of fine motor control and the control of posture and thus their growth could be indicative of changes in locomotor function [43]. Primary dorsal horn afferent fibers are known to sprout into more medial lamina of the spinal cord following SCI, again making it challenging to ascertain whether the increasing number of CGRP-positive fibers was due to regenerating sensory afferents or collateral sprouts [44]. Like 5HT⁺ axon growth, acute administration of putrescine following SCI and SC implantation generated the greatest amount of CGRP⁺ fiber growth, almost four times as many fibers compared to SCs alone and more than twice as many fibers as delayed supplementation. These CGRP⁺ axons may have arisen from DRGNs present at the level of the lesion or from DRGNs located more distally. Further investigation is needed to explore the mechanisms by which putrescine encourages primary sensory afferents to surmount the inhibitory environment of the host cord-implant interface and penetrate deeply into the SC implants as well as the use of tracing techniques to identify the level(s) from which responding DRGNs are located.

Putrescine supplementation of SC implants also resulted in significant functional improvement, as measured in the open field with the BBB score and on the grid walk test. Irrespective of the timing of putrescine delivery, enhanced locomotor ability, as measured by using the BBB score and subscore, was obtained with treatment compared to SC implanted, vehicle controls. Overall, both acute and delayed putrescine administration generated similar improvements in hind limb performance and tail posturing, including a one-point higher BBB score and five-point higher BBB subscore. Only the acute delivery of putrescine, however, reduced footfall errors on the horizontal grid walk test, by 25% compared to the vehicle control. The effectiveness of acute putrescine only on this outcome measure would indicate that tissue preservation would be a likely mechanistic explanation for this effect. The observed functional improvements following supplementation of SC implants with putrescine are in addition to those that are known to be provided when SC implants alone are used after SCI [4, 13]. The most pronounced behavioral improvement was displayed by the BBB subscore, in which a persistent improvement in outcome was observed starting at 1 week after implantation. This highly acute benefit may imply that these effects acted through

putrescine-mediated neuro- or axopreservation. The later improvements in BBB score and the continuous improvement in subscore may in turn be due to the reparative actions instigated by the initial delivery of putrescine.

5. Conclusions

In conclusion, we supply evidence that modulating polyamines in conjunction with cell implantation is an effective approach for enhancing the functionality of the implant as well as locomotor recovery after SCI. Future research should seek to gain a greater understanding of the mechanisms underlying putrescine's effects on SC function, migration, and survival, as well as its ability to promote axon sparing, growth, and/or sprouting.

Conflict of Interests

The authors declare that there is no conflict of interests regarding the publication of this paper.

Acknowledgments

The authors gratefully acknowledge the Miami Project Animal Core Facility for performing spinal cord contusions and the postoperative animal care, in particular, Alexander Marcillo, Paulo Diaz, Santiago Castro, Denise Koivisto, Kim Loor, and Rosa Abril. In addition, The authors thank Yelena Pressman for Schwann cell culture, Devin Bustin for histology, Beata Frydel, Crystal Portocarrero, and Michael Bild for image analysis, and Raisa Puzis for immunohistochemistry. This work was supported by NIH NINDS Grant no. R01NS056281 (D. D. Pearse), The Miami Project to Cure Paralysis, The Buoniconti Fund, and The Lois Pope Neuroscience Summer Research Fellowship (J. B. Iorgulescu). J. Bryan Iorgulescu was supported by the Doris Duke Clinical Research Fellowship.

References

- [1] G. Yiu and Z. He, "Glial inhibition of CNS axon regeneration," *Nature Reviews Neuroscience*, vol. 7, no. 8, pp. 617–627, 2006.
- [2] D. Cai, J. Qiu, Z. Cao, M. McAtee, B. S. Bregman, and M. T. Filbin, "Neuronal cyclic AMP controls the developmental loss in ability of axons to regenerate," *Journal of Neuroscience*, vol. 21, no. 13, pp. 4731–4739, 2001.
- [3] D. D. Pearse, A. R. Sanchez, F. C. Pereira et al., "Transplantation of Schwann cells and/or olfactory ensheathing glia into the contused spinal cord: Survival, migration, axon association, and functional recovery," *Glia*, vol. 55, no. 9, pp. 976–1000, 2007.
- [4] D. D. Pearse, F. C. Pereira, A. E. Marcillo et al., "cAMP and Schwann cells promote axonal growth and functional recovery after spinal cord injury," *Nature Medicine*, vol. 10, no. 6, pp. 610–616, 2004.
- [5] Y. Gao, K. Deng, J. Hou et al., "Activated CREB is sufficient to overcome inhibitors in myelin and promote spinal axon regeneration in vivo," *Neuron*, vol. 44, no. 4, pp. 609–621, 2004.
- [6] D. Cai, K. Deng, W. Mellado, J. Lee, R. R. Ratan, and M. T. Filbin, "Arginase I and polyamines act downstream from cyclic AMP in overcoming inhibition of axonal growth MAG and myelin in vitro," *Neuron*, vol. 35, no. 4, pp. 711–719, 2002.
- [7] M. L. DeGeorge, D. Marlowe, E. Werner et al., "Combining glial cell line-derived neurotrophic factor gene delivery (AdGDNF) with L-arginine decreases contusion size but not behavioral deficits after traumatic brain injury," *Brain Research*, vol. 1403, pp. 45–56, 2011.
- [8] H.-S. Kuo, M.-J. Tsai, M.-C. Huang et al., "Acid fibroblast growth factor and peripheral nerve grafts regulate Th2 cytokine expression, macrophage activation, polyamine synthesis, and neurotrophin expression in transected rat spinal cords," *Journal of Neuroscience*, vol. 31, no. 11, pp. 4137–4147, 2011.
- [9] H.-S. Kuo, M. J. Tsai, M.-C. Huang et al., "The combination of peripheral nerve grafts and acidic fibroblast growth factor enhances arginase I and polyamine spermine expression in transected rat spinal cords," *Biochemical and Biophysical Research Communications*, vol. 357, no. 1, pp. 1–7, 2007.
- [10] Y. M. Park, S. H. Han, S. K. Seo, K. A. Park, W. T. Lee, and J. E. Lee, "Restorative benefits of transplanting human mesenchymal stromal cells overexpressing arginine decarboxylase genes after spinal cord injury," *Cytotherapy*, vol. 17, no. 1, pp. 25–37, 2015.
- [11] T. K. Morrissey, N. Kleitman, and R. P. Bunge, "Isolation and functional characterization of Schwann cells derived from adult peripheral nerve," *Journal of Neuroscience*, vol. 11, no. 8, pp. 2433–2442, 1991.
- [12] M. F. L. Meijs, L. Timmers, D. D. Pearse et al., "Basic fibroblast growth factor promotes neuronal survival but not behavioral recovery in the transected and Schwann cell implanted rat thoracic spinal cord," *Journal of Neurotrauma*, vol. 21, no. 10, pp. 1415–1430, 2004.
- [13] T. Takami, M. Oudega, M. L. Bates, P. M. Wood, N. Kleitman, and M. B. Bunge, "Schwann cell but not olfactory ensheathing glia transplants improve hindlimb locomotor performance in the moderately contused adult rat thoracic spinal cord," *Journal of Neuroscience*, vol. 22, no. 15, pp. 6670–6681, 2002.
- [14] J. A. Gruner, "A monitored contusion model of spinal cord injury in the rat," *Journal of Neurotrauma*, vol. 9, no. 2, pp. 123–128, 1992.
- [15] D. J. Barakat, S. M. Gaglani, S. R. Neravetla et al., "Survival, integration, and axon growth support of glia transplanted into the chronically contused spinal cord," *Cell Transplantation*, vol. 14, no. 4, pp. 225–240, 2005.
- [16] T. P. Lo Jr., K.-S. Cho, M. S. Garg et al., "Systemic hypothermia improves histological and functional outcome after cervical spinal cord contusion in rats," *Journal of Comparative Neurology*, vol. 514, no. 5, pp. 433–448, 2009.
- [17] M. Kudou, K. Shiraki, S. Fujiwara, T. Imanaka, and M. Takagi, "Prevention of thermal inactivation and aggregation of lysozyme by polyamines," *European Journal of Biochemistry*, vol. 270, no. 22, pp. 4547–4554, 2003.
- [18] D. D. Pearse, T. P. Lo Jr., K. S. Cho et al., "Histopathological and behavioral characterization of a novel cervical spinal cord displacement contusion injury in the rat," *Journal of Neurotrauma*, vol. 22, no. 6, pp. 680–702, 2005.
- [19] H. Kanno, Y. Pressman, A. Moody et al., "Combination of engineered Schwann cell grafts to secrete neurotrophin and chondroitinase promotes axonal regeneration and locomotion after spinal cord injury," *Journal of Neuroscience*, vol. 34, no. 5, pp. 1838–1855, 2014.
- [20] D. M. Basso, M. S. Beattie, and J. C. Bresnahan, "A sensitive and reliable locomotor rating scale for open field testing in rats," *Journal of Neurotrauma*, vol. 12, no. 1, pp. 1–21, 1995.

- [21] S. M. Schaal, B. M. Kitay, K. S. Cho et al., "Schwann cell transplantation improves reticulospinal axon growth and forelimb strength after severe cervical spinal cord contusion," *Cell Transplantation*, vol. 16, no. 3, pp. 207–228, 2007.
- [22] G. Flora, G. Joseph, S. Patel et al., "Combining neurotrophin-transduced Schwann cells and rolipram to promote functional recovery from subacute spinal cord injury," *Cell Transplantation*, vol. 22, no. 12, pp. 2203–2217, 2013.
- [23] P. L. Wood, M. A. Khan, S. R. Kulow, S. A. Mahmood, and J. R. Moskal, "Neurotoxicity of reactive aldehydes: the concept of 'aldehyde load' as demonstrated by neuroprotection with hydroxylamines," *Brain Research*, vol. 1095, no. 1, pp. 190–199, 2006.
- [24] K. Deng, H. He, J. Qiu, B. Lorber, J. B. Bryson, and M. T. Filbin, "Increased synthesis of spermidine as a result of upregulation of arginase I promotes axonal regeneration in culture and in vivo," *The Journal of Neuroscience*, vol. 29, no. 30, pp. 9545–9552, 2009.
- [25] N. A. V. Bellé, G. D. Dalmolin, G. Fonini, M. A. Rubin, and J. B. T. Rocha, "Polyamines reduces lipid peroxidation induced by different pro-oxidant agents," *Brain Research*, vol. 1008, no. 2, pp. 245–251, 2004.
- [26] T. Imagama, K. Ogino, K. Takemoto et al., "Regulation of nitric oxide generation by up-regulated arginase I in rat spinal cord injury," *Journal of Clinical Biochemistry and Nutrition*, vol. 51, no. 1, pp. 68–75, 2012.
- [27] Y. Huang, D. S. Higginson, L. Hester, H. P. Myung, and S. H. Snyder, "Neuronal growth and survival mediated by eIF5A, a polyamine-modified translation initiation factor," *Proceedings of the National Academy of Sciences of the United States of America*, vol. 104, no. 10, pp. 4194–4199, 2007.
- [28] A. Buss, K. Pech, B. A. Kakulas et al., "Growth-modulating molecules are associated with invading Schwann cells and not astrocytes in human traumatic spinal cord injury," *Brain*, vol. 130, part 4, pp. 940–953, 2007.
- [29] M. Oudega, "Schwann cell and olfactory ensheathing cell implantation for repair of the contused spinal cord," *Acta Physiologica*, vol. 189, no. 2, pp. 181–189, 2007.
- [30] A. Banan, S. A. McCormack, and L. R. Johnson, "Polyamines are required for microtubule formation during gastric mucosal healing," *The American Journal of Physiology—Gastrointestinal and Liver Physiology*, vol. 274, no. 5, pp. G879–G885, 1998.
- [31] B. Kamińska, L. Kaczmarek, and B. Grzelakowska-Sztabert, "Inhibitors of polyamine biosynthesis affect the expression of genes encoding cytoskeletal proteins," *FEBS Letters*, vol. 304, no. 2–3, pp. 198–200, 1992.
- [32] S. A. McCormack, R. M. Ray, P. M. Blanner, and L. R. Johnson, "Polyamine depletion alters the relationship of F-actin, G-actin, and thymosin beta4 in migrating IEC-6 cells," *American Journal of Physiology*, vol. 276, no. 2, part 1, pp. C459–C468, 1999.
- [33] H. Hirata, H. Hibasami, T. Hineno et al., "Role of ornithine decarboxylase in proliferation of Schwann cells during Wallerian degeneration and its enhancement by nerve expansion," *Muscle and Nerve*, vol. 18, no. 11, pp. 1341–1343, 1995.
- [34] S. Ohkaya, H. Hibasami, H. Hirata et al., "Nerve expansion in nerve regeneration: effect of time on induction of ornithine decarboxylase and Schwann cell proliferation," *Muscle and Nerve*, vol. 20, no. 10, pp. 1314–1317, 1997.
- [35] T. Thomas and T. J. Thomas, "Polyamines in cell growth and cell death: molecular mechanisms and therapeutic applications," *Cellular and Molecular Life Sciences*, vol. 58, no. 2, pp. 244–258, 2001.
- [36] K. Nishimura, K. Murozumi, A. Shirahata, M. H. Park, K. Kashiwagi, and K. Igarashi, "Independent roles of eIF5A and polyamines in cell proliferation," *Biochemical Journal*, vol. 385, no. 3, pp. 779–785, 2005.
- [37] J. J. Parkkinen, M. J. Lammi, U. Ågren et al., "Polyamine-dependent alterations in the structure of microfilaments, Golgi apparatus, endoplasmic reticulum, and proteoglycan synthesis in BHK cells," *Journal of Cellular Biochemistry*, vol. 66, no. 2, pp. 165–174, 1997.
- [38] A. N. Lopatin, E. N. Makhina, and C. G. Nichols, "Potassium channel block by cytoplasmic polyamines as the mechanism of intrinsic rectification," *Nature*, vol. 372, no. 6504, pp. 366–369, 1994.
- [39] H. Komulainen and S. C. Bondy, "Transient elevation of intrasynaptosomal free calcium by putrescine," *Brain Research*, vol. 401, no. 1, pp. 50–54, 1987.
- [40] N. A. Khan, J. P. Moulinoux, and P. Deschaux, "Putrescine modulation of depolarization-induced [³H]serotonin release from fish brain synaptosomes," *Neuroscience Letters*, vol. 212, no. 1, pp. 45–48, 1996.
- [41] M. G. Ribotta, J. Provencher, D. Feraboli-Lohnherr, S. Rossignol, A. Privát, and D. Orsal, "Activation of locomotion in adult chronic spinal rats is achieved by transplantation of embryonic raphe cells reinnervating a precise lumbar level," *The Journal of Neuroscience*, vol. 20, no. 13, pp. 5144–5152, 2000.
- [42] M. J. Eaton, D. D. Pearce, J. S. McBroom, and Y. A. Berrocal, "The combination of human neuronal serotonergic cell implants and environmental enrichment after contusive SCI improves motor recovery over each individual strategy," *Behavioural Brain Research*, vol. 194, no. 2, pp. 236–241, 2008.
- [43] A. Schorscher-Petcu, J.-S. Austin, J. S. Mogil, and R. Quirion, "Role of central calcitonin gene-related peptide (CGRP) in locomotor and anxiety- and depression-like behaviors in two mouse strains exhibiting a CGRP-dependent difference in thermal pain sensitivity," *Journal of Molecular Neuroscience*, vol. 39, no. 1–2, pp. 125–136, 2009.
- [44] N. R. Krenz and L. C. Weaver, "Sprouting of primary afferent fibers after spinal cord transection in the rat," *Neuroscience*, vol. 85, no. 2, pp. 443–458, 1998.

Clinical Study

Clinical Trial of Human Fetal Brain-Derived Neural Stem/Progenitor Cell Transplantation in Patients with Traumatic Cervical Spinal Cord Injury

Ji Cheol Shin,^{1,2} Keung Nyun Kim,³ Jeehyun Yoo,^{1,2} Il-Sun Kim,⁴
Seokhwan Yun,⁵ Hyejin Lee,⁵ Kwangsoo Jung,⁵ Kyujin Hwang,⁵ Miri Kim,⁵
Il-Shin Lee,⁴ Jeong Eun Shin,⁴ and Kook In Park^{4,5}

¹Department of Rehabilitation Medicine, Yonsei University College of Medicine, Seoul 120-752, Republic of Korea

²Research Institute of Rehabilitation Medicine, Yonsei University College of Medicine, Seoul 120-752, Republic of Korea

³Department of Neurosurgery, Yonsei University College of Medicine, Seoul 120-752, Republic of Korea

⁴Department of Pediatrics, Severance Children's Hospital, Yonsei University College of Medicine, Seoul 120-752, Republic of Korea

⁵BK21 Plus Project for Medical Science, Yonsei University College of Medicine, Seoul 120-752, Republic of Korea

Correspondence should be addressed to Kook In Park; kipark@yuhs.ac

Received 13 February 2015; Accepted 1 July 2015

Academic Editor: Young Wook Yoon

Copyright © 2015 Ji Cheol Shin et al. This is an open access article distributed under the Creative Commons Attribution License, which permits unrestricted use, distribution, and reproduction in any medium, provided the original work is properly cited.

In a phase I/IIa open-label and nonrandomized controlled clinical trial, we sought to assess the safety and neurological effects of human neural stem/progenitor cells (hNSPCs) transplanted into the injured cord after traumatic cervical spinal cord injury (SCI). Of 19 treated subjects, 17 were sensorimotor complete and 2 were motor complete and sensory incomplete. hNSPCs derived from the fetal telencephalon were grown as neurospheres and transplanted into the cord. In the control group, who did not receive cell implantation but were otherwise closely matched with the transplantation group, 15 patients with traumatic cervical SCI were included. At 1 year after cell transplantation, there was no evidence of cord damage, syrinx or tumor formation, neurological deterioration, and exacerbating neuropathic pain or spasticity. The American Spinal Injury Association Impairment Scale (AIS) grade improved in 5 of 19 transplanted patients, 2 (A → C), 1 (A → B), and 2 (B → D), whereas only one patient in the control group showed improvement (A → B). Improvements included increased motor scores, recovery of motor levels, and responses to electrophysiological studies in the transplantation group. Therefore, the transplantation of hNSPCs into cervical SCI is safe and well-tolerated and is of modest neurological benefit up to 1 year after transplants. This trial is registered with Clinical Research Information Service (CRIS), Registration Number: KCT0000879.

1. Introduction

Acute traumatic spinal cord injury (SCI) occurs most commonly in the cervical segments due to the great flexibility of neck. Cervical SCI is a devastating disorder, which can result in quadriplegia, ventilator dependency, a requirement for total assistance with all major functions, and a significant reduction in quality of life. However, there is currently no curative or effective therapy for SCI [1]. Therapeutic transplantation of different types of stem cells and their derivatives, alone or in combination with other treatments, has been

reported to improve functional outcome in animal models of SCI, probably through cell replacement, trophic support, facilitation of axonal growth, remyelination, or modulation of inflammation [2, 3]. Based on these experimental findings, although the field of stem cell therapy is in its infancy, some stem cell or cell-based transplantation using bone marrow-derived cells, umbilical cord blood cells, olfactory ensheathing cells, Schwann cells, activated macrophages, or T cells have already been used in patients with SCI [4–12]. To date, the existing data from clinical trials have shown some stem cell or cell transplants to be safe, but with very limited

or no therapeutic efficacy. Thus, stem cell therapies are not yet approved for SCI [3, 13].

Neural stem/progenitor cells (NSPCs) are characterized by a capacity for self-renewal, differentiation into multiple neural lineages, and migration toward damaged sites in the central nervous system (CNS), all of which are currently considered to be promising components for SCI repair and regeneration [14–19]. Recent studies have shown that human fetal CNS-derived NSPCs (hNSPCs) implanted into mice with subacute or chronic SCI were found to successfully engraft, migrate, differentiate into oligodendrocytes and neurons, and improve long-term locomotor recovery [20, 21]. This functional recovery was likely to have been mediated through the integration of donor-derived neurons with host neural circuitry and contact with host motor neurons [22, 23]. Based on these preclinical data, a clinical trial by the company StemCells, Inc., is undergoing to assess the effect of the company's proprietary human neural stem cell transplantation into patients with cervical SCI [24].

The objective of this study was to evaluate the safety, tolerability, and neurological status of patients with traumatic sensorimotor complete (AIS grade A, AIS-A) or motor complete (AIS grade B, AIS-B) cervical SCI following transplantation of hNSPCs into the injured cord. The American Spinal Injury Association (ASIA) Impairment Scale (AIS), which forms part of the International Standards for Neurological Classification of SCI (ISNCSCI) examinations, has been widely used for the diagnosis and prognosis of SCI and represents a toolbox of validated outcomes for use in the forthcoming clinical trials [25]. This is a report of the outcome of the trial, 1 year after transplantation. Our results demonstrate that the direct administration of hNSPCs into the injured cervical cord is safe and well-tolerated and of modest benefit neurologically.

2. Materials and Methods

2.1. Patient Selection. This phase I/IIa open-label and non-randomized controlled clinical study was reviewed and approved by the Institutional Review Board (IRB) of the Severance Hospital, Yonsei University College of Medicine, Seoul, Korea (Permit number: 4-2005-0057), Korean Food and Drug Administration (Permit number: BM-473), and was monitored by the responsible ethics committees. This study was conducted in accordance with the Declaration of Helsinki (1964). All procedures were performed after obtaining written informed consent. Patients were fully aware of the experimental nature of the treatment, unclear outcomes, and possible side effects, such as pain, spasticity, autonomic dysfunction, worsening of motor or sensory function, infection, tumor formation, and unforeseen adverse events.

Participants were eligible when they were admitted to the hospital if they were between 18 and 60 years old and had AIS-A or AIS-B cervical SCI of traumatic etiology. Patients first underwent spinal cord decompression and stabilization therapy and then rehabilitation. They showed persistent complete or incomplete paralysis below the level of the injury. Exclusion criteria were SCI at multiple levels, spinal vertebral instability, major concurrent medical or neurological illness,

substance abuse, psychiatric illness, traumatic brain injury associated with SCI, and concomitant skeletal fracture or joint atrophy. Subjects who had concurrent peripheral nerve, nerve root injury, or accompanying neuropathy that might influence spontaneous recovery and recordings of evoked potentials [26, 27] were also excluded. To verify peripheral nerve injury or neuropathy, peripheral nerve conduction studies (NCS), including median sensory, ulnar sensory, superficial peroneal, sural, median motor, ulnar motor, peroneal, and tibial nerves, were made in all patients with SCI [28]. If there was any abnormality in the NCS, the patient was excluded.

Nineteen patients were selected for hNSPCs transplantation from among those who were admitted to the hospital between May 2005 and August 2008. According to the time window between the injury onset and hNSPCs transplantation, eligible patients were divided into four groups: acute (<1 week), early subacute (1–8 weeks), late subacute (9 weeks–6 months), and chronic (>6 months). In the control group, all 15 patients with traumatic cervical SCI were managed with decompression surgery of the spinal canal and then referred to the rehabilitation clinic of the hospital. They did not receive hNSPCs implantation for SCI. They were randomly selected from AIS-A or AIS-B patients who were admitted to the hospital from May 2005 to April 2008. The inclusion and exclusion criteria for the control group were the same as the transplantation group. Demographic data and clinical characteristics of patients in both groups are presented in Table 1.

2.2. Peripheral Nerve Conduction Study. To verify peripheral nerve injury or neuropathy, peripheral nerve conduction studies, including median sensory, ulnar sensory, superficial peroneal, sural, median motor, ulnar motor, peroneal, and tibial nerves, were conducted before transplantation. For median sensory nerve conduction studies, the recording electrode was placed over the second finger and stimulation was done at the wrist between the tendons of the flexor carpi radialis laterally and the palmaris longus muscles medially. For ulnar sensory nerve conduction studies, the recording electrode was placed over the fifth finger and stimulation was done at the wrist, just lateral to the tendon of the flexor carpi ulnaris muscle. For superficial peroneal nerve conduction studies, the recording electrode was placed 1–2 cm medial to the lateral malleolus and stimulation was done at 12 cm proximal to the recording electrode, just anterior to the anterior margin of the fibular. For sural nerve conduction studies, the recording electrode was placed at 3 cm posterior to the lateral malleolus and stimulation was done at 14 cm proximal to the recording electrode, just lateral to the leg midline. For median motor nerve conduction studies, the recording electrode was placed over the abductor pollicis brevis muscle and stimulation was done at the wrist and the antecubital fossa. For ulnar motor nerve conduction studies, the recording electrode was placed over the adductor digiti quinti muscle and stimulation was done at the wrist and just below the medial epicondyle. For peroneal nerve conduction studies, the recording electrode was placed over the extensor digitorum brevis muscle and stimulation was done at the

TABLE 1: Demographic, clinical, and neurological features of the patients.

Transplantation group						Control group					
Patient	Sex	Age (years)	Time (days) ^a	SCI level	AIS grade ^b	Patient	Sex	Age (years)	Time (days) ^c	SCI level	AIS grade ^d
1	M	34	38	C3	A	1	M	37	168	C6	A
2	M	36	46	C3	A	2	M	56	19	C4	A
3	M	33	81	C7	A	3	M	28	7	C6	A
4	M	45	52	C4	A	4	M	29	58	C6	A
5	M	26	141	C4	A	5	M	34	33	C5	A
6	M	56	75	C4	A	6	F	54	92	C5	A
7	F	45	21	C3	A	7	M	41	35	C3	A
8	M	24	48	C5	A	8	F	35	37	C3	A
9	M	53	123	C3	A	9	F	22	60	C3	A
10	M	32	28	C3	A	10	M	28	92	C6	A
11	M	27	59	C5	A	11	M	35	17	C7	A
12	M	54	213	C3	A	12	M	51	97	C3	A
13	M	57	16	C4	A	13	M	24	66	C4	A
14	M	29	34	C4	A	14	M	39	19	C5	B
15	M	23	18	C4	A	15	M	46	38	C7	B
16	F	23	141	C3	A						
17	M	51	24	C4	A						
18	F	41	25	C7	B						
19	M	18	22	C8	B						

Patients are listed according to AIS grade. M = male. F = female. ^aTime between the injury onset and hNSPC transplantation, ^bAIS grade before transplantation, ^ctime between the injury onset and the initial evaluation of AIS examination in the hospital, and ^dAIS grade at the initial evaluation.

ankle, just lateral to the tibialis anterior tendon and distal to the fibular head. For tibial nerve conduction studies, the recording electrode was placed over the abductor hallucis muscle and stimulation was done at the ankle just posterior to the medial malleolus and the popliteal fossa.

2.3. Maintenance and Propagation of Human NSPCs in Culture. Human fetal tissue from a cadaver at 13 weeks of gestation was obtained with full parental consent and approval of the IRB of the hospital (Permit number: 4-2003-0078). In this study, hNSPCs for transplantation were derived from such a single donated fetal brain. The methods of acquisition conformed to NIH and Korean Government guidelines. The freshly dissected telencephalic tissue of a fetal brain was transferred from the Good Tissue Practice (GTP) to the Good Manufacturing Practice (GMP) facility. Brain tissue was in dissociation in trypsin (0.1% for 30 min, Sigma) and seeded into tissue culture-treated 100-mm plates (Corning) at a density of 400,000 cells/mL of serum-free growth medium, which consisted of a 1:1 mixture of Dulbecco's modified Eagle's medium and Ham's F12 (DMEM/F12; Gibco), supplemented with penicillin/streptomycin (1% v/v; Gibco) and N2 formulation (1% v/v; Gibco). Mitogenic stimulation was achieved by adding 20 ng/mL of fibroblast growth factor-2 (FGF2; R&D Systems) and 10 ng/mL of leukemia inhibitory factor (LIF; Sigma). Heparin (8 µg/mL; Sigma) was added to stabilize FGF2 activity. All cultures were maintained in a humidified incubator at 37°C and 5% CO₂ in air, and half of

the growth medium was replenished every 3-4 days. Proliferating single cells isolated from the fetal brain gave rise to free-floating neurospheres during the first 2-5 days of growth. Passaging was undertaken every 7-8 days by dissociation of bulk neurospheres with 0.05% trypsin/EDTA (T/E; Gibco). hNSPCs, cultured as neurospheres, were reseeded in fresh growth medium at a density equivalent to ~400,000 cells/mL. Under these culture conditions, hNSPCs continued to proliferate and generate a large number of progenies for over 1 year [29]. For cryopreservation of hNSPCs, trypsinized cells taken at each passage were resuspended in a freezing solution consisting of 10% dimethyl sulfoxide, 50% fetal bovine serum, and 40% growth medium and brought slowly to -140°C. Human neurospheres were continuously expanded from the initial outgrowths to avoid repeated freezing and thawing. Cells were pooled and frozen at each passage (P4-30; passage number 4-30) as primary cell banks and following additional expansion cryopreserved (P7-25) as secondary cell banks.

The growth rate of hNSPCs in the presence of mitogens was assessed *in vitro*. Initially, 4×10^6 cells were plated on tissue culture-treated 100-mm plates. At 5 time points up to 50 days, the cells were harvested with T/E and the average number of hNSPCs was determined by using the trypan blue exclusion method. Cell counts were then plotted versus the time of cells harvest and the doubling time was calculated. The doubling time of hNSPCs was between 4 and 5 days. To analyze the cellular composition of the neurospheres, sectioned neurospheres were immunostained for various neural cell markers. Under proliferative conditions, the majority of

cells (~99%) within the neurospheres expressed immature cell markers: nestin, vimentin, glial fibrillary acidic protein (GFAP), Pax6, excitatory amino acid transporter 1 (EAAT1), and Sox2 [29]. These results indicated that the cells within the neurospheres consisted mostly of hNSPCs.

2.4. Cell Culture Quality Control. Before releasing hNSPCs for transplantation, in-process quality testing for the cells at each passage was carried out for cellular differentiation pattern, karyotyping, endotoxins, mycoplasmas, bacteria, fungi, or viruses. Endotoxins and mycoplasmas were checked using the Limulus Amebocyte Lysate test and MycoAlert Mycoplasma Detection Assay (Cambrex), respectively. HIV-1/2, HTLV-1/2, hepatitis A/B/C, herpes (HSV-1/2), cytomegalovirus, syphilis, toxoplasmosis, fungi, and aerobic or anaerobic bacterial infection were assessed. At any step, if any sample was detected to be positive, it was discarded immediately. For cytogenetic studies of hNSPCs, a standard G-banding procedure to visualize chromosomes was regularly given by the analysis of about at least 20 metaphases per cultural passage. The data from this study confirmed that hNSPCs were diploid soon after derivation and retained a normal karyotype after long-term passage and cryopreservation. Array-based comparative genomic hybridization (aCGH), a technique that allows for high-resolution genome-wide detection of unbalanced structural and numerical chromosomal alterations [30], was performed regularly using MacArray Karyo (Macrogen, Seoul, Korea) according to the manufacturer's protocol. The data from this study showed no evidence for genomic alteration in hNSPCs.

To evaluate the differentiation potential of hNSPCs into neural cell types, whole neurospheres taken at sequential passages in culture were dissociated into single-cell suspensions and plated directly onto poly-L-lysine-coated, 8-well chamber slides (Nunc) in serum-free medium. After a 7-day period following plating, cells were fixed with 4% paraformaldehyde in PIPES buffer (Sigma) and immunostained with antibodies to Nestin, glial fibrillary acidic protein (GFAP), neuron-specific β -tubulin III (TUJ1, polyclonal, 1:1000; Covance), NF (pan-neurofilament, 1:500; Sternberger), rabbit anti-Olig2 (1:500; Millipore), O4 (1:30; Chemicon), CNPase (2,3-cyclic nucleotide-3-phosphohydrolase, 1:500; Sternberger), choline acetyltransferase (ChAT; 1:200; Chemicon), glutamate (1:500; Sigma), γ -aminobutyric acid (GABA, 1:500; Sigma), and tyrosine hydroxylase (TH, 1:50; Chemicon). Primary antibodies were labeled with a fluorescent secondary antibody. Cells were examined and quantified microscopically and photographed digitally.

About 40–50% of cells from the neurospheres at P10–20 expressed early neuronal cell marker TUJ1, ~2% of cells expressed early oligodendrocyte marker O4, and more than 80% of cells expressed astrocyte marker GFAP. Although the percentages of GFAP⁺ cells from hNSPCs were very high, more than 90% of the cells were dual-labeled with human nestin immature cell marker. Thus, the high percentages of GFAP⁺ cells in hNSPCs do not reflect their differentiation into astrocytes, but they suggest that cells still retain many characteristics of stem cells or progenitors. Before transplantation, the differentiation patterns of hNSPCs taken at

between P10–20 were examined immunocytochemically to identify the multipotency of differentiation. In this study, all transplanted hNSPCs met these criteria of differentiation.

2.5. Preparation and Transplantation of Human NSPCs. hNSPCs were maintained by passaging through the dissociation of bulk neurospheres and cryopreserved at each passage in the GMP facility. For transplantation, hNSPCs taken between P10 and P20 were selected and prepared. On the day of transplantation, cells were harvested by trypsinization after which the enzymatic activity was stopped with soybean trypsin inhibitor (Sigma). The cells were centrifuged (900 g, 3 min), the cell pellet was washed three times with Hank's balanced salt solution-HEPES (H-H) buffer, and the entire cell pellet was then resuspended in 1.0 mL of H-H buffer at a density of 1.0×10^5 cells per μ L. The concentrated hNSPCs in a sterile freezing tube (Nunc) were then delivered to the operation room [31].

Surgical intervention was performed under general anesthesia with endotracheal intubation. All surgical procedures were performed by the same neurosurgical team. A midline incision and posterior laminectomy was performed to expose the dura at the site of injury. Using magnification of an operating microscope (Zeiss Corporation), a midline durotomy was performed away from the site of injury and the opening completed by splitting the normal dura and sharp dissection. A dorsal adhesiolysis was carefully performed using sharp and blunt dissection methods through the injury to remove the scar tissue and detether the cord. After exposure of sufficient surface at the contusion site, cells (1.0 mL , 1.0×10^5 cells per μ L) were injected into the spinal cord using a 23-gauge needle attached to a 1-mL syringe. Five hundred microliters of cell suspension was injected at the lesion center, as demonstrated on preoperative magnetic resonance imaging (MRI), and then 250 μ L was injected, 5 mm rostral and caudal to the lesion center, respectively. The needle was set at the lesion center along the midline and inserted into the cord 5 mm deep from the dorsal surface of the spinal cord. The needle was removed from the first injection site and moved on the midline 5 mm rostrally and caudally and inserted into the cord 5 mm deep from the dorsal surface of the spinal cord. Each injection was performed over a 3-min infusion period. To prevent cell leakage through the injection track, the injection needle was left in position for additional 2 min after completing the injection. The dura was primarily closed with absorbable sutures and a wound drain was placed. The wound was then closed in layers. Sham operations in the control group were not considered because of the difficulty of ethical justification, given that this would entail an increased risk for the placebo group.

Although NSPCs are minimally immunogenic, low-grade rejection of transplanted NSPCs remains possible [32]. Therefore, many investigators believe that some form of temporary immunosuppression is necessary to optimize fetal donor cell engraftment and survival in humans [33]. For the induction of temporary immunosuppression in this study, cyclosporine (3 mg/kg BID, Novartis, Korea) was orally given to patients for 3 days preoperatively, and it was intravenously given for 4 days after the transplant and orally supplied for

the next 2 weeks. The oral cyclosporine dose was reduced to 2 mg/kg BID at 4 weeks after implantation and then reduced to 1 mg/kg BID 3 weeks later and discontinued at 9 weeks postoperatively. Toxicity monitoring included checks of cyclosporine blood trough concentrations, urine analysis, blood urea nitrogen, and creatinine every 48 h during the first week after surgery, biweekly until 5 weeks, and then at the cessation of drug administration. No patient showed side effects due to the cyclosporine.

2.6. Outcome Measures. Preoperative and postoperative assessments included AIS neurological examination, according to the revised 2006 ISNCSCI assessments guidelines [25], somatosensory evoked potentials (SSEPs), motor evoked potentials (MEPs), spinal cord magnetic resonance imaging (MRI) scanning, and pain and spasticity assessments. All assessments were made by physicians specially trained for AIS who also had expertise in treating SCI patients. Variability was reduced by using the same assessors throughout the study, obviating interobserver variability.

2.7. Neurological Assessments. The neurological status of the patients was determined in terms of AIS grade, ASIA motor scores (AMS), ASIA sensory scores (ASS), ASS-pin prick scores (ASS-P), ASS-light touch scores (ASS-L), and neurological level prior to and at 2, 6, and 12 months after hNSPC transplantation. A five-scale subdivision of the AIS grade was used to evaluate changes in patient motor and sensory function. AIS-A grade has no motor or sensory function at the level of S4-S5 sacral segments. AIS-B has some sensory function below the neurological level, including S4-S5, but no motor function. AIS-C has some motor function below the neurological level, but more than half of the key muscles involved have a muscle strength score that is less than 3. AIS-D has motor function below the neurological level, but more than half of the key muscles have a muscle grade of 3 or more. AIS-E indicates normal motor and sensory function. AMS involves a qualitative grading of the strength of contraction within 10 representative key muscles, five for the upper extremity (upper extremity motor score (UEMS)) and five for the lower extremity (lower extremity motor score (LEMS)) on each side of the body. ASS involves a qualitative grading of sensory responses to touch (ASS-L) and pin prick (ASS-P) at each of 28 dermatomes along each side of the body [25].

The neurological level of spinal injury is generally the lowest segment of the spinal cord with normal sensory and motor function on both sides of the body. Motor level is defined as the most caudal spinal level, as indexed by the key muscle group for that level having a muscle strength of 3/5 or above while the key muscle for the spinal segment, immediately above, is normal (5/5; right/left side). In this study, all AIS-A patients and a motor level of C4-C7 at the baseline assessment in both transplantation and control groups were included in the analysis of motor level. C4 motor level of SCI was determined based on the normal preservation of sensory function on the C4 dermatome [34]. Because there is no key muscle delineating the C4 spinal segment, it is difficult to reliably track deterioration from an

initial C4 motor level. Thus, these individuals were analyzed separately for changes in motor level. However, individuals with an initial C4 motor level SCI were included in the analysis of motor level from baseline. An analysis of motor level (right and left side) changes was also performed for the combined group of C5-C7 SCI patients. Sensory level is defined as the spinal segment corresponding with the most caudal dermatome having a normal score for both pin prick and light touch.

2.8. Electrophysiological Studies. To assess the functional integrity of the corticospinal tract and the dorsal columns, SSEP and MEP studies of the lower and upper limbs were conducted prior to and at 2, 6, and 12 months after transplantation.

For SSEP studies of median, ulnar, tibial, and peroneal nerves, stimulating electrodes were placed over the median nerve at the wrist, ulnar nerve at the wrist, tibial nerve at the medial ankle, and peroneal nerve at the popliteal fossa, respectively. For pudendal nerve SSEP studies, the stimulating electrode was placed on the shaft of the penis by a ring electrode in males or on the clitoris by a bar electrode in females. Recording electrodes were placed on the C3'-Fz for median and ulnar nerve SSEP studies. For tibial, peroneal, and pudendal nerve SSEP studies, recording electrodes were placed on the Cz'-Fz. The stimulation frequency was 3 Hz and the stimulation duration was 0.1 ms. The stimulation intensity was able to produce a visual contraction of the abductor pollicis brevis (APB) for the median nerve, the abductor digiti quinti (ADQ) for the ulnar nerve, the abductor hallucis (AH) for the tibial nerve, and the extensor digitorum brevis (EDB) for the peroneal nerve. The sweep speed was 5 ms/division and sensitivity was 2 μ V/division. With median nerve and ulnar nerve SSEPs, we obtained N20 latency by applying 250 repeated stimulations twice each. For the tibial, peroneal, and pudendal nerve SSEPs, P40 latency was acquired through 250 repeated stimulations that were applied twice. SSEP was performed using Synergy (Medelec Synergy-Oxford Instruments, UK). Normal values are median SSEP: 16.9–20.6 ms, ulnar SSEP: 18.1–20.5 ms, tibial SSEP: 32–46 ms, peroneal SSEP: 32.3–36.3 ms, and pudendal nerve SSEP: 40.4–44.2 ms for men and 38.5–41.1 ms for women. A positive SSEP response was defined as the presence of a cortical response (prolonged latency time or normalization of SSEP) to peripheral stimulation at 1 year after hNPSC implantation, while there was no response before transplantation.

For MEP studies, transcranial magnetic stimulation was performed using Magstim (Magstim Company Limited, UK). The surface recording electrodes were placed over the biceps brachii and abductor pollicis brevis (APB) muscles for the upper limbs and over the tibial anterior (TA) muscle for the lower limbs [28]. The resting motor threshold was the lowest transcranial magnetic stimulation (TMS) intensity that could yield MEP more than 50 μ V in amplitude in muscles at rest in at least 5 of 10 stimulations; it was established by increasing the stimulus intensity slowly. We then stimulated the motor cortex 10 times at 1.2 times the intensity of the resting motor threshold and obtained a mean amplitude and latency of

MEP. Normal values are biceps brachii MEP: latency 9.1–14.7 ms, amplitude 0.21–1.08 mV; APB MEP: latency 12.2–18.4 ms, amplitude 0.25–1.10 mV; TA MEP: latency 20.2–32.5 ms, amplitude 0.19–0.88 mV. A positive MEP response was defined as the presence of a peripheral response (prolonged or normal latency time, or low or normal amplitude) to transcranial stimulation at 1 year after NSPC implantation, while there was no response before transplantation.

2.9. Spine MRI Studies. Spine MRI studies were conducted prior to and at 2, 6, and 12 months after transplantation. MRI examinations were performed with a 1.5/3.0-T magnet using T1- and T2-weighted images (WI) (Signa, GE Medical Systems). For the classification of MRI patterns of acute SCI before hNSPC transplantation, criteria based on alterations in the signal intensity in the spine MRI, as detected by T1- and T2-WI (weighted images) sequences, with respect to time elapsed since the trauma, were used [35]. These criteria are as follows: Type I pattern (hemorrhage): within the first 72 h after the trauma, the spinal cord on T1-WI is heterogeneous; on T2-WI, there is a large central area with low signal intensity surrounded by a thin high intensity peripheral ring. At 72 h to the first week from the trauma, the spinal cord shows hyperintensity on T1- and T2-WI. Type II pattern (edema): there are normal images on T1-WI with high signal intensity on T2-WI. Type III pattern (contusion or mixed): there are normal images on T1-WI, while, on T2-WI, the spinal cord presents with a small central area of isointensity and a thick peripheral ring of high intensity, which persists through the subacute phase. Type IV pattern (compression): there is severe obliteration of the spinal cord with significant alteration of its morphology.

To assess posttraumatic abnormalities and possible complications arising during chronic SCI, MRI findings at 1 year after implantation were evaluated and classified as follows: cord atrophy, myelomalacia, cyst, or syrinx [36]. Cord atrophy is abnormal narrowing of the cervical cord region in the sagittal plane two segments or more beyond the vertebral injury (<7 mm in anteroposterior dimension). Myelomalacia is an area of ill-defined contours and irregular shapes, which is hypointense on T1-WI and hyperintense on T2-WI. Cyst is an oval or round intramedullary lesion with the same signal intensity as cerebrospinal fluid, which is confined to the vertebral level of maximum bony protrusion into the spinal canal. Syrinx is a tubular and well-defined fluid-filled region, which is usually tapered at one or both ends and extends beyond the length of maximal bony damage.

The location of SCI was named for the nearest vertebral segment [37]. Each segment was subdivided into three parts: the upper half of the vertebral body was named segment 1 (e.g., C4.1), the lower part of the vertebral body segment is 2 (e.g., C4.2), and the intervertebral disc below the body segment is 3 (C4.3). In all patients, the lesion length was determined where intramedullary cord signal intensity change was depicted on T1- and T2-WI. Lesion length was defined as the distance between the most cephalic and the most caudal extent of the cord signal intensity change.

2.10. Pain and Spasticity Assessments. The development of pain and spasticity in patients following hNSPC implantation was evaluated serially. Pain was assessed using a visual analog scale (VAS) [38]. The VAS frame used a 10-cm bar. Patients indicated their pain score from 0 to 10; zero means no pain and ten means the worst pain imaginable.

Spasticity was evaluated clinically using a modified Ashworth scale with definitions as follows [39]: 0 = no increase in tone, 1 = slight increase in muscle tone, manifested by a catch and release or minimal resistance at the end of the ROM when the affected part(s) is moved in flexion or extension, 1+ = slight increase in muscle tone, manifested by a catch, followed by minimal resistance throughout the remainder (less than half) of the ROM, 2 = more marked increase in muscle tone through most of the ROM, but the affected part(s) easily moved, 3 = considerable increase in muscle tone, passive movement difficult, and 4 = affected part(s) rigid in flexion or extension. Patients were allowed to take medications for the control of spasticity or pain according to their needs.

2.11. Western Blot and PCR. hNSPCs were lysed in tissue protein extraction reagent (Thermo) containing protease and phosphatase inhibitors (Sigma), and lysates were centrifuged (16,000 ×g, 30 min, 4°C). The supernatant was collected and stored at -70°C. Protein concentrations were determined using the Bradford assay. Samples were electrophoresed in 10% Tris-glycine gels, 4–15% Mini-PROTEAN TGX precast gels (Bio-Rad), or 16.5% Tris-tricine gels and transferred to nitrocellulose membranes. After being blocked with 5% skim milk or BSA in TBS containing 0.1 or 0.05% Tween 20 (TBS-T), the membranes were incubated with the following antibodies: rabbit anti-neurotrophin-3 (NTF3; Santa Cruz Biotechnology), rabbit anti-nerve growth factor (NGF), rabbit anti-brain-derived neurotrophic factor (BDNF; Santa Cruz Biotechnology), rabbit anti-neurotrophin-4 (NTF4; Santa Cruz Biotechnology), and mouse anti-human vascular endothelial growth factor (VEGF; BD). Next, the membranes were incubated with peroxidase-conjugated antibodies (Jackson ImmunoResearch) and treated with SuperSignal West Pico or Dura chemiluminescent substrate (Thermo).

For PCR analysis, total RNA was isolated from hNSPCs under proliferation and differentiation conditions *in vitro* using TRI reagent (Molecular Research Center). The RNA quantity was spectrophotometrically determined, and 4-μg isolated RNA was reverse-transcribed into cDNA using SuperScript III Reverse Transcriptase (Invitrogen). Reverse transcriptase PCR was carried out in a 20-μL reaction mixture containing 1-μL cDNA following cycle parameters: 30 s at 95°C, 30 s at 53°C for 30 s, and 30 s at 72°C for 31 cycles. Forward and reverse primers were designed to evaluate the expression levels of trophic factors in hNSPCs (*GAPDH*: sense, 5' ACCACAGTCCATGCCATCAC 3'; antisense, 5' TCCACCACCCTGTTGCTGTA 3'; *BDNF*: sense, 5' AACATAAGGACGCAGACTT 3'; antisense, 5'

TGCAGTCTTTTGTCTGCCG 3'; *NTF3*: sense, 5' TACGCGGAGCATAAGAGTCAC 3'; antisense, 5' GGCACACACAGGACGTGTC 3'; *NTF4*: sense, 5' CCTCCCCATCCTCCTCCTTTT 3'; antisense, 5' ACTCGCTGGTGCA GTTTCGCT 3'; *VEGFA*: sense, 5' CCATGGCAGAAGGAGGAGG 3'; antisense, 5' ATTGGATGGCAGTAGCTGCG3'; *GDNF*: sense, 5' CTGACTTGGGTCTGGGCTATG 3'; antisense, 5' TTGTCACTCACCAGCCTTCTATT; *FGF2*: sense, 5' GTGTGCTAACCGTACCTGGC 3'; antisense, 5' CTGGTGATTTCCCTTGACCGG 3'; *NGF*: sense, 5' ATGTCCATGTTGTTCTACACT 3'; antisense, 5' AAGTCCAGATCCTGAGTGTCT 3'). qPCR was performed in 384-well plates using 0.5- μ L cDNA in a 10- μ L reaction volume with LightCycler 480 SYBR Green I Master mix (Roche) on a LightCycler 480 System (Roche) as follows: 95°C for 5 min and 45 cycles of 95°C for 10 s, 60°C for 20 s, and 72°C for 15 s, followed by a melting curve program. The forward and reverse primers were designed following the PrimerBank database and RTPrimerDB [40].

2.12. Preclinical Studies. Thoracic spinal cord contusion injuries were performed on adult male Sprague-Dawley rats. Rats were housed in groups of 4-5 under a 12-h light/12-h dark cycle at 22°C, fed *ad libitum*, and maintained in a facility accredited by the Association for the Assessment and Accreditation of Laboratory Animal Care International. This study was performed under a protocol approved by the Institutional Animal Care and Use Committee, Yonsei University College of Medicine, Seoul, Korea. Spinal cord contusion was performed under Ketamine (80~90 mg/kg), Rompun (0.2 mL/kg), and Promazine (0.8~1 mg/kg) anesthesia and prophylactic administration of cefazolin (50 mg/kg). A dorsal laminectomy was performed on the T9 to expose the spinal cord. Contusion injury was induced using the Infinite Horizon Impactor (Precision Systems, Kentucky, IL, USA) with a force of 230 Kdyn. After contusion, the deep and superficial muscle layers were sutured. Animals received manual bladder expression twice daily and were inspected for weight loss, dehydration, and distress with appropriate veterinary care as needed.

Both cell- and vehicle-injected groups received intraperitoneal injections of 10 mg/kg/d cyclosporine a day before injection and then daily for the duration of the study. Cell- or vehicle-injection occurred 7 days after the induction of SCI. Animals were anesthetized as above and the laminectomy site was reexposed. Totally, 12 μ L of hNSPCs (8×10^4 cells/ μ L) suspended in H-H buffer was slowly injected along the midline of the spinal cord at a depth of 1.2 mm into one segment cranial and one segment caudal to the lesion epicenter using a 26-gauge needle. Control animals received an equal volume of H-H buffer at the same injection rate.

Animals were sacrificed, perfusion fixed, and their spinal cord removed on 12 weeks after transplantation. Fixation was accomplished using 4% paraformaldehyde (PFA; Sigma) in 0.1 M PIPES buffer, pH 6.9, within 24 hours after fixation followed by immersion and sinking in 30% sucrose in PBS. Spinal cords were cut into 16 μ m coronal section. The sections were blocked with 3% BSA and 10% normal horse serum with 0.2% Triton X-100 and incubated with primary antibodies to

mouse α -human nuclei (1:100; Chemicon), mouse α -nestin, rabbit α -GFAP, rabbit α - β -tubulin III, rabbit α -olig2 (1:500; Millipore, Billerica, MA, USA), and rabbit α -APCC1 (1:50; Abcam, Cambridge, MA, USA). Following the rinsing in PBS, the cultures were incubated with species-specific secondary antibodies conjugated with fluorescein (1:180; Vector) or Texas Red (1:180; Vector) secondary antibodies.

For the evaluation of hind limb motor function, Basso-Beattie-Bresnahan (BBB) locomotor rate scaling was performed prior to cell- or vehicle-injection and weekly following injection until sacrificed. For the evaluation of nociceptive ability of animals, the Von Frey test was performed. The behavioral responses were used to calculate the 50% paw withdrawal threshold by increasing and decreasing stimulus intensity between 0.4 and 26 g equivalents of force and estimated using a Dixon nonparametric test.

2.13. Statistical Analyses. Statistical analyses included the Mann-Whitney *U* test for nonparametric variables between the transplantation and control groups. Fisher's exact test was used to analyze nominal or ordinal variables. Absolute differences between baseline and end values were calculated for AMS, UEMS, LEMS, ASS-P, and ASS-L and analyzed using the Wilcoxon signed rank test for both transplantation and control groups. In the transplantation group, VAS scores were also measured prior to and at 2, 6, and 12 months after implantation to assess pain. These data were analyzed using a one-way repeated measure analysis of variance (ANOVA). All tests were considered significant at *p* values < 0.05. Statistical comparisons were made using the SPSS software (ver. 18.0; SPSS, Chicago, IL, USA).

3. Results

3.1. Patients. Nineteen patients were enrolled for hNSPC transplantation and followed over 1 year after implantation (16 men, 3 women). All had SCI between C3 and C8 of traumatic etiology. Seventeen patients were AIS-A and two were AIS-B before transplantation. The mean age of the patients was 37.2 (range: 18–57) years and hNSPC transplantation was performed from 16 to 213 days after SCI (mean: 63.4 days). In the control group, 15 patients were included and followed neurologically for 1 year after the initial evaluation of AIS neurological examination in the rehabilitation clinic of our hospital (12 men, 3 women). All had SCI between C3 and C7 of traumatic etiology. Thirteen patients were AIS-A and two were AIS-B. The mean age of the patients was 37.3 (range: 22–56) years, and the time between the injury onset and the initial evaluation of AIS neurological examination was 55.9 days on average (range: 7–168 days). The patients are listed according to AIS grade and baseline characteristics of the patients are summarized in Table 1. Age, gender, and duration from the injury onset to transplantation and to the initial evaluation of neurological examination, neurological level of injury, and AIS grade did not differ significantly between the transplantation and control groups (*p* > 0.05 for each).

3.2. Safety Issues. There was no mortality. No patient experienced infection, leakage of cerebrospinal fluid, serious

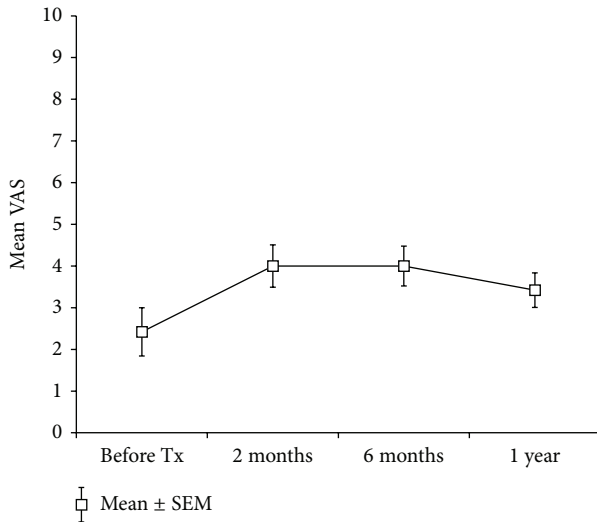


FIGURE 1: Visual analog scores (VAS).

life-threatening autonomic dysreflexia, or progressive spinal deformity following hNSPC implantation. There was no deterioration in sensory and motor function, urinary bladder complications, or neurological level postoperatively due to direct cell injection into the injured spinal cord. No patients showed worsening of respiratory function and all participants appeared to be coping well.

3.3. Pain. It has been suggested that pain is a frequent and major consequence of SCI. Estimates of study participants experiencing chronic, disabling pain that interfered with daily activity ranged from 39% to 84% [41, 42]. Furthermore, some studies have reported that cell transplantation strategies increased the risk of neuropathic pain postoperatively [14, 43]. To identify the potential risk of neuropathic pain under the current protocol, pain was assessed prior to and at 2, 6, and 12 months after transplantation with a 10-cm VAS, ranging from 0 to 10. The mean baseline VAS for the 19 patients was 2.4 ± 0.6 (mean \pm standard error of mean (SEM)), and, following implantation, the mean VAS changed to 4.0 ± 0.5 , 4.0 ± 0.5 , and 3.4 ± 0.4 at 2, 6, and 12 months, respectively (Figure 1). No statistically significant difference was found between the baseline and follow-up times ($F = 2.918$, $p = 0.066$), although hNSPC implantation tended to increase mean VAS values at 2- and 6-month follow-up times compared to those prior to cell injection. These results indicate that hNSPCs transplantation was not associated with a greater risk of developing neuropathic pain in patients with SCI, compared with the general population of SCI patients.

3.4. Spasticity. Spasticity, defined as increased muscle tone with hyperexcitability of flexor and extensor muscles, exaggerated reflexes, weakness, and joint contractures, is a common complication of SCI [25]. Spasticity was self-reported by 59% and 71% of study participants with SCI [42, 44]. The principal clinical outcome measure for spasticity has been the long-established Ashworth Scale or the modified Ashworth scale, although both scales have less-than-ideal

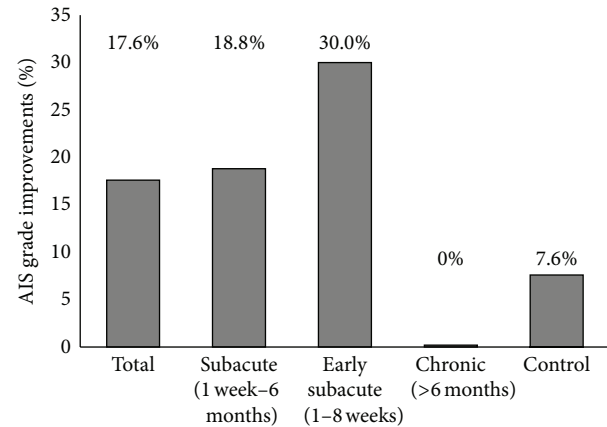


FIGURE 2: Percentage of individuals converting from sensorimotor complete (AIS-A) to incomplete cervical SCI (AIS-B or AIS-C) in the transplantation and control groups.

interrater reliability [39] and have a poor correlation with self-rated assessments of spasticity [45]. In this study, to recognize the potential risk of spasticity associated with hNSPC transplantation, spasticity was measured using the modified Ashworth scale in the upper and lower extremities of the 19 patients prior to and at 2, 6, and 12 months after transplantation (Tables 2 and 3). Collectively, only one patient (patient 14) appeared to have clinically significant spasticity in both upper and lower extremities, which affected the activities of daily living. However, he already showed a marked increase in muscle tone of the lower extremities prior to cell implantation and his spasticity was not well controlled with medications over 1 year. Other patients who developed spasticity or displayed an increase in muscle tone during follow-up times did not demonstrate serious spasticity. Their spasticity was relieved with medications and did not have significant effects on their activities of daily living. Thus, given the reported incidence of spasticity associated with the SCI condition, as described above, these results suggest that hNSPC transplantation is not associated with a greater risk of developing spasticity in patients with SCI, compared with the general population of SCI patients.

3.5. ASIA Assessments. The ASIA Impairment Scale has become a standardized and routinely adopted classification for most patients suspected of suffering a SCI [46]. Data obtained using AIS, AMS, and ASS are summarized in Tables 4–9. Figure 2 provides histograms of the estimated mean change in the percentage of patients converting from complete SCI to incomplete SCI. Overall, three (17.6%) of the 17 AIS-A patients improved their AIS grades at 1 year after transplantation: two patients (patients 7 and 15) improved to AIS-C and one (patient 8) improved to AIS-B. If AIS-A patients are classified according to the time window between the injury onset and hNSPC transplantation, 18.8% (3/16) of the patients in the subacute treatment group and 30.0% (3/10) of the patients in the early subacute treatment group showed AIS grade conversion. However, both AIS-B patients (patients 18 and 19) improved to AIS-D at 1 year

TABLE 2: Changes of spasticity in upper extremities of patients with cervical SCI using modified Ashworth scale.

Patient	Before transplantation		2 months ^a		6 months ^b		1 year ^c	
	Right	Left	Right	Left	Right	Left	Right	Left
1	0	0	1	1	1	1	1+	1+
2	0	0	0	0	1	1	0	0
3	0	0	0	0	0	0	0	0
4	0	0	0	0	0	0	1	0
5	1	1	0	0	1	1	1	1
6	0	0	1	1	1	0	1	1
7	0	0	0	0	0	0	0	0
8	0	0	0	0	1	1	0	0
9	0	0	1+	1+	1	1	1	1
10	0	0	1	1	2	2	1+	1+
11	0	0	0	0	0	0	0	0
12	0	0	0	0	1	1	1	1
13	0	0	0	0	0	0	0	0
14	0	0	0	0	1+	1+	2	2
15	0	0	0	0	0	0	0	0
16	0	0	1	1	1	1	1+	1+
17	0	0	0	0	1	1	2	1
18	0	0	0	0	0	0	0	0
19	0	0	0	0	0	0	0	0

^{a,b,c}2, 6, and 12 months after hNSPC transplantation.

TABLE 3: Changes of spasticity in lower extremities of patients with cervical SCI using modified Ashworth scale.

Patient	Before transplantation		2 months ^a		6 months ^b		1 year ^c	
	Right	Left	Right	Left	Right	Left	Right	Left
1	1+	1+	1+	1+	1+	1+	1+	1+
2	0	0	0	0	1	1	1	1
3	1	1	1	1	1	1	1	1
4	1	1	1	1	1+	1+	1+	1+
5	1	1	1	1	1	1	1	1
6	0	0	1	1	0	0	1	1
7	0	0	1	1	1	1	1	1
8	1	1	1	1	2	2	1	1
9	1	1	1+	1+	1+	1+	1	1
10	0	0	0	0	2	1+	2	1+
11	0	0	0	0	1	1	1	1
12	0	0	0	0	1	1	1	1
13	0	0	0	0	1	1	1	1
14	2	2	1+	1+	2	2	2	2
15	1+	1+	1	1	1+	1+	2	2
16	1	1	1	1	1	1	1	1
17	1	1	1	1	1	1	2	2
18	1	1	1+	1+	1+	1+	1+	1+
19	0	0	1+	1+	1+	1+	2	2

^{a,b,c}2, 6, and 12 months after hNSPCs transplantation.

TABLE 4: AIS grade conversion and motor level changes after cervical SCI.

Transplantation group					Control group				
Patient	Before AIS ^a	After AIS ^b	Prelevel (R/L) ^c	Postlevel (R/L) ^d	Patient	Initial AIS ^e	1 year AIS ^f	Initial level (R/L) ^g	1 year level (R/L) ^h
1	A	A	C4/— ⁱ	C4/C4	1	A	A	C7/C6	C7/C7
2	A	A	— ⁱ /— ⁱ	—/—	2	A	A	C4/C4	C4/C4
3	A	A	C7/C7	C8/C8	3	A	A	C6/C6	C7/C7
4	A	A	C5/C5	C6/C6	4	A	A	C6/C6	C6/C6
5	A	A	C5/C6	C6/C6	5	A	A	C6/C5	C6/C6
6	A	A	C4/C4	C4/C4	6	A	B	C6/C6	C6/C6
7	A	C	C5/C5	C7/C6	7	A	A	—/—	—/—
8	A	B	C5/C6	C6/C6	8	A	A	C4/C4	C5/C4
9	A	A	C5/C5	C5/C5	9	A	A	—/—	C4/C4
10	A	A	—/—	C5/—	10	A	A	C6/C6	C6/C6
11	A	A	C6/C7	C7/C8	11	A	A	C7/C7	C7/C7
12	A	A	C4/—	C5/—	12	A	A	—/—	—/—
13	A	A	C5/C5	C7/C7	13	A	A	C4/C4	C5/C5
14	A	A	C5/C5	C6/C6	14	B	B	C5/C6	C6/C7
15	A	C	C5/C5	C6/C5	15	B	B	C7/C7	C8/C8
16	A	A	—/C4	C5/C5					
17	A	A	C5/C4	C6/C6					
18	B	D	C5/C5	C8/C8					
19	B	D	C8/C8	T1/T1					

^a AIS grade before transplantation, ^b AIS grade 1 year after transplantation, ^c motor level before transplantation (R/L: right side/left side), ^d motor level 1 year after transplantation, ^e AIS grade at the initial evaluation of AIS examination in the hospital after SCI, ^f AIS grade 1 year after initial assessment, ^g motor level at the initial evaluation, ^h motor level 1 year after initial evaluation, and ⁱ—motor levels C1 to C3. There was no zone of partial preservation below the neurological level of injury in complete SCI patients in both groups at baseline.

TABLE 5: Summary of AMS and ASS changes in patients with complete cervical SCI.

	Transplantation group			Initial score ^d	Control group		<i>P</i> ^j
	Prescore ^{a,g}	Postscore ^{b,h}	After-before ^c		1 year score ^e	Initial 1 year ^{f,i}	
AMS	9.5 ± 2.1 ^k	17.4 ± 2.7	7.9 ± 1.2	15.5 ± 2.1	19.5 ± 2.1	3.9 ± 0.6	0.013
UEMS	9.5 ± 2.1	17.2 ± 2.7	7.8 ± 1.1	15.5 ± 2.1	19.5 ± 2.1	3.9 ± 0.6	0.014
LEMS	0.0 ± 0.0	0.1 ± 0.1	0.1 ± 0.1	0.0 ± 0.0	0.0 ± 0.0	0.0 ± 0.0	0.391
ASS-P	14.1 ± 1.1	18.9 ± 1.6	4.8 ± 1.3	19.4 ± 2.8	22.3 ± 2.9	2.9 ± 0.6	0.551
ASS-L	14.7 ± 1.2	21.6 ± 3.7	6.9 ± 3.1	19.5 ± 2.8	21.8 ± 2.9	2.3 ± 0.5	0.309

^a AMS/ASS before transplantation, ^b AMS/ASS 1 year after transplantation, ^c AMS/ASS changes over 1-year follow-up period, ^d AMS/ASS at the initial evaluation in the hospital after SCI, ^e AMS/ASS 1 year after initial evaluation, ^f AMS/ASS changes over 1-year follow-up period, ^g $p > 0.05$, between pre-AMS/ASS in the transplantation group and initial AMS/ASS in the control group, ^h $p < 0.01$, between before AMS/ASS and after AMS/ASS in the transplantation group, ⁱ $p < 0.01$, between initial AMS/ASS and 1-year after AMS/ASS in the control group, ^j p -values, between AMS/ASS changes in both transplantation and control groups, and ^k mean ± SEM.

after transplantation. In contrast, in the control group, only one of the 13 AIS-A patients (patient 6) showed AIS grade conversion (AIS-B) at 1 year (Table 4).

The changes in data obtained using ASIA scores between the baseline and the 1-year follow-up in the transplantation and control groups are summarized in Tables 6–9 and Figure 3. In AIS-A patients, there was no statistically significant difference in any neurological measure (AMS, UEMS, LEMS, ASS-P, or ASS-L) at baseline between the groups ($p > 0.05$; Table 5). AMS, UEMS, ASS-P, and ASS-L, but not LEMS, increased significantly from baseline to 1 year in AIS-A patients in both groups ($p < 0.01$; Table 5). These results suggest that neurologic examinations showed a minor, but

significant, increase in both motor and sensory scores over time in complete SCI patients in both groups. However, the mean change of UEMS over 1 year in the transplantation group was significantly greater than that in the control group (7.8 ± 1.1 versus 3.9 ± 0.6 ; $p < 0.01$) while the mean changes in ASS-P and ASS-L over 1 year were not significantly different in either group (Table 5). No strong correlation between AIS grade conversion and the change in AMS and ASS over 1 year was evident in AIS-A patients in the transplantation group. However, patients 7 and 8, who converted to AIS-C and AIS-B, respectively, showed an increase of 2 points in LEMS and 54 points in ASS-L at 1 year after transplantation, respectively (Tables 7 and 9). In incomplete SCI, two patients in the

TABLE 6: AMS upper extremity motor score (UEMS).

Patient	Transplantation group					Patient	Control group		
	Before ^a	2 months ^b	6 months ^c	1 year ^d	UEMS changes ^e		Initial ^f	1 year ^g	UEMS changes ^h
1	0	0	0	6	6	1	25	27	2
2	0	3	5	8	8	2	14	15	1
3	29	37	38	38	9	3	21	26	5
4	12	23	23	24	12	4	21	26	5
5	13	15	18	18	5	5	17	21	4
6	2	2	3	3	1	6	20	23	3
7	15	18	22	27	12	7	5	13	8
8	18	18	20	24	6	8	11	14	3
9	6	6	6	6	0	9	9	11	2
10	0	2	4	5	5	10	23	24	1
11	26	33	36	36	10	11	26	33	7
12	1	1	1	7	6	12	2	7	5
13	10	20	26	32	22	13	8	13	5
14	9	17	18	18	9	14	14	25	11
15	9	19	16	15	6	15	30	38	8
16	3	6	6	10	7				
17	8	10	12	16	8				
18	28	42	44	44	16				
19	44	50	50	50	6				

^aUEMS before transplantation, ^{b,c,d}UEMS 2, 6, and 12 months after transplantation, ^eUEMS change over 1-year follow-up period, ^fUEMS at the initial evaluation in the hospital after SCI, ^gUEMS 1 year postinitial evaluation, and ^hUEMS change over 1-year follow-up period.

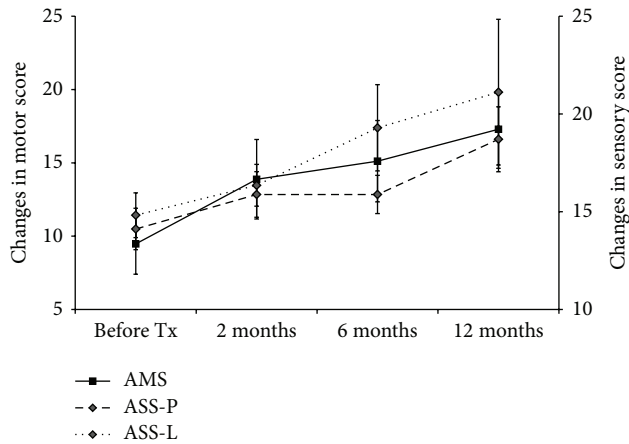


FIGURE 3: Changes in motor and sensory score over time in patients with complete cervical SCI following hNSPC transplantation. The cervical cohort of patients was followed for 1 year. The mean (mean \pm SEM) change in AMS, ASS-P, and ASS-L is shown at each time point (before transplantation (before Tx) and 2, 6, and 12 months after transplantation).

transplantation group showed greater increase in LEMS and ASS-P at 1 year, compared with those in the control group (Tables 6–9).

3.6. Motor Level Recovery. Of AIS-A SCI subjects with initial motor levels C4 to C7 in both transplantation and control groups, no patient deteriorated by one or more motor levels

over 1 year (Table 4). The proportion of individuals with initial C4–C7 or C5–C7 SCI having a stable or recovering motor level on the right and left side in both groups at 1 year after the baseline assessment is shown in Figure 4. For subjects with initial C5–C7 SCI in the transplantation group, motor level remained the same in 9.1% and 36.3% (right and left side, resp.) and improved by one level in 72.7% and 45.5% and by two levels in 18.2% and 18.2%. AIS grade conversion appeared not to influence motor level changes. However, in the control group, motor level remained the same in 85.7% and 50.0% (right and left side, resp.) and improved by one level in 14.3% and 50.0%, and no patient recovered two levels (Figure 4(b)). The proportion of individuals with initial C4–C7 motor level SCI having a stable or recovering motor level in both groups at 1 year was similar to that of patients with initial C5–C7 motor levels (Figure 4(a)). Thus, a greater proportion of AIS-A patients in the transplantation group recovered one or more motor levels, compared with the control group, at 1 year. There was no zone of partial preservation below the neurological level of injury in complete SCI patients in both groups at baseline.

3.7. Electrophysiological Assessments. Complementary to the neurological assessment, electrophysiological measurements provide objective tools for SCI assessment. They provide informative, quantitative data on changes that occur in neural circuitry [47, 48]. A series of SSEP and MEP studies of the upper and lower limbs was conducted for patients in the transplantation group, and detailed data of the latencies and amplitudes of SSEPs and MEPs from patients who showed

TABLE 7: AMS lower extremity motor score (LEMS).

Patient	Transplantation group					Patient	Control group		
	Before	2 months	6 months	1 year	LEMS changes		Initial	1 year	LEMS changes
1	0	0	0	0	0	1	0	0	0
2	0	0	0	0	0	2	0	0	0
3	0	0	0	0	0	3	0	0	0
4	0	0	0	0	0	4	0	0	0
5	0	0	0	0	0	5	0	0	0
6	0	0	0	0	0	6	0	0	0
7	0	0	0	2	2	7	0	0	0
8	0	0	0	0	0	8	0	0	0
9	0	0	0	0	0	9	0	0	0
10	0	0	0	0	0	10	0	0	0
11	0	0	0	0	0	11	0	0	0
12	0	0	0	0	0	12	0	0	0
13	0	0	0	0	0	13	0	0	0
14	0	0	0	0	0	14	0	0	0
15	0	0	0	0	0	15	0	0	0
16	0	0	0	0	0				
17	0	0	0	0	0				
18	0	21	32	32	32				
19	0	17	22	22	22				

TABLE 8: ASS-pin prick (ASS-P).

Patient	Transplantation group					Patient	Control group		
	Before	2 months	6 months	1 year	ASS-P changes		Initial	1 year	ASS-P changes
1	12	12	12	12	0	1	32	33	1
2	11	11	11	11	0	2	13	14	1
3	25	25	25	25	0	3	29	33	4
4	13	13	13	14	1	4	33	35	2
5	16	18	18	18	2	5	16	16	0
6	12	14	14	14	2	6	28	33	5
7	13	17	17	22	9	7	8	10	2
8	19	19	20	24	5	8	11	18	7
9	9	12	12	12	3	9	9	16	7
10	8	9	9	14	6	10	28	30	2
11	22	22	24	24	2	11	30	34	4
12	10	10	12	12	2	12	8	9	1
13	16	16	18	18	2	13	7	9	2
14	16	18	24	37	21	14	45	56	11
15	12	26	18	22	10	15	56	60	4
16	12	12	14	16	4				
17	14	16	18	26	12				
18	31	40	46	46	15				
19	38	38	43	70	32				

responses in electrophysiological parameters over 1 year after implantation are summarized in Tables 10 and 11. Following hNSPC transplantation, no patients showed negative changes in neurophysiological measures during follow-up (data not shown). This postoperative longitudinal assessment demonstrates the safety of intraspinal hNSPC injections, even

though a relatively large number of cells were injected three times, into the core, rostral and caudal to the lesion.

In the SSEP study of upper limbs, the median and ulnar nerves were stimulated. Of the 17 AIS-A patients, 6 (35.3%) showed positive response at 1 year, while there was no response before transplantation (patients 1, 2, 4,

TABLE 9: ASS-light touch (ASS-L).

Patient	Transplantation group					Control group			
	Before	2 months	6 months	1 year	ASS-L changes	Patient	Initial	1 year	ASS-L changes
1	10	12	12	12	2	1	32	33	1
2	11	12	13	13	2	2	13	13	0
3	25	26	26	26	1	3	28	32	4
4	13	19	19	19	6	4	33	37	4
5	17	17	18	18	1	5	16	16	0
6	12	14	14	14	2	6	30	31	1
7	13	17	18	19	6	7	8	12	4
8	22	22	48	76	54	8	11	14	3
9	12	12	12	12	0	9	10	14	4
10	8	10	14	15	7	10	30	32	2
11	21	23	24	26	5	11	28	32	4
12	11	12	12	12	1	12	8	8	0
13	19	19	19	19	0	13	6	9	3
14	19	19	29	40	21	14	46	54	8
15	10	15	16	16	6	15	54	61	7
16	11	12	15	15	4				
17	16	16	16	16	0				
18	68	68	70	70	2				
19	65	90	92	93	28				

TABLE 10: Latency measured by evoked potentials of the upper and lower limbs in patients with cervical SCI who showed response of SSEP over 1 year after hNSPC transplantation.

Patient	Before		2 months		6 months		1 year	
	Right ^a	Left ^b	Right	Left	Right	Left	Right	Left
Median nerve								
1	0.00 ^c	0.00	0.00	0.00	0.00	0.00	19.00	17.95
2	0.00	0.00	0.00	0.00	33.15	22.95	25.15	31.50
10	0.00	0.00	17.80	18.75	19.40	16.00	17.71	20.95
15 ^d	0.00	0.00	19.00	18.65	0.00	0.00	0.00	0.00
Ulnar nerve								
1	0.00	0.00	0.00	0.00	0.00	0.00	23.40	28.95
2	0.00	0.00	0.00	0.00	26.40	0.00	24.85	0.00
4	0.00	0.00	0.00	0.00	37.30	35.30	22.20	23.95
6	0.00	0.00	16.10	0.00	18.05	0.00	18.50	0.00
7	0.00	0.00	0.00	0.00	0.00	0.00	19.35	20.65
10	0.00	0.00	20.10	25.50	18.85	19.35	17.05	20.25
5 ^d	0.00	0.00	0.00	0.00	20.90	21.60	0.00	0.00
8 ^d	0.00	0.00	27.95	27.95	0.00	0.00	0.00	0.00
15 ^d	0.00	0.00	19.45	18.15	0.00	0.00	0.00	0.00
Tibial nerve								
7	0.00	0.00	0.00	0.00	0.00	0.00	61.90	43.10
15 ^d	0.00	0.00	42.70	44.70	0.00	0.00	0.00	0.00
Peroneal nerve								
7	0.00	0.00	0.00	0.00	0.00	0.00	44.80	44.60
15 ^d	0.00	0.00	39.10	48.00	0.00	0.00	0.00	0.00
Pudendal nerve ^e								
7		0.00		0.00		0.00		61.80
19		0.00		0.00		44.40		48.00

^aRight side, ^bleft side, ^cms, and ^dpatients showed recovery of SSEPs at 2- or 6-month follow-up times. However, the cortical response to peripheral stimulation disappeared at 1 year after transplantation. ^eThere is no division into right and left side in pudendal nerve stimulation.

TABLE 11: Latency and amplitude measured by evoked potentials of the upper limbs in patients with cervical SCI who showed response of MEP over 1 year after hNSPC transplantation.

Patient	Before		2 months		6 months		1 year	
	Right ^a	Left ^b	Right	Left	Right	Left	Right	Left
Biceps brachii muscle (latency)								
6	0.00 ^c	0.00	0.00	0.00	14.49	14.31	15.99	17.37
9	0.00	0.00	13.01	13.27	14.57	14.40	14.50	14.60
10	0.00	0.00	0.00	0.00	12.39	0.00	12.16	0.00
Biceps brachii muscle (amplitude)								
1	0.00 ^d	0.00	0.00	0.00	0.79	0.87	0.69	0.61
2	0.00	0.00	0.00	0.00	0.22	0.00	0.62	0.00
6	0.00	0.00	0.00	0.00	0.75	1.25	0.88	0.53
9	0.00	0.00	0.36	0.20	0.65	0.40	0.84	0.54
10	0.00	0.00	0.00	0.00	1.37	0.00	1.66	0.00
12	0.00	0.00	0.00	0.00	0.00	0.00	0.51	0.42
14	0.55	0.00	0.62	0.38	2.14	1.39	1.07	0.66
16	0.00	0.00	0.85	0.76	0.91	2.49	1.57	1.00
17	0.00	0.00	0.82	0.84	0.93	1.24	1.21	1.58
Abductor pollicis brevis muscle (latency)								
3	0.00	0.00	24.85	0.00	25.95	0.00	28.59	0.00
11 ^e	0.00	0.00	0.00	0.00	0.00	30.06	0.00	0.00
Abductor pollicis brevis muscle (amplitude)								
3	0.00	0.00	0.39	0.00	0.07	0.00	0.18	0.00
11 ^e	0.00	0.00	0.00	1.06	0.00	0.00	0.00	0.00

^aRight side, ^bleft side, ^cms, ^dmicrovolts, and ^ethe patient showed recovery of MEPs at 2- or 6-month follow-up times. However, the peripheral response to transcranial stimulation disappeared at 1 year after transplantation.

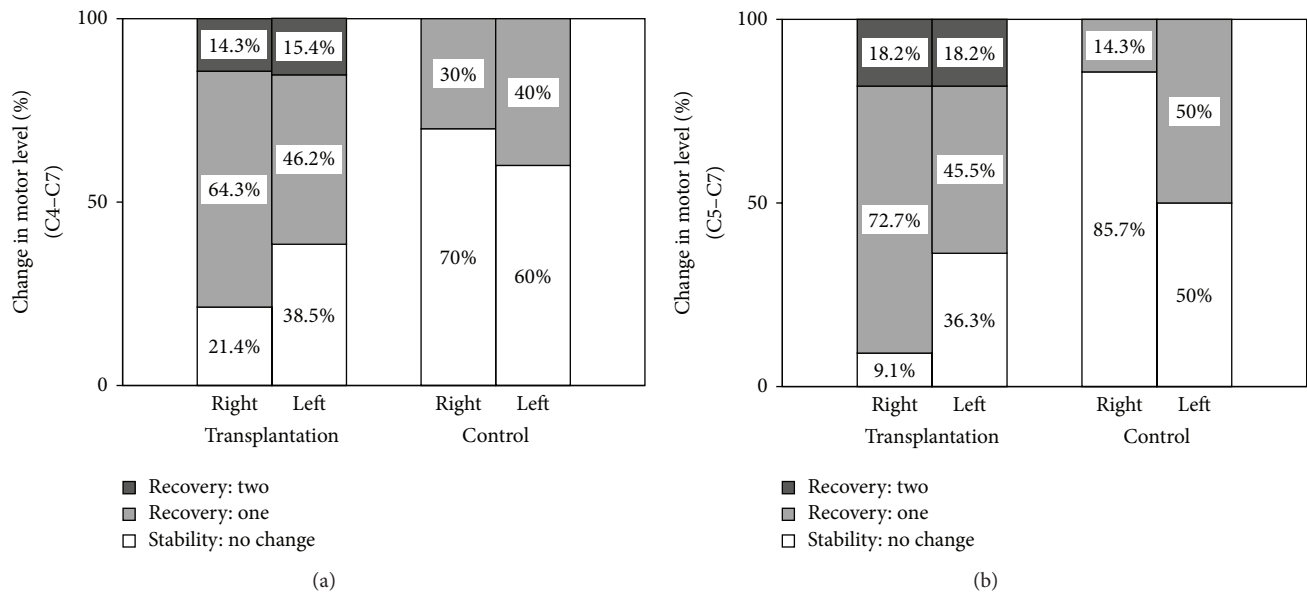


FIGURE 4: Proportion of AIS-A SCI individuals with initial C4-C7 (a) or C5-C7 (b) motor level remaining stable or gaining motor levels from the baseline to 1-year follow-up in the transplantation and control groups. The cervical motor level is indicated separately in the right and left sides of the cord. The percentage of individuals in each category of motor level change or stability at 1 year after the baseline assessment in both groups is displayed in each bar graph.

6, 7, and 10; Table 10). Three patients (patients 5, 8, and 15) showed transient responses in SSEPs during follow-up; however, the cortical response disappeared at 1 year. In the SSEP study of lower limbs, the tibial, peroneal, and pudendal nerves were stimulated. Only one patient (patient 7) who converted to AIS-C showed positive responses in the SSEPs of the tibial and peroneal nerves at 1 year. Another patient (patient 15) who also converted to AIS-C exhibited no response at 1 year although a transient response at 2 months could be observed (Table 10). Thus, in a patient (patient 7) with complete SCI, hNSPC transplantation may repair the injured ascending spinal tract from the upper and lower limbs, which was supported by the SSEP findings, objectively validating conductivity repair in SCI [26]. However, no strong correlation between ASIA motor and sensory scores and SSEP measurements was evident in the transplanted patients. Of the two AIS-B patients, one (patient 19) showed a positive response in the SSEP study of the pudendal nerve at 1 year (Table 10).

Motor evoked responses were measured over the biceps brachii and abductor pollicis brevis muscles for the upper limbs and the tibialis anterior muscle for the lower limbs. Of the 17 AIS-A patients, 10 (58.8%) showed positive response in the MEPs of upper limbs at 1 year, while there was no response before transplantation (patients 1–3, 6, 9, 10, 12, 14, 16, and 17; Table II). One patient (patient 11) showed a transient response in MEPs in the abductor pollicis brevis muscle during follow-up; however, the response disappeared at 1 year. Unlike the SSEP studies, three patients with AIS grade conversions did not show a positive response in MEPs following transplantation. No strong correlation between ASIA motor and sensory scores and MEP measurements was evident in the transplanted patients. Additionally, in AIS-B patients, the MEP study did not show a positive response at 1 year.

3.8. Spinal MRI Findings. Changes in the MRI findings of patients in the transplantation group are given in Table 12 and Figure 5. Nine of the 19 patients (47.4%) showed progressive posttraumatic myelomalacic change in the spinal cord at the site of cell transplantation; however, three (15.8%) showed a decrease in the diameter of the spinal cord and seven (36.8%) demonstrated no change. The lesion length of SCI was decreased in all patients at 1 year. Other findings, including spinal cord atrophy (3 patients), myelomalacia (17 patients), and cystic degeneration (4 patients), were observed during follow-up. However, no significant change, such as tumor formation or syringomyelia, was found on any of the MRI sequences, at the implantation site, or at any other point in the neuraxis. Additionally, qualitative MRI imaging patterns, the extent of the cord compression, and lesion length in acute SCI appeared not to correlate with neurological or electrophysiological improvements at 1 year after transplantation.

4. Discussion

Attempts to induce recovery after SCI by transplanting cells or tissues have been a major focus of much research

over the last several decades. Many studies have evaluated the effects of transplanting a wide variety of cell types in SCI animal models and, remarkably, many studies have indicated improved functional outcomes [5]. However, there are difficulties in directly comparing studies because of the varying degree of characterization of the transplanted cells, different injury models, implantation at different time points after SCI, and different evaluation methods. Recent studies have reported that implanted human fetal brain-derived NSPCs can become integrated into injured mice spinal cord and induce locomotor recovery [20, 22, 49]. They have shown that engrafted cells differentiate predominantly into oligodendrocytes and that survival of donor-derived cells is required to sustain locomotor recovery, suggesting that oligodendrocyte integration with the host is likely to be a key mechanism in recovery. This differentiation pattern of donor-derived cells is in contrast to many studies that have demonstrated predominant astroglial fate or differentiation failure following acute or subacute NSPCs transplantation [49].

In our preclinical study, we induced contusive thoracic spinal cord injury (T9) in adult Sprague-Dawley rats using the Infinite Horizon Impactor [50] and transplanted hNSPCs used in this study into the epicenter of the injured cord at 7 days following the induction of SCI. Grafted cells exhibited robust engraftment, extensive migration, integration with host cells, and differentiation into neurons and glial cells at 12 weeks after transplant (Figure 6). Additionally, hNSPC-implanted animals showed improved locomotor recovery and no detectable mechanical allodynia (data not shown). On average, 21.3% of donor-derived cells differentiated into neurons, 3.5% into astrocytes, and 1.5% into mature oligodendrocytes. However, more than 80% of engrafted cells expressed the immature cell marker nestin, suggesting that they may still remain as undifferentiated neural precursors. The sum of all quantification markers was more than 100%, suggesting that there is an overlap between some cell markers. Nestin, in particular, has been found to colocalize with β -tubulin III, GFAP, and the oligodendroglial progenitor cell marker Olig2 [51]. These findings indicate that in our preclinical study the predominant differentiation of hNSPCs into oligodendroglia and the induction of remyelination may not be a major mechanism of locomotor recovery. Several studies from other labs have also observed limited oligodendroglial differentiation *in vivo* after transplantation [51–53]. Thus, further studies to examine the mechanisms underlying the cell fate determination of transplanted hNSPCs in the injured spinal cord are necessary. In fact, there are many other variables that may be involved in neuronal or glial differentiation of transplanted hNSPCs after SCI, including the source of the human cells, culturing techniques, and cell preparation, as well as potential differences between injury models.

A comprehensive knowledge of how transplanted hNSPCs exert their therapeutic effects in SCI is still lacking and alternative pathways of hNSPCs-mediated repair should also be considered. Neuronal differentiation of implanted NSPCs could promote restoration of disrupted circuitry by formation of bridges or bypass connections [54] or may

TABLE 12: Changes in spinal MRI findings in patients with cervical SCI before and 1 year after hNSPC transplantation.

Patient	Before transplantation			1 year after transplantation		
	Types ^a	Location	Lesion length	Types ^b	Location	Lesion length
1	I	C2.3–C7.1	81.2 mm	B, C	C4.1–C5.2	29.3 mm
2	I	C2.3–C4.2	33.5 mm	A, B	C3.2–C4.1	12.3 mm
3	III	C5.1–C7.1	30.5 mm	B	C6.2–C6.3	10.3 mm
4	IV	C3.1–C7.2	70.3 mm	B	C5.2–C7.2	32.9 mm
5	IV	C2.1–C7.2	99.6 mm	B	C5.1–C6.3	37.5 mm
6	N/A ^c	C3.3–C5.3	34.6 mm	B	C3.3–C5.2	33.8 mm
7	II	C3.3–C7.1	62.2 mm	B	C5.1–C6.1	24.2 mm
8	IV	C2.1–C7.3	57.1 mm	B	C5.1–C6.1	25.4 mm
9	N/A ^c	C3.3–C4.1	13.8 mm	B	C3.3–C4.1	12.6 mm
10	III	C2.3–C5.3	59.9 mm	C	C3.2–C4.1	13.5 mm
11	IV	C4.3–T1.3	76.7 mm	B, C	C6.1–T1.2	42.9 mm
12	I	C2.1–C5.3	70.0 mm	B	C2.3–C4.3	43.0 mm
13	IV	C3.1–T2.1	101.6 mm	B	C5.2–C6.2	19.3 mm
14	III	C4.2–T1.1	58.4 mm	B	C5.2–C7.1	36.0 mm
15	IV	C2.3–C7.1	89.8 mm	A, B	C3.2–C6.2	59.4 mm
16	I	C2.3–C6.2	67.6 mm	A, B	C4.1–C6.1	41.8 mm
17	III	C4.2–T1.1	84.0 mm	B	C5.1–C6.3	33.7 mm
18	III	C5.2–T1.1	42.3 mm	C	C7.1–C7.2	9.0 mm
19	III	C6.1–T1.2	40.7 mm	B	C7.2	6.9 mm

^aTypes of acute SCI pattern: Type I: hemorrhage, Type II: edema, Type III: mixed or contusion, and Type IV: compression. ^bTypes of subacute and chronic SCI pattern: type A: atrophy, type B: myelomalacia, type C: cyst, and type D: syrinx. ^cSpine MRI studies were not available in the acute phase of SCI; however, MRI scan showed myelomalacia before hNSPC transplantation.

provide trophic support, enhancing neuroprotection and regeneration [23]. In a preclinical study, we could also observe that hNSPCs expressed a variety of neurotrophic factors in culture, including BDNF, GDNF, NTF3, NTF4, NGF, VEGF, and FGF2 (Figure 7), and engrafted hNSPCs induced host axonal regrowth in injured spinal cord of rats following transplantation (Figure 6). Thus, neurotrophic factors secreted by implanted hNSPCs may promote host axonal growth along the engrafted cells and contribute to improved locomotor recovery. In addition, recent evidence suggests that transplanted NSPCs can have a variety of effects on the host microenvironment [5]. It is increasingly clear that NSPCs, especially undifferentiated cells, release anti-inflammatory or immune-regulatory molecules at the site of tissue damage, and, in turn, promote functional recovery from CNS injuries [55, 56]. We also observed that a vast majority of hNSPCs remained undifferentiated in injured spinal cord of rats following transplantation which might therefore promote recovery from SCI via a multifaceted response including axonal regeneration, white matter sparing, decrease of glial scar formation or neuronal apoptotic death, or reduction of inflammation.

4.1. Safety and Tolerability. In this study, the safety and feasibility of hNSPC transplantation were supported. There was no adverse finding over 1 year after allogeneic hNSPC implantation into patients with cervical SCI. The neurosurgical procedure did not result in any deteriorating sequelae; any ascending damage to one or two spinal cord segments

above an injury would be of great clinical significance in cervical injuries. No patient showed serious life-threatening autonomic dysreflexia, worsening of respiratory function, or deterioration in neurological level, sensory or motor function, and urinary bladder complications. Patients also tolerated short-term cyclosporine therapy for immunosuppression. hNSPCs, grown as neurospheres in long-term cultures, did not acquire chromosomal aberrations, maintained their multipotency in neural cell differentiation, and did not introduce pathogens into the cultures. Their transplantation was not obviously associated with any fever, inflammation, immunological rejection, or graft-versus-host reaction. The presence of either undifferentiated NSPCs or inappropriate inflammation may trigger aberrant changes in CNS networks that could lead to neurological dysfunction, such as hyperreflexia, spasticity, dystonia, pain, or allodynia [14, 43]. In this study, hNSPC transplantation tended to increase mean VAS values at 2- and 6-month follow-up times compared to those prior to cell injection, although there was no significant difference between the baseline and follow-up times over 1 year. Additionally, only one patient complained of clinically significant spasticity in both upper and lower extremities; however, he already showed a marked increase in muscle tone of the lower extremities prior to cell implantation. Thus, hNSPC transplantation appeared not to be associated with a greater risk of developing any significant neuropathic pain and spasticity in patients with cervical SCI. Their pain or spasticity was well relieved with medications.

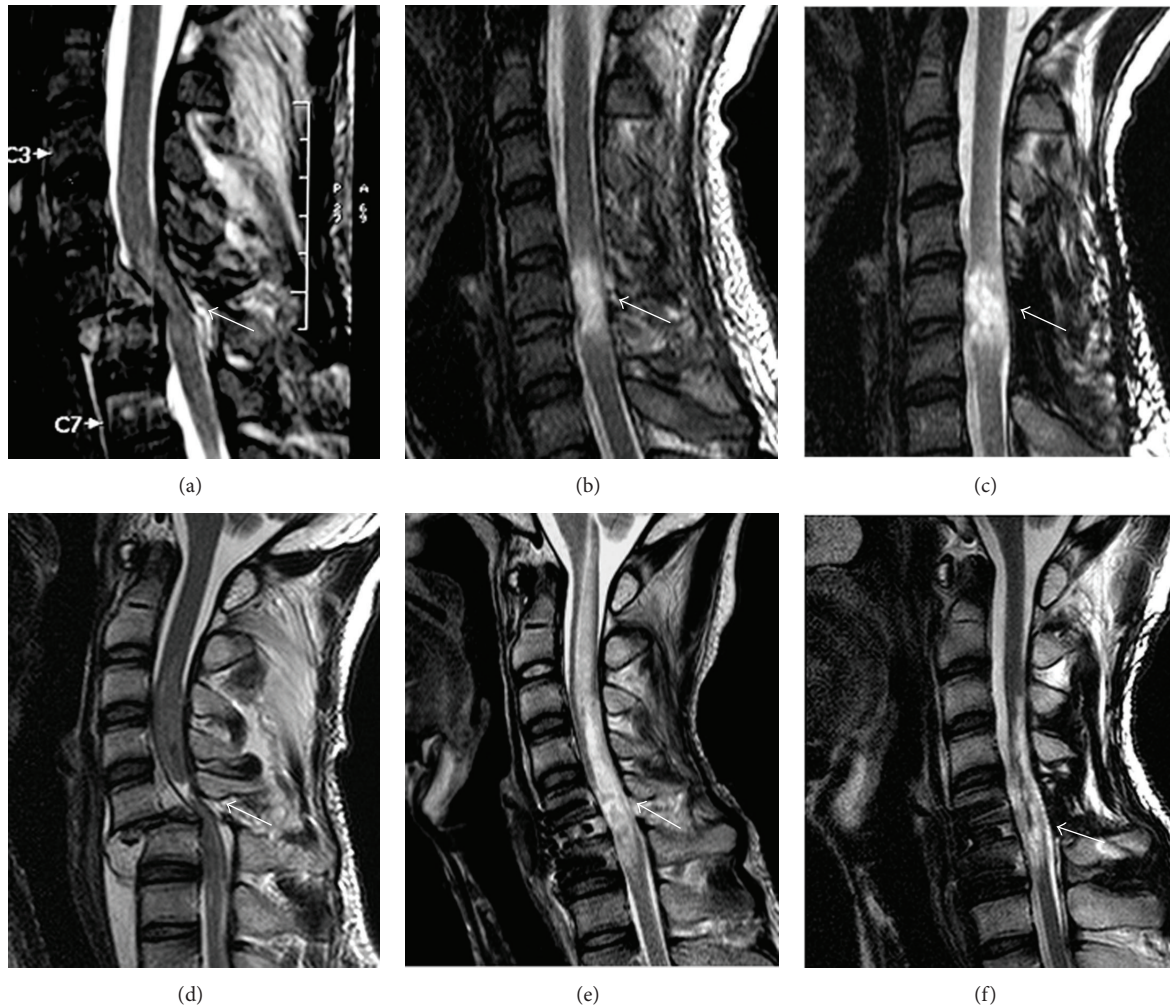


FIGURE 5: Sagittal T2W MRI scan of two SCI patients (upper panel: patient 8; lower panel: patient 15) at the time of injury (a, d), before transplantation as a baseline (b, e), and 1 year after transplantation (c, f). Follow-up findings showed progressive myelomalacic change at the site of cell transplantation (c) or myelomalacia and atrophy of the cord (f) in cell implantation areas. The white arrows mark the site of injury.

Spine MRIs showed no evidence of any tumor formation, development of posttraumatic syringomyelia, or other adverse radiological findings. However, although this procedure appears safe at 1 year, further follow-up MRIs are necessary to assess the possibility of the development of other abnormalities. MRI has been useful in determining the extent of extrinsic cord compression, outlining qualitative findings, such as cord hemorrhage, edema, soft tissue injury, and hematoma, and in assessing any progressive changes during the course of the trial after SCI. These qualitative MRI imaging parameters have been proposed to correlate with the degree of neurological injury, recovery, and eventual outcome in patients with SCI. However, MRI is still largely a qualitative measure, and quantitative standards, in relation to SCI outcomes, will need to be developed and validated before MRI can be used as an outcome tool [25]. In this study, MRI images were taken with instruments with 1.5 or 3 T field-strength. Higher resolution MRI with a field-strength of 3 T provided better resolution; however, it could not detect transplanted cells. Additionally, we could not

find any correlation between qualitative or quantitative MRI findings in acute SCI and neurological outcome at 1 year after transplantation (Table 12). Thus, it is hoped that MRI technologies will develop rapidly such that imaging will become a useful tool for following recovery or predicting outcome of an intervention after SCI.

4.2. Neurological Improvements. Spontaneous recovery of neurological function in patients with complete SCI is fairly limited. Prior studies reported spontaneous conversion rates of complete (AIS-A) to incomplete (AIS-B, AIS-C, and AIS-D) status ranging from 4% to 13% [57–61]. The baseline examinations in two of these studies were performed later than 1 week after injury, which would be expected to lower the conversion rate [60, 61]. The recent International Campaign for Cures of Spinal Cord Injury Paralysis (ICCP) systematic review of multiple existing SCI databases reported that about 20% of AIS-A patients on initial acute examination (<1 week after injury) converted to incomplete status during the first postinjury year. However, many patients with SCI show

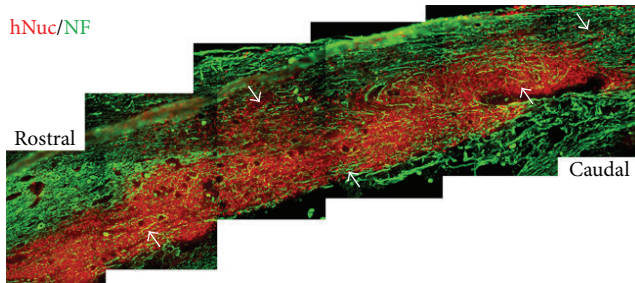


FIGURE 6: Direct transplantation of hNSPCs into the injured thoracic spinal cord (T9) of adult Sprague-Dawley rats with contusive SCI showed robust long-term engraftment and extensive migration of donor-derived cells and induced host axonal growth along engrafted cells. At 12 weeks after transplantation, immunohistochemistry was conducted in the sectioned spinal cord tissues using anti-human nuclei marker (hNuc) and anti-NF and visualized with fluorescein or Texas red-labeled secondary antibodies. Many hNuc-positive cells (colored red) survived and migrated extensively to rostral and caudal parts of the injury site, including the spared tissue surrounding the lesion. Multiple neuronal processes expressing NF (colored green) extended over the engrafted human cells, as indicated by arrows. Scale bar: 200 μ m.

some neurological recovery after the first few days and the AIS grade conversions occurred mostly within the first 2-3 months after injury [62]. It should be noted that a number of variables may also influence the rate of neurological recovery in SCI. These include medical or surgical treatment variables for acute SCI, effect of specialized rehabilitation centers on care for SCI, timing and quality of initial examination of neurological status, formal training and reliability testing of neurologic examiners, and factors affecting the reliability of examinations. For this reason, review of these data should be undertaken with a full understanding of the specific clinical or research context. Additionally, spinal damage in spinal contusions involves not only tract fibers, but also closely packed motor neurons and roots, usually over 2-3 segments that supply arm or leg muscles. Thus, a large part of the motor deficit has to be attributed to the peripheral nervous system, and recovery after complete SCI occurs due to recovery of nerve roots adjacent to the level of the lesion or peripheral axonal sprouting, as well as regeneration of the spinal cord at the level of the lesion [63–65]. However, the influence of extensive damage to peripheral nerves or nerve roots associated with spinal cord contusion on spontaneous recovery is not addressed in the current translational studies or existing SCI databases.

In this study, hNSPC transplantation was not done at the acute stage of SCI, but at an average of 63.4 days after injury, and peripheral nerve or nerve root injuries did not accompany the SCI, as verified by NCS before transplantation. As a result, 18.8% (3/16) of AIS-A patients in the subacute treatment group and 30% (3/10) in the case of the early subacute treatment group improved to AIS-B or AIS-C at 1 year. All three AIS-A patients exhibiting AIS grade conversion were transplanted with hNSPCs in the early subacute stage of SCI. In contrast, only one patient in the

control group showed AIS grade conversion. Thus, although further long-term, larger-scale, and randomized clinical trials are required to establish evidence of safety and efficacy, our results suggest that hNSPC transplantation into AIS-A patients within less than 2 months after SCI would result in better neurological outcome. In patients initially assessed as AIS-B, the extent of spontaneous recovery was significantly greater than those in AIS-A; AIS-B conversion to AIS-D has been reported to be as high as 30–40% at 1 year after injury [62]. In this study, both AIS-B patients improved to AIS-D at 1 year following transplantation, albeit the small number of patients. Thus, future clinical trials are required to assess the efficacy of hNSPC transplantation in AIS-B patients to investigate whether AIS-B patients may be a preferable target population to AIS-A patients.

Neurological recovery can also be measured by changes in AMS and ASS, which are often used in phase I/II SCI trials to determine whether an experimental intervention has potentially beneficial effects. Spontaneous motor score recovery in subjects with tetraplegia is also fairly limited. Cervical-injured AIS-A patients showed a mean improvement in AMS of ~8–10 points at 1 year after SCI [62]. However, if changes in AMS are calculated not immediately after SCI, but at different time points after SCI, AIS-A patients are expected to spontaneously improve by 5.7 AMS points, on average, from 8 weeks to the first year after SCI [62]. In this study, we observed a mean improvement of 7.9 AMS points at 1 year after transplantation in AIS-A patients who underwent hNSPC implantation at an average of 63.4 days after injury. The continued improvement of AMS that we observed over 1 year after transplantation is also encouraging (Figure 3). If some recovery was caused by regeneration of injured fibers, this would be expected to be a slow process, similar to what we observed. In contrast, AIS-A patients in the control group showed significantly smaller improvement in AMS compared with the transplantation group (Table 5). Analogous to the findings with motor scores, patients in the cohort showed improvement in sensory scores following transplantation (Figure 3). AIS-B patients also exhibited greater improvement in motor and sensory scores following transplantation, as compared to the control group.

It seems reasonable to suggest that an experimental therapy applied locally to the site of SCI, such as cell transplantation, will have maximum effect within the spinal levels just below the injury. Thus, for patients with complete cervical SCI, an improvement in motor level may readily show a subtle therapeutic effect and could accurately identify a clinically important difference (e.g., improvement in hand function). A number of studies have looked at spontaneous changes in motor levels in patients with SCI. In several studies, the majority of individuals (~55–85%) with complete tetraplegia recovered at least one motor level in the injured cervical cord within 1 year after SCI, whereas, based on initial assessment within 30 days of SCI, only 27% of subjects showed one motor level recovery [34, 60, 66, 67]. This variation in spontaneous recovery rates may be due to different definitions of motor level recovery, different timing of the initial examination, or a different distribution of motor function in the segment below the initial motor level. In this study, the initial examination

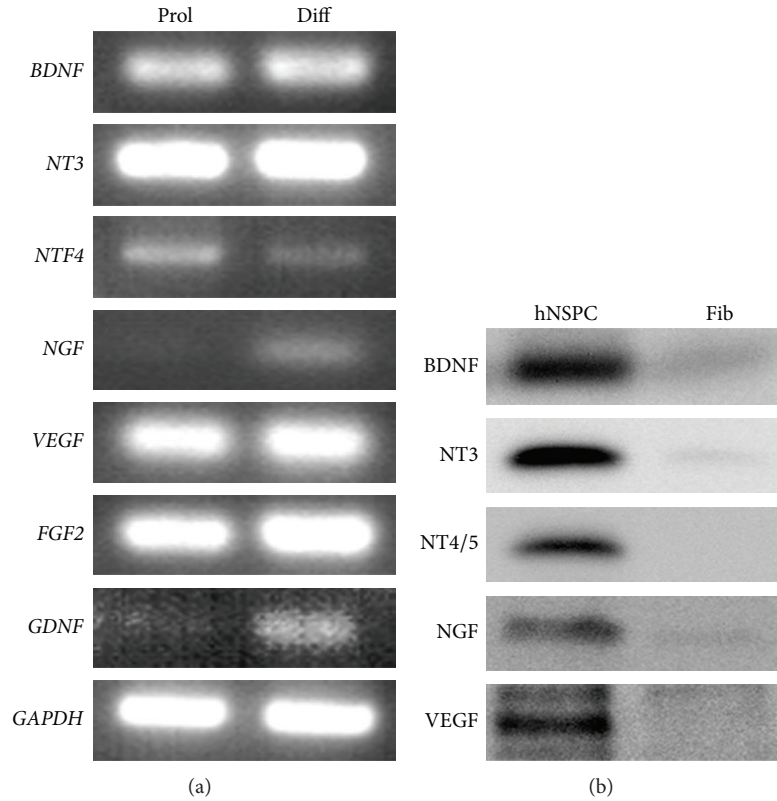


FIGURE 7: Human NSPCs express diverse trophic factors. (a) *In vitro*, proliferating (Prol) and differentiated (Diff) hNSPCs, respectively, expressed *FGF2*, *GDNF*, *VEGF*, and neurotrophins including *BDNF*, *NT3*, *NTF4*, and *NGF*. (b) hNSPCs notably secreted *BDNF*, *NT3*, *NT4/5*, *NGF*, and *VEGF* into the cultured media, compared to human foreskin fibroblasts (Fib).

of motor level was not done at the acute stage of SCI and peripheral nerve injuries did not accompany the SCI. Under this condition, we could observe that higher percentage of AIS-A patients recovered at least one motor level at 1 year after transplantation compared with control group. These results suggest that hNSPC transplantation may improve motor function in spinal segments adjacent to cell injection sites and facilitate endogenous neural substrate repair.

4.3. Electrophysiological Evidence of Recovery. Electrophysiological examinations could help in understanding the mechanism(s) of new therapeutic interventions directed at enhancing recovery of spinal cord function. Repair mechanisms, such as remyelination/regeneration and reconnection of damaged spinal tract fibers, may be reflected in changes in spinal impulse conductivity. In a multicenter study, SSEP and MEP recordings remained absent over 1 year in AIS-A patients, and SSEP and MEP latencies remained unchanged over time in AIS-B patients, indicating that neurological and functional recovery in SCI patients were apparently not related to improvements in spinal conductivity [26]. Thus, it was assumed that spontaneous functional recovery occurs primarily through compensation in complete SCI and through neural plasticity in incomplete SCI, rather than through repair of damaged spinal pathways. In this study, electrophysiological recordings showed no response below the level of injury before hNSPC transplantation, confirming

the completeness of the SCI. However, we demonstrated a positive response in SSEP and MEP activities in 35.3% and 58.8% of AIS-A patients, respectively, below the level of injury at 1 year after transplantation. Additionally, a patient with complete SCI showed a positive response in SSEP studies of upper and lower limbs following transplantation. In incomplete SCI, a patient also exhibited a positive response in the SSEP study of lower limbs. These findings suggest that hNSPC transplantation may mediate repair across the injury site in the spinal cord. However, the relationship between changes in electrophysiological measures and different outcome tools of recovery has not been fully explored yet, and the hNSPC-mediated recovery mechanisms in complete and incomplete SCI are also still in need of further investigation.

5. Conclusion

Our studies offer support for the safety and tolerability of hNSPC transplantation in sensorimotor or motor complete cervical SCI. At 1 year after cell transplantation, there was no evidence of cord damage, syrinx or tumor formation, neurological deterioration, and exacerbating neuropathic pain or spasticity. There are some indications of efficacy, based on neurological and electrophysiological testing with a limited number of patients that justify moving forward to a larger, controlled clinical trial. Therefore, the transplantation of hNSPCs into cervical SCI is safe and well-tolerated and is

of modest neurological benefit up to 1 year after transplants. However, further basic and clinical research is also required to achieve neurological improvement more significantly, identify the maximum safely tolerated or optimal dose of intraspinal grafting of hNSPCs, develop appropriate microsurgical transplantation techniques, evaluate the optimal timing of hNSPC transplantation in SCI, and monitor the long-term safety issue related to hNSPC transplantation.

Conflict of Interests

The authors declare that there is no conflict of interests regarding the publication of this paper.

Authors' Contribution

Ji Cheol Shin and Keung Nyun Kim are co-first authors.

Acknowledgments

This work was supported by Grants from National Research Foundation (2013M3A9B4076545) and Korean Health Technology R&D Project (A121943, H114C1564), Faculty Grant of Yonsei University College of Medicine (6-2006-0017), and the Severance Hospital in Seoul, Korea. The authors thank Professor Chang-il Park, Department of Rehabilitation Medicine, and Professor Chul Lee, Department of Pediatrics, Yonsei University College of Medicine, for supporting the clinical trial in the Severance Hospital.

References

- [1] D. C. Baptiste and M. G. Fehlings, "Update on the treatment of spinal cord injury," *Progress in Brain Research*, vol. 161, pp. 217–233, 2007.
- [2] F. Barnabé-Heider and J. Frisén, "Stem cells for spinal cord repair," *Cell Stem Cell*, vol. 3, no. 1, pp. 16–24, 2008.
- [3] V. Sahni and J. A. Kessler, "Stem cell therapies for spinal cord injury," *Nature Reviews Neurology*, vol. 6, no. 7, pp. 363–372, 2010.
- [4] F. Féron, C. Perry, J. Cochrane et al., "Autologous olfactory ensheathing cell transplantation in human spinal cord injury," *Brain*, vol. 128, no. 12, pp. 2951–2960, 2005.
- [5] J. Hernández, A. Torres-Espín, and X. Navarro, "Adult stem cell transplants for spinal cord injury repair: current state in preclinical research," *Current Stem Cell Research & Therapy*, vol. 6, no. 3, pp. 273–287, 2011.
- [6] N. Knoller, G. Auerbach, V. Fulga et al., "Clinical experience using incubated autologous macrophages as a treatment for complete spinal cord injury: phase I study results," *Journal of Neurosurgery: Spine*, vol. 3, no. 3, pp. 173–181, 2005.
- [7] C. Lima, P. Escada, J. Pratas-Vital et al., "Olfactory mucosal autografts and rehabilitation for chronic traumatic spinal cord injury," *Neurorehabilitation and neural repair*, vol. 24, no. 1, pp. 10–22, 2010.
- [8] A. Mackay-Sim, F. Féron, J. Cochrane et al., "Autologous olfactory ensheathing cell transplantation in human paraplegia: a 3-year clinical trial," *Brain*, vol. 131, no. 9, pp. 2376–2386, 2008.
- [9] G. A. Moviglia, R. Fernandez Viña, J. A. Brizuela et al., "Combined protocol of cell therapy for chronic spinal cord injury. Report on the electrical and functional recovery of two patients," *Cytotherapy*, vol. 8, no. 3, pp. 202–209, 2006.
- [10] H. Saberi, P. Moshayedi, H.-R. Aghayan et al., "Treatment of chronic thoracic spinal cord injury patients with autologous Schwann cell transplantation: an interim report on safety considerations and possible outcomes," *Neuroscience Letters*, vol. 443, no. 1, pp. 46–50, 2008.
- [11] E. Syková, A. Homola, R. Mazanec et al., "Autologous bone marrow transplantation in patients with subacute and chronic spinal cord injury," *Cell Transplantation*, vol. 15, no. 8–9, pp. 675–687, 2006.
- [12] H. Y. Seung, S. S. Yu, H. P. Yong et al., "Complete spinal cord injury treatment using autologous bone marrow cell transplantation and bone marrow stimulation with granulocyte macrophage-colony stimulating factor: phase I/II clinical trial," *Stem Cells*, vol. 25, no. 8, pp. 2066–2073, 2007.
- [13] O. Lindvall and Z. Kokaia, "Stem cells in human neurodegenerative disorders—time for clinical translation?" *Journal of Clinical Investigation*, vol. 120, no. 1, pp. 29–40, 2010.
- [14] C. P. Hofstetter, N. A. V. Holmström, J. A. Lilja et al., "Allodynia limits the usefulness of intraspinal neural stem cell grafts; directed differentiation improves outcome," *Nature Neuroscience*, vol. 8, no. 3, pp. 346–353, 2005.
- [15] S. Karimi-Abdolrezaee, E. Eftekharpour, J. Wang, C. M. Morshead, and M. G. Fehlings, "Delayed transplantation of adult neural precursor cells promotes remyelination and functional neurological recovery after spinal cord injury," *The Journal of Neuroscience*, vol. 26, no. 13, pp. 3377–3389, 2006.
- [16] H. S. Keirstead, G. Nistor, G. Bernal et al., "Human embryonic stem cell-derived oligodendrocyte progenitor cell transplants remyelinate and restore locomotion after spinal cord injury," *The Journal of Neuroscience*, vol. 25, no. 19, pp. 4694–4705, 2005.
- [17] P. Lu, L. L. Jones, E. Y. Snyder, and M. H. Tuszynski, "Neural stem cells constitutively secrete neurotrophic factors and promote extensive host axonal growth after spinal cord injury," *Experimental Neurology*, vol. 181, no. 2, pp. 115–129, 2003.
- [18] Y. D. Teng, E. B. Lavik, X. Qu et al., "Functional recovery following traumatic spinal cord injury mediated by a unique polymer scaffold seeded with neural stem cells," *Proceedings of the National Academy of Science of the United States of America*, vol. 99, no. 5, pp. 3024–3029, 2002.
- [19] Y. Ziv, H. Avidan, S. Pluchino, G. Martino, and M. Schwartz, "Synergy between immune cells and adult neural stem/progenitor cells promotes functional recovery from spinal cord injury," *Proceedings of the National Academy of Sciences of the United States of America*, vol. 103, no. 35, pp. 13174–13179, 2006.
- [20] B. J. Cummings, N. Uchida, S. J. Tamaki et al., "Human neural stem cells differentiate and promote locomotor recovery in spinal cord-injured mice," *Proceedings of the National Academy of Sciences of the United States of America*, vol. 102, no. 39, pp. 14069–14074, 2005.
- [21] D. L. Salazar, N. Uchida, F. P. T. Hamers, B. J. Cummings, and A. J. Anderson, "Human neural stem cells differentiate and promote locomotor recovery in an early chronic spinal cord injury NOD-scid mouse model," *PLoS ONE*, vol. 5, no. 8, Article ID e12272, 2010.
- [22] M. J. Hooshmand, C. J. Sontag, N. Uchida, S. Tamaki, A. J. Anderson, and B. J. Cummings, "Analysis of host-mediated repair mechanisms after human CNS-stem cell transplantation for spinal cord injury: correlation of engraftment with recovery," *PLoS ONE*, vol. 4, no. 6, Article ID e5871, 2009.

- [23] J. Yan, L. Xu, A. M. Welsh et al., "Extensive neuronal differentiation of human neural stem cell grafts in adult rat spinal cord," *PLoS Medicine*, vol. 4, no. 2, Article ID e39, 2007.
- [24] Globe Newswire, Stem Cells, Inc. initiates phase II clinical trial in cervical spinal cord injury, <http://investor.stemcellsinc.com/phoenix.zhtml?c=86230&p=irol-newsArticle&ID=1974747>.
- [25] J. D. Steeves, D. Lammertse, A. Curt et al., "Guidelines for the conduct of clinical trials for spinal cord injury (SCI) as developed by the ICCP panel: clinical trial outcome measures," *Spinal Cord*, vol. 45, no. 3, pp. 206–221, 2007.
- [26] A. Curt, H. J. A. Van Hedel, D. Klaus, and V. Dietz, "Recovery from a spinal cord injury: significance of compensation, neural plasticity, and repair," *Journal of Neurotrauma*, vol. 25, no. 6, pp. 677–685, 2008.
- [27] J. F. Ditunno Jr., A. E. Flanders, S. Kirshblum et al., "Predicting outcome in traumatic spinal cord injury," in *Spinal Cord Medicine*, S. Kirshblum, D. I. Campagnolo, and J. A. Delisa, Eds., Lippincott Williams & Wilkins, Philadelphia, Pa, USA, 2002.
- [28] D. Dumitru, A. A. Amato, and M. J. Zwarts, *Electrodiagnostic Medicine*, Hanley & Belfus, Philadelphia, Pa, USA, 2002.
- [29] H.-T. Kim, I.-S. Kim, I.-S. Lee, J.-P. Lee, E. Y. Snyder, and K. In Park, "Human neurospheres derived from the fetal central nervous system are regionally and temporally specified but are not committed," *Experimental Neurology*, vol. 199, no. 1, pp. 222–235, 2006.
- [30] M. Shinawi and S. W. Cheung, "The array CGH and its clinical applications," *Drug Discovery Today*, vol. 13, no. 17-18, pp. 760–770, 2008.
- [31] H. Lee, S. Yun, I.-S. Kim et al., "Human fetal brain-derived neural stem/progenitor cells grafted into the adult epileptic brain restrain seizures in rat models of temporal lobe epilepsy," *PLoS ONE*, vol. 9, no. 8, Article ID e104092, 2014.
- [32] Z. Kokaia, G. Martino, M. Schwartz, and O. Lindvall, "Cross-talk between neural stem cells and immune cells: the key to better brain repair?" *Nature Neuroscience*, vol. 15, no. 8, pp. 1078–1087, 2012.
- [33] L. Titomanlio, A. Kavelaars, J. Dalous et al., "Stem cell therapy for neonatal brain injury: perspectives and Challenges," *Annals of Neurology*, vol. 70, no. 5, pp. 698–712, 2011.
- [34] J. D. Steeves, J. K. Kramer, J. W. Fawcett et al., "Extent of spontaneous motor recovery after traumatic cervical sensorimotor complete spinal cord injury," *Spinal Cord*, vol. 49, no. 2, pp. 257–265, 2011.
- [35] S. Ramón, R. Domínguez, L. Ramírez et al., "Clinical and magnetic resonance imaging correlation in acute spinal cord injury," *Spinal Cord*, vol. 35, no. 10, pp. 664–673, 1997.
- [36] K. Potter and A. Saifuddin, "Pictorial review: MRI of chronic spinal cord injury," *British Journal of Radiology*, vol. 76, no. 905, pp. 347–352, 2003.
- [37] A. E. Flanders, C. M. Spettell, L. M. Tartaglino, D. P. Friedman, and G. J. Herbison, "Forecasting motor recovery after cervical spinal cord injury: value of MR imaging," *Radiology*, vol. 201, no. 3, pp. 649–655, 1996.
- [38] M. P. Jensen and P. Karoly, "Self-report scales and procedures for assessing pain in adults," in *Handbook of Pain Assessment*, D. C. Turk and R. Melzack, Eds., Guilford Press, New York, NY, USA, 1992.
- [39] A. D. Pandyan, G. R. Johnson, C. I. M. Price, R. H. Curless, M. P. Barnes, and H. Rodgers, "A review of the properties and limitations of the Ashworth and modified Ashworth Scales as measures of spasticity," *Clinical Rehabilitation*, vol. 13, no. 5, pp. 373–383, 1999.
- [40] A. Spandidos, X. Wang, H. Wang, and B. Seed, "Primer-Bank: a resource of human and mouse PCR primer pairs for gene expression detection and quantification," *Nucleic Acids Research*, vol. 38, supplement 1, Article ID gkp1005, pp. D792–D799, 2009.
- [41] H. Barrett, J. M. McClelland, S. B. Rutkowski, and P. J. Siddall, "Pain characteristics in patients admitted to hospital with complications after spinal cord injury," *Archives of Physical Medicine and Rehabilitation*, vol. 84, no. 6, pp. 789–795, 2003.
- [42] V. K. Noonan, J. A. Kopeck, H. Zhang, and M. F. Dvorak, "Impact of associated conditions resulting from spinal cord injury on health status and quality of life in people with traumatic central cord syndrome," *Archives of Physical Medicine and Rehabilitation*, vol. 89, no. 6, pp. 1074–1082, 2008.
- [43] M. Y. Macias, M. B. Syring, M. A. Pizzi, M. J. Crowe, A. R. Alexanian, and S. N. Kurpad, "Pain with no gain: allodynia following neural stem cell transplantation in spinal cord injury," *Experimental Neurology*, vol. 201, no. 2, pp. 335–348, 2006.
- [44] S. L. Hitzig, M. Tonack, K. A. Campbell et al., "Secondary health complications in an aging canadian spinal cord injury sample," *American Journal of Physical Medicine & Rehabilitation*, vol. 87, no. 7, pp. 545–555, 2008.
- [45] H. E. Lechner, A. Frotzler, and P. Eser, "Relationship between self- and clinically rated spasticity in spinal cord injury," *Archives of Physical Medicine and Rehabilitation*, vol. 87, no. 1, pp. 15–19, 2006.
- [46] R. J. Marino, T. Barros, F. Biering-Sorensen et al., "International standards for neurological classification of spinal cord injury," *The journal of spinal cord medicine*, vol. 26, supplement 1, pp. S50–S56, 2003.
- [47] A. Curt and V. Dietz, "Electrophysiological recordings in patients with spinal cord injury: significance for predicting outcome," *Spinal Cord*, vol. 37, no. 3, pp. 157–165, 1999.
- [48] J. Xie and M. Boakye, "Electrophysiological outcomes after spinal cord injury," *Neurosurgical Focus*, vol. 25, no. 5, article E11, 2008.
- [49] D. L. Salazar, N. Uchida, F. P. T. Hamers, B. J. Cummings, and A. J. Anderson, "Human neural stem cells differentiate and promote locomotor recovery in an early chronic spinal cord injury NOD-*scid* mouse model," *PLoS ONE*, vol. 5, no. 8, Article ID e12272, 2010.
- [50] T. Cheriyan, D. J. Ryan, J. H. Weinreb et al., "Spinal cord injury models: a review," *Spinal Cord*, vol. 52, no. 8, pp. 588–595, 2014.
- [51] E. Åkesson, J.-H. Piao, E.-B. Samuelsson et al., "Long-term culture and neuronal survival after intraspinal transplantation of human spinal cord-derived neurospheres," *Physiology & Behavior*, vol. 92, no. 1-2, pp. 60–66, 2007.
- [52] C. N. Svendsen, M. A. Caldwell, and T. Ostensfeld, "Human neural stem cells: Isolation, expansion and transplantation," *Brain Pathology*, vol. 9, no. 3, pp. 499–513, 1999.
- [53] S.-C. Zhang, M. Wernig, I. D. Duncan, O. Brüstle, and J. A. Thomson, "In vitro differentiation of transplantable neural precursors from human embryonic stem cells," *Nature Biotechnology*, vol. 19, no. 12, pp. 1129–1133, 2001.
- [54] M. Abematsu, K. Tsujimura, M. Yamano et al., "Neurons derived from transplanted neural stem cells restore disrupted neuronal circuitry in a mouse model of spinal cord injury," *The Journal of Clinical Investigation*, vol. 120, no. 9, pp. 3255–3266, 2010.
- [55] M. Bacigaluppi, S. Pluchino, L. P. Jametti et al., "Delayed post-ischaemic neuroprotection following systemic neural stem cell

- transplantation involves multiple mechanisms,” *Brain*, vol. 132, no. 8, pp. 2239–2251, 2009.
- [56] S. Pluchino, A. Quattrini, E. Brambilla et al., “Injection of adult neurospheres induces recovery in a chronic model of multiple sclerosis,” *Nature*, vol. 422, no. 6933, pp. 688–694, 2003.
 - [57] A. S. Burns, B. S. Lee, J. F. Ditunno Jr., and A. Tessler, “Patient selection for clinical trials: the reliability of the early spinal cord injury examination,” *Journal of Neurotrauma*, vol. 20, no. 5, pp. 477–482, 2003.
 - [58] Consortium for Spinal Cord Medicine, “Outcomes following traumatic spinal cord injury: clinical practice guidelines for health-care professionals,” *Journal of Spinal Cord Medicine*, vol. 23, no. 4, pp. 289–316, 2003.
 - [59] R. J. Marino, J. F. Ditunno Jr., W. H. Donovan, and F. Maynard Jr., “Neurologic recovery after traumatic spinal cord injury: data from the model spinal cord injury systems,” *Archives of Physical Medicine and Rehabilitation*, vol. 80, no. 11, pp. 1391–1396, 1999.
 - [60] R. L. Waters, R. H. Adkins, J. S. Yakura, and I. Sie, “Motor and sensory recovery following complete tetraplegia,” *Archives of Physical Medicine and Rehabilitation*, vol. 74, no. 3, pp. 242–247, 1993.
 - [61] R. L. Waters, R. H. Adkins, J. S. Yakura, and I. Sie, “Recovery following complete paraplegia,” *Archives of Physical Medicine and Rehabilitation*, vol. 73, no. 9, pp. 784–789, 1992.
 - [62] J. W. Fawcett, A. Curt, J. D. Steeves et al., “Guidelines for the conduct of clinical trials for spinal cord injury as developed by the ICCP panel: spontaneous recovery after spinal cord injury and statistical power needed for therapeutic clinical trials,” *Spinal Cord*, vol. 45, no. 3, pp. 190–205, 2007.
 - [63] V. Dietz and A. Curt, “Neurological aspects of spinal-cord repair: promises and challenges,” *The Lancet Neurology*, vol. 5, no. 8, pp. 688–694, 2006.
 - [64] J. F. Ditunno Jr., A. E. Flanders, S. Kirshblum, V. Graziani, and A. Tessler, “Predicting outcome in traumatic spinal cord injury,” in *Spinal Cord Medicine*, S. Kirshblum, D. I. Campagnolo, and J. A. Delisa, Eds., Lippincott Williams & Wilkins, Philadelphia, Pa, USA, 2002.
 - [65] R. J. Marino, G. J. Herbison, and J. F. Ditunno Jr., “Peripheral sprouting as a mechanism for recovery in the zone of injury in acute quadriplegia: a single-fiber EMG study,” *Muscle and Nerve*, vol. 17, no. 12, pp. 1466–1468, 1994.
 - [66] J. F. Ditunno Jr., M. E. Cohen, W. W. Hauck, A. B. Jackson, and M. L. Sipski, “Recovery of upper-extremity strength in complete and incomplete tetraplegia: a multicenter study,” *Archives of Physical Medicine and Rehabilitation*, vol. 81, no. 4, pp. 389–393, 2000.
 - [67] C. G. Fisher, V. K. Noonan, D. E. Smith, P. C. Wing, M. F. Dvorak, and B. Kwon, “Motor recovery, functional status, and health-related quality of life in patients with complete spinal cord injuries,” *Spine*, vol. 30, no. 19, pp. 2200–2207, 2005.

Review Article

The Effects of Exercise on Cognitive Recovery after Acquired Brain Injury in Animal Models: A Systematic Review

Elise Wogensen, Hana Malá, and Jesper Mogensen

The Unit for Cognitive Neuroscience, Department of Psychology, University of Copenhagen, Øster Farimagsgade 2A, 1354 Copenhagen K, Denmark

Correspondence should be addressed to Jesper Mogensen; jesper.mogensen@psy.ku.dk

Received 9 February 2015; Accepted 9 June 2015

Academic Editor: Midori A. Yenari

Copyright © 2015 Elise Wogensen et al. This is an open access article distributed under the Creative Commons Attribution License, which permits unrestricted use, distribution, and reproduction in any medium, provided the original work is properly cited.

The objective of the present paper is to review the current status of exercise as a tool to promote cognitive rehabilitation after acquired brain injury (ABI) in animal model-based research. Searches were conducted on the *PubMed*, *Scopus*, and *psycINFO* databases in February 2014. Search strings used were: exercise (and) animal model (or) rodent (or) rat (and) traumatic brain injury (or) cerebral ischemia (or) brain irradiation. Studies were selected if they were (1) in English, (2) used adult animals subjected to acquired brain injury, (3) used exercise as an intervention tool after inflicted injury, (4) used exercise paradigms demanding movement of all extremities, (5) had exercise intervention effects that could be distinguished from other potential intervention effects, and (6) contained at least one measure of cognitive and/or emotional function. Out of 2308 hits, 22 publications fulfilled the criteria. The studies were examined relative to cognitive effects associated with three themes: exercise type (forced or voluntary), timing of exercise (early or late), and dose-related factors (intensity, duration, etc.). The studies indicate that exercise in many cases can promote cognitive recovery after brain injury. However, the optimal parameters to ensure cognitive rehabilitation efficacy still elude us, due to considerable methodological variations between studies.

1. Introduction

Physical exercise has long been known to be effective in the treatment and prevention of many physical conditions such as type 2 diabetes, hypertension, obesity, dyslipidemia, and cardiovascular disease [1–3]. Furthermore, exercise has been found to reduce symptoms of depression and anxiety [4–7]. Exercise has also garnered considerable interest as a tool to promote cognitive health. Studies of healthy older adults have shown positive effects of exercise on measures of cognitive function [8, 9]. Research into the effects of physical activity on enhancing cognitive/academic abilities in children shows some promise. However, the findings are still fairly limited and more randomized, controlled trials are needed [10–12]. Similarly, there is some evidence that physical activity can improve cognition or prevent mental decline in people with neurological and neurodegenerative disorders. The overall results, however, remain inconclusive due to differences in methodologies and quality of studies [13–16].

Physical exercise after acquired brain injury (ABI) has received attention as a cost-effective, noninvasive, and practicable rehabilitation tool. Preclinical research has shown that post-ABI exercise can increase cerebral growth factor levels [17–21], reduce apoptosis-related processes [22–24], promote neurogenesis, neuronal survival, and regeneration [25–28], reduce lesion size [29, 30], modulate inflammatory responses [31], reduce astrogliosis [32, 33], and improve cerebral blood flow [34, 35]. However, less is known about the potential effects of exercise on cognitive recovery after ABI. Cognitive dysfunctions after brain injury, such as memory, attentional, and executive function impairments, are common and can negatively affect work performance, social competencies, and experienced quality of life [36].

In this paper, the preclinical research investigating the effects of post-ABI exercise on cognitive recovery will be systematically reviewed. Within brain injury rehabilitation, several factors (e.g., timing, repetition, intensity) have been shown to be of importance for promoting brain plasticity

mechanisms and enhancing recovery outcome [37]. Such factors are also believed to be essential when using exercise as a cognitive rehabilitation tool. In the following, parameters that are believed to play a role in the efficacy of exercise, including type of exercise, starting point, and dose-related issues, will be examined.

2. Inclusion Criteria

Relevant research studies were found using the search terms “exercise (and) animal model (or) rodent (or) rat (and) traumatic brain injury (or) cerebral ischemia (or) brain irradiation,” all in all 9 search strings. The searches were performed in February of 2014 on the *PubMed*, *Scopus*, and *PsycINFO* databases, providing a total of 2308 hits. Articles were then selected using the following inclusion criteria:

- (i) In English.
- (ii) Animal model based.
- (iii) Employing adult animals (rat models: min. 7 weeks old or min. 200 g; mouse models: min. 6 weeks old or min. 20 g; gerbil models: min. 11 weeks old or min. 55 g).
- (iv) Animals were subjected to acquired brain injury (ABI) in their adult life, either through mechanical injury, neurotoxic injection, irradiation, or induction of cerebral ischemia.
- (v) Exercise was used as an intervention/treatment tool *after* cerebral injury (habituation to the exercise apparatuses prior to injury was accepted).
- (vi) The exercise regimens consisted of a general motor activation of all of the animals' extremities (i.e., running, swimming). Sole training of a single muscle group or extremity (i.e., forced limb use, grip training) was not included.
- (vii) The effects of the exercise intervention could be clearly distinguished from effects of nonexercise interventions if such were also investigated.
- (viii) Studies contained at least one measure of cognitive and/or emotional function after (or during) exercise treatment. Studies solely investigating motor abilities (i.e., balance tests, physical strength tests) or neural/molecular mechanisms were excluded.

Twenty-two research articles fulfilled the above inclusion criteria. Examination of the references in these articles did not uncover further publications that fulfilled the inclusion criteria.

Of the 22 papers, 14 used rats, five used mice, and three used gerbils as their experimental subjects. All used male animals except two (see Table 1). Regarding type of brain injury, eight were ischemia models (common carotid artery occlusion, middle cerebral artery occlusion, and photothrombosis), five used cortical impact injury, four used fluid percussion injury, one used closed head injury equipment, another used neurotoxic injection, and three used gamma irradiation.

Experimental groups fell into four types of exercise: nonmotorized running wheel exercise (nine studies), motorized treadmill exercise (11 studies), motorized running wheel (one study), swimming in a circular pool (one study), and swimming or running wheel exercise (one study).

Cognitive measures applied in these studies were spatial learning/retention paradigms administered in a water maze (12 studies) or in a Barnes maze (one study), visual discrimination and retention in a water maze (one study), object recognition tests (three studies), an object location test (one study), conditioning based learning paradigms (seven studies) (i.e., contextual fear learning, step-down avoidance task, passive avoidance task, stop-signal reaction time task, conditioned learning in a Y-maze), open field tests (three studies), and tail suspension tests (two studies). Some studies used more than one test.

3. Voluntary or Forced?

Within animal model based research, exercise is often differentiated into voluntary or forced paradigms. In voluntary paradigms, the animals are given a choice between movement and inactivity while having access to the exercise apparatus. In forced exercise, activity levels are controlled by external factors. Exercise in a nonmotorized running wheel allows animals to exercise at their own accord, while motorized treadmill running/running wheel exercise and swimming exercise do not offer such movement autonomy. The following section examines whether the type of exercise (voluntary or forced) exerts differential effects on cognitive recovery after ABI.

3.1. Voluntary Exercise. Nine studies included experimental groups subjected to voluntary (running wheel) exercise.

Wu et al. [38] subjected rats to lateral fluid percussion injury (IFPI) immediately followed by 12 days of running wheel exercise (7 of those days prior to cognitive testing), a diet high in docosahexaenoic acid (DHA), or both. They found that IFPI exercised animals did significantly better in a spatial learning task in a water maze (as shown by reduced latency to find a platform) in comparison to nonexercised IFPI animals kept on a normal diet. The DHA diet was also associated with improved spatial learning. Furthermore, injured rats on the combined exercise and DHA diet significantly outperformed all other IFPI groups. Molecular analysis showed increased levels of DHA, Acox1, and 17 β -HSD4 (enzymes involved in DHA metabolism), Sir2 (involved in mitochondrial function), iPLA2 (molecules involved in membrane homeostasis), p-TrkB (BDNF receptor), and lower levels of 4-HHE (marker for lipid peroxidation) in the groups subjected to either exercise or the DHA diet (compared to controls) and a further increase/decrease in the combined group. The combined group also showed increased STX-3 (also involved in membrane homeostasis) and brain derived neurotrophic factor (BDNF) levels. The study indicates that early initiated voluntary exercise and/or the DHA diet can positively affect cognitive recovery after TBI, possibly

TABLE 1: Summary of exercise protocols and postexercise cognitive/emotional and cerebral changes in ABI animal models.

Reference	ABI model	Animal, gender (age/weight)	Exercise type	Intervention start*	Dose parameters	Mean daily exercise distance	Cognitive/emotional effects	Cerebral changes
de Araujo et al. [52]	CCAO	Mongolian gerbils, male (60–80 g)	Treadmill	Early (12, 24, 48, or 72 hours postinjury)	Max. 3 days (4 sessions), min. 1 day (1 session), 15 min/session. Speed: 10 m/min	150 m	CCAO + EX after 12 hours showed a decreased number of field crossings and an increase in grooming in an open field test compared to sham + SED. No other group differences	CCAO + EX after 12 hours: number of cells ↓ in CA1 + striatum compared to CCAO + EX after 24 hours
Cechetti et al. [47]	CCAO	Wistar rats, male (3 months)	Treadmill	Early (24 hours postinjury [†])	12 weeks, 3 times/week, 20 min/session. Weeks 1-2: 12 m/min for 3 min, 24 m/min for 4 min, 36 m/min for 6 min, 24 m/min for 4 min, and 12 m/min for 3 min; weeks 3–6, at 24 m/min for 4 min, 36 m/min for 12 min, and 24 m/min for 4 min; weeks 7–10: 24 m/min for 2 min, 36 m/min for 16 min, and 24 m/min for 2 min; weeks 11-12: 36 m/min for 2 min, 48 m/min for 16 min, and 36 m/min for 2 min.	480 m/session up to 912 m/session (graded protocol)	All EX groups did significantly better in a spatial acquisition and retention task as well as a working memory task than CCAO + SED	No differences between groups in levels of free radicals or SOD. CCAO + SED: hippocampal lipoperoxidation and thiol-levels ↑ compared to the other groups
Chen et al. [55]	NTI	Sprague-Dawley rats (12–14 weeks)	Motorized running wheel	Early (2nd postinjury day)	7 consecutive days, 30 min twice daily. LowEX: 3 m/min for 10 min., 4.2 m/min for 10 min, and 5.4 m/min for 10 min. ModEX: 4.8 m/min for 10 min, 6 m/min for 10 min, and 7.2 m/min for 10 min. HighEX: 9.6 m/min for 10 min, 10.8 m/min for 10 min, and 12 m/min for 10 min	NTI + LowtEX: 252 m; NTI + ModEX: 360 m; NTI + HighEX: 648 m	NTI + ModEX showed significantly better acquisition of conditioning task in Y-maze than NTI + SED. No acquisition differences between NTI + LowEX and NTI + SED or NTI + HighEX and NTI + SED	BrdU-positive cells in dentate gyrus ↑ in NTI + ModEX compared to NTI + SED. No BrdU-staining differences between other NTI + exercise intensity groups and NTI + SED. Positive correlation between acquisition and BrdU-positive cells

TABLE 1: Continued.

Reference	ABI model	Animal, gender (age/weight)	Exercise type	Intervention start*	Dose parameters	Mean daily exercise distance	Cognitive/emotional effects	Cerebral changes
Chen et al. [57]	CHI	ICR mice, male (7 weeks)	Treadmill	Early + late (2 or 9 days postinjury)	7 or 14 days (early) or 7 days (late). 1 hour/daily. Speed: 9 m/min progressively increased to 13.5 m/min	Between 540 m and 810 m (graded protocol)	CHI + earlyEX spent significantly more time exploring new object in an object recognition task than CHI + SED. CHI + lateEX and CHI + SED had less time exploration time with the new object than sham animals	EarlyEX hindered progressive cell loss in the cortex and hippocampus more than lateEX. EarlyEX ↑ neurite regeneration in the early postinjury stages, lateEX hindered later stage cell loss. EarlyEX for 14 days restored lesion-induced reduction in BDNF and MKP-1
Clark et al. [45]	IRR	C57BL/6J mice, male + female (min. 50 days)	Running wheel	Late (114/142 days postinjury)	54 days total, 24-hour daily access	IRR + EX: 5.8 km; sham + EX: 5.7 km	No differences in spatial learning + retention between IRR + EX and IRR + SED. Spatial learning and retention improved in sham + EX. Exercise improved retention in a contextual fear conditioning test	Exercise ↑ hippocampal neurogenesis. Exercise counteracted radiation-induced reductions in neurogenesis, neuronal differentiation, and glia cell levels
Crane et al. [40]	CCI	Long Evans rats, male (ca. 50 days)	Running wheel	Early (immediately postinjury)	7 days	7-8 km	CCI + EX performed significantly worse in complex stop-signal reaction time task for the first five test days compared CCI + SED and sham groups. After a week of testing, CCI + EX returned to baseline levels	CCI + EX: GFAB and IBA1 positive cells ↑ in the cortex and hippocampus, respectively; all CCI-animals: DAPI positive cells ↓ in the cortex, hippocampus, mediodorsal nucleus and corpus callosum compared to sham + SED

TABLE 1: Continued.

Reference	ABI model	Animal, gender (age/weight)	Exercise type	Intervention start*	Dose parameters	Mean daily exercise distance	Cognitive/emotional effects	Cerebral changes
Griesbach et al. [39]	FPI	Sprague-Dawley rats, male (ca. 312 g)	Running wheel	Early + late (0 or 14 days postinjury)	7 days total, 24-hour daily access. Wheel resistance: 100 g	N/A (mean ranges of nightly running distances between approximately 300 m and approximately 3400 m)	FPI + earlyEX performed significantly worse on a spatial acquisition task than all other groups. FPI + lateEX performed to the level of the sham operated animals. All FPI animals performed worse than noninjured animals on retention task	FPI + lateEX and sham groups: hippocampal pCREB and BDNF ↑. FPI + earlyEX: Synapsin-I and CREB ↓
Griesbach et al. [42]	FPI	Sprague-Dawley rats, male (ca. 265 g)	Running wheel	Late (14 days postinjury)	7 days total, 24-hour daily access. Wheel resistance: 100 g	N/A	FPI + EX acquired a spatial learning task and reached six criterium scores significantly faster than FPI + SED	Exercise ↑ hippocampal levels of BDNF. FPI + EX: mBDNF and CREB ↑ compared to FPI + SED. Sham + EX: Synapsin-I ↑. When blocking trk-B receptors: mBDNF ↓ in FPI + EX
Hicks et al. [50]	FPI	Sprague-Dawley rats, male (360–410 g)	Treadmill	Early (1 day postinjury)	18 days, 11.3 m/min. Day 1: 5 min, increased by 5 min daily for 14 days until reaching 60 min. After this running 60 min again for 4 days. Inclination: 6°	56.5 m/daily up to 678 m/daily (time graded protocol)	No differences in spatial acquisition or retention between FPI + EX and FPI + SED	BDNF mRNA levels in CA1 and CA3 ↑ in FPI + EX compared to FPI + SED. No group differences in hippocampal injury or cortical lesion volume. Left neocortex < right neocortex in FPI + SED compared to FPI + EX
Itoh et al. [46]	CCI	Wistar rats, male (10 weeks)	Treadmill	Early (1 day postinjury)	7 days, 30 min/day. Speed: 22 m/min	660 m	CCI + EX did significantly better in a spatial acquisition and retention task than CCI + SED	Lesion size ↓ in CCI + EX compared to CCI + SED. ssDNA immunopositive cells around the damaged cortical area ↓ in CCI + EX (postinjury days 1, 3, and 7), number of NeuN positive cells ↑ and GFAP positive cells ↓ (postinjury day 7) compared to CCI + SED

TABLE 1: Continued.

Reference	ABI model	Animal, gender (age/weight)	Exercise type	Intervention start*	Dose parameters	Mean daily exercise distance	Cognitive/emotional effects	Cerebral changes
Kim et al. [56]	CCI	Sprague-Dawley rats, male (7 weeks)	Treadmill	Early (2 days postinjury)	10 days, 30 min/day. Speed: 2 m/min for 5 min, 5 m/min for 5 min, and 8 m/min for 20 min	195 m (graded protocol)	CCI + EX had shorter latency times in a step-down avoidance test than CCI + SED	Hippocampal DNA fragmentation, Caspase-3, and Bax ↓ in CCI + EX compared to CCI + SED. Levels of Bcl2 ↑ in CCI + EX compared to CCI + SED. No group differences in corticosterone levels
Luo et al. [41]	MCAO	C57BL/6 mice, male (25–30 g)	Running wheel + swimming	Late (1 week postinjury)	RW: 43 days total, 24-hour daily access. SWIM: 43 days total, 2 trials/day, and 60 sec/trial	N/A	MCAO + RW had significantly shorter latency time to find the platform in a water maze task compared to MCAO + SED. No differences between MCAO + SWIM and MCAO + SED	Dentate gyrus progenitor cell survival and pCREB levels ↑ in MCAO + RW compared to control group

TABLE 1: Continued.

Reference	ABI model	Animal, gender (age/weight)	Exercise type	Intervention start*	Dose parameters	Mean daily exercise distance	Cognitive/emotional effects	Cerebral changes
Piao et al. [31]	CCI	C57BL/6 mice, male (10 weeks)	Running wheel	Late (1 week or 5 weeks postinjury)	4 weeks total, 24-hour daily acces.	103.2 m (1 week), 97.2 m (5 weeks).	CCI + lateEX performed significantly better in a spatial acquisition and retention task than CCI + SED. CCI + lateEX showed significant improvement in a cognitive flexibility task compared to CCI + earlyEX and CCI + SED. Retention of the flexibility task was significantly better in CCI + lateEX compared to CCI + SED. In a novel object recognition task, CCI + lateEX spent significantly longer time exploring a new object than CCI + earlyEX and CCI + SED. No locomotor differences in an open field test. In a tail suspension test, all CCI groups had increased immobility times	CCI + lateEX: ↓ lesion size compared to CCI + earlyEX and CCI + SED. IL-1 β levels ↑ in CCI + earlyEX (week 5) and ↓ in CCI + lateEX (week 9) compared to CCI + SED. IL-6 and IL-10 ↑ CCI + lateEX (week 9). Cortical Galectin-3 and C1qB levels ↑ increased in CCI + earlyEX, but ↓ in CCI + lateEX. Gp91phox and p22phox ↓ in CCI + lateEX. Hippocampal CREB gene expression, BDNF, IGF-1, neurogenesis, and cell survival ↑ in CCI + lateEX
Shen et al. [49]	CCI	Sprague-Dawley rats, male (250–270 g)	Treadmill	Early (24 hours postinjury)	14 days, 30 min/day. LowEX: week 1: 3 m/min; week 2: 3 m/min for 5 min, 5 m/min for 5 min, and 8 m/min for 20 min. HighEX: Day 1: 3 m/min; day 2: 3 m/min for 10 min, 6 m/min for 10 min, and 9 m/min for 10 min; day 3: 6 m/min for 10 min, and 9 m/min for 10 min, and 12 m/min for 10 min; day 4–14: 12 m/min	Week 1: 90 m, week 2: 200 m (lowEX). Day 1: 90 m, day 2: 180 m, day 3: 270 m, day 4–14: 360 m (highEX) (graded protocols)	CCI + lowEX performed better on a spatial acquisition task compared to CCI + highEX and CCI + SED. CCI + lowEX showed better task retention than CCI + SED	Contralateral hippocampal BDNF and pCREB ↑ in CCI + lowEX compared to CCI + SED. No group differences in levels of Synapsin-I and CREB

TABLE 1: Continued.

Reference	ABI model	Animal, gender (age/weight)	Exercise type	Intervention start*	Dose parameters	Mean daily exercise distance	Cognitive/emotional effects	Cerebral changes
Shih et al. [48]	MCAO	Sprague-Dawley rats, male (8 weeks)	Treadmill	Early (24 hours postinjury)	14 days, 30 min/day. LowEX: 8 m/min, highEX: 20 m/min	240 m (lowEX); 600 m (highEX)	MCAO + lowEX performed better in a spatial acquisition than the two other groups and showed better retention than MCAO + SED	Hippocampal BDNF, Synapsin-I (contralaterally), PSD-95, dendritic complexity and dendrite spines ↑ in MCAO + lowEX compared to MCAO + SED. Corticosterone levels ↑ in MCAO + highEX compared to MCAO + SED
Shimada et al. [58]	MCAO	Wistar rats, male (7 weeks)	Treadmill	Early (4th postinjury day)	28 days, 30 min/day. LowEX: 2 m/min for 5 min, 5 m/min for the next 5 min, and 8 m/min for 20 min. HighEX: 8 m/min for 5 min, 11 m/min for 5 min, and 22 m/min for 20 min	195 m (lowEX); 535 m (highEX) (graded protocols)	MCAO + lowEX spent more time exploring the novel object/newly placed object in object recognition/object location tasks than MCAO + SED. MCAO + highEX explored less than MCAO + lowEX. Both EX groups showed longer latency time in a passive avoidance test compared to MCAO + SED. No group differences in locomotor activity in an open field test	EX groups ↓ lesion size. EX groups ↑ number of neurons in the dentate gyrus compared with non-EX groups – higher in the ipsilateral dentate gyrus in MCAO + lowEX than MCAO + highEX. Ipsilateral dentate gyrus MAP-2 levels ↑ in MCAO + lowEX compared to MCAO + SED. Ipsilateral hippocampal MAP-2 ↓ in MCAO + highEX compared with MCAO + lowEX and sham group. Contralaterally, MAP-2 ↓ in CA1 and CA3 in MCAO + highEX compared with MCAO + lowEX
Sim et al. [53]	CCAO	Mongolian gerbils, male (11–13 weeks)	Treadmill	Early (2nd postinjury day)	10 days, 30 min/day. Speed: 2 m/min for the first 5 min, 5 m/min for the next 5 min, and 8 m/min 20 min	195 m (graded protocol)	CCAO + EX showed longer latency times in a step-down avoidance task than CCAO + SED	TUNEL-positive and Caspase-3 positive cells ↓ in CCAO + EX compared to CCAO + SED. Cell proliferation ↑ in CCAO + SED and sham + EX

TABLE 1: Continued.

Reference	ABI model	Animal, gender (age/weight)	Exercise type	Intervention start*	Dose parameters	Mean daily exercise distance	Cognitive/emotional effects	Cerebral changes
Sim et al. [54]	CCAO	Mongolian gerbils, male (11–13 weeks)	Treadmill	Early (1st postinjury day)	4 weeks, 30 min/day. Speed: 2 m/min for the first 5 min, 5 m/min for the next 5 min, and 8 m/min 20 min	195 m (graded protocol)	CCAO + EX showed longer latencies in a step-down avoidance task than CCAO + SED	TUNEL-positive and Caspase-3 positive cells ↓ in CCAO + EX compared to CCAO + SED
Song et al. [51]	PT	Sprague-Dawley rats, male (10 weeks)	Swimming	Early (1 day postinjury)	4 weeks, 5 days/week, 20 min/day	N/A	No significant differences between any treatment groups and lesioned controls on a spatial acquisition task	Hippocampal SOD-levels ↑ and MDA-levels ↓ in all treatment groups compared to lesioned controls. Number of cells in CA3 ↑ in the treatment groups compared to controls
Winocur et al. [44]	IRR	Long Evans rats, male (5 months)	Running wheel	Late (25th postinjury day)	25 days total, 24-hour daily access	IRR + EX: 8.4 km; sham + EX: 3.6 km	No group differences in visual discrimination task acquisition. IRR + EX in high-interference group performed significantly better in retention task than IRR + SED in low-interference group. Sham + EX performed significantly better in retention task than Sham + SED	Exercise ↑ hippocampal DCX and ki67 in all groups
Wong-Goodrich et al. [43]	IRR	C57BL/6 mice, female (8 weeks)	Running wheel	Late (1 month postinjury)	111 days total, 8–12-hour daily access	IRR + EX: 0.56 km; sham + EX: 0.52 km	IRR + EX: longer latency to complete spatial acquisition task on day 1; by day 3 no group differences. IRR + EX also showed improved task retention. No group differences in tail suspension test	No group differences in dentate gyrus size. Hippocampal BrdU- and NeuN-positive cells ↑ in IRR + EX. Levels of TNF-α, INF-γ, and IL-6 ↑ in IRR groups. Levels of IGF ↑ in IRR + EX compared to IRR + SED. Levels of BDNF and VEGF ↓ in IRR + EX and IRR + SED. Running partially restored VEGF-levels in IRR

TABLE 1: Continued.

Reference	ABI model	Animal, gender (age/weight)	Exercise type	Intervention start*	Dose parameters	Mean daily exercise distance	Cognitive/emotional effects	Cerebral changes
Wu et al. [38]	FPI	Sprague-Dawley rats, N/A (200–240 g)	Running wheel	Early (postinjury day 0)	12 days total, daily access: N/A	N/A	FPI + EX + REG and FPI + SED + DHA did significantly better in a spatial acquisition task compared to FPI + SED + REG. FPI + EX + DHA did significantly better than all other FPI groups	Levels of DHA, Acox1, 17 β -HSD4, Sir2, iPLA2, and p-TrkB \uparrow and 4-HHE \downarrow in FPI groups subjected to either EX or DHA; this was even more pronounced in FPI + EX + DHA compared to FPI + SED + REG. Levels of STX-3 and BDNF \uparrow in FPI + EX + DHA

* Early: postinjury days 0–6; late: postinjury days 7 and onwards. [†] Data from personal communication with corresponding author. CCAO: common carotid artery occlusion; CCI: controlled cortical impact; CHI: closed head injury; DHA: docosahexaenoic acid diet; earlyEX: early initiated exercise; EX: exercised animals; FPI: fluid percussion injury; highEX: high intensity exercise; IRR: irradiation; lateEX: late initiated exercise; lowEX: low intensity exercise; MCAO: middle cerebral artery occlusion; ModEX: moderate intensity exercise; N/A: information not available; NTI: neurotoxic injury; PT: photothrombosis; REG: regular diet; RW: running wheel exercise; SED: sedentary (nonexercised) animals; Sham: nonlesioned animals; SWIM: swimming exercise.

through counteracting membrane damage and coordinating DHA metabolism.

Contrary to these results, Griesbach et al. [39] found that animals exposed to IFPI and early initiated exercise (from post-injury day 0) performed significantly worse on a spatial acquisition task in a water maze than all other groups, including an IFPI group starting exercise at a later point in time (at postinjury day 14) and IFPI nonexercised controls. Animals exercised later performed at the level of the sham operated animals. During a retention test (probe trial), all IFPI animals performed worse than noninjured animals, regardless of exercise treatment. The late exercise and sham groups showed increased hippocampal levels of the transcriptional regulator phosphorylated cyclic AMP response element-binding protein (pCREB) and BDNF. Moreover, there was a positive correlation between BDNF-levels and the amount of exercise. No BDNF-increase was seen in the early exercised group, which also showed lower levels of Synapsin-I (involved in synaptic vesicle clustering and release) and CREB.

Also finding detrimental effects, Crane et al. [40] subjected animals to a cortical contusion injury immediately followed by a 7-day running wheel exercise regimen. In a complex stop-signal reaction time task (a conditioning-based learning task requiring either inhibition or execution of a learned behavior depending on stimuli given), the exercised animals performed significantly worse for the first five test days compared with both the nonexercised injured animals and the sham animal groups. However, after a week of testing, the exercised animals returned to their baseline levels. The contused, exercised animals showed larger inflammatory responses (more GFAB and IBA1 positive cells) in the cortex and hippocampus, respectively. All contused groups had fewer surviving cells (less DAPI positive cells) in the cortex, hippocampus, mediodorsal nucleus of the thalamus, and corpus callosum compared to the nonexercised, sham animals.

The conflicting results of the two first studies are somewhat surprising, as they use similar models and setups. Discrete differences, for example, in the duration of the exercise protocol, could potentially account for these divergent findings. While the studies by Griesbach et al. [39] and Crane et al. [40] both found detrimental effects of early exercise on cognitive performance, it appears that these effects are transient, as the animals seem to catch up during the rather short-time course of task acquisition.

Initiating exercise a little later after injury, Luo et al. [41] subjected C57/BL6 mice to middle cerebral artery occlusion (MCAO) followed by a one week postinjury break. Subsequently, the animals were exercised for 39 days in either running wheels or by swimming in a circular pool before starting a spatial acquisition task in a water maze. The MCAO running group found the platform significantly faster than the nonexercised MCAO group. This was not the case for the swimming group, whose performance did not differentiate from the nonexercised MCAO group. Progenitor cell survival in the dentate gyrus and pCREB levels were increased in the MCAO running wheel group compared to the control group. This suggests that different exercise types can affect cognitive

recovery differently and that voluntary exercise initiated after the first postinjury week can induce functional recovery and help promote cell survival.

However, in another study by Piao et al. [31] starting exercise 1 week after injury did not produce similar results. Examining the timing effects of a 4-week running wheel regimen after controlled cortical impact injury (CCI), animals were exercised beginning either 1 week ("early") or 5 weeks ("late") postinjury. The study found that the late exercised CCI-group had a significantly reduced latency to find the platform in a spatial water maze learning task and better retention of the task compared to a nonexercised CCI-group. In a reversed platform test, a test of cognitive flexibility, they found that the late exercised animals showed a significant improvement compared to both the early exercised CCI-group and the nonexercised CCI-group. Retention of the reversed platform task was significantly better in the late exercised CCI-animals compared to the nonexercised CCI-group. There were no differences between the early initiated group and the nonexercised CCI-group on any of the above parameters. In a novel object recognition task, the late exercised CCI-animals spent significantly longer time exploring a new object than both the early exercised CCI-group and a nonexercised CCI-group, indicating improved short-term memory abilities; in fact their exploration time was at the level of uninjured, naïve animals. There were no group differences in locomotor activity in an open field test. In a tail suspension test, all CCI-groups showed increased immobility times regardless of exercise status, suggesting more pronounced behavioral despair due to injury. Furthermore, the late exercised CCI-group had a reduced lesion size compared to the early exercised CCI-group and the nonexercised CCI-group. There were time-dependent increases and decreases in different microglia activation markers: IL-1 β levels (a proinflammatory marker) increased in the early exercise group in week 5 after CCI and levels reduced in the late exercise group in postinjury week 9 (both compared to the nonexercised CCI-group). There were also increased levels of IL-6 (a proinflammatory marker) and IL-10 (an anti-inflammatory marker) in the late exercise group in week 9. Cortical (ipsilateral) Galectin-3 and C1qB levels (microglial activation markers) were increased in the early exercised animals, while they were reduced in the late exercised group together with levels of gp91phox and p22phox (membrane components of NADPH oxidase enzyme). Late exercise increased hippocampal CREB gene expression, BDNF, and IGF-1 (insulin-like growth factor 1) levels and increased neurogenesis and cell survival in the late exercise group (but not in the early exercise group). The study concludes that the improved cognitive performance in the group subjected to late exercise is possibly due to a more optimal coordination/balance of microglia expression and increased growth factor levels.

Similar to studies initiating exercise immediately after ABI, starting a voluntary exercise paradigm one week after injury produces conflicting results, suggesting that the exercise type (voluntary versus forced) is not the only factor determining the efficacy of exercise.

As already mentioned, Griesbach et al. [39] found improved cognitive performance in animals exercised 14 days

after injury. In a later study, Griesbach et al. [42] reproduced this finding. Animals exercised 14 days after IFPI acquired a spatial learning task in a water maze significantly faster than nonexercised IFPI animals. In addition, they reached six out of seven criterion scores (e.g., reaching a platform from 10 sec down to 4 sec) significantly faster than the nonexercised IFPI group. Exercise increased hippocampal levels of BDNF in all animals regardless of lesion status. However, mBDNF and CREB levels were higher in the IFPI exercised animals than in the IFPI control animals. This also held true for the exercised sham animals, who showed increased levels of Synapsin-I. When blocking trkB receptors in IFPI animals, the exercise-induced increase in mBDNF was reduced. The two studies by Griesbach et al. [39, 42] suggest that voluntary exercise started at a later stage (14 days) is beneficial for cognitive recovery, possibly through upregulation of BDNF and downstream effectors of synaptic transmission.

Wong-Goodrich et al. [43] subjected female C57BL/6 mice to whole brain irradiation (5 Gy, single dose). The animals were then given access to running wheels outside of their home cages for 8–12 hours a day, starting 1 month after irradiation. Prior to initiation of exercise, all animals were tested in a spatial learning and retention test in a Barnes maze as well as a tail suspension test. After 6 weeks of wheel running, the animals were once again tested in the Barnes maze (both 3 and 4 months after irradiation) and in the tail suspension test (2.5 months after irradiation). Results from the first testing period in the Barnes maze (preexercise) showed no differences between the groups: the sham animals learned the task by day 2, the irradiated animals by day 3. There were no differences in retention as assessed by probe trials. The tests performed after exercise showed that irradiated, exercised animals had longer latency to complete the task on the first test-day compared to all other groups; however, by day 3 there were no differences. The irradiated, sedentary animals did not exhibit target quadrant preferences in retention trials (which they did during the first test period). However, the irradiated, exercised animals spent more time in the target quadrant, indicating improved memory. This picture was also seen on the test performed 4 months after irradiation. There were no differences between the groups in immobility times in the tail suspension test at any test point. Histology showed no differences in dentate gyrus size in any of the groups. Running elevated the number of hippocampal BrdU and NeuN positive cells (markers of newborn cells and mature neurons, resp.) in the irradiated animals. Levels of proinflammatory cytokines (tumor necrosis factor- α (TNF- α), interferon- γ (IFN- γ), and interleukin-6 (IL-6)) were elevated in the irradiated groups (compared to shams). Levels of IGF were increased in the irradiated, exercised animals compared to irradiated, sedentary animals. Levels of BDNF and VEGF (vascular endothelial growth factor) were decreased in all irradiated animals (both exercised and nonexercised). However, running partially restored VEGF-levels in the irradiated, exercised animals. The study shows that later-initiated voluntary running can prevent memory decline at a later stage in irradiation-exposed animals.

Showing similar positive recovery effects of late-initiated voluntary exercise after brain irradiation, Winocur et al.

[44] irradiated adult rats at a single dose of 8 Gy. Twenty-five days after irradiation approximately half the animals were allowed to exercise in running wheels in their home cages. After two weeks of running, all animals were tested in a visual discrimination task in a water maze, followed by either a high-interference task (an unsolvable task) or a low-interference task (demanding no visual discrimination for task solution). Lastly, a retention test for the original discrimination task was performed. There were no differences between the groups in acquiring the visual discrimination task. In the retention task, the irradiated animals had the most errors; this was especially pronounced in the animals that had previously performed the high-interference task. Further analysis showed that irradiated, exercised animals in the high-interference group performed significantly better in the retention test than the irradiated, sedentary animals in the low-interference group. The exercised, sham animals performed better in the retention test than the sedentary sham animals regardless of interference group affiliation. Analysis of hippocampal DCX and ki67 positive neurons (neurogenesis markers) showed that irradiation decreased their levels, but running increased the levels in all exercised groups. The authors conclude that neurogenesis is a part of the mechanism that controls memory interference, as suppressing neurogenesis disrupts retention in the high-interference groups. However, this effect can be diminished by promoting neurogenesis through exercise.

While three studies found cognitive improvement in animals starting exercise 25 days after injury or later [31, 43, 44], Clark et al. [45] administered running wheel exercise between 114 and 142 days after gamma irradiation of the hippocampal area of both male and female C57BL/6J mice. They found that 54 days of wheel exercise did not have an effect on spatial learning and retention in a water maze in the gamma radiated group compared with a nonexercised radiated group. Running did, however, have a positive effect on sham operated animals. In a contextual fear conditioning test, running increased freezing time (indicating increased memory of a formerly presented painful stimulus); however, this was regardless of radiation status. In other words, in the spatial tasks no effects of exercise were found in the irradiated animals, yet running did improve performance in the conditioning task in all exercise groups. Running increased hippocampal neurogenesis regardless of lesion status. Exercise counteracted radiation-induced reductions in neurogenesis, neuronal differentiation, and glia cell levels.

Five studies [31, 39, 42–44] found positive effects of later initiated voluntary exercise on measures of spatial learning and retention. However, this was not the case in the study by Clark et al. [45], who waited 3–4 months with exercise administration. This opens the question whether there is a window of rehabilitation opportunity that closes after certain amount of time has passed. Other factors could also account for the conflicting results such as different injury types and duration of exercise. Interestingly, running affected performance positively in the fear conditioning task in the Clark et al. study, indicating that exercise effects can be task specific.

All in all, the above research shows a somewhat mixed picture of using voluntary exercise in cognitive rehabilitation after ABI. Later starting points (from 14-days post-injury) appear to have the most consistent effects on cognitive recovery. However, further research is needed to determine if exercise interventions can be administered too late to produce cognitive improvements. Moreover, caution should be taken in making general recommendations based on such a limited and methodologically diverse set of studies. The results indicate that the voluntary aspect of exercise is not the sole determinant of effect; other variables such as starting point and duration may also play a significant role.

3.2. Forced Exercise. Fourteen studies have looked into the effects of forced exercise on cognitive recovery after ABI.

Itoh et al. [46] subjected rats to CCI injury followed by a 7-day treadmill exercise regimen beginning one day after injury. In acquisition and retention of a spatial task in a water maze, the lesioned, exercised animals did significantly better than the lesioned, nonexercised animals; the former performing to the functional level of the sham animals. There was a significant reduction in lesion size in the exercised group compared to the controls. Additionally, there was a significant reduction in ssDNA immunopositive cells (a marker of apoptosis) around the damaged cortical area in the exercised group on postinjury days 1, 3, and 7, an increase in the number of NeuN positive cells, and a reduction in GFAP positive cells (marker for astrocytes) 7 days after TBI compared to the lesioned, nonexercised control group. This suggests that early initiated forced exercise can improve cognitive function while reducing apoptosis and impacting the glial scarring.

Cechetti et al. [47] looked at effects of both pre- and postinjury treadmill exercise in a bilateral common carotid artery occlusion (CCAO) rat model. The postinjury trained group started exercising 24 hours following surgery and continued for 12 weeks, 3 days a week. They found that all exercised groups, including the postinjury exercised group, did significantly better on three of the five testing days in acquisition of a spatial task in a water maze compared to a lesioned, nonexercised group. This pattern was also seen in a retention (probe trial) test and in a working memory test in a water maze. There were no differences between groups in levels of free radicals or SOD (superoxide dismutase, an antioxidant enzyme) levels. However, there were heightened hippocampal lipoperoxidation (evaluated by TBARS test) and thiol-levels (antioxidants) in the lesioned, nonexercised group compared to the other groups. Like the study by Itoh et al. [46], this study shows that early initiated forced exercise can positively affect cognitive recovery, potentially through reducing oxidative damage by regulation of antioxidant levels.

Shih et al. [48] subjected rats to right hemisphere MCAO. After 24 hours, the animals began exercising at either a low or a high-intensity (speed) on a treadmill for 14 days. They found that the lesioned, low-intensity group had shorter latencies on three out of the four testing days in a spatial learning task in a water maze (compared to the lesioned, high-intensity

group and a lesioned, nonexercised control group). The low-intensity group also showed better retention than the control group. Furthermore, the low-intensity paradigm increased levels of hippocampal BDNF, Synapsin-I (contralaterally), and PSD-95 (membrane scaffolding protein) as well as the dendritic complexity (measured by Sholl analysis) and the number of dendritic spines compared to the control group. There were higher levels of corticosterone (stress-hormone) in the high-intensity group compared to the controls. The study is interesting as it investigates the effects of exercise intensity on cognitive measures. While both groups initiated exercise 24 hours after injury, only the low-intensity group showed positive cognitive effects concomitant with increases in plasticity-related proteins and dendrite development. Furthermore, the high-intensity group displayed higher levels of stress-hormone, which may have inhibited the efficacy of exercise.

In another study investigating the effects of different exercise intensities, Shen et al. [49] subjected rats to CCI immediately followed by two different intensities of treadmill exercise for 14 days. They found that the lesioned, low-intensity group performed better on two out of the four days of the acquisition part of a spatial task in a water maze compared to the high-intensity group and a lesioned, nonexercised control group. The low-intensity group also showed better retention than the control group. On a neurological deficit score all CCI animals did worse than the sham animals, but they all improved by day 6 post-TBI. BDNF and phosphorylated CREB measurements showed higher levels in the contralateral hippocampus in the low-intensity group compared to the control group. There were no differences in measurements of Synapsin-I and CREB in any of the groups.

While the above studies suggest that early forced exercise can promote cognitive recovery, these results are not unchallenged. Hicks et al. [50] found that animals exposed to lFPI and 18 days of treadmill exercise initiated the day following injury differed in neither spatial acquisition nor retention tasks in a water maze compared to a lesioned, nonexercised group. They saw no differences between groups in neuromotor scores. They found increased BDNF mRNA levels in CA1 and CA3 in the exercised, lesioned animals compared to lesioned, sedentary animals. There were no differences in hippocampal injury or cortical lesion volume between groups. However, the left neocortex (ipsilaterally to the injury) was significantly smaller than the right neocortex in the nonexercised, lesioned animals compared to the exercised, lesioned animals. These results are in contrast to many of the above studies, as they fail to find cognitive effects of early initiated forced exercise, but do find BDNF and some histological effects of exercise.

The findings of Hicks et al. [50] were echoed by Song et al. [51], who used photothrombosis to induce cerebral stroke in rats. One day after injury the animals were swim-exercised in a circular pool for 4 weeks (a total of 20 days), or given Acetyl-L-carnitine (ALC) injections, or both. They found no significant differences in any of their treatment groups compared to lesioned controls on acquisition of a spatial task in a water maze tested the first, second, and fourth week after injury. Hippocampal SOD-levels were increased in all

treatment groups compared to the lesioned controls; these were significantly higher in the combined (exercise + ALC-injection) group in comparison to the other groups. MDA-levels (related to lipid peroxidation) were reduced in the treatment groups compared to the controls. Histologically, there were an increased number of cells in CA3 in the treatment groups compared to the controls.

Investigating emotional parameters, de Araujo et al. [52] exercised gerbils on treadmills either 12, 24, 48, or 72 hours after CCAO for 1 up to 3 days. In an open field, animals exercised 12 hours after injury showed a decreased number of field crossings and an increase in grooming (indicating increased anxiety and stereotyped behavior) compared to a nonlesioned, nonexercised group. There were no differences in any other groups. All CCAO animals showed a reduced time spent on a rotarod compared with the nonlesioned, nonexercised group. There were a decreased number of cells in CA1 and striatum in the group exercised after 12 hours compared to the group exercised after 24 hours. This study indicates that very early initiated short-duration exercise (12 hours after injury) can lead to increased anxiety-like behavior and cell death, while exercise starting 24 hours (or later) does not induce these emotional responses. Unfortunately, the experimental groups did not exercise the same amount. Exercise doses were decreased with later initiation points (down to a single 15 min session), making it difficult to decipher starting point effects from dose-related effects in the exercised groups.

Some studies have opted for exercise initiation two days after injury. After inflicting bilateral CCAO in gerbils, Sim et al. [53] found that treadmill exercise for 10 days resulted in longer latencies (i.e., better short-term memory for a noxious stimulus) in a step-down avoidance task than in a nonexercised, lesioned group. They also found reduced levels of TUNEL positive and Caspase-3 positive cells (markers for apoptosis) in the lesioned, exercise group compared with the lesioned, nonexercised group. Cell proliferation was increased in the nonexercised, lesioned group and the exercised, sham group, but not in the lesioned, exercise group. The authors hypothesized that this finding might be due to reduced cell death in the exercised group, reflected in less cell proliferation. In a later experiment, using the same injury model but a longer exercise regimen (4 weeks, starting on the first postinjury day), Sim et al. [54] found that the lesioned, exercised animals did better than the nonexercised lesioned group in the step-down avoidance task. The exercised, lesioned group presented with fewer TUNEL and Caspase-3 positive cells than the nonexercised, lesioned group. The studies indicate that exercise might protect the brain from neuronal cell death, which could play a part in the functional recovery. Interestingly, this finding goes for both a shorter and longer duration exercise paradigm at the same running speed.

Chen et al. [55] exposed rats to hippocampal injury via unilateral kainic acid injection to the CA1 area. Starting on the second postinjury day, the animals were exercised in a motorized running wheel for seven consecutive days at one of three different intensities: light, moderate, and heavy. Exercise took place twice a day (morning and afternoon) for

30 minutes. The animals were then tested in a conditioning (pain-avoidance) learning task in a Y-maze for one session of 20 trials. The study found that lesioned animals that had been exercised at moderate intensity performed significantly better in the learning task than nonexercised, lesioned animals, as well as showing significantly higher numbers of BrdU positive cells. There were no learning or BrdU staining differences between the other lesioned, exercised groups and the nonexercised, lesioned animals. Furthermore, a positive correlation between learning and BrdU positive labelled cells in the dentate gyrus was found, indicating that neurogenesis may have supported the functional recovery.

Positive recovery effects of second day postinjury initiation were also found by Kim et al. [56]. Using electromagnetic contusion in rats followed by 10 days of treadmill exercise, they found that lesioned, exercised animals had shorter latency times in a step-down avoidance test than a lesioned, nonexercised group, indicating better (short-term) memory for a noxious stimulus in the exercised group. Measurements of hippocampal DNA fragmentation (a marker for apoptosis), Caspase-3, and Bax (pro-apoptosis molecules) showed reduced levels in the lesioned, exercised group compared to the lesioned, nonexercised group. Levels of Bcl2 (antiapoptosis molecules) were increased in the lesioned, exercised group compared to the control group. There were no differences in corticosterone levels between the groups. Besides improvement in short-term memory, the study, like those by Sim et al. [53, 54], shows effects on markers of apoptosis further supporting the assumption that enhanced functional recovery after exercise could be mediated by regulation of neuronal cell death mechanisms.

Chen et al. [57] compared the timing of treadmill exercise initiated two days (early, for either 7 or 14 days) or nine days after injury (late, for 7 days) in a closed head injury mouse model. In an object recognition task, they found that the early initiated groups spent significantly more time exploring a new object compared to a lesioned, nonexercised group indicating better memory for the previously encountered object. The late initiated group and the nonexercised, lesioned group spent less time exploring the new object than the sham animals. Furthermore, early exercise hindered progressive cell loss in the cortex and the hippocampus to a larger extent than in the late exercised group. Early exercise boosted neurite regeneration in the early postinjury stages, but late exercise only hindered later stage cell loss. Early exercise for 14 days restored the lesion-induced reduction in BDNF and MKP-1 (an anti-inflammation marker). When animals were given triptolide (a MKP-1 synthesis inhibitor) neither this nor cognitive recovery was seen; however, there were positive effects on neuronal loss and neuroinflammation. These findings show that different starting points can generate different outcomes in short-term memory, cell survival, and plasticity-related protein levels.

Starting exercise on the fourth day after injury, Shimada et al. [58] subjected rats to left MCAO followed by one of two different treadmill intensities (low or high) for 28 days. In both an object recognition and an object location task, the low-intensity group spent more time exploring the novel object/newly placed object than the lesioned, nonexercised

control group. The high-intensity group explored less than the low-intensity group. In a passive avoidance test, both exercise groups showed longer latencies than the controls, indicating that exercise resulted in better memory for noxious stimuli. An open field analysis did not reveal any locomotor differences between the groups. Exercise reduced lesion size, but there were no differences between the intensity groups. Both intensity groups had increased number of neurons in the dentate gyrus compared with the controls and the shams; this was higher in the ipsilateral dentate gyrus in the low-intensity group versus the high-intensity group. In the ipsilateral dentate gyrus, MAP-2 levels (microtubule-associated protein 2) were increased in the low-intensity group compared to the controls. MAP-2 was lower in the high-intensity group compared with the low-intensity group and the shams ipsilaterally in all examined hippocampal areas. Contralaterally, the levels were lower in CA1 and CA3 in the high-intensity group than in the low-intensity group. The findings of this study echo the findings of Shih et al., Shen et al., and Chen et al. [48, 49, 55] underlining the potential differential effects of varying exercise intensities in the early stages of recovery. As in the studies by Shih et al. and Shen et al., this study shows that low-intensity forced exercise is able to produce cognitive recovery effects after ABI; however, in this study there were also positive effects of high-intensity exercise on one of the cognitive parameters (passive avoidance).

Two studies have begun forced exercise 1 week after ABI or later. The previously mentioned study by Luo et al. [41] compared a forced exercise protocol (swimming) with a voluntary exercise protocol starting one week after MCAO. They found no cognitive effects of the forced exercise paradigm. Chen et al. [57] (see above) did not find any effects of exercise starting 9 days after injury on cognitive parameters. This opens the question as to whether there exists a window of opportunity for rehabilitation via forced exercise that closes after a certain time point. Compared to what appears to be the case regarding voluntary exercise, this window may be substantially smaller.

The studies of forced exercise, like those of voluntary exercise, show a somewhat conflicting, pattern of outcome. Though only one study shows detrimental effects (in one group) on anxiety-related behavior, the above studies generally show that especially early forced exercise can lead to improvement in animals exposed to low or moderate intensity exercise. One may therefore ask whether exercise needs to be maintained at a certain intensity level in order to produce cognitive gains. Neither of the two studies using swimming exercise produced cognitive recovery effects. However, more studies are needed to determine whether this is a result of the type of exercise or protocol related issues. Unfortunately, only two studies investigated effects of exercise starting later than a week, leaving us with limited knowledge about the effects of forced exercise initiated at a later stage.

4. Sooner or Later?

As already described, the above research varies in the time points of exercise initiation. Of the 22 studies included in this

overview, we find that 16 studies had experimental groups starting exercise from postinjury days 0–4, while eight studies had experimental groups starting exercising at the earliest from postinjury day 7.

Examining common traits or dissimilarities of the early intervention groups with positive or no effects does not render a clear picture. Almost all early initiation studies with positive effects of exercise on cognition use forced exercise paradigms. However, as early initiation voluntary exercise studies are much fewer in number, this might be a paradigm bias. Moreover, the studies vary on most parameters including types of injury and animal as well as exercise duration and intensity.

The three studies showing groups with adverse effects [39, 40, 52] started exercising the animals immediately after injury, that is, within the first 24 hours. They also had fairly short duration exercise protocols (3 or 7 days). This indicates that very acute, relatively short duration exercise can induce unwanted effects. However, positive cognitive outcomes using very early exercise have also been reported [38] (see above).

Later initiation studies are fewer and with starting points spanning from 1 week to almost 4 months after injury; it is difficult to obtain a coherent picture. Studies with groups starting 7 to 9 days after injury [31, 41, 57] showed either positive and/or no effects, and a 14 day postinjury start showed cognitive improvement effects in two studies [39, 42]. Starting at even later time points showed some variability: starting 25–30 days post-ABI induced positive effects in three studies [31, 43, 44], while an approximately 4-month postinjury start generated both an improvement and no effects depending on the cognitive measure [45]. Thus it would appear that later initiated exercise, in most cases, can promote cognitive recovery. However, once again, there are considerable methodological variations between the studies.

It is quite surprising that we know relatively little about the cognitive effects of exercise starting relatively late post-TBI. In clinical rehabilitation settings exercise is often initiated in later recuperation stages, when patients are stabilized and able to perform physical activities. It therefore seems clinically relevant to further investigate the potential effects of late-initiation exercise.

5. Easy Does It?

Exercise dose encompasses many variables including total length of intervention (how many days), session duration (how many minutes), distribution (how often), distance moved (how far), and intensity (how fast).

In the 22 studies included in this review, the total length of intervention varied considerably, ranging from 1 day to almost 4 months. Regarding individual session durations, most of the voluntary exercise studies gave the animals unlimited access to the running wheels, that is, 24 hour access. The forced exercise paradigm sessions lasted between 5 min and 1 hour; eight of those studies used 30 min session durations. By and large, the animals exercised/or had access to exercise apparatuses on a daily basis throughout

the intervention period except in two studies that distributed the intervention somewhat differently [47, 51], as well as one study that exercised animals twice daily [55].

Average group distances and/or intensities are not stated in all studies (see Table 1). This information is provided in five voluntary paradigms and 12 forced paradigms. Intensities are mostly reported in meters exercised *pr. minute* and often vary within individual exercise sessions or over days/weeks. In some cases, exercise duration (number of minutes) is increased over a period of days. While such graduation of intensity or duration of exercise might in itself be an important rehabilitative factor, the individual protocols vary too much for meaningful comparisons to be carried out. When calculating mean daily/session distances over the total duration of exercise, they range between 97.2 m and 8.4 km. Such a wide variation is also found in the total exercise distances over time (i.e., total distance over all exercise days/sessions) that range from 150 m to 313.2 km.

Four studies explicitly examined the cognitive effects of different exercise intensities [48, 49, 55, 58]. Interestingly, all of these studies found that the low or moderate exercise intensity groups produced positive results, while the higher intensity groups did not produce any results (or only produced results in one test [58]) (see above). This indicates that intensity is indeed an important factor when using exercise as a cognitive rehabilitation tool. While it would appear that average doses up to around 250 m daily in many cases produce positive results [31, 48, 49, 53, 54, 56, 58], this is not always the case [31, 52, 55]. The picture becomes more blurred when using higher daily doses. In the studies specifically looking into exercise intensities, daily doses exceeding an average of 320 m daily did not produce cognitive results in three of the studies. It did, however, produce positive results in one study [55]. In other cases [43, 44, 46, 47, 57] average session distances of 320 m and above improved cognitive recovery, but this was in some cases contingent upon other variables such as starting point. In some studies, doses exceeding 320 m daily did not produce any results on the spatial tasks [45, 50] or had detrimental effects [40].

Interestingly, in the case of the Chen et al. study [55], the moderate exercise group (that showed positive recovery effects) ran 180 m twice daily, making the individual exercise trials fall below the 320 m mark (but the total daily running distance was slightly above). However, their heavy intensity group ran 324 m twice daily (to a total of 648 m) and did not show recovery effects. One may therefore ask whether total running distances are a good dose measure, or whether the intensity of individual training trials are of more importance for cognitive recovery. Although an unresolved matter, this could be another explanatory factor for the differential results in studies examining voluntary running effects, where intensity and duration of individual running bouts are not experimentally controlled.

All in all, the substantial variations in exercise protocols among the studies make it difficult to make general dose recommendations. While it does appear that dose, duration, and intensity are important factors for cognitive recovery, more systematic research looking into these aspects and how

they interact with other variables such as starting point is needed to elucidate this further.

6. Post-ABI Exercise and Brain-Derived Neurotrophic Factor (BDNF)

While many neural mechanisms behind the effects of exercise are being investigated, special attention has been given to neurotrophic factors, in particular BDNF. BDNF is highly expressed in the cortex and hippocampus and is involved in many neural processes including neuronal differentiation and survival, as well as axonal path-finding [59]. Furthermore, the relationship between forced exercise and stress-hormone levels has garnered considerable interest. In the following these topics will be investigated further in relation to exercise type, timing, and intensity.

6.1. Exercise Type, BDNF, and Stress-Hormone. In relation to exercise type, a special focus has been placed on the connection between exercise and the release of stress-hormones, as forced exercise is believed to be more stressful than voluntary exercise. However, studies dealing with this topic show somewhat inconsistent results. Griesbach et al. [60] found that early stage postinjury forced exercise elevated corticosterone and ACTH levels in IFPI animals. This was not the case in a group exercised in a voluntary paradigm. Neither exercise regimens elevated BDNF-levels. In another experiment starting exercise at a later stage, Griesbach et al. [61] found that forced exercise stimulated the corticotrophic axis in all animals. BDNF-levels were unaffected by forced exercise, yet they were elevated in all rats exposed to voluntary exercise. In two other studies [42, 62] the same lab also found an increase in BDNF-levels as a result of voluntary exercise. Similarly, Ke et al. [20] found that voluntary exercise improved motor function and elevated BDNF-levels, an effect not seen in the group exposed to forced exercise, although these animals did present higher levels of corticosterone. Wong-Goodrich et al. [43] did not see any exercise-related BDNF-changes in their late voluntary paradigm; however, they did find that the intervention improved cognition in their irradiated animals.

Several studies using forced exercise after TBI have found BDNF-elevations [21, 57, 63–65], indicating that forced exercise paradigms can increase BDNF-levels after injury. Using both forced and voluntary exercise, Ploughman et al. [66] found that corticosterone levels were elevated in all exercise groups but were highest in animals exposed to forced exercise running at greater speed or duration. Exercise did not increase BDNF, IGF-1, or Synapsin-I in the ischemic hemisphere. Furthermore, they found that voluntary exercise decreased serum levels of IGF-1 and increased hippocampal levels of IGF-1 in the ischemic hemisphere. Shih et al. [48] (see above) also found corticosterone elevations in their high-intensity group. However, in the study by Kim et al. [56] (see above), no differences in stress-hormone levels were found between the treadmill exercised and nonexercised groups. Ploughman et al. [67] found that forced exercise created a rapid, but more short-lived BDNF-increase compared to

voluntary exercise. The group exposed to forced exercise also showed increased levels of corticosterone in several brain regions.

Thus, it appears that forced exercise does lead to elevated stress-hormone levels. When it comes to impact on BDNF-levels, the picture is more unclear. It seems that the type of exercise (voluntary or forced) cannot solely account for variation in neurotrophic factor levels, but other factors such as timing and intensity are also key players. How stress-hormones and neuroplasticity-related proteins are affected by exercise, how they interact, and, importantly, what consequences this has for functional recovery remain to be resolved. As discussed above, though the efficacy of forced exercise on cognitive parameters is inconclusive, detrimental effects on cognition are practically unseen. This poses the question of whether elevations in stress-hormones during physical activity are necessarily harmful when it comes to the recovery of cognitive functions.

6.2. Exercise Starting Point and BDNF Responses. Like exercise type, some research indicates that starting point affects BDNF-levels after ABI. Early exercise initiation (defined here from day 0–6 postinjury) has been shown to elevate BDNF-levels in several studies [21, 50, 57, 62, 63, 65]; in some cases this elevation is also dependent upon exercise intensity [48, 49] (see below) or type of exercise [20, 67] (see above). In other cases, early exercise did not affect BDNF-levels [38, 39, 60]. Later post-ABI exercise (defined here from postinjury day 7 and onwards) has also been shown to produce BDNF-elevations [31, 39, 42], in some cases this is dependent on type of exercise [60] or injury severity [68]. A few studies have found that later initiated exercise did not produce BDNF-elevations [31, 43, 57].

These studies indicate that both early and later initiated exercise regimens can increase BDNF-levels in some cases. Whether such BDNF-elevations are part of the neural processes mediating cognitive recovery is still unclear. Griesbach et al. [39] did not find BDNF-elevations after early initiated exercise and this group also showed delayed learning. Wu et al. [38] found no BDNF-effects either but did see improvements in their cognitive measure after early initiated exercise. Reversely, Hicks et al. [50] found BDNF-elevations after early initiation, but no cognitive effects. Chen et al. [57] found elevated BDNF-levels (in their early initiated group running for 14 days) as well as a cognitive improvement. Shih et al. [48] and Shen et al. [49] also found both BDNF-elevations and cognitive improvements (in their low-intensity running groups).

Initiating exercise at later points, Griesbach et al. [39, 42] found BDNF-elevations and concomitant cognitive improvement. The same holds for the study by Piao et al. [31]; however only in one of their two (late) exercised groups. Wong-Goodrich et al. [43] found no exercise-related BDNF-level changes in their irradiated animals; they did, however, find a cognitive improvement.

It seems that the relationship between BDNF-responses and cognitive recovery outcome at different exercise initiation points is still largely unresolved. Currently, there are

a limited number of studies investigating this, underlining a need for additional research.

6.3. BDNF and Post-ABI Exercise Intensity. Not many studies have investigated the relationship between BDNF-levels and exercise intensity in post-ABI exercise. Shih et al. [48] and Shen et al. [49] found hippocampal BDNF-elevations (contralaterally) in their low-intensity exercise groups concomitant with cognitive improvement. In a study by Ploughman et al. [66], rats were subjected to focal stroke using endothelin-I. After 4 days of recovery, the animals were given either a 30 min or a 60 min walk in a motorized running wheel (both 11 m/min), a 30 min run in a motorized running wheel (14 m/min), or a 12-hour voluntary run in a (nonmotorized) running wheel. The animals in the 30 min motorized walking group and the voluntary running group had increased hippocampal BDNF-levels (in the noninjured hemisphere) compared to noninjured, nonexercised animals. Furthermore, the 30 min walking group showed increased BDNF-levels in the intact sensorimotor cortex compared to the 60 min walking group and nonexercised animals. Placed together, these studies indicate that exercise of a lower intensity can increase BDNF-levels in areas contralaterally to the inflicted injury. However, intensity and duration of intervention (and thereby total distance run) vary between the studies, restricting what overall information can be derived regarding the relationship between BDNF and post-ABI intensity parameters.

7. General Considerations

The above studies provide some information as to the effects of exercise on cognition in the brain injured individual. They also stress some of the parameters that are important for the efficiency of this intervention. However, there are still many unresolved issues.

Voluntary and forced exercise paradigms vary on parameters of choice of movement and, potentially, level of stress-hormone activation. The studies included in this review also reveal other differences between the two exercise paradigms. Most of the voluntary paradigms allow animals access to the exercise apparatus in their home environment, while the forced paradigms require moving and handling of the animals to initiate (and sometimes prompt) exercise. Whether such environmental differences can affect the outcome in terms of cognitive recovery will have to be clarified in the future.

In all but two of the studies using voluntary exercise, animals were housed individually either permanently or during intervention. Most of the forced exercise studies do not report housing conditions; however those that do have animals pair or group housed. Some studies have looked into the effects of social deprivation and exercise in animals. Stranahan et al. [69] found that both single and group housed male rats had corticosterone elevations due to running. However, only group housed animals also presented increased neurogenesis induced by running. When exposing these animals to additional stressors, the socially isolated animals

showed decreased neurogenesis compared to the controls. In another study using female rats, Leasure and Decker [70] found that social isolation suppressed the cell-proliferation effects of exercise that were seen in group housed animals. Furthermore, there was a correlation between BrdU+ cells and the running distance in the group housed animals, but not in the single housed animals. In a study looking into the emotional effects of housing, Berry et al. [71] found that single housing triggered anxiety and depression-like behaviors in the animals, increased HPA-axis reactivity, and reduced BDNF-levels. Such findings indicate that housing-paradigms (and animal gender) can influence the effects of exercise as well as emotional reactivity. Whether single housing would also influence cognitive performance in animals subjected to ABI remains unknown. It is therefore relevant to investigate whether cognitive effects in exercise studies using single housing are related to the exercise intervention per se, boredom-factors due to isolation, or other variables.

Furthermore, there are considerable differences in relation to exercise dose and duration. Animals in the voluntary paradigms have 24-hour access to the exercise apparatuses (except in one study) and can administer their treatment when they choose and in the intensity and duration that they prefer. This is a marked difference from forced exercise paradigms that mainly offer single exercise bouts of limited duration (up to 1 hour) under controlled running speeds. These differences underline that paradigms of voluntary and forced exercise vary on many variables that can affect the cognitive (and neural) outcome.

Epidemiological research shows that premenopausal women have decreased risk of stroke compared to age-matched males as well as to postmenopausal women [72]. Animal studies have shown that female hormones regulate and protect against a variety of pathological processes associated with stroke [73]. Both estrogen and progesterone have been shown to have neuroprotective effects after stroke in animal models [73, 74]. This indicates that gender-specific hormonal environments can influence the recovery outcome after brain injury. However, all but two of the studies discussed in this review use male animals (see Table 1), leaving us with very limited data about the effects of exercise in the traumatized female brain.

The type and severity of injuries in the above studies are quite different. Some types of injury cause more focal tissue damage; others are more wide-spread and diffuse in nature. Some injuries are unilateral, while some affect both hemispheres. The studies using cerebral ischemia models inhibit blood flow for varied time periods. The studies using traumatic brain injury models (i.e., an external force afflicting the brain) use different techniques, impact velocities, and depths of compression. The models inducing injury by irradiation use different doses and afflict different cerebral areas. As different types of brain injury and injury severities can cause different injury patterns, both in terms of tissue responses as well as their spatial and temporal occurrence [75], this can also affect the efficacy of the employed exercise protocols.

Another issue relates to the genetic make-up of the experimental animals. Much research has shown that the

same brain injury method can induce significantly different cerebral (and behavioral) responses depending on the rodent strain/stock used [76–90]. Even animals of the same stock, but purchased from different breeders, have been shown to differ in their cerebral responses when exposed to the same injury [91–93]. Thus, strain/stock choice is an important factor to take into account when assessing brain injury outcomes as well as the efficacy of treatment interventions. In the 22 studies included in this review, six different rodent strains/stocks were used (see Table 1). However, due to the considerable procedural differences in performing “the same” brain injury (see above) as well as substantial interstudy variations in the exercise protocols and outcome measures, meaningful comparisons of the studies on the basis of strain are very difficult to make. Further research is needed to elucidate the effects of strain on post-ABI exercise on cognitive recovery.

The applied cognitive tests are generally brief, limiting our knowledge to mainly short-term learning effects. Potential long-term effects of exercise have not been examined in any of the studies, leaving us with little knowledge as to whether the observed cognitive effects are lasting or transient. Furthermore, the majority of studies use tests that motivate learning through avoidance, that is, the ability to avoid an unwanted stimulus (escaping water or a previously presented painful stimulus). Testing animals in nonavoidance based tasks would help to clarify whether the outcome is related to the treatment or the method of testing.

Another discussion related to the cognitive tests pertains to the individual test protocols and setups. While many of the studies used spatial acquisition tasks in a water maze, the individual testing protocols were very varied, in terms of both number of acquisition trials and sessions. Such differences could potentially affect the learning outcome if some animals were to be trained more intensively than others [94]. Furthermore, the visual surroundings when performing spatial acquisition tasks (i.e., the number and salience of visual cues as well as their distance to the animals) have been shown to be of importance for both the neural substrate and cognitive mechanisms of task solution in rodents [95–97]. It is generally taken for granted that different cognitive tasks reflect different neural substrates and cognitive mechanisms. However, within what is generally considered the same cognitive tasks, various experimental and/or test setups can also vary with respect to the underlying neural and cognitive mechanisms [98, 99]. Consequently, what may superficially appear to be the same cognitive test may result in different cognitive recovery effects of a given exercise protocol; even minor variations in experimental setups can be essential. Thus, it appears that research in this area would benefit greatly from more homogenous use of cognitive tests/setups to facilitate comparisons between labs and help eliminate test protocol differences as a source of variation when assessing the effects of exercise on cognition.

Postinjury depression and anxiety are common after brain injury [100]. As already mentioned, exercise is often used in the treatment of depression and anxiety-related disorders.

It is known that depression can lead to cognitive impairment. However, whether these impairments are primarily psychosocially or neurobiologically founded, transient or enduring, is still debated [101]. Though some of the above studies have included tests of emotional behavior in their experimental protocols, we still know very little about how post-TBI exercise affects emotional states, and how this potentially affects cognitive performance. Knowing more about the relationship between injury-related emotional and cognitive problems will help to further clarify when (and in what way) exercise promotes cognitive recovery after ABI.

8. Conclusion

In this review we have examined the effects of exercise on cognitive measures after acquired brain injury in animal models. Although there is cause for optimism in using exercise as a rehabilitation tool in the treatment of cognitive sequelae after ABI, research in this area is still fairly limited. Overall, there is evidence that exercise in some cases can improve cognitive recovery. However, what distinguishes these cases from others that do not produce effects (or have adverse effects) remains unclear. Considerable variations in models and experimental protocols, including differences in animal strains, injury type, exercise type, post-injury starting point, dose-related differences, and cognitive measures, should presently warrant caution in making general protocol recommendations. More research is needed to clarify these issues as well as the potential long-term effects of postinjury exercise.

Conflict of Interests

The authors declare that there is no conflict of interests regarding the publication of this paper.

Acknowledgment

The present study was supported by a grant from the Danish Council for Independent Research.

References

- [1] A. Cordero, M. D. Masiá, and E. Galve, "Physical Exercise and Health," *Revista Española de Cardiología (English Edition)*, vol. 67, no. 9, pp. 748–753, 2014.
- [2] F. J. Penedo and J. R. Dahn, "Exercise and well-being: a review of mental and physical health benefits associated with physical activity," *Current Opinion in Psychiatry*, vol. 18, no. 2, pp. 189–193, 2005.
- [3] A. B. Pérez, "Exercise as the cornerstone of cardiovascular prevention," *Revista Espanola de Cardiologia*, vol. 61, no. 5, pp. 514–528, 2008.
- [4] G. Cooney, K. Dwan, and G. Mead, "Exercise for depression," *JAMA*, vol. 311, no. 23, pp. 2432–2433, 2014.
- [5] T. Josefsson, M. Lindwall, and T. Archer, "Physical exercise intervention in depressive disorders: meta-analysis and systematic review," *Scandinavian Journal of Medicine & Science in Sports*, vol. 24, no. 2, pp. 259–272, 2014.
- [6] J. C. Strickland and M. A. Smith, "The anxiolytic effects of resistance exercise," *Frontiers in Psychology*, vol. 5, article 753, 2014.
- [7] A. Ströhle, "Physical activity, exercise, depression and anxiety disorders," *Journal of Neural Transmission*, vol. 116, no. 6, pp. 777–784, 2009.
- [8] N. T. Lautenschlager and O. P. Almeida, "Physical activity and cognition in old age," *Current Opinion in Psychiatry*, vol. 19, no. 2, pp. 190–193, 2006.
- [9] P. J. Smith, G. G. Potter, M. E. McLaren, and J. A. Blumenthal, "Impact of aerobic exercise on neurobehavioral outcomes," *Mental Health and Physical Activity*, vol. 6, no. 3, pp. 139–153, 2013.
- [10] N. A. Khan and C. H. Hillman, "The relation of childhood physical activity and aerobic fitness to brain function and cognition: a review," *Pediatric Exercise Science*, vol. 26, no. 2, pp. 138–146, 2014.
- [11] L. B. Käll, M. Nilsson, and T. Lindén, "The impact of a physical activity intervention program on academic achievement in a Swedish elementary school setting," *Journal of School Health*, vol. 84, no. 8, pp. 473–480, 2014.
- [12] A. Singh, L. Uijtdewilligen, J. W. R. Twisk, W. van Mechelen, and M. J. M. Chinapaw, "Physical activity and performance at school: a systematic review of the literature including a methodological quality assessment," *Archives of Pediatrics & Adolescent Medicine*, vol. 166, no. 1, pp. 49–55, 2012.
- [13] D. Aarsland, F. S. Sardahae, S. Anderssen, and C. Ballard, "Is physical activity a potential preventive factor for vascular dementia? A systematic review," *Aging & Mental Health*, vol. 14, no. 4, pp. 386–395, 2010.
- [14] M. N. McDonnell, A. E. Smith, and S. F. MacKintosh, "Aerobic exercise to improve cognitive function in adults with neurological disorders: a systematic review," *Archives of Physical Medicine and Rehabilitation*, vol. 92, no. 7, pp. 1044–1052, 2011.
- [15] Y. Rolland, G. Abellan van Kan, and B. Vellas, "Physical activity and Alzheimer's disease: from prevention to therapeutic perspectives," *Journal of the American Medical Directors Association*, vol. 9, no. 6, pp. 390–405, 2008.
- [16] H. Öhman, N. Savikko, T. E. Strandberg, and K. H. Pitkälä, "Effect of physical exercise on cognitive performance in older adults with mild cognitive impairment or dementia: a systematic review," *Dementia and Geriatric Cognitive Disorders*, vol. 38, no. 5–6, pp. 347–365, 2014.
- [17] H.-C. Chang, Y.-R. Yang, P. S. Wang, C.-H. Kuo, and R.-Y. Wang, "Insulin-like growth factor I signaling for brain recovery and exercise ability in brain ischemic rats," *Medicine & Science in Sports & Exercise*, vol. 43, no. 12, pp. 2274–2280, 2011.
- [18] J.-Y. Chung, M.-W. Kim, M.-S. Bang, and M. Kim, "The effect of exercise on trkA in the contralateral hemisphere of the ischemic rat brain," *Brain Research*, vol. 1353, pp. 187–193, 2010.
- [19] J. Y. Chung, M. W. Kim, M. S. Bang, and M. Kim, "Increased expression of neurotrophin 4 following focal cerebral ischemia in adult rat brain with treadmill exercise," *PLoS ONE*, vol. 8, no. 3, Article ID e52461, 2013.
- [20] Z. Ke, S. P. Yip, L. Li, X.-X. Zheng, and K.-Y. Tong, "The effects of voluntary, involuntary, and forced exercises on brain-derived neurotrophic factor and motor function recovery: a rat brain ischemia model," *PLoS ONE*, vol. 6, no. 2, Article ID e16643, 2011.
- [21] M.-W. Kim, M.-S. Bang, T.-R. Han et al., "Exercise increased BDNF and trkB in the contralateral hemisphere of the ischemic rat brain," *Brain Research*, vol. 1052, no. 1, pp. 16–21, 2005.

- [22] H.-C. Chang, Y.-R. Yang, P. S. Wang, and R.-Y. Wang, "Quercetin enhances exercise-mediated neuroprotective effects in brain ischemic rats," *Medicine and Science in Sports and Exercise*, vol. 46, no. 10, pp. 1908–1916, 2014.
- [23] M.-H. Lee, H. Kim, S.-S. Kim et al., "Treadmill exercise suppresses ischemia-induced increment in apoptosis and cell proliferation in hippocampal dentate gyrus of gerbils," *Life Sciences*, vol. 73, no. 19, pp. 2455–2465, 2003.
- [24] P. Zhang, Y. Zhang, J. Zhang et al., "Early exercise protects against cerebral ischemic injury through inhibiting neuron apoptosis in cortex in rats," *International Journal of Molecular Sciences*, vol. 14, no. 3, pp. 6074–6089, 2013.
- [25] N. F. Ho, S. P. Han, and G. S. Dawe, "Effect of voluntary running on adult hippocampal neurogenesis in cholinergic lesioned mice," *BMC Neuroscience*, vol. 10, article 57, 2009.
- [26] J. Jin, H.-M. Kang, and C. Park, "Voluntary exercise enhances survival and migration of neural progenitor cells after intracerebral haemorrhage in mice," *Brain Injury*, vol. 24, no. 3, pp. 533–540, 2010.
- [27] H. H. Lee, M. S. Shin, Y. S. Kim et al., "Early treadmill exercise decreases intrastriatal hemorrhage-induced neuronal cell death and increases cell proliferation in the dentate gyrus of streptozotocin-induced hyperglycemic rats," *Journal of Diabetes and its Complications*, vol. 19, no. 6, pp. 339–346, 2005.
- [28] L. Zhang, X. Hu, J. Luo et al., "Physical exercise improves functional recovery through mitigation of autophagy, attenuation of apoptosis and enhancement of neurogenesis after MCAO in rats," *BMC Neuroscience*, vol. 14, article 46, 2013.
- [29] F. Matsuda, H. Sakakima, and Y. Yoshida, "The effects of early exercise on brain damage and recovery after focal cerebral infarction in rats," *Acta Physiologica*, vol. 201, no. 2, pp. 275–287, 2011.
- [30] Y.-R. Yang, R.-Y. Wang, and P. S.-G. Wang, "Early and late treadmill training after focal brain ischemia in rats," *Neuroscience Letters*, vol. 339, no. 2, pp. 91–94, 2003.
- [31] C.-S. Piao, B. A. Stoica, J. Wu et al., "Late exercise reduces neuroinflammation and cognitive dysfunction after traumatic brain injury," *Neurobiology of Disease*, vol. 54, pp. 252–263, 2013.
- [32] S.-U. Lee, D.-Y. Kim, S.-H. Park, D.-H. Choi, H.-W. Park, and T. R. Han, "Mild to moderate early exercise promotes recovery from cerebral ischemia in rats," *Canadian Journal of Neurological Sciences*, vol. 36, no. 4, pp. 443–449, 2009.
- [33] T.-B. Seo, B.-K. Kim, I.-G. Ko et al., "Effect of treadmill exercise on Purkinje cell loss and astrocytic reaction in the cerebellum after traumatic brain injury," *Neuroscience Letters*, vol. 481, no. 3, pp. 178–182, 2010.
- [34] Y. Ma, L. Qiang, and M. He, "Exercise therapy augments the ischemia-induced proangiogenic state and results in sustained improvement after stroke," *International Journal of Molecular Sciences*, vol. 14, no. 4, pp. 8570–8584, 2013.
- [35] P. Zhang, H. Yu, N. Zhou et al., "Early exercise improves cerebral blood flow through increased angiogenesis in experimental stroke rat model," *Journal of NeuroEngineering and Rehabilitation*, vol. 10, no. 1, article 43, 2013.
- [36] A. R. Rabinowitz and H. S. Levin, "Cognitive sequelae of traumatic brain injury," *Psychiatric Clinics of North America*, vol. 37, no. 1, pp. 1–11, 2014.
- [37] J. A. Kleim and T. A. Jones, "Principles of experience-dependent neural plasticity: implications for rehabilitation after brain damage," *Journal of Speech, Language, & Hearing Research*, vol. 51, no. 1, pp. S225–S239, 2008.
- [38] A. Wu, Z. Ying, and F. Gomez-Pinilla, "Exercise facilitates the action of dietary DHA on functional recovery after brain trauma," *Neuroscience*, vol. 248, pp. 655–663, 2013.
- [39] G. S. Griesbach, D. A. Hovda, R. Molteni, A. Wu, and F. Gomez-Pinilla, "Voluntary exercise following traumatic brain injury: brain-derived neurotrophic factor upregulation and recovery of function," *Neuroscience*, vol. 125, no. 1, pp. 129–139, 2004.
- [40] A. T. Crane, K. D. Fink, and J. S. Smith, "The effects of acute voluntary wheel running on recovery of function following medial frontal cortical contusions in rats," *Restorative Neurology and Neuroscience*, vol. 30, no. 4, pp. 325–333, 2012.
- [41] C. X. Luo, J. Jiang, Q. G. Zhou et al., "Voluntary exercise-induced neurogenesis in the postischemic dentate gyrus is associated with spatial memory recovery from stroke," *Journal of Neuroscience Research*, vol. 85, no. 8, pp. 1637–1646, 2007.
- [42] G. S. Griesbach, D. A. Hovda, and F. Gomez-Pinilla, "Exercise-induced improvement in cognitive performance after traumatic brain injury in rats is dependent on BDNF activation," *Brain Research*, vol. 1288, pp. 105–115, 2009.
- [43] S. J. E. Wong-Goodrich, M. L. Pfau, C. T. Flores, J. A. Fraser, C. L. Williams, and L. W. Jones, "Voluntary running prevents progressive memory decline and increases adult hippocampal neurogenesis and growth factor expression after whole-brain irradiation," *Cancer Research*, vol. 70, no. 22, pp. 9329–9338, 2010.
- [44] G. Winocur, S. Becker, P. Luu, S. Rosenzweig, and J. M. Wojtowicz, "Adult hippocampal neurogenesis and memory interference," *Behavioural Brain Research*, vol. 227, no. 2, pp. 464–469, 2012.
- [45] P. J. Clark, W. J. Brzezinska, M. W. Thomas, N. A. Ryzhenko, S. A. Toshkov, and J. S. Rhodes, "Intact neurogenesis is required for benefits of exercise on spatial memory but not motor performance or contextual fear conditioning in C57BL/6J mice," *Neuroscience*, vol. 155, no. 4, pp. 1048–1058, 2008.
- [46] T. Itoh, M. Imano, S. Nishida et al., "Exercise inhibits neuronal apoptosis and improves cerebral function following rat traumatic brain injury," *Journal of Neural Transmission*, vol. 118, no. 9, pp. 1263–1272, 2011.
- [47] F. Cechetti, P. V. Worm, V. R. Elsner et al., "Forced treadmill exercise prevents oxidative stress and memory deficits following chronic cerebral hypoperfusion in the rat," *Neurobiology of Learning and Memory*, vol. 97, no. 1, pp. 90–96, 2012.
- [48] P.-C. Shih, Y.-R. Yang, and R.-Y. Wang, "Effects of exercise intensity on spatial memory performance and hippocampal synaptic plasticity in transient brain ischemic rats," *PLoS ONE*, vol. 8, no. 10, Article ID e78163, 2013.
- [49] X. Shen, A. Li, Y. Zhang et al., "The effect of different intensities of treadmill exercise on cognitive function deficit following a severe controlled cortical impact in rats," *International Journal of Molecular Sciences*, vol. 14, no. 11, pp. 21598–21612, 2013.
- [50] R. R. Hicks, A. Boggs, D. Leider et al., "Effects of exercise following lateral fluid percussion brain injury in rats," *Restorative Neurology and Neuroscience*, vol. 12, no. 1, pp. 41–47, 1998.
- [51] M.-K. Song, H.-J. Seon, I.-G. Kim, J.-Y. Han, I.-S. Choi, and S.-G. Lee, "The effect of combined therapy of exercise and nootropic agent on cognitive function in focal cerebral infarction rat model," *Annals of Rehabilitation Medicine*, vol. 36, no. 3, pp. 303–310, 2012.
- [52] F. L. B. de Araujo, G. Bertolino, C. A. R. Funayama, N. C. Coimbra, and J. E. de Araujo, "Influence of treadmill training on motor performance and organization of exploratory behavior in

- Meriones unguiculatus* with unilateral ischemic stroke: histological correlates in hippocampal CA1 region and the neostriatum," *Neuroscience Letters*, vol. 431, no. 2, pp. 179–183, 2008.
- [53] Y.-J. Sim, S.-S. Kim, J.-Y. Kim, M.-S. Shin, and C.-J. Kim, "Treadmill exercise improves short-term memory by suppressing ischemia-induced apoptosis of neuronal cells in gerbils," *Neuroscience Letters*, vol. 372, no. 3, pp. 256–261, 2004.
- [54] Y.-J. Sim, H. Kim, J.-Y. Kim et al., "Long-term treadmill exercise overcomes ischemia-induced apoptotic neuronal cell death in gerbils," *Physiology & Behavior*, vol. 84, no. 5, pp. 733–738, 2005.
- [55] L. Chen, S. Gong, L.-D. Shan et al., "Effects of exercise on neurogenesis in the dentate gyrus and ability of learning and memory after hippocampus lesion in adult rats," *Neuroscience Bulletin*, vol. 22, no. 1, pp. 1–6, 2006.
- [56] D.-H. Kim, I.-G. Ko, B.-K. Kim et al., "Treadmill exercise inhibits traumatic brain injury-induced hippocampal apoptosis," *Physiology & Behavior*, vol. 101, no. 5, pp. 660–665, 2010.
- [57] M. F. Chen, T. Y. Huang, Y. M. Kuo, L. Yu, H. I. Chen, and C. J. Jen, "Early postinjury exercise reverses memory deficits and retards the progression of closed-head injury in mice," *Journal of Physiology*, vol. 591, no. 4, pp. 985–1000, 2013.
- [58] H. Shimada, M. Hamakawa, A. Ishida, K. Tamakoshi, H. Nakashima, and K. Ishida, "Low-speed treadmill running exercise improves memory function after transient middle cerebral artery occlusion in rats," *Behavioural Brain Research*, vol. 243, no. 1, pp. 21–27, 2013.
- [59] C. Phillips, M. A. Baktir, M. Srivatsan, and A. Salehi, "Neuroprotective effects of physical activity on the brain: a closer look at trophic factor signaling," *Frontiers in Cellular Neuroscience*, vol. 8, article 170, 2014.
- [60] G. S. Griesbach, D. L. Tio, J. Vincelli, D. L. McArthur, and A. N. Taylor, "Differential effects of voluntary and forced exercise on stress responses after traumatic brain injury," *Journal of Neurotrauma*, vol. 29, no. 7, pp. 1426–1433, 2012.
- [61] G. S. Griesbach, D. L. Tio, S. Nair, and D. A. Hovda, "Recovery of stress response coincides with responsiveness to voluntary exercise after traumatic brain injury," *Journal of Neurotrauma*, vol. 31, no. 7, pp. 674–682, 2014.
- [62] G. S. Griesbach, D. A. Hovda, F. Gomez-Pinilla, and R. L. Sutton, "Voluntary exercise or amphetamine treatment, but not the combination, increases hippocampal brain-derived neurotrophic factor and synapsin I following cortical contusion injury in rats," *Neuroscience*, vol. 154, no. 2, pp. 530–540, 2008.
- [63] H.-C. Chang, Y.-R. Yang, S.-G. P. Wang, and R.-Y. Wang, "Effects of treadmill training on motor performance and extracellular glutamate level in striatum in rats with or without transient middle cerebral artery occlusion," *Behavioural Brain Research*, vol. 205, no. 2, pp. 450–455, 2009.
- [64] J. Chen, J. Qin, Q. Su, Z. Liu, and J. Yang, "Treadmill rehabilitation treatment enhanced BDNF-TrkB but not NGF-TrkA signaling in a mouse intracerebral hemorrhage model," *Neuroscience Letters*, vol. 529, no. 1, pp. 28–32, 2012.
- [65] Q.-W. Zhang, X.-X. Deng, X. Sun, J.-X. Xu, and F.-Y. Sun, "Exercise promotes axon regeneration of newborn striatonigral and corticonigral projection neurons in rats after ischemic stroke," *PLoS ONE*, vol. 8, no. 11, Article ID e80139, 2013.
- [66] M. Ploughman, S. Granter-Button, G. Chernenko, B. A. Tucker, K. M. Mearow, and D. Corbett, "Endurance exercise regimens induce differential effects on brain-derived neurotrophic factor, synapsin-I and insulin-like growth factor I after focal ischemia," *Neuroscience*, vol. 136, no. 4, pp. 991–1001, 2005.
- [67] M. Ploughman, S. Granter-Button, G. Chernenko et al., "Exercise intensity influences the temporal profile of growth factors involved in neuronal plasticity following focal ischemia," *Brain Research*, vol. 1150, no. 1, pp. 207–216, 2007.
- [68] G. S. Griesbach, F. Gómez-Pinilla, and D. A. Hovda, "Time window for voluntary exercise-induced increases in hippocampal neuroplasticity molecules after traumatic brain injury is severity dependent," *Journal of Neurotrauma*, vol. 24, no. 7, pp. 1161–1171, 2007.
- [69] A. M. Stranahan, D. Khalil, and E. Gould, "Social isolation delays the positive effects of running on adult neurogenesis," *Nature Neuroscience*, vol. 9, no. 4, pp. 526–533, 2006.
- [70] J. L. Leasure and L. Decker, "Social isolation prevents exercise-induced proliferation of hippocampal progenitor cells in female rats," *Hippocampus*, vol. 19, no. 10, pp. 907–912, 2009.
- [71] A. Berry, V. Bellisario, S. Capoccia et al., "Social deprivation stress is a triggering factor for the emergence of anxiety- and depression-like behaviours and leads to reduced brain BDNF levels in C57BL/6J mice," *Psychoneuroendocrinology*, vol. 37, no. 6, pp. 762–772, 2012.
- [72] R. A. M. Haast, D. R. Gustafson, and A. J. Kilian, "Sex differences in stroke," *Journal of Cerebral Blood Flow and Metabolism*, vol. 32, no. 12, pp. 2100–2107, 2012.
- [73] M. Liu, M. H. Kelley, P. S. Hersen, and P. D. Hurn, "Neuroprotection of sex steroids," *Minerva Endocrinologica*, vol. 35, no. 2, pp. 127–143, 2010.
- [74] S. J. Murphy, L. D. McCullough, and J. M. Smith, "Stroke in the female: role of biological sex and estrogen," *ILAR Journal*, vol. 45, no. 2, pp. 147–159, 2004.
- [75] H. M. Bramlett and W. D. Dietrich, "Pathophysiology of cerebral ischemia and brain trauma: similarities and differences," *Journal of Cerebral Blood Flow and Metabolism*, vol. 24, no. 2, pp. 133–150, 2004.
- [76] A. A. Tan, A. Quigley, D. C. Smith, and M. R. Hoane, "Strain differences in response to traumatic brain injury in Long-Evans compared to Sprague-Dawley rats," *Journal of Neurotrauma*, vol. 26, no. 4, pp. 539–548, 2009.
- [77] W. M. Reid, A. Rolfe, D. Register, J. E. Levasseur, S. B. Churn, and D. Sun, "Strain-related differences after experimental traumatic brain injury in rats," *Journal of Neurotrauma*, vol. 27, no. 7, pp. 1243–1253, 2010.
- [78] C. G. Markgraf, S. Kraydieh, R. Prado, B. D. Watson, W. D. Dietrich, and M. D. Ginsberg, "Comparative histopathologic consequences of photothrombotic occlusion of the distal middle cerebral artery in Sprague-Dawley and Wistar rats," *Stroke*, vol. 24, no. 2, pp. 286–292, 1993.
- [79] R. C. G. Herz, P. J. Gaillard, D. J. de Wildt, and D. H. G. Versteeg, "Differences in striatal extracellular amino acid concentrations between Wistar and Fischer 344 rats after middle cerebral artery occlusion," *Brain Research*, vol. 715, no. 1–2, pp. 163–171, 1996.
- [80] F. J. van der Staay, K.-H. Augstein, and E. Horváth, "Sensorimotor impairments in rats with cerebral infarction, induced by unilateral occlusion of the left middle cerebral artery: strain differences and effects of the occlusion site," *Brain Research*, vol. 735, no. 2, pp. 271–284, 1996.
- [81] J. P. McLin and O. Steward, "Comparison of seizure phenotype and neurodegeneration induced by systemic kainic acid in inbred, outbred, and hybrid mouse strains," *European Journal of Neuroscience*, vol. 24, no. 8, pp. 2191–2202, 2006.

- [82] J. Fuzik, L. Gellért, G. Oláh et al., "Fundamental interstrain differences in cortical activity between Wistar and Sprague-Dawley rats during global ischemia," *Neuroscience*, vol. 228, pp. 371–381, 2013.
- [83] F. Al Nimer, R. Lindblom, M. Ström et al., "Strain influences on inflammatory pathway activation, cell infiltration and complement cascade after traumatic brain injury in the rat," *Brain, Behavior, and Immunity*, vol. 27, no. 1, pp. 109–122, 2013.
- [84] G. B. Fox, R. A. Levasseur, and A. I. Faden, "Behavioral responses of C57BL/6, FVB/N, and 129/SvEMS mouse strains to traumatic brain injury: implications for gene targeting approaches to neurotrauma," *Journal of Neurotrauma*, vol. 16, no. 5, pp. 377–389, 1999.
- [85] G. Yang, K. Kitagawa, K. Matsushita et al., "C57BL/6 strain is most susceptible to cerebral ischemia following bilateral common carotid occlusion among seven mouse strains: selective neuronal death in the murine transient forebrain ischemia," *Brain Research*, vol. 752, no. 1-2, pp. 209–218, 1997.
- [86] M. Schroeter, P. Küry, and S. Jander, "Inflammatory gene expression in focal cortical brain ischemia: differences between rats and mice," *Molecular Brain Research*, vol. 117, no. 1, pp. 1–7, 2003.
- [87] J. A. D'Abbondanza, E. Lass, J. Ai, and R. L. Macdonald, "Mouse genetic background is associated with variation in secondary complications after subarachnoid hemorrhage," in *Neurovascular Events After Subarachnoid Hemorrhage*, vol. 120 of *Acta Neurochirurgica Supplement*, pp. 29–33, Springer, Cham, Switzerland, 2015.
- [88] A. Majid, Y. Y. He, J. M. Gidday et al., "Differences in vulnerability to permanent focal cerebral ischemia among 3 common mouse strains," *Stroke*, vol. 31, no. 11, pp. 2707–2714, 2000.
- [89] J. Bardutzky, Q. Shen, N. Henninger, J. Bouley, T. Q. Duong, and M. Fisher, "Differences in ischemic lesion evolution in different rat strains using diffusion and perfusion imaging," *Stroke*, vol. 36, no. 9, pp. 2000–2005, 2005.
- [90] M. Fujii, H. Hara, W. Meng, J. P. Vonsattel, Z. Huang, and M. A. Moskowitz, "Strain-related differences in susceptibility to transient forebrain ischemia in SV-129 and C57Black/6 mice," *Stroke*, vol. 28, no. 9, pp. 1805–1811, 1997.
- [91] M. Marosi, G. Rákos, H. Robotka et al., "Hippocampal (CA1) activities in Wistar rats from different vendors. Fundamental differences in acute ischemia," *Journal of Neuroscience Methods*, vol. 156, no. 1-2, pp. 231–235, 2006.
- [92] H. S. Oliff, E. Weber, G. Eilon, and P. Marek, "The role of strain/vendor differences on the outcome of focal ischemia induced by intraluminal middle cerebral artery occlusion in the rat," *Brain Research*, vol. 675, no. 1-2, pp. 20–26, 1995.
- [93] H. S. Oliff, E. Weber, B. Miyazaki, and P. Marek, "Infarct volume varies with rat strain and vendor in focal cerebral ischemia induced by transcranial middle cerebral artery occlusion," *Brain Research*, vol. 699, no. 2, pp. 329–331, 1995.
- [94] H. Malá, M. Rodríguez Castro, H. Pearce et al., "Delayed intensive acquisition training alleviates the lesion-induced place learning deficits after fimbria-fornix transection in the rat," *Brain Research*, vol. 1445, pp. 40–51, 2012.
- [95] J. Mogensen, L. H. Christensen, A. Johansson, G. Wörtwein, L. E. Bang, and S. Holm, "Place learning in scopolamine-treated rats: the roles of distal cues and catecholaminergic mediation," *Neurobiology of Learning and Memory*, vol. 78, no. 1, pp. 139–166, 2002.
- [96] G. Wörtwein, L. H. Saerup, D. Charlottenfeld-Starpov, and J. Mogensen, "Place learning by fimbria-fornix transected rats in a modified water maze," *International Journal of Neuroscience*, vol. 82, no. 1-2, pp. 71–81, 1995.
- [97] J. Mogensen, T. K. Pedersen, S. Holm, and L. E. Bang, "Pre-frontal cortical mediation of rats' place learning in a modified water maze," *Brain Research Bulletin*, vol. 38, no. 5, pp. 425–434, 1995.
- [98] I. Wilms and J. Mogensen, "Dissimilar outcomes of apparently similar procedures as a challenge to clinical neurorehabilitation and basic research: when the same is not the same," *Neurorehabilitation*, vol. 29, no. 3, pp. 221–227, 2011.
- [99] J. Mogensen, "Animal models in neuroscience," in *Handbook of Laboratory Animal Science, Volume II. Animal Models*, J. Hau and S. J. Schapiro, Eds., pp. 47–73, CRC Press, 2011.
- [100] R. E. Jorge and D. B. Arciniegas, "Mood disorders after TBI," *Psychiatric Clinics of North America*, vol. 37, no. 1, pp. 13–29, 2014.
- [101] M.-P. Austin, P. Mitchell, and G. M. Goodwin, "Cognitive deficits in depression: possible implications for functional neuropathology," *British Journal of Psychiatry*, vol. 178, pp. 200–206, 2001.

Research Article

Spinal Cord Hemisection Facilitates Aromatic L-Amino Acid Decarboxylase Cells to Produce Serotonin in the Subchronic but Not the Chronic Phase

Bushra Azam,¹ Jacob Wienecke,^{1,2} Dennis Bo Jensen,²
Aleena Azam,¹ and Mengliang Zhang^{1,3}

¹Department of Neuroscience and Pharmacology, University of Copenhagen, 2200 Copenhagen, Denmark

²Department of Nutrition, Exercise and Sports, University of Copenhagen, 2200 Copenhagen, Denmark

³Department of Experimental Science, Neuronano Research Center, Lund University, 223 81 Lund, Sweden

Correspondence should be addressed to Mengliang Zhang; mzhang@sund.ku.dk

Received 13 February 2015; Revised 12 May 2015; Accepted 19 May 2015

Academic Editor: Tae Hong Lim

Copyright © 2015 Bushra Azam et al. This is an open access article distributed under the Creative Commons Attribution License, which permits unrestricted use, distribution, and reproduction in any medium, provided the original work is properly cited.

Neuromodulators, such as serotonin (5-hydroxytryptamine, 5-HT) and noradrenalin, play an essential role in regulating the motor and sensory functions in the spinal cord. We have previously shown that in the rat spinal cord the activity of aromatic L-amino acid decarboxylase (AADC) cells to produce 5-HT from its precursor (5-hydroxytryptophan, 5-HTP) is dramatically increased following complete spinal cord transection. In this study, we investigated whether a partial loss of 5-HT innervation could similarly increase AADC activity. Adult rats with spinal cord hemisection at thoracic level (T11/T12) were used with a postoperation interval at 5 days or 60 days. Using immunohistochemistry, first, we observed a significant reduction in the density of 5-HT-immunoreactive fibers in the spinal cord below the lesion on the injured side for both groups. Second, we found that the AADC cells were similarly expressed on both injured and uninjured sides in both groups. Third, increased production of 5-HT in AADC cells following 5-HTP was seen in 5-day but not in 60-day postinjury group. These results suggest that plastic changes of the 5-HT system might happen primarily in the subchronic phase and for longer period its function could be compensated by plastic changes of other intrinsic and/or supraspinal modulation systems.

1. Introduction

Spinal cord injury (SCI) has a devastating effect on daily life of the patients. The foremost and frustrating symptoms are the losses of sensory, motor, and/or autonomic functions [1–5]. Spinal cord injury can be either complete or incomplete, and the symptoms for different SCI individuals may vary according to the severity of the trauma. Neural plasticity occurs over time at sites both above and below the level of injury, which results in both the pathophysiological complications and the functional recovery [6, 7]. The monoaminergic system is one of the systems that undergo drastic plastic changes in the spinal cord following SCI [8–16]. In the mammalian spinal cord monoamine neurotransmitters, for example, serotonin (5-hydroxytryptamine, 5-HT), dopamine, and noradrenaline, are important modulators of

both sensory and motor functions. It is commonly believed that monoamines in the spinal cord originate from different supraspinal brain regions [17, 18]. Accordingly in complete SCI the monoamines are largely gone although residual amounts still remain [11, 19], whereas in incomplete SCI monoamines in the spinal cord are lost at a varied degree depending on the severity of the injury [20].

Recently our research group has focused on the plastic changes of serotonergic system in the spinal cord. Using a sacral spinal cord transection rat model we have found that 5-HT₂ (A and C) receptors are upregulated in response to complete SCI [13, 14, 16]. More importantly, we have found that cells expressing aromatic L-amino acid decarboxylase (AADC) in the spinal cord, which normally do not contain monoamines [21], increase their activity and could potentially produce 5-HT in the presence of 5-HT precursor,

5-hydroxytryptophan (5-HTP) [22]. Following incomplete SCI, either contusion or hemisection, there remains a considerable amount of 5-HT in the spinal cord below the lesion. For instance, following hemisection the remaining amount of 5-HT below the lesion is about 8–40% of the normal level 3–8 days after the lesion according to the data from different laboratories [9, 10, 23–25]. More importantly some studies have reported a gradual recovery of 5-HT due to reinnervation to the lesion side over time [9, 10, 24] although this is not constantly observed [25, 26]. Then the question is whether this 5-HT is produced from the 5-HT sprouting fibers from the uninjured side or from the intrinsic 5-HT-producing cells, such as AADC cells. This issue is investigated by using a hemisection SCI rat model in the present study. We used rats with a postinjury time at either 5 days or 60 days to examine the expression of 5-HT based on the facts that the descending 5-HT fibers have been degenerated at 5–7 days after the transection [14, 27], that from 4 to 8 weeks after incomplete SCI significant plastic changes have occurred in the spinal cord including the descending cortical and subcortical spinal fibers [6], and that at both time points the AADC cells have shown a steady increased ability to synthesize 5-HT from 5-HTP [22].

2. Materials and Methods

2.1. Experimental Animals. All experiments followed the guidelines of EU Directive 2010/63/EU and were approved by the Danish Animal Experiments Inspectorate. Efforts were taken to minimize the number of animals and their sufferings. Twenty-nine male Sprague-Dawley rats with initial body weight of 160–490 g during the operation were used in this study. The animals were subjected to either thoracic spinal cord hemisection operation ($n = 28$) or sacral spinal cord transection ($n = 1$). All the rats had a 12/12-hour light/dark cycle and had access to food and water ad libitum. The rats subjected to hemisection were divided into four groups and the rats in each group underwent different treatments before perfusion (see further below).

2.2. Spinal Cord Hemisection and Transection Operation. Before the hemisection operation, the rat was anesthetized with 2.0% isoflurane in a mixture of gas of O₂ (500 psi) and N₂O (200 psi). The surgical area was shaved and cleaned with alcohol and the whole operation was carried out under sterile conditions. A 0.2 mL mix of sedatives and local anesthesia (Xylocaine 12.5 mg/mL and Marcaine 2.5 mg/mL) were given intramuscularly. Also, a nonsteroidal anti-inflammatory drug and a postoperation pain relieving drug (Rimadyl, 5 mg/kg) were given subcutaneously. The operation was performed under a surgery microscope. For hemisection the laminectomy was done at the thoracic vertebral level T10–T11. The dura was opened and about 1–2 mm of the spinal cord at level T11–T12 was removed at one side without damaging the dorsal vein or ventral artery. The wound was then closed by stitching the muscle, fascia and skin separately with a monofilament suture. For one rat that was subjected to spinal cord transection at the second sacral level (S2) the surgery

procedure has been described elsewhere [22]; that is, a small piece of the spinal cord tissue at S2 level was completely removed. After the operation, the rat was subcutaneously treated with analgesic (Temgesic 0.1 mg/kg) at every 8 hours for the first 48 hours. The welfare of the animals was controlled every day until the end of the experiments.

Initially the 28 spinal hemisected rats were divided into two time groups: 16 rats in a 5-day postoperation group and 12 rats in a 60-day postoperation group. In each time group the rats were further divided into two subgroups subjected to different treatments. However, due to compromised welfare of three animals in the 5-day group they had to be euthanized before the planned time. Thus in the end there were 25 rats in total in the four groups: 14 rats were used in experimental groups or treated groups (8 in the 5-day group and 6 in the 60-day group, resp., Table 1) which were subjected to intraperitoneal (i.p.) injection of 5-HTP (50 mg/kg) combined with carbidopa (20 mg/kg) in saline with a small amount of hydrochloride acid 30 min before the perfusion. The other 11 rats were used as control animals or untreated groups (5 in the 5-day group and 6 in the 60-day group, resp., Table 1) and were not injected with any drugs before perfusion. The rat whose spinal cord was transected at S2 level was treated in the same way as those in the experimental groups.

All the rats were euthanized with pentobarbital 50 mg/mL and perfused intracardially with 200–300 mL 0.01 M phosphate buffered saline (PBS) for 3–4 min, followed by a 400 mL solution of 4% paraformaldehyde in 0.1 M phosphate buffer over 15 min. The entire spinal cord was removed and postfixed in the original fixative for 24 hours at 4°C and cryoprotected in PBS with 30% sucrose for 24 hours at 4°C. Upon the removal of the spinal cord the lesion site was inspected under surgery microscope. All the spinal cord hemisected rats used in this study were demonstrated to have been hemisected at T11 or T12 level on one side. The spinal cord was separated into different segments and the lumbar and sacral parts were cut horizontally into 40 μ m sections. If the spinal cord was not cut after 48 hours, it was cryoprotected in a 0.01 M PBS solution containing 15% sucrose, 30% ethylene glycol, and 0.05% thimerosal and stored at –20°C.

2.3. 5-HT and AADC Immunohistochemistry. Every second section from lumbar (L1–L6) and sacral (S1–Ca3) levels from all the rats was processed for 5-HT and AADC double immunofluorescence staining. The sections were rinsed in PBS twice for 10 min each and in PBS with 0.1% Triton X-100 (PBST) once for 10 min. Then the sections were preincubated in PBST containing 2% bovine serum albumin and 5% normal donkey serum for an hour. After rinsing in PBST for 10 min, the sections were incubated in the same solution containing rabbit anti-5-HT (1:10000, Immunostar) and sheep anti-AADC (1:200; Millipore-Chemicon) primary antibodies diluted over 24 hours at room temperature. Following rinsing four times in PBST for 15 min each the sections were incubated for an hour in donkey anti-rabbit Alexa Fluor 594 (1:200, Invitrogen), donkey anti-sheep Alexa Fluor 488 (1:200, Invitrogen) in PBST with 1% bovine serum albumin, and normal donkey serum 2% at room temperature.

TABLE 1: Summary of the results from the different animal groups.

Group	Number of animals	Spinal cord side	Density of 5-HT fibers in IMZ ¹ (% of analyzed area)	Density of 5-HT fibers in VH ² (% of analyzed area)	Density of AADC cells (number of cells/analyzed section)	Density of 5-HT cells (% of AADC cells)
5-day control	5	Injured	0.89 ± 0.48	1.19 ± 0.51	19.99 ± 3.83	0
		Uninjured	3.80 ± 1.22	5.02 ± 1.21	22.37 ± 7.11	0
5-day 5-HTP + carbidopa	8	Injured	1.26 ± 0.78	0.73 ± 0.18	19.36 ± 8.78	42.52 ± 19.15
		Uninjured	4.20 ± 1.82	3.13 ± 0.61	15.08 ± 7.61	25.86 ± 17.81
60-day control	6	Injured	0.36 ± 0.06	0.59 ± 0.38	8.83 ± 3.45	0
		Uninjured	3.24 ± 1.24	2.72 ± 1.25	7.10 ± 3.73	0
60-day 5-HTP + carbidopa	6	Injured	0.78 ± 0.34	0.35 ± 0.08	11.42 ± 5.94	15.98 ± 18.72
		Uninjured	2.41 ± 1.16	1.54 ± 0.46	10.85 ± 4.80	9.57 ± 15.00

¹IMZ: intermediate zone; ²VH: ventral horn.

After rinsing three times in PBS for 10 min each the sections were mounted, dried, and coverslipped with Fluorescence Mounting Medium (Dako).

2.4. Data Analysis. The spinal sections were observed with a fluorescence microscope (Leica DM6000B, Leica Microsystems, Wetzlar, Germany). All the images were captured digitally (Leica DFC420 C Digital Camera System) and processed with Adobe Photoshop CS6. To compare with the results from our previous study where the rat spinal cord was transected at S2 level [22] we only analyzed the data acquired from sacrocaudal level in this study.

For the analysis of the density of 5-HT-immunoreactive (IR) fibers, images were taken from 5 or 6 spinal sections. Paired images were taken with an imaging area of $1000 \mu\text{m} \times 750 \mu\text{m}$ from the intermediate gray matter/zone and the ventral motoneuron region from both sides of the selected sections. To avoid bias in the quantitative data analysis due to varied spinal locations images from the injured and uninjured sides were taken from the same rostrocaudal level (mostly at S2–S4 level). The density of 5-HT-IR fibers was analyzed with Image J software [13, 14]. To do this the image was first thresholded and then the area above the threshold level was calculated and the data from injured and uninjured sides were compared. The distribution of AADC cells and the incidence of 5-HT-IR AADC cells at S1–Ca3 were analyzed in the intermediate zone using a MD-plotting system (Accustage) as has been described previously [22]. All the sections containing the AADC cells in the intermediate zone were plotted. The AADC cells and the 5-HT-IR AADC cells were plotted with different symbols. The relative quantity of AADC cells was expressed as cell number per section and the incidence of 5-HT-IR AADC cells was expressed as percent AADC cells for each animal.

Standard deviation (SD) was used to represent data variations from the mean value. The group average value is expressed as the mean \pm SD. The statistical analysis was done on Sigmaplot (version 11, Systat Software). Paired *t*-test (or Wilcoxon signed rank test if the data were asymmetrically distributed) or unpaired *t*-test (or Mann-Whitney rank-sum test if the data was asymmetrically distributed) was used

for the comparison of data between two groups and the significance level was set at $P < 0.05$.

3. Results

3.1. Physical Activity of Hind Limbs and Tail after Spinal Hemisection. Immediately after spinal hemisection operation the hind limb on the injured side became paralyzed in all animals. Generally, the rats expressed clumsy locomotion pattern of the affected limb at 5 days and at 7–8 days the locomotor pattern is more functional. After three weeks the affected limb looked, from a qualitative point of view, fully functional during locomotion. We did not score or quantify the level of spasticity of either limb. There was no tail spasticity developed for all the rats regardless of the injury times.

3.2. The Density of 5-HT Nerve Fibers in Different Animal Groups. To investigate whether spinal hemisection completely removed 5-HT innervations on the same side and whether the innervations recovered over time we compared the density of 5-HT-IR fibers and 5-HT-IR AADC cells on the injured and the uninjured side at the lumbar and sacrocaudal parts of the spinal cord of the untreated and treated groups at 5 days and 60 days after injury. Since we found a similar labelling pattern of 5-HT-IR fibers and AADC cells at both lumbar and sacrocaudal levels, in this study we mainly focused on the sacrocaudal part in order to compare with our previously published results on completely spinal cord transected rats [22].

First we have analyzed 5-HT fibers in the intermediate zone in 5-day and 60-day groups. In 5-day rats the density of 5-HT-IR fibers in the untreated group was dramatically reduced on the injured side as compared to the uninjured side (Figure 1(a)). When a quantitative analysis was performed in the intermediate zone 5-HT-IR fibers on the injured side were only 23.42% of that on the uninjured side (Table 1). Thus on the uninjured side 5-HT-IR fibers occupied on average $3.80 \pm 1.22\%$ of the analyzed area, whereas on the injured side 5-HT-IR fibers occupied only $0.89 \pm 0.48\%$ of the analyzed area. This difference was statistically significant ($P < 0.01$, paired *t*-test) (Figure 1(e)). In the treated group, we observed an increase

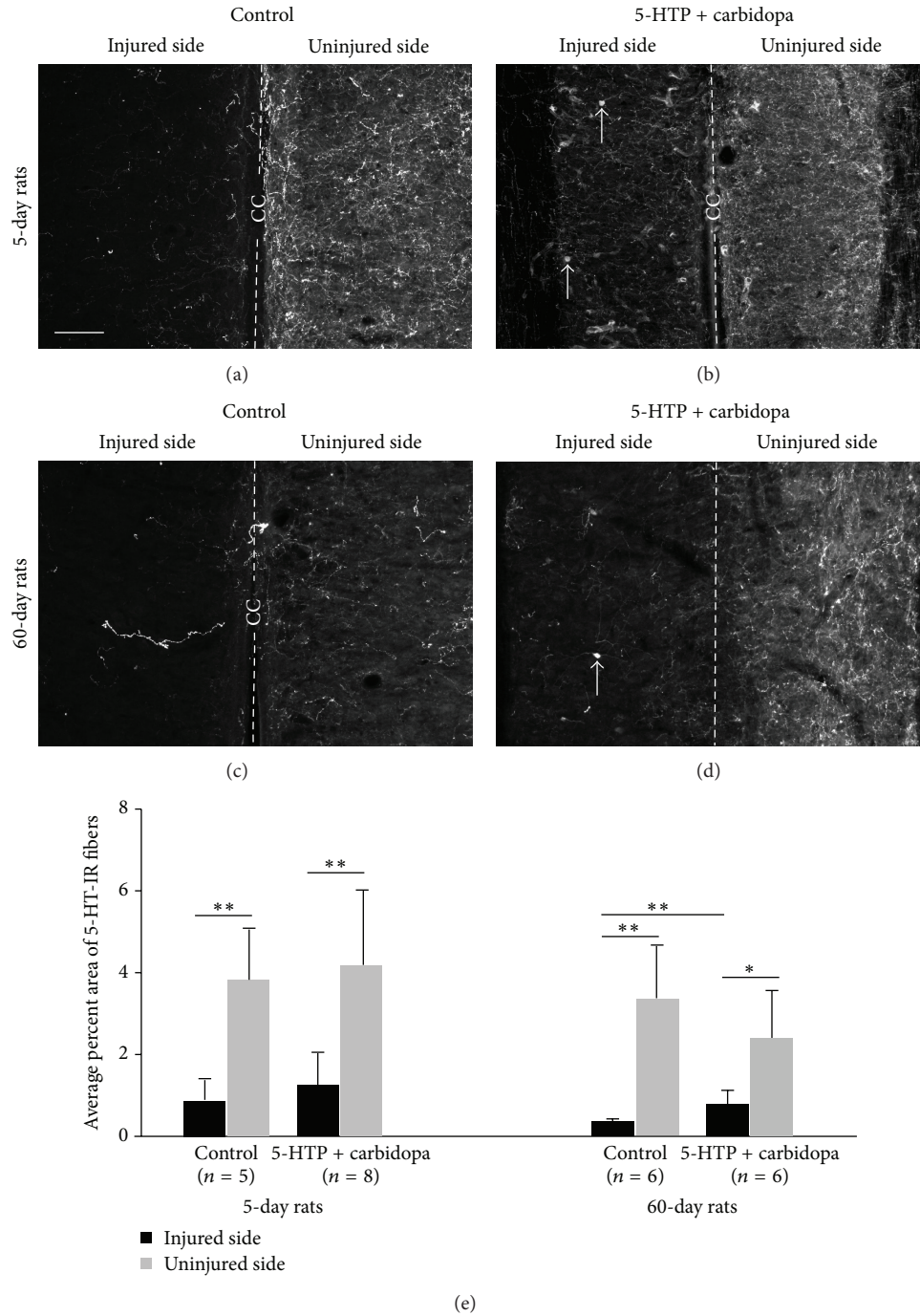


FIGURE 1: 5-HT-immunoreactive (IR) nerve fibers in the intermediate zone in the sacrocaudal spinal cord on the injured and uninjured side in different animal groups. (a–d) Photomicrographs of 5-HT-IR fibers in 5-day untreated group (a) and 5-HTP plus carbidopa treated group (b) and in 60-day untreated group (c) and 5-HTP plus carbidopa treated group (d). Dashed line represents the midline in each horizontal section. CC: central canal. Arrows in (b) and (d) indicate 5-HT-immunoreactive cells. Scale bar in (a), 100 μ m. (e) Quantitative data of the density of 5-HT-IR fibers in different animals groups. * $P < 0.05$, ** $P < 0.01$.

of 5-HT-IR fibers on both the injured and the uninjured side although the 5-HT-IR fibers on the injured side were significantly lower than the uninjured side (Figures 1(b) and 1(e)) ($P < 0.01$, paired t -test). Thus, the percent area of 5-HT-IR fibers on the injured side reached $1.26 \pm 0.78\%$, which was 1.4-fold higher than the injured side in the untreated group

although no significant difference was reached (unpaired t -test). On the uninjured side the 5-HT-IR fiber density was $4.20 \pm 1.82\%$, which was 1.1-fold higher than the uninjured side in the untreated group. Quantitatively in the treated group the density of 5-HT-IR fibers in the injured side was 30.0% ($1.26/4.2$) of the uninjured side, which was 1.3-fold higher

than the untreated group (23.42%). However, for the same side there was no significant difference between treated and untreated groups (unpaired *t*-test) (Figure 1(e)).

Following 60-day injury the density of 5-HT-IR fibers in the untreated group was dramatically reduced on the injured side as compared to the uninjured side (Table 1, Figure 1(c)). The density of 5-HT-IR fibers on the injured side was reduced to 11.11% of that on the uninjured side. Thus on the injured side the density of 5-HT-IR fibers was only $0.36 \pm 0.06\%$ on average, whereas on the uninjured side it was $3.24 \pm 1.24\%$. The difference was statistically significant ($P < 0.01$, paired *t*-test) (Figure 1(e)). In the treated group, the density of 5-HT-IR fibers on the injured side was clearly increased (Figure 1(d)), which reached 32.59% of that on the uninjured side although the density on the uninjured side was still significantly higher than the injured side ($P < 0.05$, paired *t*-test) (Figure 1(e)). Thus the density of 5-HT-IR fibers on the injured side was $0.78 \pm 0.34\%$, which was 2.2-fold higher than the injured side in the untreated group and the difference was statistically significant ($P < 0.01$, Mann-Whitney rank-sum test) (Figure 1(e)). On the uninjured side the 5-HT-IR fiber density was $2.41 \pm 1.16\%$, which appeared 41% lower than the uninjured side in the untreated group but the difference was not statistically different (unpaired *t*-test) (Figure 1(e)).

Because spinal motoneurons receive dense 5-HT fiber innervations, to investigate whether 5-HT fibers undergo similar plastic changes around the motoneurons, we have examined 5-HT fiber density in different animal groups with the same method. As shown in Table 1 and Figure 2, the density of 5-HT fibers on the injured side was significantly lower than the uninjured side for both 5-day and 60-day groups regardless of the treatment with 5-HTP and carbidopa. Thus the density of 5-HT fibers on the injured side was counted for consistently about 21–24% of that on the uninjured side in the different groups. These density differences on the two sides were somehow similar to those in the intermediate zone (11–33%, see above) in the different groups. However, to our surprise, the density of 5-HT fibers was lower in the treated groups than in the untreated groups for both 5-day and 60-day groups. We will discuss these results further in the Discussion.

We did not try to make a comparison for the 5-HT-IR fiber density between 5-day and 60-day postinjury groups. The key issue we were interested in was that whether 5-HT-IR fibers became denser following 5-HTP + carbidopa application in each group. However, in general the 5-HT-IR density at the 5-day postinjury group was higher than the 60-day postinjury on both sides regardless of locations of the gray matter and the drug applications.

3.3. The Distribution of the AADC Cells in Different Experimental Groups. To investigate whether spinal hemisection affects the expression of AADC cells in the spinal cord we investigated the distribution of the AADC cells on the injured and the uninjured side at the sacrocaudal spinal segment in different animal groups. As we have reported previously [22] the AADC cells were found in the dorsal horn, the intermediate zone, and the region around the central canal on both sides (data not shown). To facilitate the comparison

with the results from our spinal transection experiments [22] the quantitative analysis was only performed on the data from the intermediate zone.

The results showed that in both 5-day and 60-day groups AADC cells showed a similar distribution on the injured and uninjured side regardless of whether the rat was treated with 5-HTP and carbidopa or not ($P > 0.05$ for the two time groups), indicating that hemisection and drug application did not alter the expression of AADC cells in the injured side (Table 1). Therefore we decided to pool the data from the untreated group and the treated group together. In the 5-day group the number of AADC cells in the intermediate zone on the injured side was $19.60 \pm 7.07/\text{section}$ whereas on the uninjured side it was $17.88 \pm 8.02/\text{section}$ ($n = 13$). No significant difference was found between the two sides ($P = 0.721$, paired *t*-test). Similarly, in the 60-day group the number of AADC cells in the intermediate zone on the injured side was $10.13 \pm 4.82/\text{section}$ whereas on the uninjured side it was $8.98 \pm 4.56/\text{section}$ ($n = 12$). No significant difference was found between the two sides ($P = 0.128$, paired *t*-test). Since we did not systematically plot the AADC cells in all the sections no attempt was made to make a quantitative comparison of AADC cells between the 5-day and the 60-day groups.

3.4. The Ability of the AADC Cells to Produce 5-HT from Extraneously Applied 5-HTP following Hemisection. Because the main purpose of this study was to investigate whether AADC cells increased their ability to produce 5-HT from 5-HTP following hemisection, we have examined 5-HT expression in AADC cells in two different animal groups following 5-HTP + carbidopa application. 5-HT-positive AADC cells were examined at the sacrocaudal level in both the untreated and the treated group in 5-day and 60-day rats. In addition 5-HT-positive AADC cells were also examined in the spinal cord from the rat subjected to a complete spinal transection at S2 level and the results showed that 100% of the AADC cells in the intermediate zone became 5-HT-IR in this rat (data not shown).

In the untreated groups no AADC cells became 5-HT-positive on both the injured and the uninjured side of the spinal cord in both 5-day and 60-day groups. In the 5-day treated group we have observed a certain number of 5-HT-IR AADC cells on both the injured side and uninjured side in 7 out of 8 cases (Figures 3(a) and 3(b)). Quantitative analysis showed that $42.52 \pm 19.15\%$ ($n = 8$) of AADC cells became 5-HT-positive on the injured side whereas only $25.25 \pm 17.81\%$ ($n = 8$) of the AADC cells became 5-HT-IR on the uninjured side. The difference was significantly different ($P < 0.01$, power = 0.85 with $\alpha = 0.05$, paired *t*-test) (Figure 3(c)). In 60-day treated group we observed a certain number of 5-HT-IR AADC cells in 3 out of 6 rats in the injured side and 2 out of 6 rats in the uninjured side (Figures 3(d) and 3(e)). Quantitative analysis showed that $15.98 \pm 18.72\%$ ($n = 6$) of the AADC cells on the injured side became 5-HT-IR while $9.57 \pm 15.00\%$ ($n = 6$) of AADC cells on the uninjured side became 5-HT-IR. The difference between the injured and uninjured sides was not statistically significant ($P = 0.25$, Wilcoxon signed rank test) (Figure 3(f)). Further, we have compared the data

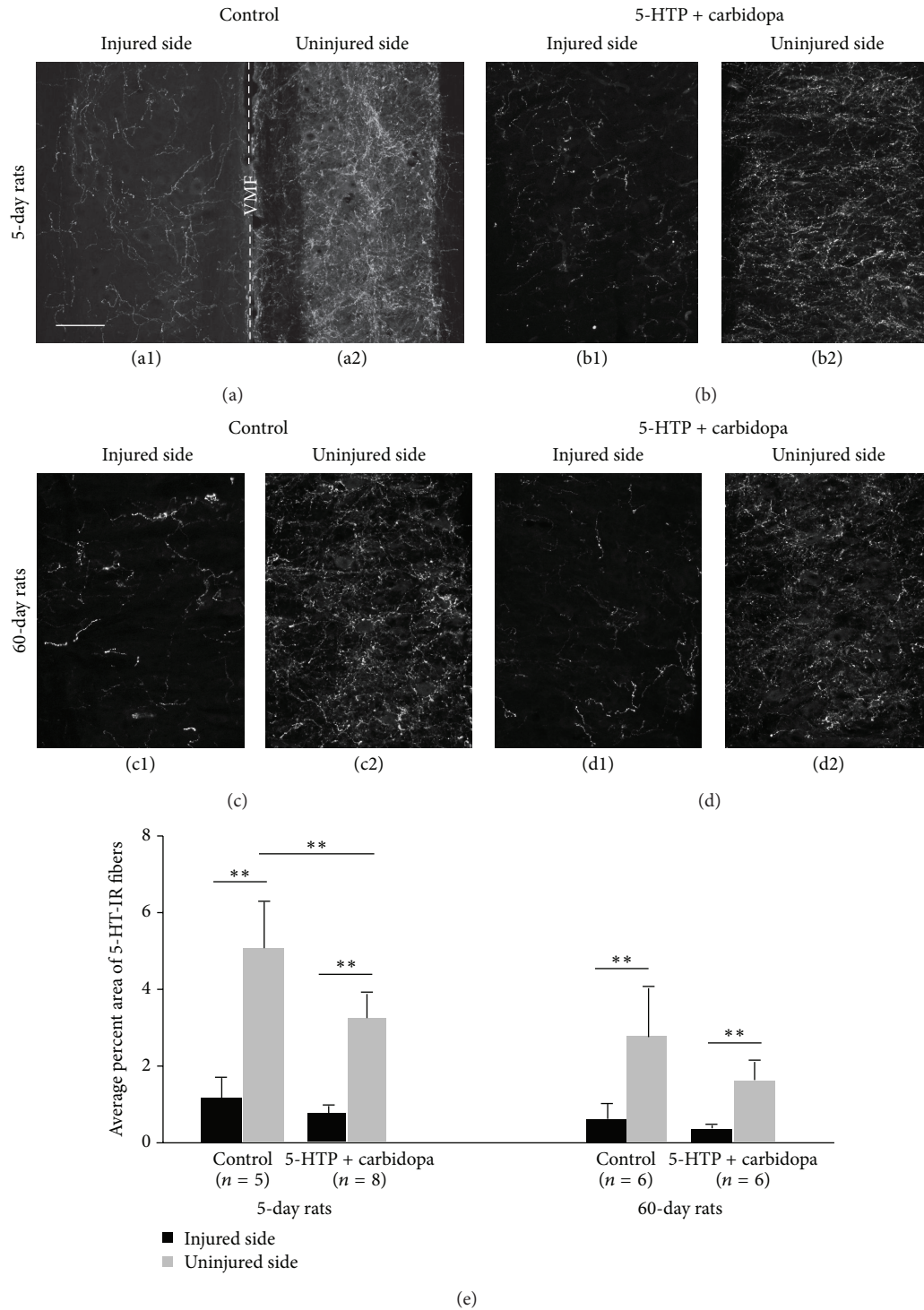


FIGURE 2: 5-HT-immunoreactive (IR) nerve fibers in the ventral horn motoneuron region in the sacrocaudal spinal cord on the injured and uninjured side in different animal groups. (a1–d2) Photomicrographs of 5-HT-IR fibers in 5-day untreated group (a1, a2) and 5-HTP plus carbidopa treated group (b1, b2) and in 60-day untreated group (c1, c2) and 5-HTP plus carbidopa treated group (d1, d2). (a1) and (a2) were from the same horizontal section. Dashed line indicates the midline. VMF: ventral median fissure. Other pairs of photomicrographs were from different sections. Scale bar in (a1), 100 μ m. (e) Quantitative data of the density of 5-HT-IR fibers in different animals groups. ** $P < 0.01$.

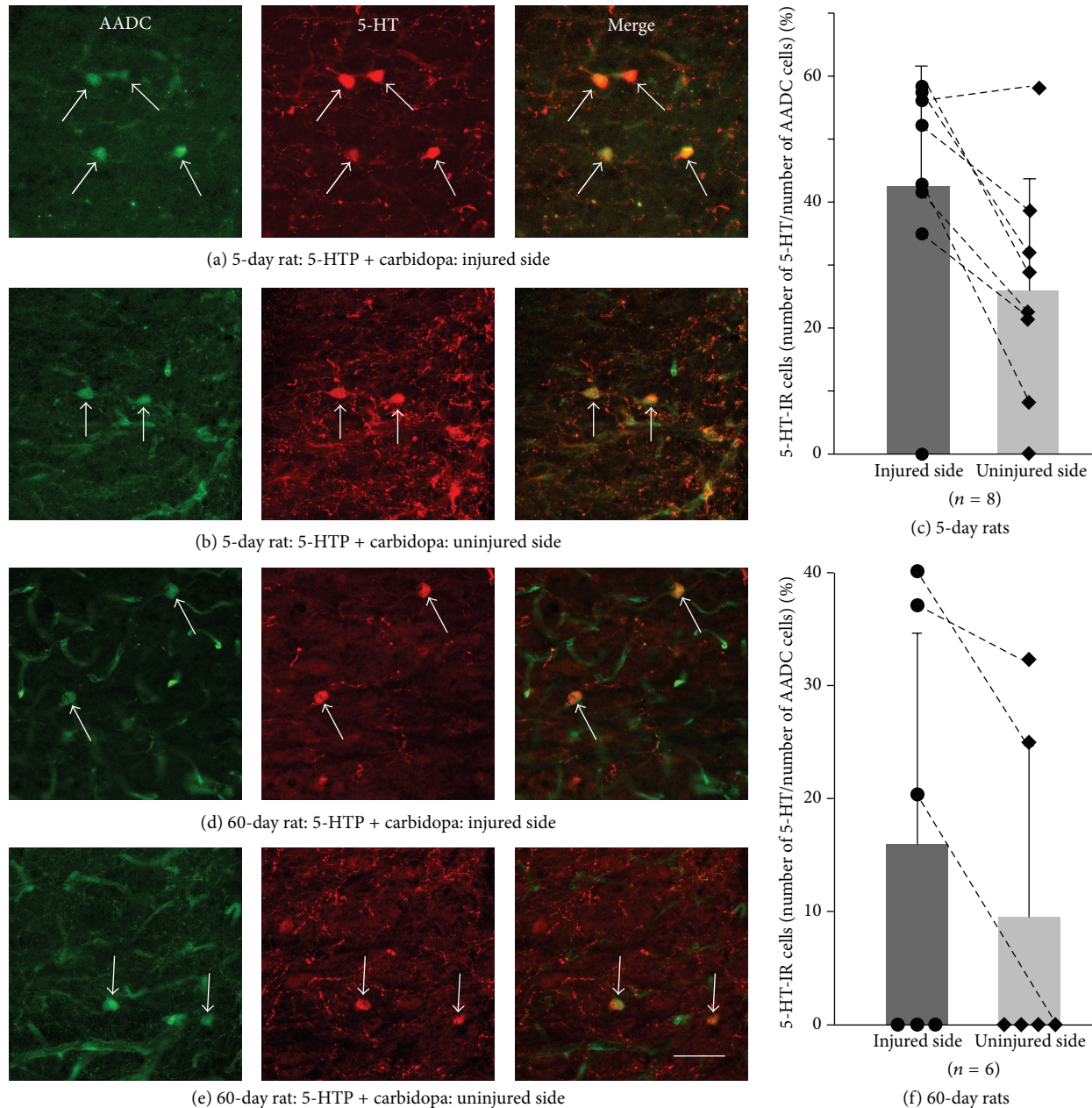


FIGURE 3: 5-HT expression in AADC cells in the intermediate zone in the sacrocaudal spinal cord on the injured and uninjured side in the animal groups injected with 5-HTP and carbidopa. (a) Photomicrograph showing 5-HT-immunoreactive (IR) AADC cells on the injured side in a rat at 5 days after injury. (b) On the uninjured side in a rat at 5 days after injury. Arrows indicate the 5-HT-IR AADC cells. (c) Group data of the incidence of 5-HT-IR AADC cells on the injured side with respect to uninjured side. Dots/squares represent data from different individual cases. Dashed lines connect the data from the same cases. There was significant difference of 5-HT-IR cells between the two sides (** $P < 0.05$). (d–f) Data from 60-day postinjury group with the same format as in 5-day postinjury group.

in the two time groups treated with 5-HTP and carbidopa. The results revealed that on the injured side the incidence of 5-HT-IR AADC cells in 5-day group was significantly higher than that in 60-day group ($P < 0.05$, power = 0.59 with $\alpha = 0.05$, t -test), whereas on the uninjured side the difference was not significant ($P = 0.096$, power = 0.27 with $\alpha = 0.05$, t -test).

Due to large variations for the 5-HT-IR AADC cells in different drug treated groups we speculate whether this was

related to the variations of 5-HT fiber denervation. Thus we have made a Pearson product-moment correlation analysis between incidences of 5-HT-IR AADC cells and the densities of 5-HT fibers in different drug treated groups and the results showed no correlation between the density of the 5-HT-IR fibers and the number of 5-HT-IR AADC cells. Actually, the variation of the density of 5-HT-IR fibers was relatively small within a specific group/side (Table 1), which indicates that

the higher incidences of 5-HT-IR AADC cells in some cases were due to other facts (see Discussion).

4. Discussion

In the present study using thoracic hemisection rat model we found that, first, 5-HT-IR nerve fibers in both the intermediate zone and the ventral horn motoneuron region were dramatically reduced on the injured side in comparison with the uninjured side for both 5-day and 60-day groups, and this decrease did not recover in animals with a longer survival time; second, there was no significant expression difference for the AADC cells on the injured side and uninjured side for both time groups; and third, the AADC cells increased their ability to synthesize 5-HT from its precursor, 5-HTP, at 5 days but not at 60 days after injury. These results indicate different plastic changes may occur for the spinal cord which is subjected to a partial or a complete injury.

4.1. Plastic Changes of 5-HT Fibers following Partial Spinal Cord Injury. There are many investigations to examine the plastic changes of 5-HT fibers with different SCI animal models. The density of 5-HT fibers in the spinal cord after SCI varies in relation to many different factors which include, among others, the severity of the injury, the postinjury time, and the locations in the spinal cord. For example, when the spinal cord was completely transected usually just a few 5-HT-IR fibers were observed below the lesion in the intermediate zone and/or the ventral horn following more than two months of injury [14, 15, 28]. In contusion injury the density of remaining 5-HT fibers below the lesion depends on the locations along the dorsoventral axis and the severity of the injury [20]. In hemisection the density of 5-HT fibers in the ventral horn was reported at a range from 8% to 30% of the control value according to different studies with a postinjury time window from 4 to 7 days [9, 23, 25, 26]. Hains et al. [10] found that, in the dorsal horn (laminae I-II), following 3-day of hemisection at thoracic level, ~30% 5-HT-IR fibers remain in the lumbar spinal cord. Our 5-HT fiber data from 5-day animals in the intermediate zone and the motoneuron region are in general agreement with that reported in the dorsal horn and the ventral horn, indicating that 5-HT fibers may undergo a similar degradation process in different parts of the gray matter.

An apparent discrepancy exists in the literature as to whether 5-HT fibers recover over time after spinal hemisection. Some studies have reported a gradual increase of 5-HT-IR fibers on the ipsilateral side below the lesion [9, 10, 24] whereas some others did not (e.g., [25]). For example, Saruhashi et al. [9] observed that from first week to the fourth week the 5-HT-IR fibers recovered from 20% to about 75% of the normal value in the ventral horn. Camand et al. [24] and Hains et al. [10] also reported similar results although with slight variations in the intermediate zone and dorsal horn, respectively. On the contrary, Filli et al. [25] reported a decrease to about 10% by 4 weeks from about 30% at day 4. Our results are quite similar to Filli et al.'s in that by 60 days the density of 5-HT-IR fibers in the intermediate zone was reduced to 11% from 23% at 5 days. In

the motoneuron region although the value was not reduced so much (23% versus 22%) it neither increased. There might be several explanations for this discrepancy. First, the different locations in the spinal gray matter may undergo different plastic changes of 5-HT innervations. In our study 5-HT fiber density in the ipsilateral intermediate zone decreased more than in the motoneuron region upon 60 days, which may indicate that the intermediate zone is less affected by 5-HT axon reinnervation. Second, upon 5 days after injury the 5-HT fibers may not drop to the lowest level. It may take 2-3 weeks for the degenerated 5-HT fibers to completely disappear [14]. In this case the reinnervation will take some time to reach a certain level. Thus more experimental groups with narrower time intervals are needed. Third, it might be more logical to compare the data from the injured side with the normal control animal rather than the uninjured sides, since hemisection could also affect the 5-HT fiber density in the uninjured side considering the existence of crossing 5-HT fibers. In addition, different lesion level, slight lesion variations, and different analysis methods may also result in different 5-HT density output. In any way, further studies are needed to find out which factor(s) is (are) involved in causing this discrepancy.

We observed that the density of 5-HT-IR fibers in the intermediate zone increased on both sides in 5-day group and on injured side in 60-day group after combining 5-HTP and carbidopa injections, and the density decreased in the motoneuron region for both sides in the two time groups. It is easy to understand the increase due to the increased availability of 5-HT precursor in the 5-HT fibers. However, it is bewildering that 5-HT fiber density decreased with addition of 5-HTP. One possible explanation may be that the contribution of 5-HT fibers from the AADC cells is very limited presumably due to their poor fiber arborization. In this case, what we saw in the motoneuron region is just the results representing approximately those prior to 5-HTP application.

4.2. Plasticity of AADC Cells following SCI. Similar to our study using complete spinal transection rat model [22] we did not observe AADC cell expression changes on the injured side. This result is different from Li et al.'s [29] observation that AADC cells are only expressed in the region around the central canal and that only after spinal transection they start to appear in the intermediate zone. The results from our group thus indicate that the number of AADC cells is not increased in response to SCI although AADC plastic changes at molecular level cannot be excluded.

One of the main purposes of the present study is to examine whether AADC cells increase their ability to produce 5-HT from its precursor, 5-HTP. It has been reported both from our and Bennett's research group that after complete spinal transection AADC cells in the spinal cord increase their efficacy to catalyze 5-HTP [22, 29]. In the present study we have observed an increased enzymatic ability in spinal AADC cells on the injured side at 5 days but, to our surprise, not at 60 days although the results are not conclusive due to the lower statistical power in the 60-day group. Thus we have observed a different AADC activity in response to

complete spinal transection and hemisection. At 5 days after either complete spinal transection or hemisection AADC cells dramatically increase their ability to use 5-HT precursor to synthesize 5-HT ([22]; present study). This rapid response of AADC cells in the spinal cord may be a response to a sudden loss of supraspinal 5-HT innervation, and thus through the deactivation of 5-HT_{1B} receptors AADC cells are activated [22]. After spinal hemisection both intraspinal and supraspinal plasticity occur which will help eventually to reestablish anatomical and functional circuits in the spinal cord. In addition to the descending 5-HT pathway other descending pathways, such as corticospinal, rubrospinal, and reticulospinal pathway, may also have an inhibitory effect on the spinal AADC cells. A large body of evidence has indicated that extensive plasticity occurs usually after 2-3 weeks of injury (reviewed by Nardone et al. [30]). Indeed, using microdialysis technique Gerin et al. [31] have found that 5-HT release in the lumbar ventral horn showed about 200% increase at day 18 relative to day 8 following subhemisection. Meanwhile plastic changes of many other pathways, including intraspinal and descending pathways, may reorganize and reestablish functional circuits in the spinal cord [6, 32]. All the above factors may contribute to reestablishing an inhibitory network for the AADC cells in the chronic phase following hemisection. In spinal transection these descending pathways, including 5-HT pathway, will not recover below the lesion; thus AADC cells will continue to be active in the chronic phase.

4.3. Significance of Plastic Changes of AADC System in the Spinal Cord. 5-HT is an important neuromodulator for both motor and sensory functions in the spinal cord [11, 30]. Numerous studies have illustrated that locomotor activity can be recovered following 5-HT or its precursor application or transplantation of 5-HT-producing cells in the spinal cord after spinal cord transection [30, 33–36]. Thus it is extremely important that after SCI there are sources in the spinal cord that could produce 5-HT. Evidence from complete spinal cord transection studies showed that the activity of AADC cells is increased in both the subchronic and chronic phase and 5-HT produced from these cells could induce increased motoneuron excitability and thus muscle spasms. Our results in the present study indicate that after hemisection a plastic change occurs for AADC cells in that in the subchronic phase they could increase their ability to potentially provide 5-HT if its precursor is available. Although AADC cell activity is not significantly increased in chronic phase the cells may help to maintain the reestablished spinal network which is essential for functional recovery of the spinal cord in later phase. Actually in agreement with many other studies (e.g., [9, 25]) we observed a motor function recovery over time in the body parts below the hemisection in 60-day rats without giving any external interventions. It deserves further investigation as to how much AADC cells contribute to this functional recovery.

Conflict of Interests

The authors declare that there is no conflict of interests regarding the publication of this paper.

Acknowledgments

We are grateful to Lillian Grøndahl and Britta Karlsson for their technical assistance. This project was supported by the Lundbeck Foundation, the Danish Multiple Sclerosis Foundation, and the Danish Medical Research Council.

References

- [1] J. N. Kornegay, "Paraparesis (paraplegia), tetraparesis (tetraplegia), urinary/fecal incontinence. Spinal cord diseases," *Problems in Veterinary Medicine*, vol. 3, no. 3, pp. 363–377, 1991.
- [2] M. D. Christensen and C. E. Hulsebosch, "Chronic central pain after spinal cord injury," *Journal of Neurotrauma*, vol. 14, no. 8, pp. 517–537, 1997.
- [3] S. Hou and A. G. Rabchevsky, "Autonomic consequences of spinal cord injury," *Comprehensive Physiology*, vol. 4, no. 4, pp. 1419–1453, 2014.
- [4] E. M. Hagen, "Acute complications of spinal cord injuries," *World Journal of Orthopedics*, vol. 6, no. 1, pp. 17–23, 2015.
- [5] N. Sezer, S. Akkuş, and F. G. Uğurlu, "Chronic complications of spinal cord injury," *World Journal of Orthopaedics*, vol. 6, no. 1, pp. 24–33, 2015.
- [6] O. Raineteau and M. E. Schwab, "Plasticity of motor systems after incomplete spinal cord injury," *Nature Reviews Neuroscience*, vol. 2, no. 4, pp. 263–273, 2001.
- [7] C. Darian-Smith, "Synaptic plasticity, neurogenesis, and functional recovery after spinal cord injury," *Neuroscientist*, vol. 15, no. 2, pp. 149–165, 2009.
- [8] H. Barbeau and S. Rossignol, "Initiation and modulation of the locomotor pattern in the adult chronic spinal cat by noradrenergic, serotonergic and dopaminergic drugs," *Brain Research*, vol. 546, no. 2, pp. 250–260, 1991.
- [9] Y. Saruhashi, W. Young, and R. Perkins, "The recovery of 5-HT immunoreactivity in lumbosacral spinal cord and locomotor function after thoracic hemisection," *Experimental Neurology*, vol. 139, no. 2, pp. 203–213, 1996.
- [10] B. C. Hains, A. W. Everhart, S. D. Fullwood, and C. E. Hulsebosch, "Changes in serotonin, serotonin transporter expression and serotonin denervation supersensitivity: involvement in chronic central pain after spinal hemisection in the rat," *Experimental Neurology*, vol. 175, no. 2, pp. 347–362, 2002.
- [11] B. J. Schmidt and L. M. Jordan, "The role of serotonin in reflex modulation and locomotor rhythm production in the mammalian spinal cord," *Brain Research Bulletin*, vol. 53, no. 5, pp. 689–710, 2000.
- [12] P. J. Harvey, X. Li, Y. Li, and D. J. Bennett, "Endogenous monoamine receptor activation is essential for enabling persistent sodium currents and repetitive firing in rat spinal motoneurons," *Journal of Neurophysiology*, vol. 96, no. 3, pp. 1171–1186, 2006.
- [13] X.-Y. Kong, J. Wienecke, H. Hultborn, and M. Zhang, "Robust upregulation of serotonin 2A receptors after chronic spinal transection of rats: an immunohistochemical study," *Brain Research*, vol. 1320, pp. 60–68, 2010.
- [14] X.-Y. Kong, J. Wienecke, M. Chen, H. Hultborn, and M. Zhang, "The time course of serotonin 2A receptor expression after spinal transection of rats: an immunohistochemical study," *Neuroscience*, vol. 177, pp. 114–126, 2011.
- [15] K. C. Murray, A. Nakae, M. J. Stephens et al., "Recovery of motoneuron and locomotor function after spinal cord injury

- depends on constitutive activity in 5-HT_{2C} receptors," *Nature Medicine*, vol. 16, no. 6, pp. 694–700, 2010.
- [16] L.-Q. Ren, J. Wienecke, M. Chen, M. Møller, H. Hultborn, and M. Zhang, "The time course of serotonin 2C receptor expression after spinal transection of rats: an immunohistochemical study," *Neuroscience*, vol. 236, pp. 31–46, 2013.
 - [17] A. Bjorklund and G. Skagerberg, "Evidence for a major spinal cord projection from the diencephalic A11 dopamine cell group in the rat using transmitter-specific fluorescent retrograde tracing," *Brain Research*, vol. 177, no. 1, pp. 170–175, 1979.
 - [18] B. L. Jacobs and E. C. Azmitia, "Structure and function of the brain serotonin system," *Physiological Reviews*, vol. 72, no. 1, pp. 165–230, 1992.
 - [19] T. Magnusson, "Effect of chronic transection on dopamine, noradrenaline and 5-hydroxytryptamine in the rat spinal cord," *Naunyn-Schmiedeberg's Archives of Pharmacology*, vol. 278, no. 1, pp. 13–22, 1973.
 - [20] A. I. Faden, A. Gannon, and A. I. Basbaum, "Use of serotonin immunocytochemistry as a marker of injury severity after experimental spinal trauma in rats," *Brain Research*, vol. 450, no. 1–2, pp. 94–100, 1988.
 - [21] C. B. Jaeger, G. Teitelman, T. H. Joh, V. R. Albert, D. H. Park, and D. J. Reis, "Some neurons of the rat central nervous system contain aromatic-L-amino-acid decarboxylase but not monoamines," *Science*, vol. 219, no. 4589, pp. 1233–1235, 1983.
 - [22] J. Wienecke, L. Ren, H. Hultborn et al., "Spinal cord injury enables aromatic L-amino acid decarboxylase cells to synthesize monoamines," *Journal of Neuroscience*, vol. 34, no. 36, pp. 11984–12000, 2014.
 - [23] M. Hadjiconstantinou, P. Panula, Z. Lackovic, and N. H. Neff, "Spinal cord serotonin: a biochemical and immunohistochemical study following transection," *Brain Research*, vol. 322, no. 2, pp. 245–254, 1984.
 - [24] E. Camand, M.-P. Morel, A. Faissner, C. Sotelo, and I. Dusart, "Long-term changes in the molecular composition of the glial scar and progressive increase of serotonergic fibre sprouting after hemisection of the mouse spinal cord," *European Journal of Neuroscience*, vol. 20, no. 5, pp. 1161–1176, 2004.
 - [25] L. Filli, B. Zörner, O. Weinmann, and M. E. Schwab, "Motor deficits and recovery in rats with unilateral spinal cord hemisection mimic the Brown-Séquard syndrome," *Brain*, vol. 134, no. 8, pp. 2261–2273, 2011.
 - [26] B. S. Bregman, "Development of serotonin immunoreactivity in the rat spinal cord and its plasticity after neonatal spinal cord lesions," *Brain Research*, vol. 431, no. 2, pp. 245–263, 1987.
 - [27] N. E. Andén, J. Haeggendal, T. Magnusson, and E. Rosengren, "The time course of the disappearance of noradrenaline and 5-hydroxytryptamine in the spinal cord after transection," *Acta Physiologica Scandinavica*, vol. 62, pp. 115–118, 1964.
 - [28] A. Takeoka, M. D. Kubasak, H. Zhong, R. R. Roy, and P. E. Phelps, "Serotonergic innervation of the caudal spinal stump in rats after complete spinal transection: effect of olfactory ensheathing glia," *Journal of Comparative Neurology*, vol. 515, no. 6, pp. 664–676, 2009.
 - [29] Y. Li, L. Li, M. J. Stephens et al., "Synthesis, transport, and metabolism of serotonin formed from exogenously applied 5-HTP after spinal cord injury in rats," *Journal of Neurophysiology*, vol. 111, no. 1, pp. 145–163, 2014.
 - [30] R. Nardone, Y. Höller, A. Thomschewski et al., "Serotonergic transmission after spinal cord injury," *Journal of Neural Transmission*, vol. 122, pp. 279–295, 2015.
 - [31] C. G. Gerin, A. Hill, S. Hill, K. Smith, and A. Privat, "Serotonin release variations during recovery of motor function after a spinal cord injury in rats," *Synapse*, vol. 64, no. 11, pp. 855–861, 2010.
 - [32] B. Zörner, L. C. Bachmann, L. Filli et al., "Chasing central nervous system plasticity: the brainstem's contribution to locomotor recovery in rats with spinal cord injury," *Brain*, vol. 137, no. 6, pp. 1716–1732, 2014.
 - [33] O. Kiehn and O. Kjaerulff, "Spatiotemporal characteristics of 5-HT and dopamine-induced rhythmic hindlimb activity in the in vitro neonatal rat," *Journal of Neurophysiology*, vol. 75, no. 4, pp. 1472–1482, 1996.
 - [34] D. Feraboli-Lohnherr, D. Orsal, A. Yakovlev, M. Giménez Y Ribotta, and A. Privat, "Recovery of locomotor activity in the adult chronic spinal rat after sublesional transplantation of embryonic nervous cells: specific role of serotonergic neurons," *Experimental Brain Research*, vol. 113, no. 3, pp. 443–454, 1997.
 - [35] K. A. Leech, C. R. Kinnaird, and T. G. Hornby, "Effects of serotonergic medications on locomotor performance in humans with incomplete spinal cord injury," *Journal of Neurotrauma*, vol. 31, no. 15, pp. 1334–1342, 2014.
 - [36] U. Slawinska, K. Miazga, and L. M. Jordan, "The role of serotonin in the control of locomotor movements and strategies for restoring locomotion after spinal cord injury," *Acta Neurobiologiae Experimentalis*, vol. 74, no. 2, pp. 172–187, 2014.

Research Article

Contralateral Metabolic Activation Related to Plastic Changes in the Spinal Cord after Peripheral Nerve Injury in Rats

Ran Won¹ and Bae Hwan Lee²

¹Department of Biomedical Laboratory Science, Division of Health Sciences, Dongseo University, Busan 617-716, Republic of Korea

²Department of Physiology, Brain Research Institute, Epilepsy Research Institute, Brain Korea 21 PLUS Project for Medical Science, Yonsei University College of Medicine, Seoul 120-752, Republic of Korea

Correspondence should be addressed to Bae Hwan Lee; bhlee@yuhs.ac

Received 13 February 2015; Revised 5 May 2015; Accepted 5 May 2015

Academic Editor: Michael G. Stewart

Copyright © 2015 R. Won and B. H. Lee. This is an open access article distributed under the Creative Commons Attribution License, which permits unrestricted use, distribution, and reproduction in any medium, provided the original work is properly cited.

We have previously reported the crossed-withdrawal reflex in which the rats with nerve injury developed behavioral pain responses of the injured paw to stimuli applied to the contralateral uninjured paw. This reflex indicates that contralateral plastic changes may occur in the spinal cord after unilateral nerve injury. The present study was performed to elucidate the mechanisms and morphological correlates underlying the crossed-withdrawal reflex by using quantitative ¹⁴C-2-deoxyglucose (2-DG) autoradiography which can examine metabolic activities and spatial patterns simultaneously. Under pentobarbital anesthesia, rats were subjected to unilateral nerve injury. Mechanical allodynia was tested for two weeks after nerve injury. After nerve injury, neuropathic pain behaviors developed progressively. The crossed-withdrawal reflex was observed at two weeks postoperatively. Contralateral enhancement of 2-DG uptake in the ventral horn of the spinal cord to electrical stimulation of the uninjured paw was observed. These results suggest that the facilitation of information processing from the uninjured side to the injured side may contribute to the crossed-withdrawal reflex by plastic changes in the spinal cord of nerve-injured rats.

1. Introduction

It has been shown that peripheral nerve injury can cause severe chronic pain in humans [1, 2]. Humans frequently experience neuropathic pain symptoms such as spontaneous burning painful sensations, hyperalgesia (elevated sensitivity to noxious stimulation), and allodynia (painful experience to innocuous stimulation) after peripheral nerve injury.

Occasionally, neuropathic pain symptoms can be observed on the opposite side of the nerve injury in humans or in experimental animal models of neuropathic pain [1–4]. It indicates that the intact side of the body can be sensitive and may produce secondary pain after unilateral nerve injury [5, 6]. This phenomenon has been known as the “mirror image pain.” Although the mechanism of mirror image pain remains unclear, the investigation for possible mechanisms for mirror image pain is an ongoing project. In mirror image pain, IL-6 protein and mRNA in both lumbar and cervical dorsal root ganglia were elevated bilaterally

following unilateral chronic compression injury of the sciatic nerve [7]. Also, bilateral changes of cannabinoid receptor type 2 protein and mRNA in the dorsal root ganglia of a rat neuropathic pain model were reported [8].

In our previous study [9], we observed that the rats with unilateral nerve injury showed withdrawal responses of the injured paw to stimuli applied to the contralateral uninjured paw. This phenomenon is fundamentally different from mirror image pain. Therefore, this phenomenon is called “the crossed-withdrawal reflex.” The mechanisms underlying the crossed-withdrawal reflex are still uncertain. For the crossed-withdrawal reflex to appear, the dorsal horn neurons on the intact side need to be activated by applied stimulation and then the ventral horn neurons on the injured side need to be activated by inputs from the intact side. However, the connections between the dorsal horn neurons on the intact side and the ventral horn neurons on injured side are unclear. For example, the information may be transmitted directly from the dorsal horn on the intact side to the ventral horn

of the injured side. Otherwise, the input information on the intact side may go indirectly to the ventral horn on the injured side via a relaying part of the spinal cord. Despite the lack of information of a detailed mechanism, the crossed-withdrawal reflex is a very interesting phenomenon. It appears to reflect the central neuroplastic changes, which involve various morphological, electrophysiological, and biochemical processes.

The fact that increased neuronal excitability is linked with increased metabolism has been confirmed by ^{14}C -2-deoxyglucose (2-DG) autoradiography, which is a functional mapping technique established by Sokoloff et al. [10]. 2-DG is phosphorylated by hexokinase to form 2-DG-6-phosphate, which is not metabolized further and trapped within activated cells. 2-DG technique allows simultaneous examination of metabolic activity and spatial pattern affected by a stimulus or behavioral condition [11–14]. Recently, Dedeurwaerdere et al. [15] reported patterns of brain glucose metabolism to investigate a clinically functional biomarker by using 2-DG autoradiography technique.

The present study was conducted to elucidate the mechanism of “the crossed-withdrawal reflex” and to clarify the alteration of metabolic activity of this phenomenon using the quantitative 2-DG autoradiography technique.

2. Materials and Methods

2.1. Neuropathic Model. Male Sprague-Dawley rats weighing between 200 and 250 g were used. All animal experiments were approved by the Institutional Animal Care and Use Committee of Yonsei University Health System. Twelve rats were anesthetized with pentobarbital (Entobar, 50 mg/kg, i.p.). To make a neuropathic injury model, the tibial and sural nerves were cut with fine scissors after a tight ligation with a 6-0 silk thread, while the common peroneal nerve was left intact [16].

2.2. Behavioral Tests. Mechanical allodynia was carried out in all of the rats preoperatively and again for two weeks postoperatively. An innocuous mechanical stimulus was applied with a von Frey filament (8 mN of bending force) to the sensitive area of the hind paw. Rats were placed on a metal mesh floor under a transparent plastic dome (8 × 8 × 18 cm). By poking various areas of the paw with a von Frey filament the most sensitive area was determined in advance. Afterwards, the test was conducted 10 times to each hind paw by gently poking the most sensitive spot with the filament. The frequency of foot withdrawal expressed as a percentage was used as the index of mechanical allodynia. Assessments were made on both the injured side and uninjured contralateral side.

To examine the crossed-withdrawal reflex, animals expressing response rates equal or more than 40% in mechanical allodynia were stimulated to the contralateral uninjured paw. To compare to the real stimulation, sham stimulation was applied according to the same procedure as von Frey filament except for actual contact and then the frequency of the paw withdrawal was expressed as shown above. The responses to the actual and sham applications of von Frey filament were compared using the paired *t*-test.

2.3. Autoradiography. Five nerve-injured rats and four normal controls weighing 250–350 g were used to conduct 2-DG technique. Under pentobarbital anesthesia (50 mg/kg), thoracic jugular vein catheter (Braintree Scientific, Inc. MA, USA) was inserted into the external jugular vein contralateral to the side of nerve injury. The free end of the catheter was expelled through a subcutaneous tunnel to a small incision in the top of the head. A bolus of ^{14}C -2-DG (25uCi) was then injected over 15 sec into the jugular vein 5 min before the uninjured paw was electrically stimulated. Electrical pulses (rectangular pulse, 3–6 mA, 0.4 msec, 0.5 Hz) were delivered for 20 min to bipolar needle electrodes inserted subcutaneously into the receptive field (defined in the behavior test) of the uninjured hind paw. 25 min after the electrical stimulation, the animals were sacrificed by an overdose of pentobarbital and perfused with saline and 10% formalin solution. The spinal cords (L1–L6) were rapidly removed and immediately frozen. Lumbar segments of the spinal cord were sectioned into 20 μm slices using a cryostat (Leica, Wetzlar, Germany) at -20°C .

The sections were attached to a cardboard and were exposed with precalibrated [^{14}C]-methyl methacrylate standards (Amersham, Piscataway, NJ, USA) to X-ray film (Kodak BioMax MR) for 10 days. For quantitative analysis, the spinal cord gray matter was divided into 4 regions: the dorsal horn (corresponding approximately to laminae I–IV), the intermediate horn (laminae V–VI), the ventral horn (laminae VII–IX), and the central gray (lamina X). The selected regions were digitized using computer-generated templates for each spinal lumbar segment from L1 to L6. The digitized images were quantified using the MetaMorph Imaging System (Universal Image Co., Downingtown, PA, USA).

2.4. Statistical Analysis. Data were expressed as means \pm S.E.M. Differences in changes of neuropathic pain behaviors following nerve injury were tested using Friedman’s two-way ANOVA by ranks, followed by post-hoc pairwise comparisons.

The frequency of the paw withdrawal responses to the actual applications of von Frey filament and sham stimulation was compared using the paired *t*-test. The crossed-withdrawal reflex developing after nerve injury was analyzed using Friedman’s two-way ANOVA by ranks followed by post hoc pairwise comparisons. Pearson’s product-moment correlation coefficient between responsiveness of the injured and uninjured paws to von Frey filament of the uninjured side was analyzed using *t*-test.

To evaluate the lateralization of information processing following electrical stimulation of the uninjured side of the spinal cord, data from the ventral horns both ipsilateral and contralateral to electrical stimulation were analyzed using the cross ratio, which is as follows: [metabolic activity in the contralateral ventral horn]/[metabolic activity in the ipsilateral ventral horn] \times 100.

Data were expressed as means \pm S.E.M. at each level of the lumbar spinal cord. Cross ratios of the nerve-injured rats and those of normal control rats were compared at each spinal level using the independent *t*-test.

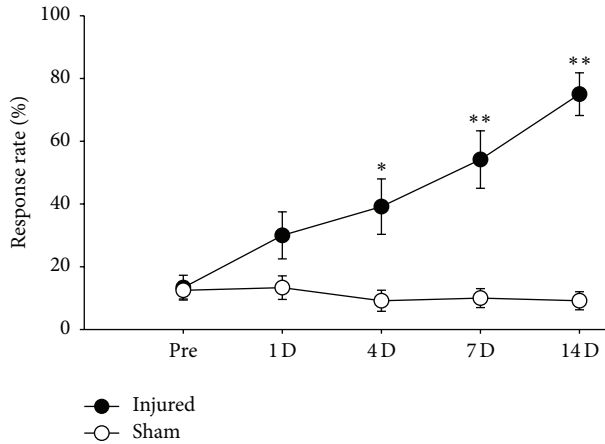


FIGURE 1: Development of mechanical allodynia in rats with injury to the tibial and sural nerves. Response rate to a von Frey filament was used as an index of mechanical allodynia. Data were expressed as means \pm S.E.M. Abscissa was marked as Pre for preoperative time and D for postoperative days (Sham: sham-operated control rats, Injured: neuropathic rats). Asterisks (*) indicate significant differences compared to preoperative values, according to Friedman's repeated ANOVA on ranks followed by Dunnett's multiple comparison test (* $P < 0.05$, ** $P < 0.01$).

3. Results

3.1. Development of Mechanical Hypersensitivity. The result of mechanical allodynia is shown in Figure 1. The response rate to a von Frey filament was used as an index of mechanical allodynia. As shown in Figure 1, the rats were rarely responsive to a von Frey filament prior to the surgery. The responsiveness of the injured foot gradually increased from the first day and reached its highest level on the 14th day postoperatively.

3.2. Behavioral Crossed-Withdrawal Reflex. In Figure 2, the result of the crossed-withdrawal reflex is shown by expressed responsiveness of the injured paw to the application of a von Frey filament to the uninjured side. The frequency of the paw withdrawal was compared between the actual stimulation of von Frey filament and sham application. The crossed-withdrawal reflexes were apparently higher than the responsiveness of the injured paws to the sham stimulation ($P < 0.05$, paired t -test) but the reflex was not observed in normal control animals.

3.3. Effects of Nerve Injury on Metabolic Activities in the Spinal Cord. To observe any increased crossing input from the uninjured side to the injured side in the spinal cord, the metabolic activities of the lumbar spinal cord in normal controls and nerve-injured rats that expressed cross-withdrawal reflexes were compared. Electrical stimulation of the uninjured paw of neuropathic rats produced significantly increased 2-DG uptake in contralateral ventral horn in the lumbar spinal cord; but, in normal controls, upregulation of

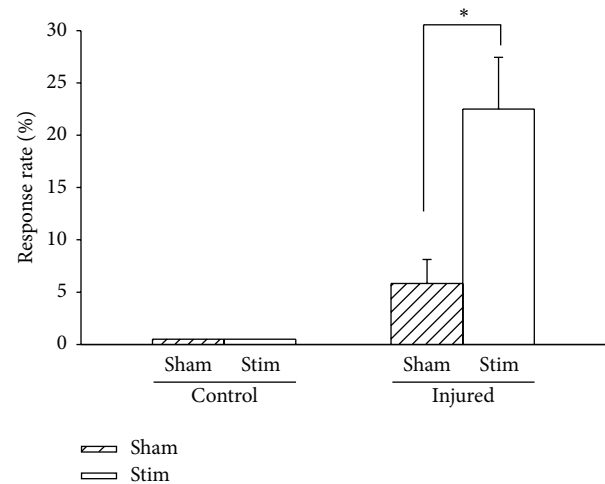


FIGURE 2: Crossed-withdrawal reflex measured by the response of the injured paw to stimulation of the uninjured paw on day 14 postoperatively. The frequency of the paw withdrawal was expressed as means \pm S.E.M. and compared between actual applications (Stim) of von Frey filament and sham stimulation (Sham). (Control: control rats, Injured: neuropathic rats). An asterisk (*) indicates significant differences between actual applications of stimuli and sham stimulation, according to the paired t -test (* $P < 0.05$).

2-DG uptake was produced in the ipsilateral ventral horn where the electrical stimulation was applied (Figure 3).

Cross ratios from different levels of the spinal cord are compared in Figure 4. Of the lumbar segments, L3 to L6 segments in nerve-injured rats were associated with significantly higher cross ratios than normal controls ($P < 0.05$, independent t -test). In the L1-L2 segments, the cross ratios of nerve-injured rats tended to be slightly higher but were not significantly different from controls ($P > 0.05$, independent t -test).

4. Discussion

After nerve injury, bilateral allodynia including original pain and mirror image pain can be found in experimental animal models as well as human patients. It has been shown that the mirror image pain develops in a minority of human patients but it recurs frequently [17].

Contralateral changes resulting from ipsilateral pain symptoms have also been reported through different experimental paradigms in the absence of lesions of the nervous systems. Subcutaneous injection of dilute formalin solution into a hind paw induced a mirror-image-like pain, and the rats frequently licked the contralateral untreated hind paw [18]. A similar phenomenon was reported using a unilateral inflammation model in the rat ankle [19]. These observations suggest that initial painful states on one side may produce hypersensitivity on the contralateral uninjured side following unilateral injury. Therefore, the secondary pain on the other side can be seen as a "mirror image pain." However, the mechanisms underlying mirror image pain may be different from those of original pain ipsilateral to injury as the original

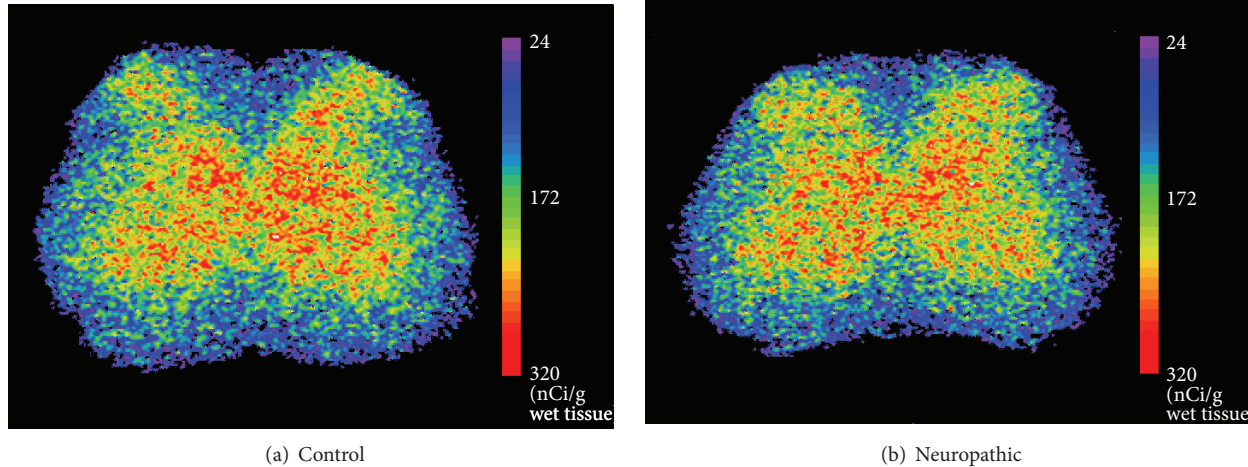


FIGURE 3: Representative pseudocolor-enhanced images showing metabolic activities in the L3 lumbar spinal cord of control (a) and neuropathic (b) rats after peripheral stimulation. The right side of the spinal cord is ipsilateral to the electrical stimulation of the hind paw. Note the increased 2-DG uptake in the contralateral ventral horn of the neuropathic rat compared to the ipsilateral ventral horn. On the contrary, 2-DG uptake increased in the ipsilateral ventral horn of the control rat compared to the contralateral ventral horn.

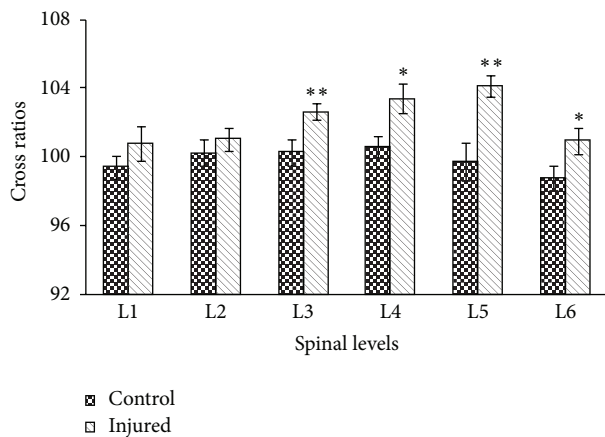


FIGURE 4: Comparison between cross ratios at different lumbar levels of the spinal cord in normal and neuropathic rats following electrical stimulation of the paw. Cross ratios were calculated as follows: [metabolic activity in the contralateral ventral horn]/[metabolic activity in the ipsilateral ventral horn] $\times 100$ (Control: control rats, Injured: neuropathic rats). Asterisks (*) indicate significant differences between cross ratios at different lumbar levels of the spinal cord in normal and neuropathic rats, according to the independent *t*-test (* $P < 0.05$, ** $P < 0.01$).

ipsilateral pain was relieved by intravenous lidocaine but not the mirror image pain [20].

In the present study, the crossed-withdrawal reflex represents information processing from input on the uninjured side to output on the injured side. This phenomenon was morphologically determined by using the 2-DG autoradiography technique. As determined by cross ratio using the 2-DG technique, the magnitude of the contralateral metabolic 2-DG activity over the ipsilateral activity by the stimulation of the uninjured side in the neuropathic rat was greater than that in the normal control animals. This result indicates that information processing from input on the uninjured side to output

on the injured side must be facilitated in rats with nerve injury. This result provides a morphological and metabolic evidence for the behavioral cross-withdrawal reflex.

Similarly, it was found that spinal cord glucose consumption increased both contralaterally and ipsilaterally after chronic constriction injury of the unilateral sciatic nerve [11, 12]. Contralateral increase of 2-DG uptake in the spinal cord was also found after unilateral noxious heat stimulation of a hind limb in cats [21] and after formalin injection into the hind paw of rats [19], but there has been no report that has shown facilitated metabolic activity from input on the uninjured side to output on the injured side. Even though it is not exactly in agreement with the report that spinal cord activity may be altered in chronic pain states [22], our own results support the hypothesis that the observed metabolic pattern in the spinal cord is mainly due to information processing from input on the uninjured side to output on the injured side. The present 2-DG data are in accordance with the behavioral and electrophysiological findings of the crossed-withdrawal reflex [9].

Our previous study [9] reported that rats show the crossed-withdrawal reflex after unilateral peripheral nerve injury. The crossed-withdrawal reflex is known as the increased responsiveness on the injured side to stimulation on the uninjured side, indicating neuroplastic changes in the spinal cord after nerve injury. In the case of conventional neuropathic pain, sensory information from the dorsal root goes to the ipsilateral ventral horn of the injured side. In the case of mirror image pain, sensory information from the dorsal root goes to the ipsilateral ventral horn on the uninjured side. Therefore, conventional neuropathic pain and mirror image pain behaviors are represented unilaterally. However, the crossed-withdrawal reflex is represented contralaterally. As a result, sensory information from the dorsal root on the uninjured side travels across the midline of the spinal cord to reach the contralateral ventral horn of the injured side (Figure 5).

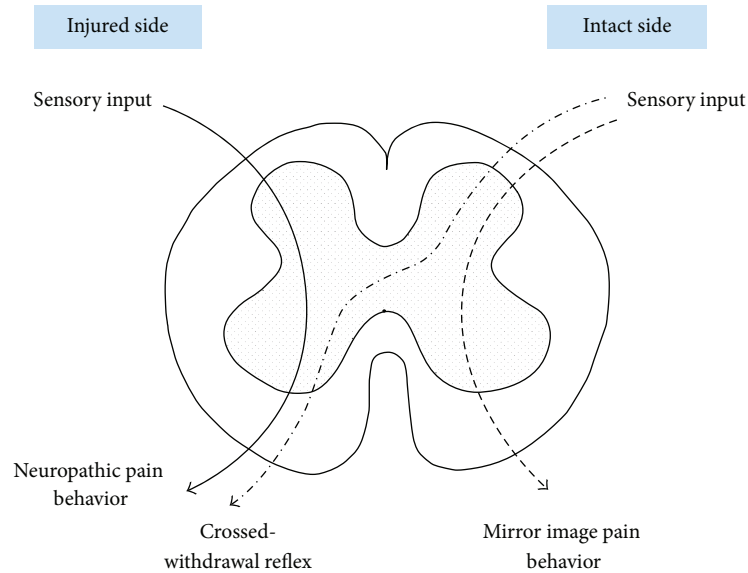


FIGURE 5: Diagram showing the neuropathic behavior, mirror image pain behavior, and crossed-withdrawal reflex. The crossed-withdrawal reflex is the increased responsiveness of the injured side to stimulation on the uninjured side. In terms of input-output information processing, conventional neuropathic pain and mirror image pain behaviors are represented unilaterally. However, the crossed-withdrawal reflex is represented contralaterally. In other words, input through the dorsal root traverses across the midline of the spinal cord toward the contralateral ventral horn.

Our present study showed that electrical stimulation on the uninjured side increased metabolic activities on the injured side through the multisegments of the spinal cord. These results suggest that maybe there exist heterotopic transneuronal signaling pathways between the uninjured side and the injured side. There are evidences supporting the existence of the transneuronal signaling pathway. The anatomical study by Fitzgerald [23] reported that a neural connection exists at the spinal cord, indicating that the transneuronal signaling pathway may be mediated via commissural tracts or interneurons in the spinal cord. In a pathological condition as shown after injury, sensations on the intact side can be frequently related to the sensations on the injured side. According to an electrophysiological study by Sotgiu and Biella [20], 88% of wide-dynamic range (WDR) neurons ipsilateral to injury were activated by noxious mechanical stimulation on the intact side in anesthetized, spinalized rats. The activated responses of WDR neurons were significantly larger in nerve-injured rats than in sham or intact animals. In the case of phantom limb pain, painful muscle areas in the intact limb were related to the painful areas in the phantom limb [24]. Light stimulation on a healthy limb often leads to touch or pain in both the injured and intact limbs (synchiria) [25, 26]. Furthermore, Casale et al. [25] found that phantom limb pain can be relieved by contralateral myofascial injection of bupivacaine, a local anaesthetic, in human patients. In addition, phantom limb pain can be attenuated by transcutaneous electric nerve stimulation (TENS) applied to the contralateral healthy limb [27]. These suggest that heterotopic treatment may relieve chronic pain through the transneuronal signaling pathway.

The detailed mechanisms of the crossed-withdrawal reflex with nerve injury still remain to be determined. However, this result is in good agreement with the report which demonstrates that peripheral nerve injury, a model for neuropathic pain, is associated with a synaptic plasticity in the spinal dorsal horn [28]. The crossed-withdrawal reflex provides a useful model for neural plasticity and may contribute to the modulation of neuropathic pain.

5. Conclusions

We observed that the rats with unilateral nerve injury showed withdrawal responses of the injured paw to stimuli applied to the contralateral uninjured paw. We called this unusual response type “the crossed-withdrawal reflex.” We determined the “crossed-withdrawal reflex” by behavioral and electrophysiological aspects in our previous report.

In the present study, electrical stimulation of the uninjured paw of neuropathic rats produced significant increase of 2-DG uptake in contralateral ventral horn in the lumbar spinal cord. This result is in accordance with the behavioral and electrophysiological findings of the crossed-withdrawal reflex and suggests that information processing from input on the uninjured side to output on the injured side may be facilitated in neuropathic rats by neuroplastic changes through the heterotopic transneuronal signaling pathway in the spinal cord after peripheral nerve injury.

Conflict of Interests

The authors declare that there is no conflict of interests regarding the publication of this paper.

Acknowledgment

This work was supported by the National Research Foundation of Korea funded by the Ministry of Science, ICT and Future Planning (NRF-2015021989).

References

- [1] S. W. Mitchell, *Injuries of Nerves and Their Consequences*, Lippincott, Philadelphia, Pa, USA, 1872.
- [2] J. J. Bonica, "Causalgia and other reflex sympathetic dystrophies," in *Advances in Pain Research and Therapy*, J. J. Bonica, J. C. Liebeskind, and D. G. Albe-Fessard, Eds., vol. 3, pp. 141–166, Raven Press, New York, NY, USA, 1979.
- [3] P. K. Thomas, "Clinical features and differential diagnosis," in *Peripheral Neuropathy*, P. J. Dyck, P. K. Thomas, E. H. Lambert, and R. Bunge, Eds., pp. 1169–1190, Saunders, Philadelphia, Pa, USA, 2nd edition, 1984.
- [4] W. K. Livingston, "The mirror image," in *Pain and Suffering*, H. L. Fields, Ed., pp. 79–85, IASP Press, Seattle, Wash, USA, 1998.
- [5] V. Kayser, A. I. Basbaum, and G. Guilbaud, "Deafferentation in the rat increases mechanical nociceptive threshold in the innervated limbs," *Brain Research*, vol. 508, no. 2, pp. 329–332, 1990.
- [6] B. P. Vos, A. M. Strassman, and R. J. Maciewicz, "Behavioral evidence of trigeminal neuropathic pain following chronic constriction injury to the rat's infraorbital nerve," *The Journal of Neuroscience*, vol. 14, no. 5, pp. 2708–2723, 1994.
- [7] P. Dubový, V. Brázda, I. Klusáková, and I. Hradilová-Sviženská, "Bilateral elevation of interleukin-6 protein and mRNA in both lumbar and cervical dorsal root ganglia following unilateral chronic compression injury of the sciatic nerve," *Journal of Neuroinflammation*, vol. 10, article 55, 2013.
- [8] I. H. Sviženská, V. Brázda, I. Klusáková, and P. Dubový, "Bilateral changes of cannabinoid receptor type 2 protein and mRNA in the dorsal root ganglia of a rat neuropathic pain model," *The Journal of Histochemistry and Cytochemistry*, vol. 61, no. 7, pp. 529–547, 2013.
- [9] R. Won, S. J. Jung, Y. G. Park, S. S. Chung, and B. H. Lee, "Crossed-withdrawal reflex in a rat model of neuropathic pain: implications in neural plasticity," *Neuroscience Letters*, vol. 369, no. 3, pp. 239–244, 2004.
- [10] L. Sokoloff, M. Reivich, and C. Kennedy, "The [¹⁴C]deoxyglucose method for the measurement of local cerebral glucose utilization: theory, procedure, and normal values in the conscious and anesthetized albino rat," *Journal of Neurochemistry*, vol. 28, no. 5, pp. 897–916, 1977.
- [11] D. D. Price, J. R. Mao, R. C. Coghill et al., "Regional changes in spinal cord glucose metabolism in a rat model of painful neuropathy," *Brain Research*, vol. 564, no. 2, pp. 314–318, 1991.
- [12] J. Mao, D. D. Price, R. C. Coghill, D. J. Mayer, and R. L. Hayes, "Spatial patterns of spinal cord [¹⁴C]-2-deoxyglucose metabolic activity in a rat model of painful peripheral mononeuropathy," *Pain*, vol. 50, no. 1, pp. 89–100, 1992.
- [13] J. Mao, D. J. Mayer, and D. D. Price, "Patterns of increased brain activity indicative of pain in a rat model of peripheral mononeuropathy," *The Journal of Neuroscience*, vol. 13, no. 6, pp. 2689–2702, 1993.
- [14] I. Quélven, A. Roussin, and J.-M. Zajac, "Functional consequences of neuropeptide FF receptors stimulation in mouse: a cerebral glucose uptake study," *Neuroscience*, vol. 126, no. 2, pp. 441–449, 2004.
- [15] S. Dedeurwaerdere, C. Wintmolders, G. Vanhoof, and X. Langlois, "Patterns of brain glucose metabolism induced by phosphodiesterase 10a inhibitors in the mouse: a potential translational biomarker," *The Journal of Pharmacology and Experimental Therapeutics*, vol. 339, no. 1, pp. 210–217, 2011.
- [16] B. H. Lee, R. Won, E. J. Baik, S. H. Lee, and C. H. Moon, "An animal model of neuropathic pain employing injury to the sciatic nerve branches," *NeuroReport*, vol. 11, no. 4, pp. 657–661, 2000.
- [17] P. H. J. M. Veldman and R. J. A. Goris, "Multiple reflex sympathetic dystrophy. Which patients are at risk for developing a recurrence of reflex sympathetic dystrophy in the same or another limb," *Pain*, vol. 64, no. 3, pp. 463–466, 1996.
- [18] A. M. Aloisi, C. A. Porro, M. Cavazzuti, P. Baraldi, and G. Carli, "Mirror pain' in the formalin test: behavioral and 2-deoxyglucose studies," *Pain*, vol. 55, no. 2, pp. 267–273, 1993.
- [19] B. D. Grubb, R. U. Stiller, and H.-G. Schaible, "Dynamic changes in the receptive field properties of spinal cord neurons with ankle input in rats with chronic unilateral inflammation in the ankle region," *Experimental Brain Research*, vol. 92, no. 3, pp. 441–452, 1993.
- [20] M. L. Sotgiu and G. Biella, "Spinal neuron sensitization facilitates contralateral input in rats with peripheral mononeuropathy," *Neuroscience Letters*, vol. 241, no. 2–3, pp. 127–130, 1998.
- [21] S. E. Abram and D. R. Kostreva, "Spinal cord metabolic response to noxious radiant heat stimulation of the cat hind footpad," *Brain Research*, vol. 385, no. 1, pp. 143–147, 1986.
- [22] R. D'Mello and A. H. Dickenson, "Spinal cord mechanisms of pain," *British Journal of Anaesthesia*, vol. 101, no. 1, pp. 8–16, 2008.
- [23] M. Fitzgerald, "The contralateral input to the dorsal horn of the spinal cord in the decerebrate spinal rat," *Brain Research*, vol. 236, no. 2, pp. 275–287, 1982.
- [24] D. Gross, "Contralateral local anaesthesia in the treatment of postamputation pain," in *Phantom and Stump Pain*, J. Siegfried and M. Zimmermann, Eds., pp. 107–109, Springer, Berlin, Germany, 1981.
- [25] R. Casale, F. Ceccherelli, A. A. E. M. Labeeb, and G. E. M. Biella, "Phantom limb pain relief by contralateral myofascial injection with local anaesthetic in a placebo-controlled study: preliminary results," *Journal of Rehabilitation Medicine*, vol. 41, no. 6, pp. 418–422, 2009.
- [26] V. S. Ramachandran, D. Rogers-Ramachandran, and S. Cobb, "Touching the phantom limb," *Nature*, vol. 377, no. 6549, pp. 489–490, 1995.
- [27] O. Giuffrida, L. Simpson, and P. W. Halligan, "Contralateral stimulation, using TENS, of phantom limb pain: two confirmatory cases," *Pain Medicine*, vol. 11, no. 1, pp. 133–141, 2010.
- [28] J. Y. Lin, B. Peng, Z. W. Yang, and S. Min, "Number of synapses increased in the rat spinal dorsal horn after sciatic nerve transection: a stereological study," *Brain Research Bulletin*, vol. 84, no. 6, pp. 430–433, 2011.

Research Article

Cortical Excitability Measured with nTMS and MEG during Stroke Recovery

Jyrki P. Mäkelä,¹ Pantelis Lioumis,^{1,2} Kristina Laaksonen,^{3,4} Nina Forss,^{3,4}
Turgut Tatlisumak,^{3,5,6} Markku Kaste,³ and Satu Mustanoja³

¹BioMag Laboratory, HUS Medical Imaging Center, Helsinki University Hospital and University of Helsinki, 00029 Helsinki, Finland

²Neuroscience Center, University of Helsinki, 00014 Helsinki, Finland

³Department of Neurology, Helsinki University Hospital and University of Helsinki, 00029 Helsinki, Finland

⁴Department of Neuroscience and Biomedical Engineering, Aalto University School of Science, P.O. Box 15100, 00076 Espoo, Finland

⁵Institute of Neuroscience and Physiology, Sahlgrenska Academy, University of Gothenburg, 41345 Gothenburg, Sweden

⁶Department of Neurology, Sahlgrenska University Hospital, 41345 Gothenburg, Sweden

Correspondence should be addressed to Jyrki P. Mäkelä; jyrki.makela@hus.fi

Received 27 February 2015; Accepted 5 May 2015

Academic Editor: Yong Jeong

Copyright © 2015 Jyrki P. Mäkelä et al. This is an open access article distributed under the Creative Commons Attribution License, which permits unrestricted use, distribution, and reproduction in any medium, provided the original work is properly cited.

Objective. Stroke alters cortical excitability both in the lesioned and in the nonlesioned hemisphere. Stroke recovery has been studied using transcranial magnetic stimulation (TMS). Spontaneous brain oscillations and somatosensory evoked fields (SEFs) measured by magnetoencephalography (MEG) are modified in stroke patients during recovery. **Methods.** We recorded SEFs and spontaneous MEG activity and motor threshold (MT) short intracortical inhibition (SICI) and intracortical facilitation (ICF) with navigated TMS (nTMS) at one and three months after first-ever hemispheric ischemic strokes. Changes of MEG and nTMS parameters attributed to gamma-aminobutyrate and glutamate transmission were compared. **Results.** ICF correlated with the strength and extent of SEF source areas depicted by MEG at three months. The nTMS MT and event-related desynchronization (ERD) of beta-band MEG activity and SICI and the beta-band MEG event-related synchronization (ERS) were correlated, but less strongly. **Conclusions.** This first report using sequential nTMS and MEG in stroke recovery found intra- and interhemispheric correlations of nTMS and MEG estimates of cortical excitability. ICF and SEF parameters, MT and the ERD of the lesioned hemisphere, and SICI and ERS of the nonlesioned hemisphere were correlated. Covarying excitability in the lesioned and nonlesioned hemispheres emphasizes the importance of the hemispheric balance of the excitability of the sensorimotor system.

1. Introduction

The motor system is a dynamic network of cortical and sub-cortical areas interacting through excitatory and inhibitory circuits, modulated by somatosensory input. The network balance is disturbed after stroke [1–3]. Modifications of cortical excitability enable recovery and reorganization of the remaining motor areas both in animal models [4, 5] and in humans [1, 6]. Transcranial magnetic stimulation (TMS) and magnetoencephalography (MEG) have both been applied in stroke patients to reveal cortical excitability changes.

Motor threshold (MT), that is, the minimal TMS intensity eliciting motor evoked potentials (MEPs), is related to membrane excitability as it is influenced by drugs affecting

neuronal ion channels. Paired pulse TMS (PP-TMS) reveals short-interval intracortical inhibition (SICI), related to the activation of GABA-A receptors and intracortical facilitation (ICF) attributed mainly to glutamatergic NMDA receptor activation (for references, see [7]). In acute stroke, the MT is increased in the lesioned hemisphere (LH) whereas in the nonlesioned (NH) hemisphere it is normal [8] or decreased one month after stroke [9]. SICI is decreased in both hemispheres early after stroke; ICF is stronger in NH in severe than mild strokes [1, 6].

Finger movements and median nerve [10] or finger stimulation [11] modify spontaneous MEG oscillations over the sensorimotor cortex in the beta band (15–25 Hz). They are suppressed at 100–300 ms after tactile stimulation

TABLE 1: Patient demographics and behavioral scores.

Pt	Sex	Age	Les. site	Hemi	Les. class	Les. size	NIHSSI	NIHSS2	mRs1	mRs2	BI1	BI2	Sense loss
1	M	60	Hand MCx	R	C	0.1	0	0	2	1	100	100	–'
2	F	68	GP	L	SC	1	2	2	1	1	100	100	+'
3	F	72	Primary MCx	L	C	0.3	0	0	1	1	100	100	–'
4	F	46	BGp	L	C + SC	70	8	6	3	3	65	85	+'
5	M	60	MCA territory	L	C + SC	48	2	2	2	2	100	100	+'
6	F	85	Hand MCx	R	C	1	0	0	1	1	100	100	–'
7	F	69	EC + insular	L	SC	3	2	0	2	2	90	100	–'
8	M	70	MCA territory	R	C + SC	297	12	12	5	5	35	40	+'
9	M	62	EC	L	C + SC	5	1	1	3	2	85	100	–'
10	F	75	Caud	R	SC	5	2	1	3	3	91	100	–'
11	M	78	Caud	L	SC	10	2	1	2	1	100	100	+'
12	F	73	Thal	L	SC	3	1	1	2	1	100	100	+'
13	F	48	Thal	L	SC	1	1	1	2	2	100	100	–'
Mean	66.8					32	2.5	2	2.2	1.9	90.4	94.6	
SD	10.7					79	3.3	3.2	1	1.1	18.7	16.2	
Max	85					297	12	12	5	5	100	100	
Min	46					0.1	0	0	1	1	35	40	

Sex: M = male; F = female. Age (years). MCx = motor cortex damage, GB = globus pallidus, BGp = basal ganglia posterior part, MCA territory = extensive involvement of the middle cerebral artery territory, EC = external capsule, Caud = caudate, and Thal = thalamus. NIHSS score (maximum 42), Modified Rankin Scale (mRs) and Barthel Index (BI) at 1 and 3 months after stroke. Hemi = hemisphere affected by stroke. L = left. R = right. Lesion classification: C = cortical, S = subcortical, and C + SC = corticostriatal lesion. Lesion size (volume in mm³).

(event-related desynchronization; ERD), reflecting increased excitability, and increased at 500–1000 ms (event-related synchronization; ERS), reflecting removal of excitation [12, 13] or reduced excitability [14]. Inhibitory GABA-A agonist diazepam increases MEG beta activity [15, 16]. Combined MEG and magnetic resonance spectroscopy showed a linear relationship between the beta ERS strength and GABA concentration [17]. Beta ERS has been shown to be significantly weaker in the LH than NH; stronger ERS amplitude was correlated with a better affected hand function up to 3 months after stroke [18]. *Reduction* of beta ERS, however, correlated with clinical improvement after physiotherapy of patients with chronic stroke [19]. Movement-related beta ERD was significantly reduced in LH of stroke patients [20].

The hand representation in the somatosensory cortex (S1), estimated by somatosensory evoked fields (SEFs), is the largest one month after stroke and its increase was correlated with the affected hand function [21]. In TMS mapping, hand motor representation expands in the LH up to 1 month [22]. In animal models, somatosensory reorganization is activated immediately after the lesion by diminished GABA-A-related inhibition and by glutamatergic activation after one month [5].

We recorded both nTMS and MEG from patients during stroke recovery. We hypothesized to see correlations between ERD and MT related to the early cortical excitability and between ERS and SICI, both attributed to GABA-A-related processes. Moreover, we expected that ICF, reflecting glutamatergic activity, would correlate with the somatosensory modifications in MEG, as glutamate is associated with late somatosensory plasticity [5].

2. Methods

MEG and nTMS were recorded from thirteen patients (age 67.3 ± 11 years, 8 women), with first-ever ischemic stroke in the middle cerebral artery territory one (T1) and three months after stroke (T2). Hand function was impaired in all patients. Six patients had a subcortical and seven patients had a subcorticocortical or cortical stroke (Table 1). At T1, one patient used amitriptyline 10 mg/day and another used citalopram 10 mg/day. One patient used zopiclone 7.5 mg for occasional sleeplessness. At T2, citalopram 10 mg/day was used by one patient. Other patients did not receive drugs known to modify cortical excitability. The ethical committee of the Hospital District of Helsinki and Uusimaa approved the project. Data from these patients has been presented previously [18, 21, 23, 24]. As the patients having both TMS and MEG recordings are a subset of the previous patient groups, we recalculated the group-level electrophysiological parameters to show that the present patient group is sufficiently similar to those reported previously (see Supplementary Tables 1 and 2 in Supplementary Material available online at <http://dx.doi.org/10.1155/2015/309546>). Only the features needed for interpretation of the present results are described.

2.1. nTMS Measurements. An eXimia navigated magnetic stimulator with a coplanar figure-of-eight coil of 70 mm wing radius (Nexstim Ltd., Helsinki, Finland) was used for nTMS. Patients' MRIs, required for navigation, were scanned at T1 and used also at T2.

The site eliciting the largest MEP amplitude in first dorsal interosseous muscle was located. The resting MT was

determined from this site as described in [25]. The site was then stimulated by single TMS pulses at 110% of MT and by the PP-TMS at 90% for conditioning and 110% of MT for test pulses. Fifteen single pulses or pairs of conditioning and test pulses were delivered in each stimulation session. The interval between stimuli was 3.3 s and the intersession interval varied between 1 and 3 min. The ISI selected for the paired-pulse stimuli was 2 ms for SICI and 12 ms for ICF. The peak-to-peak amplitudes of MEPs elicited by PP-TMS were normalized by dividing them by the corresponding single-pulse MEP amplitude to simplify subject-to-subject comparisons [6].

2.2. MEG Recordings. MEG during rest and tactile stimulation of the thumb (D1), index (D2), and little finger (D5) were recorded with a 306-sensor neuromagnetometer (Elekta Neuromag, Helsinki, Finland) in BioMag laboratory, right before the nTMS measurement. The interfering signals were suppressed by Maxfilter software [26]. The signals were filtered through 0.03–308 Hz and digitized at 941 Hz.

Time-frequency representations (TFR [27]) in the 10–30 Hz band were calculated to define the frequency range of beta modulation, which was quantified by the temporal spectral evolution method (TSE [10]) from signals of 2 to 4 MEG sensors showing the strongest reactivity. Only the contralateral beta modifications (the affected hand stimulation for the LH and the unaffected hand for NH) were analyzed. Onset and offset of the ERD and ERS were defined as a time point when the signal differed 2 SDs from the baseline. The absolute ERD and ERS strengths were calculated from the peak amplitudes and converted into relative values in relation to the 300 ms prestimulus baseline [18].

For SEFs, about 120 responses were averaged for stimulation of D2 (ISI 3005 ms), and D1 and D5 (ISI 1005 ms) in separate sessions. The size of the hand representation in the SI was determined by calculating the Euclidean distance in *xyz*-space between the equivalent current dipoles (ECDs) of the earliest responses to D1 and D5 stimulation [21]. The amplitudes of SEFs to D2 stimulation [23] were used in the analyses.

SPSS 14.0 software was employed for statistical analysis (SPSS Inc., Chicago, Illinois, USA). Spearman's correlation coefficients were calculated between nTMS and MEG parameters. Multiple comparison correction was carried out according to the number of tests ($N = 32$) suggested by the four prior hypotheses (T1 and T2 were tested separately; LH and NH variations lead to four tests in each case; $N = 4 * 4 * 2 = 32$). The significance level was set at $p < 0.05$. We also present significances of correlation values without multiple comparisons and supply all correlation coefficients and corresponding p values (cf. [1, 9, 28] for a similar approach and [29] for its statistical aspects). The differences between nTMS and MEG values obtained at T1 and T2 were tested with Student's t -test.

3. Results

3.1. Navigated TMS. In the LH, MEPs were found in 11 patients both at T1 and at T2 and were present in the NH

in all patients. Group average MTs did not change between measurements or hemispheres. Individual MT values are given in Supplementary Table 1. MT was higher for LH than NH in 9 patients at T1 ($p < 0.05$, binomial test) and in 10 patients at T2 ($p < 0.05$, binomial test). The MTs in the LH and NH correlated strongly both at T1 ($r = .82$, $p < .01$) and at T2 ($r = .78$, $p < .01$).

PP2ms stimulation of LH inhibited MEPs in 7 patients at both T1 and T2. PP2ms stimulations of NH did not inhibit MEPs (disinhibition; diminished SICI) in 5 patients at T1 and in 3 patients at T2. SICI values did not correlate significantly between the hemispheres at T1 or T2.

PP12ms stimulation of LH facilitated MEPs (ICF) in 10 out of 11 patients at T1 and in all patients at T2. In NH, ICF was induced in all patients at T1. At T2, ICF was not observed in 4 patients. MEP amplitudes elicited by PP12ms stimulations were correlated between the LH and NH at T1 ($r = .62$; $p < .05$) but not at T2 (Supplementary Table 2).

3.2. MEG. ERD started 140 ± 10 ms after tactile stimulation and peaked at 250 ± 10 ms. The subsequent ERS started at 520 ± 40 ms and peaked at 900 ± 70 ms. At T1, ERD was absent in one patient and ERS in two patients in the LH; ERS was missing from the NH in one patient. At T2, the ERD was present in every LH whereas ERS was absent in two. Both were present in all NHs. ERDs did not differ between the hemispheres. ERS was smaller in the LH than NH at T1 ($46 \pm 31\%$ versus $63 \pm 32\%$; $p < .05$); at T2, the difference was nonsignificant. SEFs from both hemispheres were detected in 12 patients at T1 and in all patients at T2. They were smaller in the LH than NH at T1 (25 nAm versus 32 nAm; $p < .04$) but not at T2. The SI hand representation area was larger in the LH than NH at T1 (12 ± 3 mm versus 10 ± 3 mm $p < .003$) but not at T2 (Supplementary Table 3).

3.3. Correlations between the nTMS and MEG. We tested the correlations indicated by the selected hypotheses. The plots of the most relevant correlations are depicted in Figure 1 to show that they were not driven by outliers. All correlations are displayed in Table 2 to enable evaluation of significance of our hypotheses against general effects of the lesions.

The MT and ERD were correlated in the LH at T1 ($r = -.66$, $p < .03$), indicating that small ERD was associated with a high MT (Figure 1(a)). At T2, this correlation was weaker ($r = -.58$, $p < .06$). However, the MT of the LH correlated with the ERD of NH ($r = -.62$, $p < .04$), and the MT of the NH correlated with ERD of the LH ($r = -.65$, $p < .02$), suggesting that high MT was associated with a small ERD in the opposite hemisphere at T2 (Table 2).

SICI and the ERS did not correlate at T1 or in LH at T2. In the NH, high ERS was associated with a strong SICI ($r = -.59$, $p < .04$; Figure 1(b)). In addition to hypothesized correlations, SICI of the NH and ERD of the LH at T2 were correlated ($r = -.82$, $p < .001$), indicating that strong ERD in the LH was associated with a strong SICI in the NH. SICI in the LH was correlated also with the SI amplitude of the LH ($r = -.64$, $p < .04$), indicating that small SI amplitude was associated with a weak SICI (Table 2).

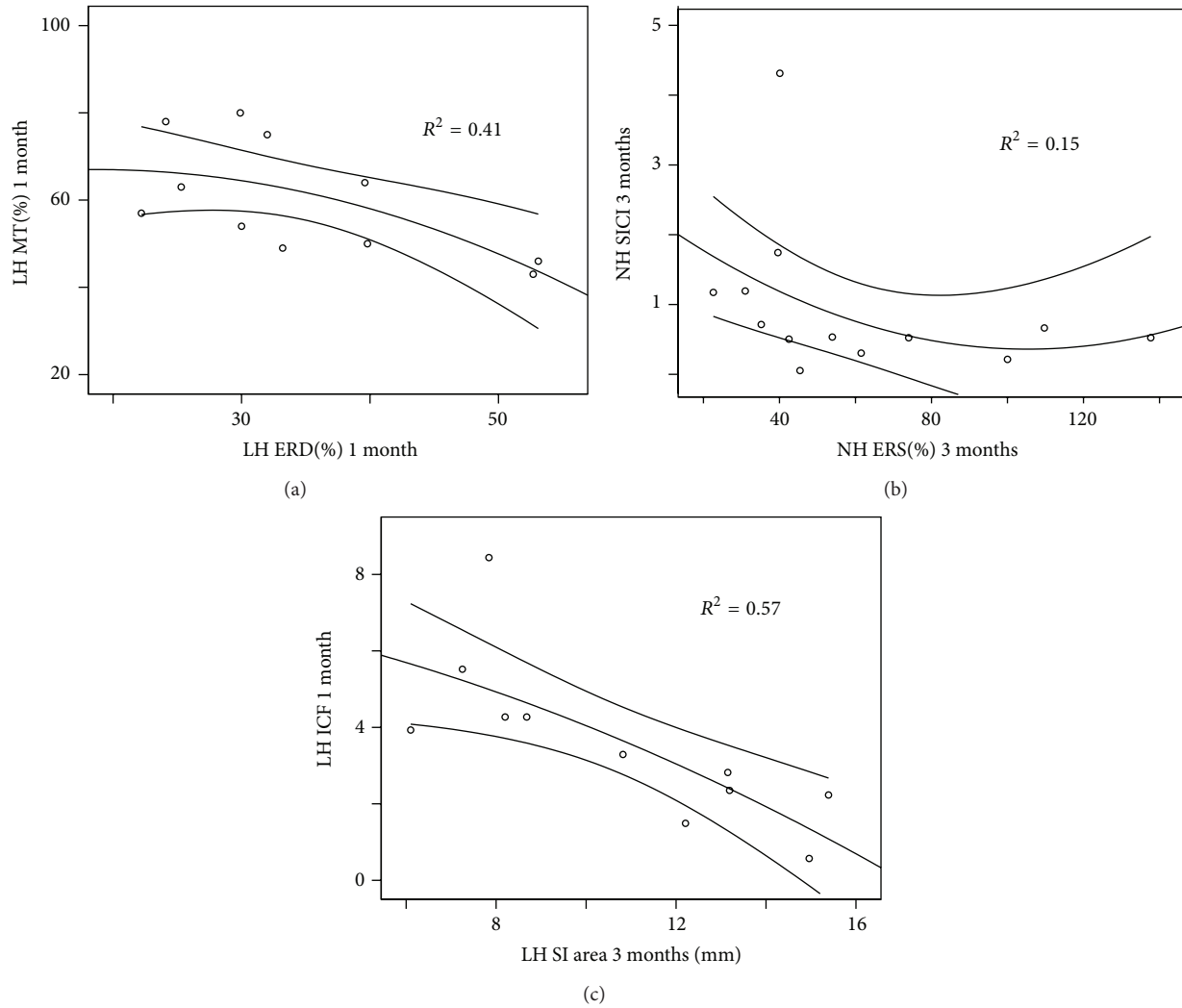


FIGURE 1: Scatterplots, quadratic fits, and 95% confidence intervals of the motor thresholds and ERD values in the lesioned hemisphere at 1 month (a), SICI and ERS values in the nonlesioned hemisphere at 3 months (b), and ICF values at 1 month and SI area at 3 months in the lesioned hemisphere (c).

ICF and SEF parameters did not correlate at T1. At T2, ICF in the LH correlated with the SI amplitude of LH ($r = -.65$, $p < .03$); if ICF was strong, the SI amplitude was small. In addition, ICF in the NH correlated ($r = -.82$, $p < .001$) with the SI finger representation area of the LH; this correlation remained significant also after Bonferroni correction (Table 2). Moreover, ICF in the LH at T1 was correlated ($r = -.83$; $p < .002$) with the SI finger representation area of LH at T2; high ICF at T1 resulted in a small hand representation area at T2 (Figure 1(c)).

4. Discussion

Our study is the first to compare MEG and nTMS excitability parameters during stroke recovery. Navigated TMS, not applied previously in longitudinal studies of stroke patients, enabled the precise replication of the stimulus site between separate measurements, adding reliability to the follow-up.

We found correlations between cortical excitability estimates derived from nTMS and MEG.

As expected, we found correlations between MT and ERD, but in only one of the four possible intrahemispheric and two out of four interhemispheric conditions. The SICI and beta ERS, both attributed to GABAergic mechanisms, were correlated in one of their four possible intrahemispheric conditions (in the NH at T2). Interhemispheric correlations of SICI were not limited to ERS. One reason for this may be that various GABA-A receptor subtypes contribute to SICI. Nonselective GABA-A receptor activators modify SICI whereas the GABA-A1 receptor specific zopiclone did not [7]. Nonselective GABA-A agonist zopiclone increased MEG beta activity whereas zopiclone suppressed beta activity in the vicinity of stroke lesion [30]. Moreover, in healthy subjects, diazepam increased MEG ERD but did not affect ERS when the increase of baseline beta activity was taken into account [16]. This nonspecificity could contribute to the correlations of SICI with the ERD and MT as well.

TABLE 2: Spearman correlations between the nTMS and MEG parameters at 1 month (1 mo) and three months (3 mo) after the stroke. The correlations between event-related desynchronization (ERD) and motor threshold (MT), event-related synchronization (ERS) and short-interval cortical inhibition (SICI), and intracortical facilitation (ICF) and somatosensory evoked field source strength (SI) and somatosensory hand representation area (SIhr), aligned with hypotheses, are depicted in bold font. *Significance of $p < .05$; **significance of $p < .01$ without multiple comparison correction; ** (marked with bold italic) statistical significance ($p < .05$) with multiple comparison correction (Bonferroni) for $N = 32$.

			1 mo							
			LH				NH			
			ERD	ERS	SI	SIhr	ERD	ERS	SI	SIhr
1 mo	LH	MT	−.66 [*]	−.06	−.36	−.21	−.48	−.53	−.41	−.27
		SICI	−.45	−.05	−.51	.42	−.22	−.04	−.28	.12
		ICF	−.39	.01	−.22	−.10	−.06	−.07	.30	−.19
	NH	MT	−.43	−.12	−.24	−.21	−.14	−.37	−.49	.02
		SICI	.17	−.03	−.22	.26	.08	.08	−.16	.26
		ICF	−.51	−.11	.16	−.02	−.18	−.19	.44	−.06
3 mo										
			LH				NH			
			ERD	ERS	SI	SIhr	ERD	ERS	SI	SIhr
3 mo	LH	MT	−.58	.11	−.14	.06	−.62 [*]	−.19	.04	.13
		SICI	−.27	.32	−.64 [‡]	.46	.06	.20	−.25	−.01
		ICF	.15	−.21	−.65 ^{**}	−.28	.46	.42	.20	−.17
	NH	MT	−.65 [*]	−.26	−.50	−.03	−.48	−.26	−.41	−.15
		SICI	−.82 ^{**}	−.51	−.44	−.13	−.62 [*]	−.59 [*]	−.07	−.05
		ICF	−.30	.04	−.22	−.82 ^{**}	.30	.27	.10	−.12

Correlations between nTMS parameters and MEG ERD/ERS were stronger at T2 than at T1. Analogously, most TMS intracortical excitability measures did not correlate with the hand function acutely but did so 3 months after stroke [1]. Recovery of sensorimotor fMRI activation to digit stimulation from 1 to 3 months was correlated with final motor function [31], emphasizing the importance of this time period for stroke recovery.

ICF correlated with SI hand area size at T2. As ICF is attributed mainly to glutaminergic mechanisms, glutamate may contribute to stroke-induced plasticity. Somewhat surprisingly, high ICF at T1 correlated with small SI hand area at T2 (Figure 1(c)); thus, the narrowing towards normal hand representation size may be supported by glutaminergic activity. ICF did not correlate with the MEG ERD/ERS, and the SI hand area and beta ERD/ERS were not correlated [18]; this suggests different mechanisms underlying SICI and ICF (see [7] for a detailed discussion).

Several correlations emphasized interhemispheric connectivity (see Figure 2 and Table 2). For example, high MT was associated with a small ERD in the opposite hemisphere, and strong ERD in the LH was associated with a strong SICI in the NH. This suggests that the hemispheric balance of excitability is important in stroke recovery. Dexterity is impaired in both hands after unilateral subcortical middle cerebral artery stroke. Increased excitability within the unaffected motor cortex may cause imbalance between the homologous cortical motor areas and worsen also the ipsilesional hand coordination (for references, see [32]). MTs between the hemispheres were strongly correlated both at

T1 and at T2. Thus, some functional correlations may relate to the modified general excitability properties of the motor system, instead of effects in the immediate vicinity of the stroke [28].

Correlations between MEG and TMS parameters of cortical excitability were relatively loose. Several factors may explain this feature. TMS results give direct information of the changes in the motor output and the immediate effects of TMS are relatively local. However, also subcortical and spinal processes affect the MEPs used to evaluate the TMS effects. MEG reveals the activity of the whole cortical mantle and enables mapping of network effects generated by stroke. MEG source analysis suggests mainly motor cortex origin of beta ERS [13, 33, 34]. However, in electrocorticography, recorded directly from the cortex, beta ERD and ERS appear outside of pre- and postcentral gyri [35], in supplementary motor cortex [36], or broadly from pre- and postcentral gyri, frontolateral and medial cortex [37, 38]. The widespread cortical generation of the ERD and ERS may make them resilient to small cortical strokes. Multitude of generators may contribute to considerable variability of source locations of beta ERD in stroke patients (cf. [20]). Multiple sources underlying MEG signals may also explain resilience of auditory evoked fields after small strokes [39]. Stronger correlations between ICF and SI parameters than between MT and SICI and ERS/ERD may, in part, result from spatially more limited source areas of SI responses than those of ERD/ERS. It can be expected that MEG and nTMS produce complementary information about the effects of stroke on cortical networks. Moreover, MEG parameters in the *affected* hemisphere and nTMS indices in

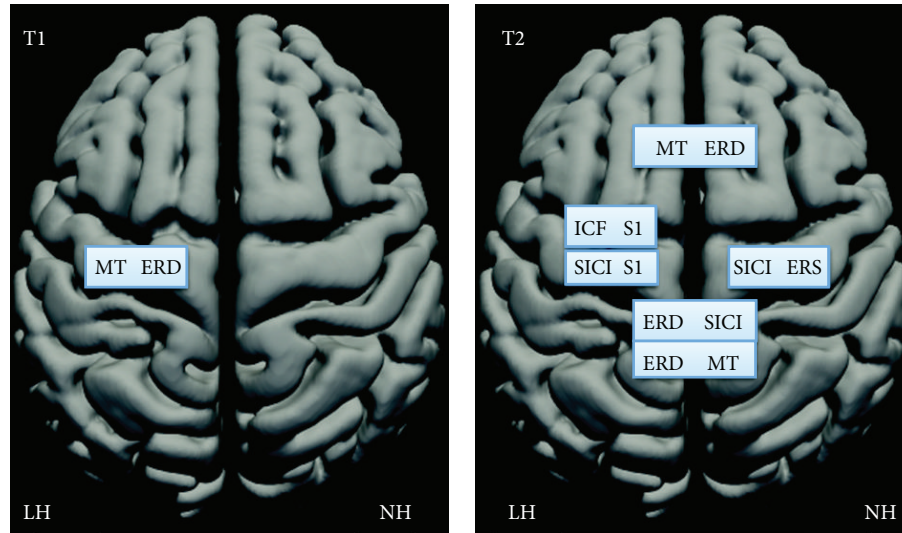


FIGURE 2: TMS and MEG parameters correlating at T1 (one month) and at T2 (three months), drawn on a schematic brain with lesioned (LH) and nonlesioned hemisphere (NH). The intrahemispheric connections are drawn on one hemisphere and interhemispheric connections on both hemispheres. Note strong increase of both intra- and interhemispheric correlations from one to three months after the stroke.

the *unaffected* hemisphere were correlated with the motor performance of the affected hand (cf. [18, 21, 24]). This emphasizes the importance of combining these two methods.

ERD in the 8–22 Hz band may reflect downregulation of intracortical inhibition in the human motor cortex, as TMS delivered during ERD is associated with increased MEP amplitudes and reduced SICI [40]. However, 1 Hz repetitive TMS over the motor cortex reduces MEPs to subsequent single TMS pulses, indicating inhibition, but *decreases* post-movement beta ERS [41], and intermittent theta burst TMS facilitates MEPs but *increases* postmovement beta ERS [42]. Beta ERS is reduced in patients with myoclonus epilepsy, indicating increased cortical excitability [43]. In line, SICI is decreased in myoclonus epilepsy patients; however, MT is *increased* [44, 45], and the silent period after the TMS pulse, reflecting motor cortical postsynaptic inhibition [7], is *prolonged*, indicating prevailing inhibitory cortical tonus [45]. Thus, only some aspects of the cortical excitability may be shared in excitability estimates obtained by TMS and MEG.

Our results suggest that some TMS and MEG excitability measures reflect the activity of the same transmitter systems. However, high MT and absence of ERD/ERS may also correlate because of severely affected sensorimotor connections between the periphery and the cortex. We detected SEFs in 12/13 patients and MEPs in 11/13 patients already at T1, indicating that both somatosensory and motor pathways were conveying signals. Motor function can be maintained despite significant damage to the corticospinal tract, as estimated from MT of stroke patients [1]. Moreover, we observed fewer correlations at T1, when the sensorimotor pathways probably were more affected, than at T2. Large lesions may create spurious correlations between the excitability parameters within LH. However, such spurious correlations

should remain stable or decrease during recovery from T1 to T2 but not increase, as in our data.

The limitations of our study include the small size of the patient group as the precise features of structural and functional changes may differ among the patients. Cortical excitability is modified differently in cortical and subcortical strokes [46, 47]. This, however, should not alter our correlations between the TMS and MEG, as both were recorded from the same patients. Possible effects of medication on excitability should go in parallel for MEG and nTMS, as the patients were tested sequentially during the same day. The patients were not tested in the acute stage with TMS, and MEG recordings showed most dramatic ERD and ERS modifications between the acute phase and T1 [18]. Although MT in the LH is correlated with the paretic hand function in acute stroke, this correlation, however, weakens during recovery, and TMS intracortical excitability parameters correlated with the clinical performance best at 3 months [1]. Longer follow-up could have produced additional correlations. The 2 ms or 12 ms ISIs, selected for our paired-pulse stimuli, produce clear SICI and ICF in healthy subjects [48] and in stroke patients [28], but we did not test other parameters, which could have produced stronger correlations between nTMS and MEG.

5. Conclusions

ICF and SI response amplitude and area size, MT and the ERD of the hemisphere harboring the stroke lesion, and SICI and ERS of the nonlesioned hemisphere are correlated in stroke patients. Numerous correlations of the excitability parameters between the LH and NH emphasize the importance of the hemispheric balance of the excitatory-inhibitory properties of the sensorimotor system in analyzing the stroke-related dysfunction during stroke recovery.

Conflict of Interests

The authors declare that there is no conflict of interests regarding the publication of this paper.

Acknowledgments

The authors thank Suvi Heikkilä and Jari Kainulainen for their help in the recordings, Jussi Nurminen for help in the data analysis, and the ergo- and physiotherapists at the Department of Neurology, HUCH, for help in the clinical testing of the patients. Dr. Ilkka Nissilä gave valuable advice about statistics. The study was financially supported by the Academy of Finland (National Centers of Excellence Program 2006–2011), the Helsinki University Central Hospital Research Fund, and the SalWe Research Program for Mind and Body (Tekes, the Finnish Funding Agency for Technology and Innovation Grant 1104/10).

References

- [1] O. B. C. Swayne, J. C. Rothwell, N. S. Ward, and R. J. Greenwood, "Stages of motor output reorganization after hemispheric stroke suggested by longitudinal studies of cortical physiology," *Cerebral Cortex*, vol. 18, no. 8, pp. 1909–1922, 2008.
- [2] N. Dancause and R. J. Nudo, "Shaping plasticity to enhance recovery after injury," *Progress in Brain Research*, vol. 192, pp. 273–295, 2011.
- [3] C. Grefkes and G. R. Fink, "Connectivity-based approaches in stroke and recovery of function," *The Lancet Neurology*, vol. 13, no. 2, pp. 206–216, 2014.
- [4] R. J. Nudo, B. M. Wise, F. SiFuentes, and G. W. Milliken, "Neural substrates for the effects of rehabilitative training on motor recovery after ischemic infarct," *Science*, vol. 272, no. 5269, pp. 1791–1794, 1996.
- [5] P. E. Garraghty, L. L. Arnold, C. L. Wellman, and T. M. Mowery, "Receptor autoradiographic correlates of deafferentation-induced reorganization in adult primate somatosensory cortex," *Journal of Comparative Neurology*, vol. 497, no. 4, pp. 636–645, 2006.
- [6] J. Liepert, F. Hamzei, and C. Weiller, "Motor cortex disinhibition of the unaffected hemisphere after acute stroke," *Muscle and Nerve*, vol. 23, no. 11, pp. 1761–1763, 2000.
- [7] U. Ziemann, "Pharmaco-transcranial magnetic stimulation studies of motor excitability," in *Handbook of Clinical Neurology*, A. M. Lozano and M. Hallett, Eds., vol. 116 of *Brain Simulation*, Elsevier, 2013.
- [8] P. Talelli, R. J. Greenwood, and J. C. Rothwell, "Arm function after stroke: neurophysiological correlates and recovery mechanisms assessed by transcranial magnetic stimulation," *Clinical Neurophysiology*, vol. 117, no. 8, pp. 1641–1659, 2006.
- [9] U. Takechi, K. Matsunaga, R. Nakanishi et al., "Longitudinal changes of motor cortical excitability and transcallosal inhibition after subcortical stroke," *Clinical Neurophysiology*, vol. 125, no. 10, pp. 2055–2069, 2014.
- [10] R. Salmelin and R. Hari, "Spatiotemporal characteristics of sensorimotor neuromagnetic rhythms related to thumb movement," *Neuroscience*, vol. 60, no. 2, pp. 537–550, 1994.
- [11] R. Enatsu, T. Nagamine, J. Matsubayashi et al., "The modulation of rolandic oscillation induced by digital nerve stimulation and self-paced movement of the finger: a MEG study," *Journal of the Neurological Sciences*, vol. 337, no. 1–2, pp. 201–211, 2014.
- [12] G. Pfurtscheller and F. H. L. da Silva, "Event-related EEG/MEG synchronization and desynchronization: basic principles," *Clinical Neurophysiology*, vol. 110, no. 11, pp. 1842–1857, 1999.
- [13] R. Salmelin, M. Hämäläinen, M. Kajola, and R. Hari, "Functional segregation of movement-related rhythmic activity in the human brain," *NeuroImage*, vol. 2, no. 4, pp. 237–243, 1995.
- [14] R. Chen, B. Corwell, and M. Hallett, "Modulation of motor cortex excitability by median nerve and digit stimulation," *Experimental Brain Research*, vol. 129, no. 1, pp. 77–86, 1999.
- [15] O. Jensen, P. Goel, N. Kopell, M. Pohja, R. Hari, and B. Ermentrout, "On the human sensorimotor-cortex beta rhythm: sources and modeling," *NeuroImage*, vol. 26, no. 2, pp. 347–355, 2005.
- [16] S. D. Hall, I. M. Stanford, N. Yamawaki et al., "The role of GABAergic modulation in motor function related neuronal network activity," *NeuroImage*, vol. 56, no. 3, pp. 1506–1510, 2011.
- [17] W. Gaetz, J. C. Edgar, D. J. Wang, and T. P. L. Roberts, "Relating MEG measured motor cortical oscillations to resting γ -aminobutyric acid (GABA) concentration," *NeuroImage*, vol. 55, no. 2, pp. 616–621, 2011.
- [18] K. Laaksonen, E. Kirveskari, J. P. Mäkelä et al., "Effect of afferent input on motor cortex excitability during stroke recovery," *Clinical Neurophysiology*, vol. 123, no. 12, pp. 2429–2436, 2012.
- [19] T. W. Wilson, A. Fleischer, D. Archer, S. Hayasaka, and L. Sawaki, "Oscillatory MEG motor activity reflects therapy-related plasticity in stroke patients," *Neurorehabilitation and Neural Repair*, vol. 25, no. 2, pp. 188–193, 2011.
- [20] H. E. Rossiter, M.-H. Boudrias, and N. S. Ward, "Do movement-related beta oscillations change following stroke?" *Journal of Neurophysiology*, vol. 112, pp. 2053–2058, 2014.
- [21] K. Roiha, E. Kirveskari, M. Kaste et al., "Reorganization of the primary somatosensory cortex during stroke recovery," *Clinical Neurophysiology*, vol. 122, no. 2, pp. 339–345, 2011.
- [22] G. F. Wittenberg, E. P. Bastings, C. Scales, and D. Good, "Evolution of TMS motor maps during recovery after stroke," *NeuroImage*, vol. 13, supplement, no. 6, 1281 pages, 2001.
- [23] N. Forss, S. Mustanoja, K. Roiha et al., "Activation in parietal operculum parallels motor recovery in stroke," *Human Brain Mapping*, vol. 33, no. 3, pp. 534–541, 2012.
- [24] P. Lioumis, S. Mustanoja, R. Bikmullina et al., "Probing modifications of cortical excitability during stroke recovery with navigated TMS," *Topics in Stroke Rehabilitation*, vol. 19, pp. 182–192, 2012.
- [25] P. M. Rossini, A. T. Barker, A. Berardelli et al., "Non-invasive electrical and magnetic stimulation of the brain, spinal cord and roots: basic principles and procedures for routine clinical application. Report of an IFCN committee," *Electroencephalography and Clinical Neurophysiology*, vol. 91, no. 2, pp. 79–92, 1994.
- [26] S. Taulu and J. Simola, "Spatiotemporal signal space separation method for rejecting nearby interference in MEG measurements," *Physics in Medicine and Biology*, vol. 51, no. 7, pp. 1759–1768, 2006.
- [27] C. Tallon-Baudry, O. Bertrand, C. Wienbruch, B. Ross, and C. Pantev, "Combined EEG and MEG recordings of visual 40 Hz responses to illusory triangles in human," *NeuroReport*, vol. 8, no. 5, pp. 1103–1107, 1997.
- [28] G. F. Wittenberg, E. P. Bastings, A. M. Fowlkes, T. M. Morgan, D. C. Good, and T. P. Pons, "Dynamic course of intracortical TMS paired-pulse responses during recovery of motor function after

- stroke," *Neurorehabilitation and Neural Repair*, vol. 21, no. 6, pp. 568–573, 2007.
- [29] T. V. Perneger, "What's wrong with Bonferroni adjustments," *The British Medical Journal*, vol. 316, no. 7139, pp. 1236–1238, 1998.
- [30] S. D. Hall, N. Yamawaki, A. E. Fisher, R. P. Clauss, G. L. Woodhall, and I. M. Stanford, "GABA(A) alpha-1 subunit mediated desynchronization of elevated low frequency oscillations alleviates specific dysfunction in stroke—a case report," *Clinical Neurophysiology*, vol. 121, no. 4, pp. 549–555, 2010.
- [31] J. D. Schaechter, C. A. M. M. van Oers, B. N. Groisser et al., "Increase in sensorimotor cortex response to somatosensory stimulation over subacute poststroke period correlates with motor recovery in hemiparetic patients," *Neurorehabilitation and Neural Repair*, vol. 26, no. 4, pp. 325–334, 2012.
- [32] D. A. Nowak, C. Grefkes, M. Dafotakis, J. Küst, H. Karbe, and G. R. Fink, "Dexterity is impaired at both hands following unilateral subcortical middle cerebral artery stroke," *European Journal of Neuroscience*, vol. 25, no. 10, pp. 3173–3184, 2007.
- [33] M. T. Jurkiewicz, W. C. Gaetz, A. C. Bostan, and D. Cheyne, "Post-movement beta rebound is generated in motor cortex: evidence from neuromagnetic recordings," *NeuroImage*, vol. 32, no. 3, pp. 1281–1289, 2006.
- [34] W. Gaetz and D. Cheyne, "Localization of sensorimotor cortical rhythms induced by tactile stimulation using spatially filtered MEG," *NeuroImage*, vol. 30, no. 3, pp. 899–908, 2006.
- [35] N. E. Crone, D. L. Miglioretti, B. Gordon et al., "Functional mapping of human sensorimotor cortex with electrocorticographic spectral analysis: I. Alpha and beta event-related desynchronization," *Brain*, vol. 121, no. 12, pp. 2271–2299, 1998.
- [36] S. Ohara, A. Ikeda, T. Kunieda et al., "Movement-related change of electrocorticographic activity in human supplementary motor area proper," *Brain*, vol. 123, no. 6, pp. 1203–1215, 2000.
- [37] W. Szurhaj, P. Derambure, E. Labyt et al., "Basic mechanisms of central rhythms reactivity to preparation and execution of a voluntary movement: a stereoelectroencephalographic study," *Clinical Neurophysiology*, vol. 114, no. 1, pp. 107–119, 2003.
- [38] D. Sochůrková, I. Rektor, P. Jurák, and A. Stančák, "Intracerebral recording of cortical activity related to self-paced voluntary movements: a Bereitschaftspotential and event-related desynchronization/synchronization. SEEG study," *Experimental Brain Research*, vol. 173, no. 4, pp. 637–649, 2006.
- [39] J. P. Mäkelä, R. Hari, L. Valanne, and A. Ahonen, "Auditory evoked magnetic fields after ischemic brain lesions," *Annals of Neurology*, vol. 30, no. 1, pp. 76–82, 1991.
- [40] M. Takemi, Y. Masakado, M. Liu, and J. Ushiba, "Event-related desynchronization reflects downregulation of intracortical inhibition in human primary motor cortex," *Journal of Neurophysiology*, vol. 110, no. 5, pp. 1158–1166, 2013.
- [41] Y. Tamura, M. Hoshiyama, H. Nakata et al., "Functional relationship between human rolandic oscillations and motor cortical excitability: an MEG study," *European Journal of Neuroscience*, vol. 21, no. 9, pp. 2555–2562, 2005.
- [42] Y.-F. Hsu, K.-K. Liao, P.-L. Lee et al., "Intermittent theta burst stimulation over primary motor cortex enhances movement-related beta synchronisation," *Clinical Neurophysiology*, vol. 122, no. 11, pp. 2260–2267, 2011.
- [43] T. Silén, N. Forss, O. Jensen, and R. Hari, "Abnormal reactivity of the ~20-Hz motor cortex rhythm in univerricht lundborg type progressive myoclonus epilepsy," *NeuroImage*, vol. 12, no. 6, pp. 707–712, 2000.
- [44] P. Brown, M. C. Ridding, K. J. Werhahn, J. C. Rothwell, and C. D. Marsden, "Abnormalities of the balance between inhibition and excitation in the motor cortex of patients with cortical myoclonus," *Brain*, vol. 119, no. 1, pp. 309–317, 1996.
- [45] N. Danner, P. Julkunen, J. Khyuppenen et al., "Altered cortical inhibition in Unverricht-Lundborg type progressive myoclonus epilepsy (EPM1)," *Epilepsy Research*, vol. 85, no. 1, pp. 81–88, 2009.
- [46] J. Liepert, C. Restemeyer, T. Kucinski, S. Zittel, and C. Weiller, "Motor strokes: the lesion location determines motor excitability changes," *Stroke*, vol. 36, no. 12, pp. 2648–2653, 2005.
- [47] M. Ameli, C. Grefkes, F. Kemper et al., "Differential effects of high-frequency repetitive transcranial magnetic stimulation over ipsilesional primary motor cortex in cortical and subcortical middle cerebral artery stroke," *Annals of Neurology*, vol. 66, no. 3, pp. 298–309, 2009.
- [48] L. Säisänen, P. Julkunen, E. Niskanen et al., "Short- and intermediate-interval cortical inhibition and facilitation assessed by navigated transcranial magnetic stimulation," *Journal of Neuroscience Methods*, vol. 195, no. 2, pp. 241–248, 2011.

Research Article

Plasticity-Related PKM ζ Signaling in the Insular Cortex Is Involved in the Modulation of Neuropathic Pain after Nerve Injury

Jeongsoo Han,^{1,2} Minjee Kwon,^{1,2} Myeounghoon Cha,¹ Motomasa Tanioka,^{1,2}
Seong-Karp Hong,³ Sun Joon Bai,⁴ and Bae Hwan Lee^{1,2}

¹Department of Physiology, Yonsei University College of Medicine, Seoul 120-752, Republic of Korea

²Brain Korea 21 PLUS Project for Medical Science, Yonsei University College of Medicine, Seoul 120-752, Republic of Korea

³Division of Bio and Health Sciences, Mokwon University, Daejeon 302-729, Republic of Korea

⁴Department of Anesthesiology and Pain Medicine, Yonsei University College of Medicine, Seoul 120-752, Republic of Korea

Correspondence should be addressed to Bae Hwan Lee; bhlee@yuhs.ac

Received 11 February 2015; Revised 16 April 2015; Accepted 17 April 2015

Academic Editor: Long-Jun Wu

Copyright © 2015 Jeongsoo Han et al. This is an open access article distributed under the Creative Commons Attribution License, which permits unrestricted use, distribution, and reproduction in any medium, provided the original work is properly cited.

The insular cortex (IC) is associated with important functions linked with pain and emotions. According to recent reports, neural plasticity in the brain including the IC can be induced by nerve injury and may contribute to chronic pain. Continuous active kinase, protein kinase M ζ (PKM ζ), has been known to maintain the long-term potentiation. This study was conducted to determine the role of PKM ζ in the IC, which may be involved in the modulation of neuropathic pain. Mechanical allodynia test and immunohistochemistry (IHC) of zif268, an activity-dependent transcription factor required for neuronal plasticity, were performed after nerve injury. After ζ -pseudosubstrate inhibitory peptide (ZIP, a selective inhibitor of PKM ζ) injection, mechanical allodynia test and immunoblotting of PKM ζ , phospho-PKM ζ (p-PKM ζ), and GluR1 and GluR2 were observed. IHC demonstrated that zif268 expression significantly increased in the IC after nerve injury. Mechanical allodynia was significantly decreased by ZIP microinjection into the IC. The analgesic effect lasted for 12 hours. Moreover, the levels of GluR1, GluR2, and p-PKM ζ were decreased after ZIP microinjection. These results suggest that peripheral nerve injury induces neural plasticity related to PKM ζ and that ZIP has potential applications for relieving chronic pain.

1. Introduction

Nerve injury-induced neural plasticity in the central nervous system (CNS) is one of the important mechanisms involved in chronic pain [1–4]. Long-term potentiation (LTP), being considered as a neural substrate of learning and memory, is an underlying mechanism of synaptic plasticity [5, 6]. Furthermore, several studies have reported that LTP is induced in the spinal cord and the cerebral cortex by acute and chronic pain states [7–9]. Thus, it is believed that there is a common mechanism between learning/memory and chronic pain [10].

Protein kinase M ζ (PKM ζ) is a key molecule required for the maintenance of late LTP (L-LTP) [11, 12]. It is one of the atypical PKC isoforms, which include PKM ζ , PKC ζ , PKC ι , and PKC λ . Because PKM ζ has only the catalytic domain of

PKC ζ , it can be activated persistently [13]. ζ -pseudosubstrate inhibitory peptide (ZIP), a selective inhibitor of PKM ζ , can reverse LTP maintenance and block L-LTP induction [14, 15]. Furthermore, ZIP can also reverse a variety of memory types, such as spatial information, fear, addiction, and conditioned taste aversion (CTA) memory [15–19]. Several studies have reported that PKM ζ -related pain memory can be erased in the spinal cord and the brain [9, 20, 21].

The insular cortex (IC) is one of the pain-processing regions of the brain which is particularly related to the emotional aspects of pain [22–25]. Clinical and animal studies have shown that lesions of the IC cause pain asym-bolia and can reverse the neuropathic pain state [26–28]. NMDA receptor-dependent plastic changes after nerve injury and PKM ζ -mediated CTA memory in the IC have been

reported [16, 29]. However, there have been no studies published on immediate-early gene (IEG) expression with respect to LTP and PKM ζ -related mechanisms of plasticity in the IC after nerve injury.

Zif268, which is also known as early growth response protein 1 (EGR-1), is required for consolidation of L-LTP in the hippocampus and the spinal cord [30, 31]. In order to determine whether there is a possibility of LTP induction in the IC after nerve injury, an immunohistochemical study on zif268 was conducted. Moreover, in order to reveal whether PKM ζ signaling in the IC is involved in the maintenance of neuropathic pain, expression levels of PKM ζ and phospho-PKM ζ (p-PKM ζ) were measured after ZIP injection into the IC, and analgesic effects following ZIP injection into the IC were observed.

2. Materials and Methods

2.1. Experimental Animals. Experimental protocols in this study complied with the National Institute of Health guidelines and were approved by the Institutional Animal Care and Use Committee of the Yonsei University Health System. Adult male Sprague-Dawley rats (Koatec, Pyeongtaek, Korea, 250–280 g) were used. Rats were allowed to accommodate to the colony room for 7 days after arrival and were housed in plastic cages. Rats were maintained under a 12-hour light/dark cycle with food pellets and water provided *ad libitum*.

2.2. Cannulation and Neuropathic Surgery. For cannula implantation, rats were anesthetized with sodium pentobarbital (50 mg/kg, i.p.). 28-gauge guide cannulas were bilaterally implanted into the IC (AP: +1.0 mm, ML: \pm 4.7 mm, and DV: –5.8 mm) on a stereotaxic frame. Rats were allowed to recover for 7 days after cannula implantation. Neuropathic pain surgery was performed after recovery. Cannula-implanted rats were anesthetized with sodium pentobarbital (50 mg/kg, i.p.) and branches of the left sciatic nerve were exposed. The tibial and sural nerves were tightly ligated with 4-0 black silk and cut, while the common peroneal nerve was left intact [32]. The same procedure was applied to the sham-operated group without nerve injury. The wound was sutured in the muscle and skin layers.

2.3. Behavioral Test for Mechanical Allodynia. In order to observe the development of neuropathic pain, the mechanical allodynia test was performed by an experimenter blinded to the experiment before nerve injury, on postoperative days (PODs) 1 and 3. Rats were placed on a metal mesh floor under rectangular-shaped transparent domes. Animals were familiarized to the test conditions for 15 minutes before testing began. Withdrawal threshold was assessed by the application of electric von Frey filament (UGO Basile, Varese, Italy) stimulation to the sensitive area of the nerve-injured hind paw. This measurement was conducted 8 times at intervals of 2–3 minutes. The mechanical force was recorded when withdrawal responses of the hind paw occurred. Positive responses to mechanical stimulation included licking, sudden withdrawal, and biting of the ipsilateral paw.

2.4. ZIP Microinjection into the Insular Cortex and Analgesia Test. ZIP microinjection was conducted on POD 3. A Hamilton syringe and PE-10 tubing were used with an injection cannula for microinjection. Saline (0.9% NaCl) or 10 nmol/ μ L of ZIP (Tocris Bioscience, Minneapolis, MN, USA) diluted in saline was infused into the IC bilaterally, 0.5 μ L per side. After injection, the injection cannulas were maintained in position as they were for at least 1 minute. The behavioral test was performed before ZIP injection and 30 minutes and 1, 2, 4, 8, 12, 24, and 48 hours after microinjection.

2.5. Immunofluorescence Double Staining. For double immunofluorescence staining, rats were deeply anesthetized with urethane and perfused transcardially with saline followed by 4% paraformaldehyde in 0.1 M sodium phosphate buffer (PB, pH 6.8). The brain was removed from the skull and postfixed with 4% paraformaldehyde in PB at 4°C overnight. After postfixation, the brain block was transferred into phosphate-buffered saline (PBS, pH 7.4) containing 30% sucrose for 24 hours. The brain sample was covered with a cryosection compound (frozen section compound FSC 22, Leica, Wetzlar, Germany) and was frozen in –70°C deep freezer. Sample tissues were cut on a coronal section of 30 μ m thickness on a cryostat (HM 525, Thermo Scientific, Waltham, MA, USA). Section slides were then washed 3 times with 1x Tris-buffered saline (TBS) containing 0.025% Triton X-100. After washing, the section slides were incubated in 10% normal goat serum (Vector Laboratories, Burlingame, CA, USA) with 1% bovine serum albumin (BSA, Thermo Scientific) in TBS for 1 hour at room temperature. The sections were incubated overnight in rabbit monoclonal anti-zif268 antibody (1:200, Santa Cruz Biotechnology, Santa Cruz, CA, USA) and mouse monoclonal anti-NeuN antibody (1:200, Abcam, Cambridge, UK) diluted in 10% normal goat serum with TBS containing 1% BSA at 4°C. The sections were then rinsed 2 times with 1x TBS plus 1% Tween-20. After washing 2 times for 10 minutes, sections were incubated in secondary antibodies which were goat anti-rabbit Alexa Fluor 488 (1:200, Abcam) and goat anti-mouse Alexa Fluor 647 (1:200, Abcam), diluted in 10% normal goat serum with TBS containing 1% BSA for 1 hour at room temperature. Finally, the slides were washed 2 times with 1x TBS containing 0.025% Triton X-100 and mounted in Vectashield mounting media (Vector Laboratories).

2.6. Immunohistochemistry. To calculate the population of zif268-positive cells, nickel-enhanced 3,3'-diaminobenzidine (DAB) immunostaining was performed on POD 3. Briefly, rat brain slices were prepared using the same steps as for immunofluorescence staining. For zif268 staining, section slides were rinsed 5 times with 1x PBS and incubated in methanol with 0.3% H₂O₂ for 15 minutes to inhibit endogenous peroxidase activity. After washing the section slides 5 times, the sections were incubated with PBS containing 1% normal horse serum (Vector Laboratories) for 30 minutes and then incubated overnight at 4°C in 0.3% Triton X-100, 2% normal horse serum (Vector Laboratories), and rabbit monoclonal anti-zif268 antibody (1:4,000, Santa Cruz

Biotechnology). The sections were rinsed 5 times with 1x PBS and incubated for 30 minutes in a universal biotinylated anti-mouse/rabbit secondary antibody (1:50, Vector Laboratories). Section slides were then washed again and incubated for 30 minutes with PBS containing avidin-biotinylated horseradish peroxidase complex (1:50, Vector Laboratories). Following washing 5 times for 15 minutes, sections were incubated for 5 minutes in a solution containing 0.1% of DAB and 0.1% ammonium nickel sulfate in 1x PBS and 0.01% H_2O_2 . Finally, the sections were washed to stop the DAB reaction, serially dehydrated in 50, 70, 95, and 100% ethanol, cleared in xylene, and coverslipped with Permount (Fisher Scientific, Waltham, MA, USA).

To quantify zif268-positive cells in the IC, 8 representative sections of the IC were chosen from each brain. The interval of each section was 300 μm . Therefore, 8 sections cover anteroposterior range (2.1 mm) of the IC. Zif268-positive cells in the IC were identified with reference to the brain atlas of Paxinos and Watson [33]. All of the zif268-labeled cells from light-field microscopy image ($\times 20$ objective, Olympus BX40, Olympus, Tokyo, Japan) were counted manually. An experimenter blinded to the treatment conditions counted zif268-labeled cells of the ipsilateral and contralateral sides.

2.7. Western Blotting. To collect insular cortices, animals were anesthetized with enflurane and decapitated. The ipsilateral and contralateral rostral insular cortices were quickly isolated and transferred into a deep freezer. Extracted samples were stored at $-70^\circ C$. For protein extraction, samples were homogenized by sonication in lysis buffer (Proprep, iNtRON Biotechnology Inc., Seongnam, Korea) containing phosphatase inhibitor (PhosStop, Roche, Penzberg, Germany). Samples were centrifuged at 22,250 g for 10 minutes at $4^\circ C$ and supernatants were collected, and total protein concentrations of lysates were assessed with a spectrophotometer (ND-1000, NanoDrop Technologies Inc., Wilmington, DE, USA). 10 μL of protein of brain tissue extracts was denatured per well and run on 10% Bis-Tris gels (Bio-Rad, Hercules, CA, USA) for detection of PKM ζ , p-PKM ζ , GluR1, and GluR2. Proteins were transferred onto polyvinylidene difluoride (PVDF) membranes (GE Healthcare, Buckinghamshire, UK). Membranes were blocked in 5% skim milk in TBS with Tween-20 for 1 hour and incubated in primary antibodies overnight on a rocking platform at $4^\circ C$. Primary antibodies against PKM ζ (1:2,000, Cell Signaling Technology, Beverly, MA, USA), p-PKM ζ (1:2,000, Cell Signaling Technology), GluR1 (1:2,000, Millipore, Temecula, MA, USA), GluR2 (1:2,000, Abcam), and GAPDH (1:10,000, Ab Frontier, Seoul, Korea), which was used as a loading control, were used for western blotting. On the following day, the membranes were incubated in the appropriate secondary antibodies for 2 hours and horseradish peroxidase activity was visualized using a chemiluminescent substrate (ECL Prime western blotting detection reagent, GE Healthcare) and processed with a local allocation system (LAS) (ImageQuant LAS 4000 Mini, GE Healthcare). The intensity of the bands for PKM ζ , GluR1, and GluR2 was normalized to the intensity of GAPDH. The intensity of the bands for p-PKM ζ was normalized to the intensity of PKM ζ .

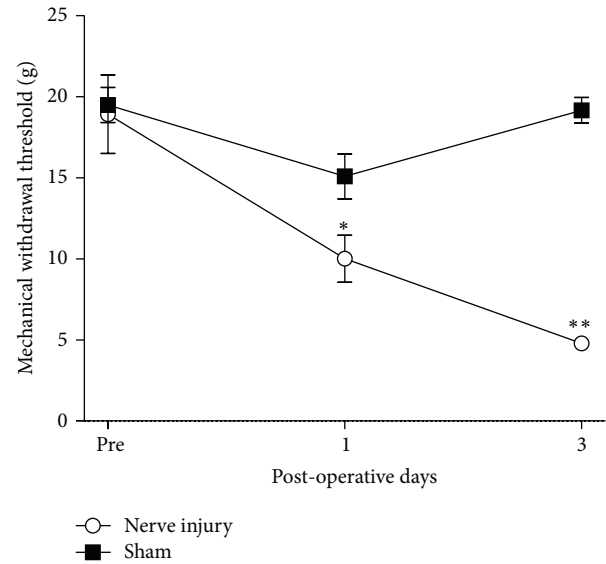


FIGURE 1: Development of mechanical allodynia after nerve injury. On PODs 1 and 3, rats developed significant neuropathic pain compared to sham group (** $P < 0.01$).

2.8. Statistical Analysis. Unpaired t -test for post hoc comparison was used for two-group comparisons while two-way ANOVA with repeated measures was used to analyze behavioral test. Western blots and IHC were compared using an unpaired t -test. All data were expressed as the mean \pm SEM. A P value less than 0.05 was considered statistically significant.

3. Results

3.1. Development of Neuropathic Pain. Injury to two major branches (sural and tibial nerves) of the sciatic nerve induced mechanical allodynia on PODs 1 and 3 (Figure 1). Repeated measures two-way ANOVA indicated effects of group ($F_{1,13} = 37.520$, $P < 0.001$), PODs ($F_{2,26} = 13.613$, $P < 0.001$), and interaction between group and PODs ($F_{2,26} = 10.305$, $P < 0.01$). The mechanical threshold of nerve-injured group decreased on POD 1 ($n = 8$, $P < 0.01$, unpaired t -test) and POD 3 ($n = 8$, $P < 0.01$, unpaired t -test) relative to sham group ($n = 8$).

3.2. Immunofluorescence Double Labeling of Zif268 and NeuN. To confirm that zif268 was co-labeled with NeuN in the IC, double labeling of zif268 and NeuN was performed. The representative images of the nerve-injured group are shown in Figures 2(d), 2(e), and 2(f), and those of the sham group are shown in Figures 2(a), 2(b), and 2(c). Zif268 immunoreactivity (green) was observed in the IC (Figures 2(a) and 2(d)). NeuN, a neuronal marker (red), was observed in the IC (Figures 2(b) and 2(e)). Colocalization of zif268 (green) and NeuN (red) was detected in the IC (Figures 2(c) and 2(f)). As shown in Figure 2, zif268-positive cells were colocalized with NeuN-positive cells. This result indicates that zif268 is expressed in IC neurons. Nerve-injured rats have more zif268-positive cells (Figure 2(d)) than the sham

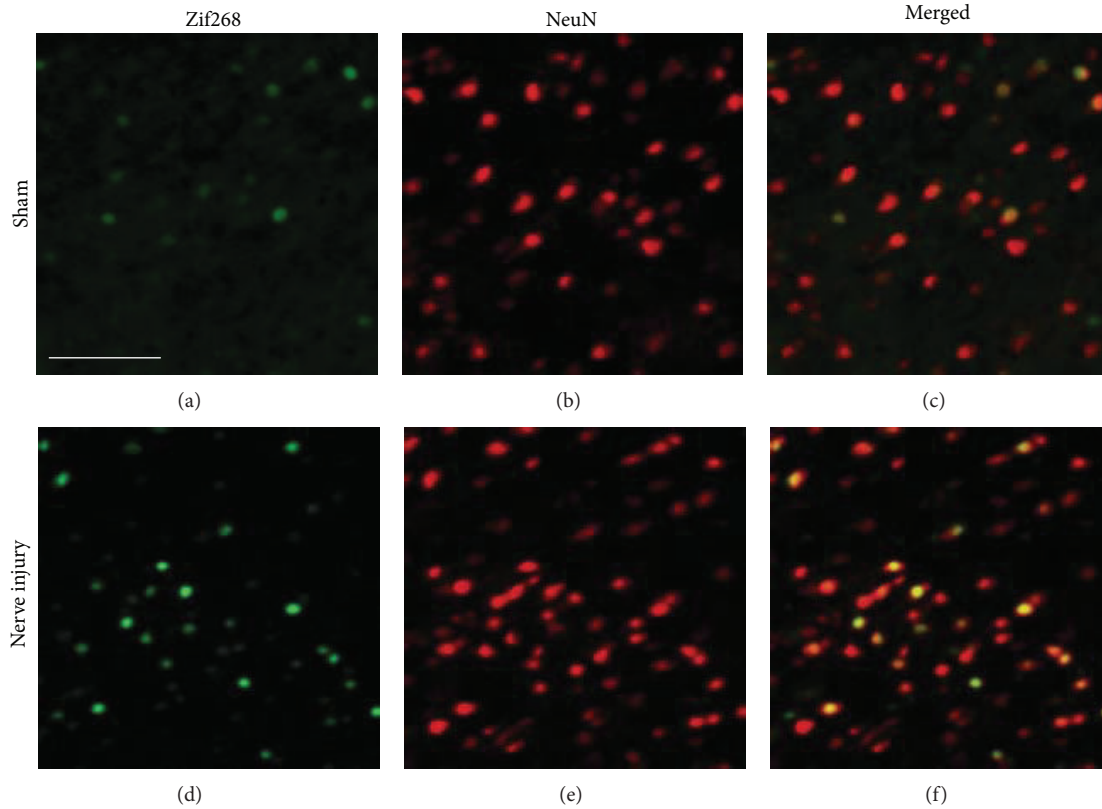


FIGURE 2: Fluorescence images of zif268 expression in the IC of nerve-injured and sham groups. (a) The sham group showed little expression of zif268-positive cells, unlike the nerve-injured group. (b) NeuN, a neuronal marker (red), was expressed in the sham group. (c) Colocalization of zif268 (green) and NeuN (red) is observed in the sham group. (d) In the nerve-injured group, the distribution of zif268 expression (green) was denser than in the sham group. (e) As in (b), NeuN was expressed in the nerve-injured group. (f) As in (c), colocalization of zif268 (green) and NeuN (red) is observed in the nerve-injured group. Scale bar, 50 μm .

group rats (Figure 2(a)). The number of NeuN-positive cells in the IC is similar between the nerve-injured (Figure 2(e)) and sham-operated groups (Figure 2(b)). The merged data of zif268 and NeuN expression show that the IC has a relationship with neuropathic pain (Figures 2(c) and 2(f)).

3.3. Immunohistochemistry of Zif268 in the Insular Cortex. Zif268-positive cells were found in the IC of nerve-injured rats (Figures 3(a) and 3(b)). Furthermore, zif268 immunohistochemistry was performed to quantify the zif268-positive cells in the nerve-injured and sham groups. The results showed that the number of zif268-positive cells in the nerve-injured group was significantly increased compared to that of the sham group ($n = 6$, $P < 0.05$, unpaired t -test; Figure 3(c)).

3.4. ZIP Injection into the Insular Cortex. Figure 4(a) shows the injection site of the IC. Injection of ZIP into the IC decreased mechanical allodynia gradually on POD 3. Repeated measures two-way ANOVA indicated effects of group ($F_{1,9} = 11.798$, $P < 0.01$), time ($F_{7,63} = 4.23$, $P < 0.01$), and interaction between group and time ($F_{7,63} = 3.93$, $P < 0.01$). The time course of mechanical allodynia in the ZIP-injected group ($n = 7$) on POD 3 shows that the analgesic effects of ZIP last for 12 hours after injection ($P < 0.05$,

unpaired t -test; Figure 4(b)), where analgesia was measured relative to the saline-injected group ($n = 5$). However, at 24 and 48 hours after injection, ZIP had no significant effect ($P > 0.05$, unpaired t -test).

3.5. Effects on PKM ζ and p-PKM ζ Expression of ZIP Microinjection into the Insular Cortex. To determine the role of ZIP, the IC was punched 3 hours after ZIP injection. The total PKM ζ in the ZIP-injected group ($n = 6$) was not changed ($P > 0.05$, unpaired t -test; Figure 5(a)) on POD 3 relative to the saline-injected group ($n = 6$). However, the expression level of p-PKM ζ was downregulated by ZIP injection into the IC on POD 3 ($P < 0.05$, unpaired t -test; Figure 5(b)).

3.6. Effects of ZIP Microinjection into the Insular Cortex on GluR1 and GluR2 Levels. We speculated that the effects of ZIP may contribute to inhibition of AMPA receptors. Accordingly, the expression levels of the AMPA receptor subunits GluR1 and GluR2 were measured after ZIP microinjection on POD 3. The results showed decreased GluR1 and GluR2 levels ($P < 0.05$, unpaired t -test; Figures 6(a) and 6(b), resp.) in the ZIP-injected group ($n = 8$), relative to the saline-injected group ($n = 8$).

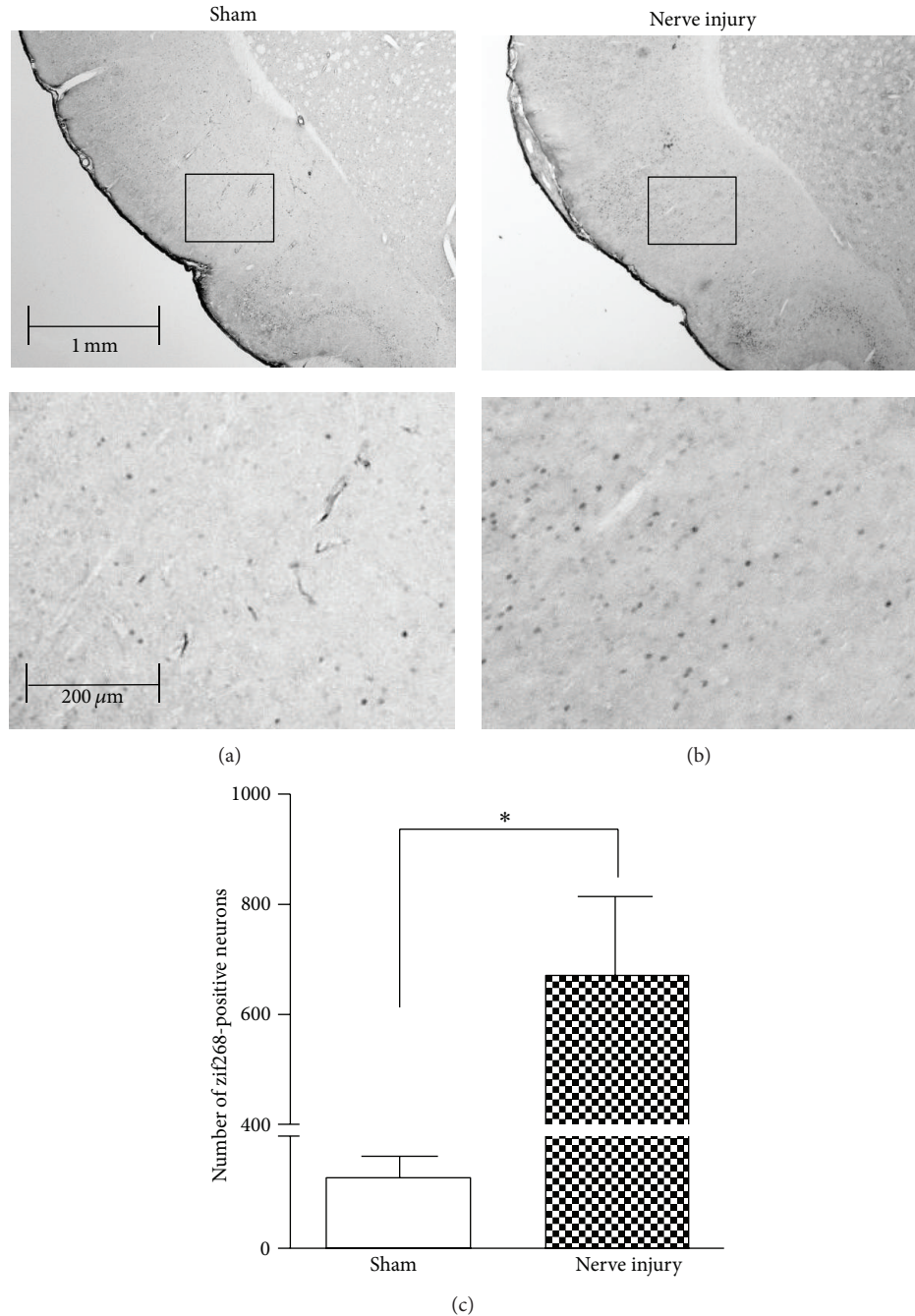


FIGURE 3: Zif268-positive cells in the IC. (a) Zif268-positive cells in the IC of a sham-operated rat. (b) Zif268-positive cells in the IC of a nerve-injured rat. (c) Comparison of zif268-positive cells in the nerve-injured and sham groups. Zif268-positive cells increased significantly in the IC after nerve injury (* $P < 0.05$). Cell counts are expressed per section.

4. Discussion

The IC plays a role in interpretation of emotional aspects of pain as one of the limbic system areas [22]. Several studies have reported that plastic changes in the IC are induced after peripheral nerve injury [29, 34]. Therefore, we focused on plastic changes of the IC and its pain modulation after nerve injury in order to understand the mechanisms of chronic pain. Recent reports have shown that functional changes in

the brain following nerve injury may be mediated by LTP [2, 9]. PKM ζ plays a key role in maintaining LTP, and inhibition of PKM ζ can reverse the chronic pain state and can erase established memories [12, 18]. Accordingly, the present study was performed to determine the plastic changes related to LTP formation, maintenance after nerve injury, and the role of the IC in pain modulation. Our findings suggest that PKM ζ in the IC can lead to nerve injury-induced plasticity which contributes to the maintenance of neuropathic pain states.

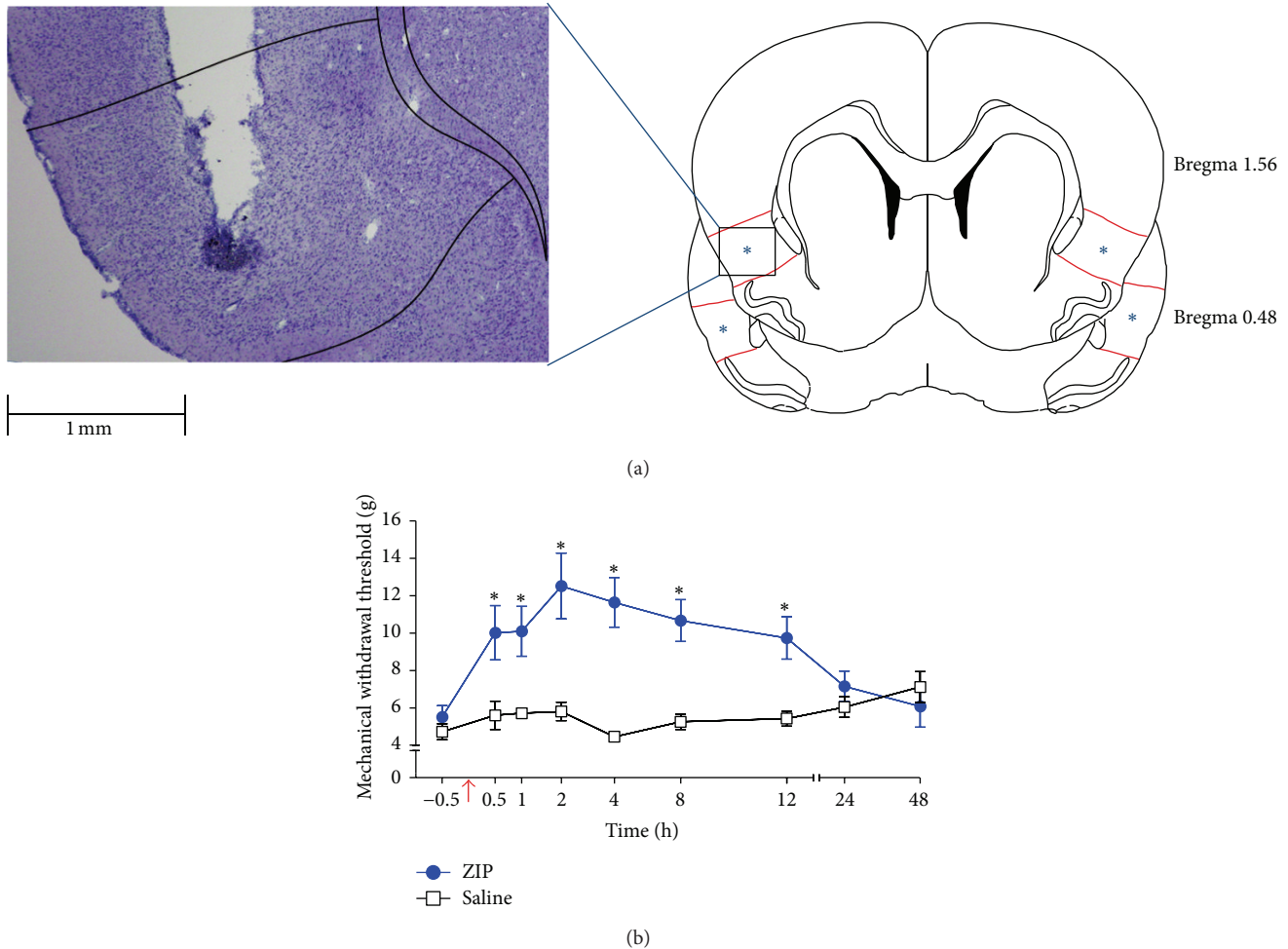


FIGURE 4: Reduction of mechanical allodynia after ZIP microinjection into the IC. (a) Identification of the ZIP injection site. ZIP was microinjected into the IC. (b) Paw withdrawal threshold to mechanical stimulation in POD 3 rats after microinjection of ZIP. Significant differences between nerve-injured and sham groups were found at the time points from 30 minutes to 12 hours after injection (* $P < 0.05$). The arrow indicates the time point of ZIP or saline injection.

Zif268 is a well-known marker related to LTP and neuronal plasticity [30]. In the hippocampus, the L-LTP phase requires the expression of IEGs such as zif268 and activity-regulated cytoskeletal-associated protein (Arc) [35, 36]. LTP-inducing stimulation increases zif268 expression levels in the hippocampus [37]. Furthermore, zif268 knockout mice displayed an absence of L-LTP and impaired long-term memory [30]. c-Fos is a neuronal activation marker and is expressed highly after nerve injury in the spinal cord and anterior cingulate cortex (ACC) [9]. Expression of c-Fos in the IC is increased by stress-induced hyperalgesia [38]. However, since zif268 is more correlated with LTP and plasticity to a greater degree than is c-Fos [39], changes in zif268 expression level in the IC after nerve injury were assessed immunohistochemically in our study. There have been several reports that zif268 is induced by nociceptive stimulation [39, 40]. However, there have been no reports on zif268 expression related to nerve injury-induced plasticity in the IC. Our results show that the number of zif268-positive cells increased after nerve injury, which is related to nerve injury-induced LTP in the IC.

Animals with lesions of the IC show reversed neuropathic or inflammatory pain behavior [27, 28]. Patients with lesions in the IC did not display appropriate responses to pain, but all other sensory and cognitive functions still remained intact [26]. Moreover, painful stimuli activate the IC, and direct stimulation of the IC can evoke sensations of pain, indicating that the IC is pronociceptive and involved in the interpretation of pain sensation [23, 41, 42].

PKM ζ is a key molecule for maintaining L-LTP and inhibition of PKM ζ can erase established LTP [12, 18]. Although the functions of PKM ζ were reported to be controversial in some studies [43–45], recent studies have suggested that atypical PKCs compensate the PKM ζ role of maintaining LTP in the constitutive PKM ζ knockout mice [46]. In fact, many studies have reported that the administration of ZIP into the spinal cord can reverse inflammatory pain, but not neuropathic pain [20, 21, 47, 48]. In contrast, ZIP injection into the ACC reverses the neuropathic pain state, but the analgesic effects disappear 24 hours after injection of ZIP [9]. Based on this report, the effects of ZIP injection into the IC were

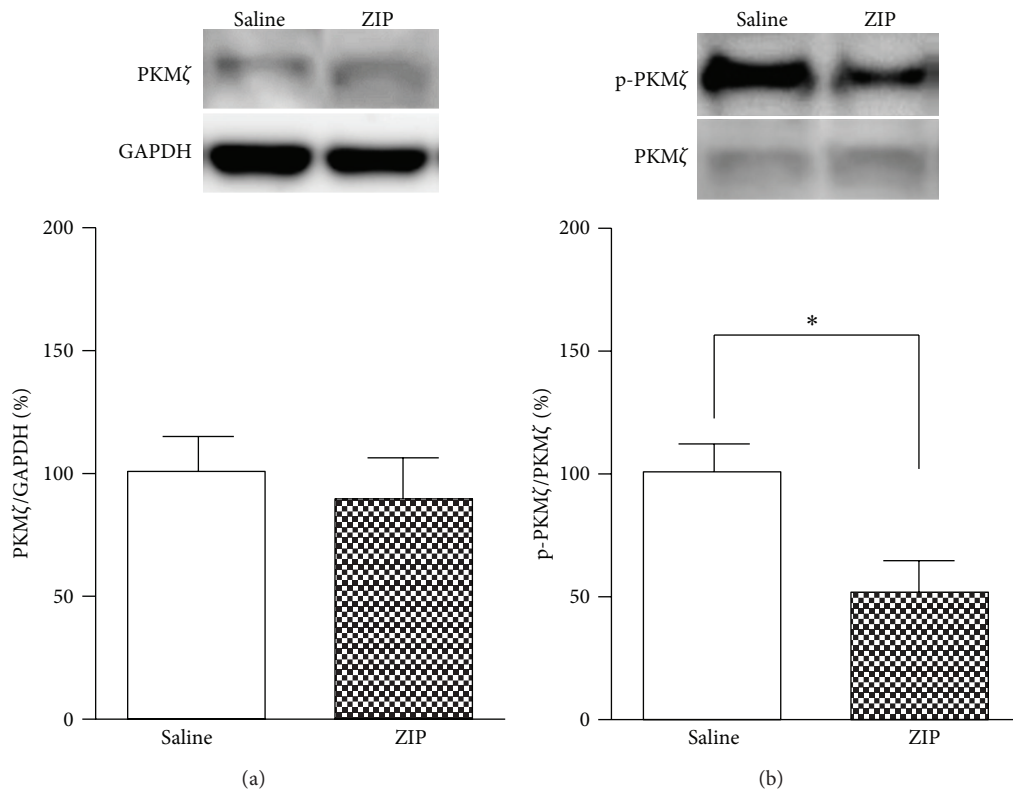


FIGURE 5: Expression levels of PKM ζ and p-PKM ζ after ZIP microinjection into the IC on POD 3. (a) Expression levels of PKM ζ normalized to GAPDH levels. There was no significant difference in PKM ζ levels between the saline injection and ZIP injection groups ($P > 0.05$). (b) Expression levels of p-PKM ζ normalized to PKM ζ levels. After ZIP injection, p-PKM ζ levels were significantly decreased (* $P < 0.05$).

investigated in the present study. The effects of ZIP lasted for 12 hours after injection into the IC. Our findings suggest that nerve injury induces plasticity related to PKM ζ in the IC and that the IC has a pain modulation function. Interestingly, the pain-relieving effect was not permanent. This phenomenon has been observed in other reports utilizing neuropathic pain models. This may be due to the reestablishment of LTP by the tonic peripheral afferent drive [9, 48].

PKM ζ is selectively upregulated in the spinal cord by formalin, capsaicin, and nerve injury [21, 48]. In the ACC, both PKM ζ and p-PKM ζ increased after nerve injury [9]. PKM ζ is activated by phosphorylation and can be inhibited by ZIP [18]. Increased levels of p-PKM ζ in the ACC contribute to neuropathic pain [9]. Similarly, increased levels of p-PKM ζ in the spinal cord contribute to formalin-induced pain [47]. Taken together, we hypothesized that upregulation of p-PKM ζ might contribute to neuropathic pain states and that ZIP can alleviate neuropathic pain. Indeed, decreased levels of p-PKM ζ were observed following ZIP injection. However, the expression levels of PKM ζ did not change after ZIP injection. In contrast, intrathecal infusion of ZIP did not reduce p-PKM ζ levels in the spinal cords of formalin model rats [47]. Although our findings are inconsistent with these studies, our results show that the function of p-PKM ζ in

the IC differs from that in the spinal cord, and these results are in line with those found with respect to the ACC [9].

Several reports have suggested that trafficking of the GluR2 subunit of the AMPA receptor in the hippocampus is related to PKM ζ [12, 49]. In addition, fear memory is maintained by PKM ζ -mediated GluR2-dependent AMPA receptor trafficking in the amygdala [50]. Other reports suggest that the GluR1 subunit of the AMPA receptor is involved in the molecular machinery of cocaine-induced plasticity in the nucleus accumbens (NAc) [51, 52]. PKM ζ -mediated LTP expression may be induced by N-ethylmaleimide-sensitive factor/GluR2-dependent trafficking in the hippocampus [49]. Interestingly, our results show that both GluR1 and GluR2 levels are downregulated by ZIP injection in the neuropathic pain model rats. Consistent with this, GluR1 levels were decreased after ZIP injection into the ACC of neuropathic pain model [9]. Other reports suggest that activation of metabotropic GluR1 (mGluR1) is required for insular L-LTP induction [53]. In addition, administration of ZIP into the NAc core can abolish long-term drug reward memory by effect on GluR2-containing AMPA receptors [54]. Taken together, we assume that PKM ζ maintains pain-related long-term plastic changes in the IC via both the GluR1 and GluR2 subunits of AMPA receptors.

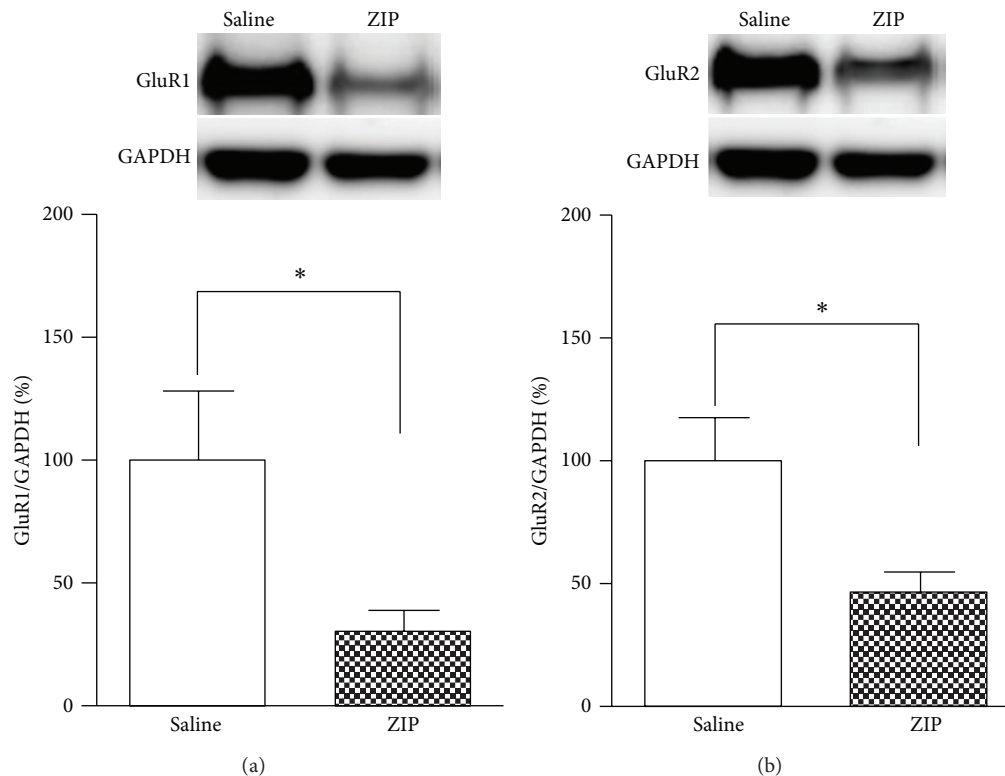


FIGURE 6: Expression levels of GluR1 and GluR2 after ZIP microinjection into the IC on POD 3. (a) Expression levels of GluR1 normalized to GAPDH levels. There was a significant difference between GluR1 levels in the saline injection and ZIP injection groups. After microinjection of ZIP, levels of GluR1 were significantly decreased ($*P < 0.05$). (b) Expression levels of GluR2 normalized to GAPDH levels. After ZIP injection, GluR2 levels were significantly decreased ($*P < 0.05$).

5. Conclusion

In this study, we demonstrated that there is a correlation between PKM ζ and neural plasticity of the IC, which might explain chronic pain mechanisms. PKM ζ seems to mediate this plasticity by regulating AMPA receptors containing GluR1 and GluR2. Moreover, the pain modulation function of the IC related to PKM ζ was revealed through administration of ZIP. Pharmacological targeting to inhibit plasticity of the IC may therefore present a strategy for chronic neuropathic pain therapy.

Conflict of Interests

The authors declare that there is no conflict of interests regarding the publication of this paper.

Authors' Contribution

Jeongsoo Han and Minjee Kwon contributed equally to this work.

Acknowledgment

This work was supported by the National Research Foundation of Korea founded by the Ministry of Science, ICT and Future Planning (NRF-2014R1A2A2A04004407).

References

- [1] R. Suzuki and A. Dickenson, "Spinal and supraspinal contributions to central sensitization in peripheral neuropathy," *Neuro-Signals*, vol. 14, no. 4, pp. 175–181, 2005.
- [2] M. Zhuo, "Cortical excitation and chronic pain," *Trends in Neurosciences*, vol. 31, no. 4, pp. 199–207, 2008.
- [3] R. Ruscheweyh, O. Wilder-Smith, R. Drdla, X.-G. Liu, and J. Sandkühler, "Long-term potentiation in spinal nociceptive pathways as a novel target for pain therapy," *Molecular Pain*, vol. 7, article 20, 2011.
- [4] C. J. Woolf and M. W. Salter, "Neuronal plasticity: increasing the gain in pain," *Science*, vol. 288, no. 5472, pp. 1765–1768, 2000.
- [5] T. V. P. Bliss and G. L. Collingridge, "A synaptic model of memory: long-term potentiation in the hippocampus," *Nature*, vol. 361, no. 6407, pp. 31–39, 1993.
- [6] S. F. Cooke and T. V. P. Bliss, "Plasticity in the human central nervous system," *Brain*, vol. 129, no. 7, pp. 1659–1673, 2006.
- [7] J. Sandkühler and X. Liu, "Induction of long-term potentiation at spinal synapses by noxious stimulation or nerve injury," *European Journal of Neuroscience*, vol. 10, no. 7, pp. 2476–2480, 1998.
- [8] H. Ikeda, J. Stark, H. Fischer et al., "Synaptic amplifier of inflammatory pain in the spinal dorsal horn," *Science*, vol. 312, no. 5780, pp. 1659–1662, 2006.
- [9] X. Y. Li, H. G. Ko, T. Chen et al., "Alleviating neuropathic pain hypersensitivity by inhibiting PKMzeta in the anterior cingulate cortex," *Science*, vol. 330, no. 6009, pp. 1400–1404, 2010.

- [10] R. R. Ji, T. Kohno, K. A. Moore, and C. J. Woolf, "Central sensitization and LTP: do pain and memory share similar mechanisms?" *Trends in Neurosciences*, vol. 26, no. 12, pp. 696–705, 2003.
- [11] D. S. F. Ling, L. S. Benardo, P. A. Serrano et al., "Protein kinase Mzeta is necessary and sufficient for LTP maintenance," *Nature Neuroscience*, vol. 5, no. 4, pp. 295–296, 2002.
- [12] T. C. Sacktor, "PKMzeta, LTP maintenance, and the dynamic molecular biology of memory storage," *Progress in Brain Research*, vol. 169, pp. 27–40, 2008.
- [13] T. C. Sacktor, P. Osten, H. Valsamis, X. Jiang, M. U. Naik, and E. Sublette, "Persistent activation of the ζ isoform of protein kinase C in the maintenance of long-term potentiation," *Proceedings of the National Academy of Sciences of the United States of America*, vol. 90, no. 18, pp. 8342–8346, 1993.
- [14] P. Serrano, Y. Yao, and T. C. Sacktor, "Persistent phosphorylation by protein kinase Mzeta maintains late-phase long-term potentiation," *The Journal of Neuroscience*, vol. 25, no. 8, pp. 1979–1984, 2005.
- [15] E. Pastalkova, P. Serrano, D. Pinkhasova, E. Wallace, A. A. Fenton, and T. C. Sacktor, "Storage of spatial information by the maintenance mechanism of LTP," *Science*, vol. 313, no. 5790, pp. 1141–1144, 2006.
- [16] R. Shema, T. C. Sacktor, and Y. Dudai, "Rapid erasure of long-term memory associations in the cortex by an inhibitor of PKM ζ ," *Science*, vol. 317, no. 5840, pp. 951–953, 2007.
- [17] P. Serrano, E. L. Friedman, J. Kenney et al., "PKM ζ maintains spatial, instrumental, and classically conditioned long-term memories," *PLoS Biology*, vol. 6, no. 12, article e318, 2008.
- [18] T. J. Price and S. Ghosh, "ZIPping to pain relief: the role (or not) of PKM ζ in chronic pain," *Molecular Pain*, vol. 9, no. 1, article 6, 2013.
- [19] M. E. Vélez-Hernández, R. Vázquez-Torres, M. C. Velasquez-Martinez et al., "Inhibition of Protein kinase Mzeta (PKMzeta) in the mesolimbic system alters cocaine sensitization in rats," *Journal of Drug and Alcohol Research*, vol. 2, Article ID 235669, 12 pages, 2013.
- [20] M. N. Asiedu, D. V. Tillu, O. K. Melemedjian et al., "Spinal protein kinase M zeta underlies the maintenance mechanism of persistent nociceptive sensitization," *The Journal of Neuroscience*, vol. 31, no. 18, pp. 6646–6653, 2011.
- [21] A. Laferrière, M. H. Pitcher, A. Haldane et al., "PKM ζ is essential for spinal plasticity underlying the maintenance of persistent pain," *Molecular Pain*, vol. 7, article 99, 2011.
- [22] A. D. Craig, "Interoception: the sense of the physiological condition of the body," *Current Opinion in Neurobiology*, vol. 13, no. 4, pp. 500–505, 2003.
- [23] L. Jasmin, S. D. Rabkin, A. Granato, A. Boudah, and P. T. Ohara, "Analgesia and hyperalgesia from GABA-mediated modulation of the cerebral cortex," *Nature*, vol. 424, no. 6946, pp. 316–320, 2003.
- [24] L. Jasmin, A. R. Burkey, A. Granato, and P. T. Ohara, "Rostral agranular insular cortex and pain areas of the central nervous system: a tract-tracing study in the rat," *The Journal of Comparative Neurology*, vol. 468, no. 3, pp. 425–440, 2004.
- [25] P. Alvarez, W. Dieb, A. Hafidi, D. L. Voisin, and R. Dallel, "Insular cortex representation of dynamic mechanical allodynia in trigeminal neuropathic rats," *Neurobiology of Disease*, vol. 33, no. 1, pp. 89–95, 2009.
- [26] M. Berthier, S. Starkstein, and R. Leiguarda, "Asymbolia for pain: a sensory-limbic disconnection syndrome," *Annals of Neurology*, vol. 24, no. 1, pp. 41–49, 1988.
- [27] A. M. Benison, S. Chumachenko, J. A. Harrison et al., "Caudal granular insular cortex is sufficient and necessary for the long-term maintenance of allodynic behavior in the rat attributable to mononeuropathy," *The Journal of Neuroscience*, vol. 31, no. 17, pp. 6317–6328, 2011.
- [28] U. Coffeen, J. Manuel Ortega-Legaspi, F. J. López-Muñoz, K. Simón-Arceo, O. Jaimes, and F. Pellicer, "Insular cortex lesion diminishes neuropathic and inflammatory pain-like behaviours," *European Journal of Pain*, vol. 15, no. 2, pp. 132–138, 2011.
- [29] S. Qiu, T. Chen, K. Koga et al., "An increase in synaptic NMDA receptors in the insular cortex contributes to neuropathic pain," *Science Signaling*, vol. 6, no. 275, article ra34, 2013.
- [30] M. W. Jones, M. L. Errington, P. J. French et al., "A requirement for the immediate early gene Zif268 in the expression of late LTP and long-term memories," *Nature Neuroscience*, vol. 4, no. 3, pp. 289–296, 2001.
- [31] F. Haugan, K. Wibrand, A. Fiskå, C. R. Bramham, and A. Tjølsen, "Stability of long term facilitation and expression of zif268 and Arc in the spinal cord dorsal horn is modulated by conditioning stimulation within the physiological frequency range of primary afferent fibers," *Neuroscience*, vol. 154, no. 4, pp. 1568–1575, 2008.
- [32] B. H. Lee, R. Won, E. J. Baik, S. H. Lee, and C. H. Moon, "An animal model of neuropathic pain employing injury to the sciatic nerve branches," *NeuroReport*, vol. 11, no. 4, pp. 657–661, 2000.
- [33] G. Paxinos and C. Watson, *The Rat Brain in Stereotaxic Coordinates*, Academic Press/Elsevier, Boston, Mass, USA, 6th edition, 2007.
- [34] S. Qiu, M. Zhang, Y. Liu et al., "GluA1 phosphorylation contributes to postsynaptic amplification of neuropathic pain in the insular cortex," *The Journal of Neuroscience*, vol. 34, no. 40, pp. 13505–13515, 2014.
- [35] J. D. Shepherd and M. F. Bear, "New views of Arc, a master regulator of synaptic plasticity," *Nature Neuroscience*, vol. 14, no. 3, pp. 279–284, 2011.
- [36] N. Granado, O. Ortiz, L. M. Suárez et al., "D₁ but not D₅ dopamine receptors are critical for LTP, spatial learning, and LTP-induced arc and zif268 expression in the hippocampus," *Cerebral Cortex*, vol. 18, no. 1, pp. 1–12, 2008.
- [37] F. Ranieri, M. V. Podda, E. Riccardi et al., "Modulation of LTP at rat hippocampal CA3-CA1 synapses by direct current stimulation," *Journal of Neurophysiology*, vol. 107, no. 7, pp. 1868–1880, 2012.
- [38] R. Takeda, Y. Watanabe, T. Ikeda et al., "Analgesic effect of milnacipran is associated with c-Fos expression in the anterior cingulate cortex in the rat neuropathic pain model," *Neuroscience Research*, vol. 64, no. 4, pp. 380–384, 2009.
- [39] W. Wisden, M. L. Errington, S. Williams et al., "Differential expression of immediate early genes in the hippocampus and spinal cord," *Neuron*, vol. 4, no. 4, pp. 603–614, 1990.
- [40] L. J. Rygh, R. Suzuki, W. Rahman et al., "Local and descending circuits regulate long-term potentiation and zif268 expression in spinal neurons," *The European Journal of Neuroscience*, vol. 24, no. 3, pp. 761–772, 2006.
- [41] L. Mazzola, J. Isnard, R. Peyron, M. Guénot, and F. Mauguière, "Somatotopic organization of pain responses to direct electrical stimulation of the human insular cortex," *Pain*, vol. 146, no. 1–2, pp. 99–104, 2009.

- [42] M. Frot, M. Magnin, F. Mauguière, and L. Garcia-Larrea, "Human SII and posterior insula differently encode thermal laser stimuli," *Cerebral Cortex*, vol. 17, no. 3, pp. 610–620, 2007.
- [43] A. M. Lee, B. R. Kanter, D. Wang et al., "*Prkcz* null mice show normal learning and memory," *Nature*, vol. 493, no. 7432, pp. 416–419, 2013.
- [44] L. J. Volk, J. L. Bachman, R. Johnson, Y. Yu, and R. L. Huganir, "PKM- ζ is not required for hippocampal synaptic plasticity, learning and memory," *Nature*, vol. 493, no. 7432, pp. 420–423, 2013.
- [45] A. X. Wu-Zhang, C. L. Schramm, S. Nabavi, R. Malinow, and A. C. Newton, "Cellular pharmacology of protein kinase M ζ (PKM ζ) contrasts with its in vitro profile: implications for PKM ζ as a mediator of memory," *The Journal of Biological Chemistry*, vol. 287, no. 16, pp. 12879–12885, 2012.
- [46] Y. Yao, P. Tsokas, D. Jothianandan, A. Tcherepanov, P. van de Nes, and T. C. Sacktor, "Compensation by PKC α / λ activation and PKM ζ / λ formation in PKM ζ knock-out mice," *Society for Neuroscience Abstract*, no. 233.22, 2013, <http://www.abstractsonline.com/Plan/ViewAbstract.aspx?mID=3236&sKey=6bc2b62b-cc81-4ad4-9245-52909d0cf884&cKey=ff4334ac-acb0-4745-8559-d4fd4a58ed1&mKey=8d2a5bec-4825-4cd6-9439-b42bb151d1cf>.
- [47] F. Marchand, R. D'Mello, P. K. Yip et al., "Specific involvement of atypical PKC ζ /PKM ζ in spinal persistent nociceptive processing following peripheral inflammation in rat," *Molecular Pain*, vol. 7, article 86, 2011.
- [48] T. King, C. Qu, A. Okun et al., "Contribution of PKM ζ -dependent and independent amplification to components of experimental neuropathic pain," *Pain*, vol. 153, no. 6, pp. 1263–1273, 2012.
- [49] Y. Yao, M. T. Kelly, S. Sajikumar et al., "PKM ζ maintains late long-term potentiation by *N*-ethylmaleimide-sensitive factor/GluR2-dependent trafficking of postsynaptic AMPA receptors," *The Journal of Neuroscience*, vol. 28, no. 31, pp. 7820–7827, 2008.
- [50] P. V. Miguez, O. Hardt, D. C. Wu et al., "PKM ζ maintains memories by regulating GluR2-dependent AMPA receptor trafficking," *Nature Neuroscience*, vol. 13, no. 5, pp. 630–634, 2010.
- [51] D. Shabashov, E. Shohami, and R. Yaka, "Inactivation of PKM ζ in the NAc shell abolished cocaine-conditioned reward," *Journal of Molecular Neuroscience*, vol. 47, no. 3, pp. 546–553, 2012.
- [52] M. A. Sutton, E. F. Schmidt, K.-H. Choi et al., "Extinction-induced upregulation in AMPA receptors reduces cocaine-seeking behaviour," *Nature*, vol. 421, no. 6918, pp. 70–75, 2003.
- [53] M.-G. Liu, S. J. Kang, T.-Y. Shi et al., "Long-term potentiation of synaptic transmission in the adult mouse insular cortex: multielectrode array recordings," *Journal of Neurophysiology*, vol. 110, no. 2, pp. 505–521, 2013.
- [54] Y.-Q. Li, Y.-X. Xue, Y.-Y. He et al., "Inhibition of PKM ζ in nucleus accumbens core abolishes long-term drug reward memory," *Journal of Neuroscience*, vol. 31, no. 14, pp. 5436–5446, 2011.

Research Article

Reactive Oxygen Species Donors Increase the Responsiveness of Dorsal Horn Neurons and Induce Mechanical Hyperalgesia in Rats

Hee Young Kim,^{1,2} Inhyung Lee,³ Sang Woo Chun,⁴ and Hee Kee Kim⁵

¹Department of Neuroscience and Cell Biology, 301 University Boulevard, University of Texas Medical Branch, TX 77555-1069, USA

²Department of Physiology, College of Korean Medicine, Daegu Haany University, Daegu 706-060, Republic of Korea

³Department of Veterinary Clinical Sciences, College of Veterinary Medicine, Seoul National University, 1 Gwanak-ro, Gwanak-gu, Seoul 151-742, Republic of Korea

⁴Department of Oral Physiology, College of Dentistry, Institute of Wonkwang Biomaterial and Implant, Wonkwang University, 344-2 Shinyong Dong, Iksan 570-749, Republic of Korea

⁵Department of Pain Medicine, The University of Texas MD Anderson Cancer Center, 1515 Holcombe Boulevard, Houston, TX 77030, USA

Correspondence should be addressed to Sang Woo Chun; physiol@wku.ac.kr and Hee Kee Kim; hkim9@mdanderson.org

Received 11 February 2015; Revised 15 April 2015; Accepted 22 April 2015

Academic Editor: Bae Hwan Lee

Copyright © 2015 Hee Young Kim et al. This is an open access article distributed under the Creative Commons Attribution License, which permits unrestricted use, distribution, and reproduction in any medium, provided the original work is properly cited.

Our previous studies suggest that reactive oxygen species (ROS) scavengers have analgesic effect on neuropathic pain through spinal mechanisms in the rat. The studies suggest that superoxide in spinal cord is one of important mediators of persistent pain. To test the hypothesis that increase of superoxide-derived intermediates leads to central sensitization and pain, the effects of an intrathecal injection of chemical ROS donors releasing either OH^\bullet , OCl^- , or H_2O_2 were examined on pain behaviors. Following treatment with *t*-BOOH (OH^\bullet donor), dorsal horn neuron responses to mechanical stimuli in normal rats and the changes of neuronal excitability were explored on substantia gelatinosa (SG) neurons using whole-cell patch clamping recordings. Intrathecal administration of *t*-BOOH or NaOCl (OCl^- donor), but not H_2O_2 , significantly decreased mechanical thresholds of hind paws. The responses of wide dynamic range neurons to mechanical stimuli increased after a local application of *t*-BOOH. The *t*-BOOH increased the frequency and the amplitude of excitatory postsynaptic potentials, depolarized membrane potential in SG neurons, and increased the frequency of action potentials evoked by depolarizing current pulses. These results suggest that elevated ROS, especially OH^\bullet , in the spinal cord sensitized dorsal horn neurons and produced hyperalgesia in normal rats.

1. Introduction

Reactive oxygen species (ROS) are generated as part of normal cell metabolism and serve both normal physiological and pathophysiological functions [1, 2]. The many types of ROS include superoxide radicals ($\text{O}_2^{\bullet-}$), hydroxyl radicals (OH^\bullet), hydrogen peroxide (H_2O_2), nitric oxide (NO), and peroxynitrite [2, 3]. The major source of ROS in the central nervous system is the electron transport chain in the inner membranes of mitochondria that produces adenosine triphosphate. Leakage of electrons during electron transport produces the superoxide anion ($\text{O}_2^{\bullet-}$), which transforms OH^\bullet

in the presence of transition metals such as free iron. The overproduction of ROS results in lipid peroxidation, protein oxidation, and nucleic acid oxidation [4].

ROS have been implicated in the pathogenesis of various diseases, including rheumatoid arthritis, asthma, inflammatory bowel disease, atherosclerosis, and Alzheimer disease. Previous studies suggested that ROS are critically involved in various pain conditions, including neuropathic and inflammatory pain. ROS scavengers such as superoxide dismutase mimetics [5], phenyl N-*t*-butylnitron [6, 7], 5,5-dimethyl-1-pyrroline-N-oxide [6], and vitamin E [8] reduce hyperalgesic behaviors in several rat models of pain. The main action site

for ROS in neuropathic [6, 8] and capsaicin-induced pain [7, 9] is the spinal cord. Also, peripheral nerve injury increases the production of ROS in the spinal cord in persistent pain conditions [10]. Those findings suggest that ROS in the spinal cord are critically involved in neuropathic and inflammatory pain. Furthermore, our previous studies have suggested that increased production of the primary ROS, $O_2^{\bullet-}$, from mitochondria mediates sensitization of spinal dorsal horn neurons and thus persistent pain [7, 11]. In brief, $O_2^{\bullet-}$ scavengers reduce persistent pain, dorsal horn neuron hyperexcitability [7], and spinal long-term potentiation [11]. The level of mitochondrial $O_2^{\bullet-}$ dismutase determines the level of central sensitization and thus hyperalgesia [12]. While it is generally accepted that $O_2^{\bullet-}$ do not diffuse across membranes [13], it is not clear how the $O_2^{\bullet-}$ formed in mitochondria diffuse into the cytoplasm and mediate spinal neuronal plasticity and pain. $O_2^{\bullet-}$ in mitochondria are rapidly converted to membrane permeable hydrogen peroxide (H_2O_2) by superoxide dismutase, are diffused in cells, and can be sequentially converted to highly reactive oxidants, such as OH^{\bullet} and hypochlorite (OCl^-) [14]. Here, we hypothesized that an increase in superoxide-derived intermediates in spinal dorsal horn neurons leads to central sensitization and hyperalgesia.

In the present study, we examined if artificial increases in possible superoxide intermediates— OH^{\bullet} , OCl^- , and H_2O_2 —in the spinal dorsal horn produce pain behaviors in normal rats. To further explore the role of OH^{\bullet} in pain, we used *in vivo* extracellular recordings to examine if *tert*-butyl hydroperoxide (*t*-BOOH, an OH^{\bullet} donor) increases the excitability of wide dynamic range (WDR) neurons in the spinal dorsal horn, and we used *in vitro* intracellular recordings to examine if *t*-BOOH produces changes in membrane excitability in substantia gelatinosa (SG) neurons in spinal cord slice preparations.

2. Materials and Methods

2.1. Experimental Animals. We used male Sprague-Dawley rats (Harlan Sprague-Dawley Co., Houston, TX, USA) for the experiments. The rats were housed under a 12/12-hour reversed light-dark cycle (dark cycle, 8:00 A.M.–8:00 P.M.) for at least 1 week before any experiments. All experiments were carried out in accordance with the National Institute of Health's Guide for the Care and Use of Laboratory Animals, and the animal use protocol was approved by the University of Texas Medical Branch Institutional Animal Care and Use Committee.

2.2. Behavioral Test

2.2.1. Intrathecal Catheterization. Intrathecal catheters were implanted into the lumbar enlargement as described previously [6, 8]. Briefly, adult rats (200–350 g) were anesthetized with isoflurane (3% for induction and 2% for maintenance) in the flow of oxygen, and then a posterior midline incision was made from the T11 vertebra to L1. The posterior articular process and lamina of the T12 vertebra were removed with a pair of rongeurs to expose the spinal meninges. A small

nick was made on the dura mater, and a prepared catheter (sterilized tubing filled with saline; PE10, Becton Dickinson) was inserted into the intrathecal space. The catheter was gently guided caudally until the tip reached the level of the lumbar enlargement of the spinal cord (approximately 1 cm caudal to the initial insert point). The remaining part of the tubing was connected with PE50 tubing and fed subcutaneously to the midthoracic level with anchors to the muscles at multiple sites in order to expose the tip to the dorsal midline position. The outside tip of the tubing was sealed, and the incision was closed. After full recovery from anesthesia, the rats were returned to their cages and housed individually for 1 week. Catheters were flushed with 10 μ L of sterile saline 3 days after catheterization to maintain patency. This experiment excluded rats showing dragging of hind paws or 5% loss of body weight 7 days after catheterization. The position of the intrathecal catheter was checked after the animals were euthanized at the end of the experiment.

2.2.2. Intrathecal Application of ROS Donors. Either *t*-BOOH or NaOCl (both from Sigma Chemical Company, St. Louis, MO, USA) was injected through an intrathecal catheter for 2–3 min while the animals were conscious at least 1 week after lumbar catheterization. The OH^{\bullet} donor *t*-BOOH was administered at 11, 28, or 55 μ mol in a volume of 15 μ L. The hypochlorite donor NaOCl was injected at 134 μ mol in 15 μ L. Control rats were treated with 15 μ L of sterile 0.9% saline. In addition, H_2O_2 was directly injected into the intervertebral space between the L5 and L6 vertebrae under light isoflurane anesthesia at 15, 44, 74, or 148 μ mol in 50 μ L.

2.2.3. Behavioral Testing for Mechanical Thresholds. Behavioral tests were conducted to measure the 50% foot mechanical thresholds in response to mechanical stimuli applied to both the left and the right hind paws under blind conditions. We recorded the mechanical threshold for the paw that was more sensitive to stimuli. For testing, each animal was placed in a plastic chamber (8.5 \times 8.5 \times 28 cm) that was placed on top of a mesh screen, and mechanical stimuli were applied to the plantar surface of one hind paw with von Frey monofilaments from underneath. Thresholds were determined by the up-down method [15] using von Frey monofilaments 4.10, 4.31, 4.52, 4.74, 4.92, and 5.16 (equivalent to 1.26, 2.04, 3.31, 5.50, 8.32, and 14.45 g, resp.). von Frey filaments were applied perpendicularly to the most sensitive area of the plantar surface—the proximal portion and base of the 2nd, 3rd, or 4th toe—with sufficient force to bend the filament slightly for 2 to 3 s. An abrupt withdrawal of the foot during stimulation or immediately after stimulus removal was counted as a positive response. The first stimulus was always initiated with the 4.74 filament. If there was a positive response, the next-lower-strength filament was used, and if not, the next-higher-strength size filament was applied. This testing pattern was continued until we had recorded responses to six von Frey stimuli counting from the first change of response (i.e., a positive response to a stimulus after a negative response to the first stimulus or a negative response to a stimulus after a positive response to the first stimulus). The responses were then converted into a 50% threshold value

using the formula $10^{(X+kd)}/10^4$, where X is the value of the final von Frey filament used in logarithmic units, k is the tabular value for positive/negative responses, and d is the mean difference between stimuli in logarithmic units (0.22) [16]. When positive or negative responses were still observed at the end of a stimulus session, values of 3.54 or 5.27 were assigned, respectively, by assuming a value of ± 0.5 for k in these cases. The behavioral data were plotted using a linear scale in von Frey values as well as in grams.

2.3. Extracellular Recordings of WDR Neurons in the Spinal Cord. Adult rats (200–350 g) were anesthetized with an intraperitoneal injection of urethane (1.5 g/kg). The trachea was cannulated to provide unobstructed ventilation, and a catheter was inserted into the left external jugular vein. A laminectomy was performed to expose the spinal cord at the T13–L2 vertebral level. The rat was placed in a stereotaxic apparatus, and the spinal cord was bathed in a pool of warm mineral oil. Core body temperature was maintained at 37°C by a controlled heating blanket. The animal was paralyzed with an initial intravenous bolus dose of pancuronium bromide (1 mg/kg) and ventilated artificially to maintain end-tidal CO_2 between 3.5 and 4.5%. The level of pancuronium was maintained by continuous intravenous infusion (0.4–0.6 mg/kg/h).

An extracellular recording was made for WDR neurons in the dorsal horn. These neurons responded to both innocuous and noxious mechanical stimuli. Cells were searched at the L4 and L5 segments of the spinal cord using a low-impedance (0.4–0.8 M Ω) carbon filament electrode (Kation Scientific, Minneapolis, MN, USA) mounted on an electronic micro-manipulator. Brush stimuli were used to search for dorsal horn neurons. WDR neurons with receptive fields located on the plantar surface of the ipsilateral hind paw were recorded extracellularly. Recordings were made only for single neurons whose spike amplitude could be easily discriminated from those of other neurons (at least twice the height). Electrophysiological activity was amplified, displayed on an oscilloscope, and transmitted into a data analysis system (CED 1401, PC, USA) with Spike2 software. Throughout the experiment, spike sizes and configurations were continuously monitored with the use of Spike2 software to confirm that the data were being acquired from the same WDR neuron and that the relationship of the recording electrode to the neuron remained constant.

After the receptive field of a WDR neuron was confirmed, graded mechanical stimuli were applied: soft-brush, nonnoxious (1 or 2 g) von Frey filaments and a noxious (20 g) von Frey filament. All stimuli were applied at a rate of once per second for 10 s with a 10 s interval between stimuli. Background activity was recorded three times before the administration of *t*-BOOH. Ten microliters of a *t*-BOOH solution (1 or 10 μmol) was applied to a small cotton ball around the electrode on the spinal cord. The cotton ball was kept on the spinal cord after application of *t*-BOOH until the end of the experiment. The discharges of WDR neurons were recorded every 30 min after administration of *t*-BOOH. Responses to mechanical stimuli were counted as discharges per second during 10 s of

stimulation, and three separate counts were obtained for each animal.

2.4. Patch Clamp Recordings of SG Neurons in the Spinal Cord

2.4.1. Spinal Cord Slice Preparation. Sprague-Dawley rats (14–20 days old, 30–55 g) were anesthetized with urethane (1.5 g/kg, intraperitoneally), and a lumbosacral laminectomy was performed. The lumbar spinal cord was rapidly dissected and submerged in ice-cold artificial cerebrospinal fluid (ACSF). The dura and arachnoid membranes and ventral/dorsal roots around the lumbar spinal cord were removed. The spinal cord was mounted on a 752M Vibroslicer (Campden Instruments, Leicestershire, UK) and cut into 300 μm thick transverse slices. The slices were then incubated in ACSF, saturated with 5% CO_2 in oxygen at 32°C for 1 h, and transferred to a recording chamber, which was continuously perfused with aerated ACSF at a rate of 3–4 mL/min. The ionic composition of the ACSF was 117 mM NaCl, 3.6 mM KCl, 1.2 mM NaH_2PO_4 , 1.2 mM MgCl_2 , 2.5 mM CaCl_2 , 11 mM glucose, and 25 mM NaHCO_3 (pH 7.4). A platinum grid was placed on top of the slice to prevent slice movement.

2.4.2. Patch Clamp Recordings. Whole-cell recordings using the patch clamp technique were performed for SG neurons in the lumbar spinal cord. Patch electrodes were made from borosilicate glass capillaries (1.5 mm diameter and 0.25 mm wall thickness) pulled on a P-80 micropipette puller (Sutter Instruments, Novato, CA, USA). When an electrode was filled with the internal solution, the resistance of patch electrodes was 6–8 M Ω . The internal solution was composed of 150 mM potassium gluconate, 5 mM KCl, 0.1 mM ethylene glycol-bis(β -aminoethylether)-N,N,N',N'-tetraacetic acid (EGTA), 10 mM N-2-hydroxyethylpiperazine-N'-2-ethanesulfonic acid (HEPES), and 5 mM MgATP (pH 7.25). Recordings were made of neurons within the SG, which was visible as a distinct translucent band across the dorsal horn under a microscope (BX51WI, Olympus, Tokyo, Japan). Current-clamp recordings were made using an Axopatch 200B amplifier (Axon Instruments, Foster City, CA, USA). After filtration at 2 KHz using a low-pass filter, data were acquired using a Digidata 1322A interface and pClamp software (version 9.0, Axon Instruments) for subsequent analysis. All recordings were made at room temperature (20–25°C).

After the formation of more than 1 G Ω , whole-cell access was achieved by rupturing the membrane with negative pressure. The resting membrane potential was measured 5–10 min after whole-cell configuration. Only neurons with a resting membrane potential more negative than –50 mV were used. Excitatory postsynaptic potentials (EPSPs) were analyzed with the Mini Analysis program (version 6.0, Synaptosoft, Decatur, GA, USA). The frequency of EPSPs was determined by setting a detection threshold level (1.0–2.0 mV). The excitability of SG neurons was quantified by examining the number of action potentials (spikes/second) evoked in response to a current of 25 pA or 50 pA (1 s duration for adapting-firing neurons (AFNs) and 3 s duration for tonic-firing neurons (TFNs)) from a holding potential

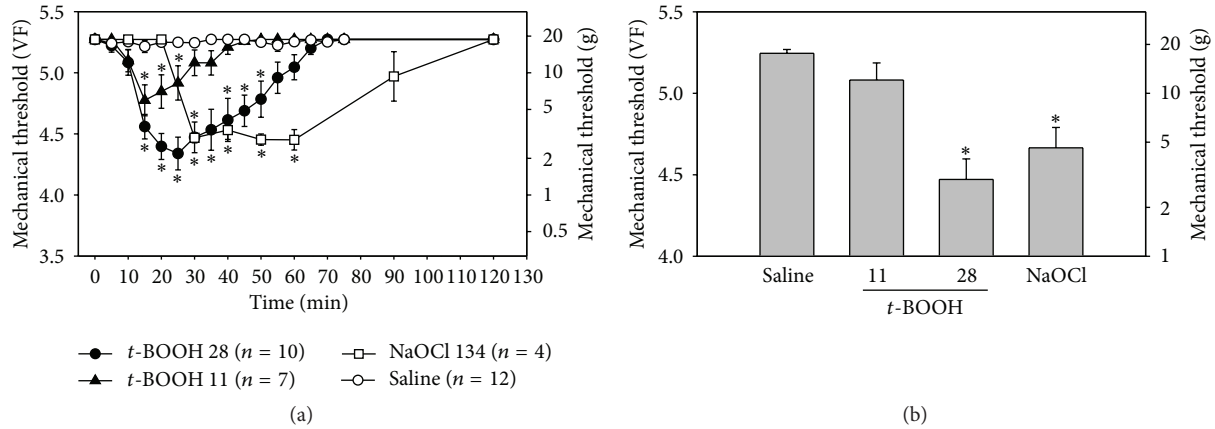


FIGURE 1: Effects of *t*-BOOH and NaOCl on mechanical thresholds in normal rats. (a) Intrathecal administration of *t*-BOOH (11 or 28 μ mol) or NaOCl (134 μ mol) temporarily decreased the mechanical threshold in a dose-dependent manner, compared to the mechanical threshold observed with administration of saline. Asterisks indicate values that are significantly different from those for the saline group as determined by a two-way repeated-measures analysis of variance with one repeated factor followed by the Duncan post hoc test ($P < 0.05$). (b) Mechanical thresholds of hind paws after intrathecal administration of *t*-BOOH (11 μ mol, $n = 7$; 28 μ mol, $n = 10$) or NaOCl (134 μ mol, $n = 4$), compared with the mechanical threshold observed with saline, 30 min after injection. Asterisks indicate values that are significantly different from that for the saline group as determined by the Kruskal-Wallis analysis of variance by ranks followed by the Dunn test ($P < 0.05$). The data are mean with standard errors of the mean. VF, von Frey filament sizes.

of -60 mV. *t*-BOOH in ACSF was applied to the perfusion bath by a gravity perfusion system (BPS-4, ALA Scientific Instruments, Westbury, NY, USA).

2.5. Statistical Analysis. The data were summarized in terms of mean and standard errors of the mean and analyzed using the statistics program SigmaStat (version 3.1, Systat Software, San Jose, CA, USA). Statistical significance ($P < 0.05$) was determined using the Student *t*-test and one- or two-way repeated-measures analyses of variance with one repeated factor followed by the Duncan test.

3. Results

3.1. Intrathecal *t*-BOOH and NaOCl Produced Transient Pain Behaviors. Intrathecal administration of *t*-BOOH (11 or 28 μ mol in 15 μ L) decreased the mechanical threshold in a dose-dependent manner (Figure 1(a)). The mechanical threshold started to decrease 10 min after the administration of 28 μ mol of *t*-BOOH, reached the lowest point (4.34 ± 0.13 on the von Frey scale) at 25 min, and recovered to near the baseline level at 55 min. The mechanical threshold after the administration of 11 μ mol of *t*-BOOH dropped to 4.77 ± 0.13 at 15 min after injection. Because, in a preliminary study, intrathecal administration of 55 μ mol of *t*-BOOH induced severe pain behaviors such as body twisting and squeaking right after administration, that dose was not tested further. The 5.5 μ mol dose of *t*-BOOH did not influence mechanical thresholds (data not shown).

Intrathecal administration of 134 μ mol of NaOCl significantly decreased the mechanical threshold between 25 min and 65 min after administration (Figure 1(a)). At 121 μ mol, NaOCl significantly decreased the mechanical threshold between 40 min (4.65 ± 0.13) and 50 min (4.69 ± 0.08).

The 100 μ mol dose of NaOCl did not have a hyperalgesic effect (data not shown), indicating that NaOCl induces hyperalgesia at a narrow range of doses.

The mechanical threshold observed with either *t*-BOOH at 28 μ mol or NaOCl at 134 μ mol was significantly lower than that observed with saline at 30 min after administration (Figure 1(b)). The administration of saline had no effect on mechanical thresholds. The areas of the paw that were the most sensitive to von Frey filaments were the base and proximal portions of the 3rd and 4th digits.

Intrathecal administration of H_2O_2 at 15, 44, or 74 μ mol did not affect the mechanical threshold until 90 min after administration. Because 148 μ mol of H_2O_2 produced serious side effects and death, doses over 148 μ mol were not tested.

Since intrathecal injection of H_2O_2 failed to produce pain behaviors in normal rats and since our recent study showed that NaOCl increases the excitability of SG neurons [17], the following experiments focused on the effects of the OH^\bullet donor *t*-BOOH on neuronal excitability.

3.2. *t*-BOOH Increased the Responsiveness of Neurons in the Spinal Dorsal Horn. Neurons in the spinal dorsal horn responded well to a variety of mechanical stimuli, including the stroking of the skin with a brush and repeated applications of von Frey filaments with weak (1 and 2 g) and strong (20 g) bending forces (Figure 2). Intrathecal *t*-BOOH was applied to a cotton ball around the electrode, and the cotton ball was kept in place until the end of experiment. After application of a *t*-BOOH dose of 1 μ mol in 10 μ L to the dorsal surface of the spinal cord, the rate of discharges of the seven WDR neurons in response to brushing and von Frey filaments started to increase by 30.0 ± 5.0 /min. The rate of discharges peaked at 60.0 ± 14.1 min after administration and returned to near the baseline level at 122.1 ± 32.1 min after administration.

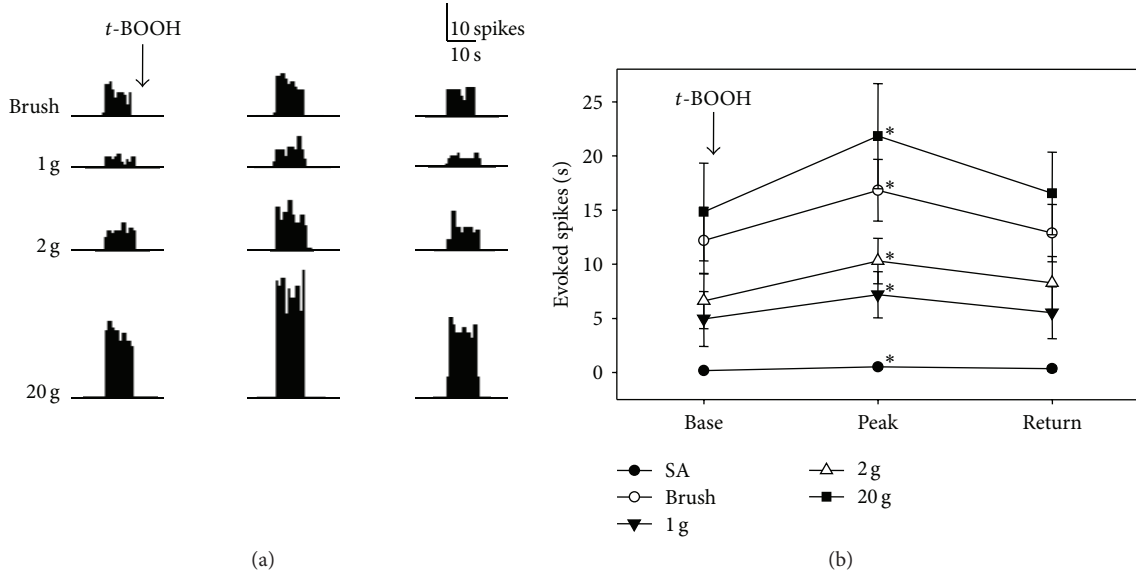


FIGURE 2: Effect of *t*-BOOH on WDR neuron activities in the spinal dorsal horn of normal rats. (a) The neurons responded well to a variety of mechanical stimuli applied to the receptive field before administration of *t*-BOOH (left column). After local application of $1 \mu\text{mol}$ of *t*-BOOH in $10 \mu\text{L}$ to the spinal cord without washout, the discharge rates started to increase, peaked by $60.0 (\pm 14.1)$ min (center column), and then returned to the baseline levels by $122.1 (\pm 32.1)$ min (right column). Stimulus duration is indicated by horizontal bars at the bottom. (b) Evoked responses of WDR neurons ($n = 7$) to various stimuli before and after *t*-BOOH application. Asterisks indicate values that are significantly different from the baseline values as determined by a one-way repeated-measures analysis of variance followed by the Duncan test ($P < 0.05$). The data are mean with standard errors of the mean.

(Figure 2(a)). After application of a *t*-BOOH dose of $10 \mu\text{mol}$ in $10 \mu\text{L}$ to the spinal cord, the rate of discharges of the WDR neurons in response to brushing and von Frey filaments started to dramatically increase by 30 min. At the same time, there was a sudden onset of discharges from the other WDR neurons. Therefore, the $10 \mu\text{mol}$ dose of *t*-BOOH was not used subsequently. Figure 2(b) shows the discharge rates after application of $1 \mu\text{mol}$ of *t*-BOOH. The peak discharge rates after treatment with *t*-BOOH increased by approximately 180% from baseline (183% for brushing, 180% for 1g, 185% for 2g, and 171% for 20g).

3.3. *t*-BOOH Increased the Excitability of SG Neurons in Spinal Cord Slices. Because the SG is a major termination site for unmyelinated afferents and plays an important role in pain mechanisms [18], we obtained whole-cell patch clamp recordings to investigate whether *t*-BOOH could change the excitability of SG neurons in spinal cord slices. Only SG neurons with a resting membrane potential more negative than -50 mV were examined. The resting membrane potential was -56.0 ± 1.1 mV ($n = 26$). When the cell was held at -60 mV, the application of *t*-BOOH (2 mM) for 7 min induced a 3.1 ± 0.5 mV depolarization, which was maintained for up to about 30 min after washout and which then recovered to baseline (Figure 3(a)). For measurement of spontaneous EPSPs of SG neurons, the baseline (control) was recorded for at least 10 min in ACSF after the whole-cell recording configuration, and the samples were superfused with *t*-BOOH (2 mM in the ACSF solution) for 7 min and then washed out for 15 min. Superfusion with *t*-BOOH significantly increased

EPSP frequency (1.1 ± 0.3 versus 0.3 ± 0.1 Hz, $P < 0.05$) and amplitude (2.1 ± 0.2 versus 1.8 ± 0.1 mV, $P < 0.05$) ($n = 26$) over the baseline (Figure 3). These data suggest that an increase in the level of hydroxyl radicals in the SG neurons affected both presynaptic and postsynaptic mechanisms of excitatory transmission in the rats.

Based on action potential (AP) discharge patterns elicited by injections of a current into a cell, SG neurons are classified as (i) AFNs, in which the frequency of an action potential is decreased during membrane depolarization; (ii) TFNs, in which a repetitive action potential is sustained during membrane depolarization; and (iii) delayed-firing neurons (DFN) with delayed-firing onset, as observed previously [19–21]. In preliminary study to determine the threshold at which a current generates an action potential in SG neurons, we stimulated neurons with depolarizing pulses using 2 to 50 pA in increments of 2 pA. An action potential was produced by current pulses of 25.7 ± 2.9 pA and 25.1 ± 4.1 pA in AFNs ($n = 10$) and TFNs ($n = 9$), respectively (data not shown). There was no statistically significant difference in the threshold current of AP generation between AFNs and TFNs. We therefore used two currents, 25 and 50 pA, to compare the numbers of action potentials before and after the application of *t*-BOOH. Mean input resistance was 660 ± 67 M Ω ($n = 26$). In AFNs ($n = 14$), the number of action potentials after the application of *t*-BOOH did not differ from the number before *t*-BOOH treatment (Figures 4(a) and 4(c)). In contrast, after treatment with *t*-BOOH, TFNs ($n = 12$) had significant increases in the frequencies of action potentials: from $6.3 \pm 1.8/\text{s}$ to $7.9 \pm 2.1/\text{s}$ and from $16.2 \pm 2.5/\text{s}$ to $18.4 \pm 2.6/\text{s}$ for

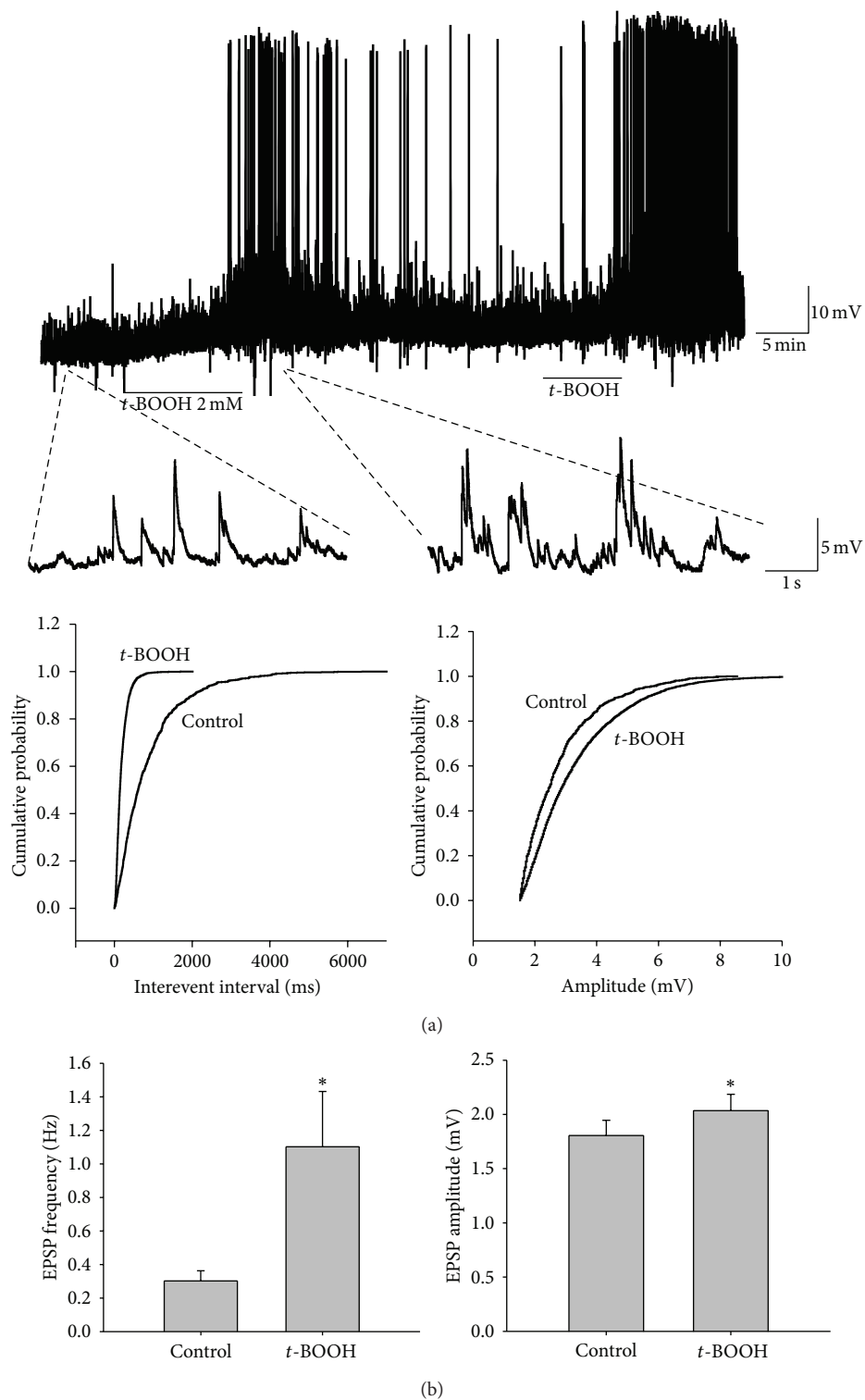


FIGURE 3: Effects of *t*-BOOH on membrane potential and EPSP in a patch clamp recording of SG neurons. (a) Original amplitude traces of EPSP in an SG neuron show that *t*-BOOH (2 mM, 7 min) increased the amplitude and frequency of EPSPs. The lower traces show EPSP at an expanded time scale. Normalized cumulative distribution analysis of EPSP amplitude and frequency (lower panels) showed that *t*-BOOH caused a significant shift toward higher frequency (left) and amplitude (right) in the neuron. (b) Average EPSP frequency (left) and amplitude (right). After application of *t*-BOOH, both the frequency and the amplitude increased significantly ($P < 0.05$, asterisks) from pre-*t*-BOOH levels as determined by a paired *t*-test. The data are mean with standard errors of the mean.

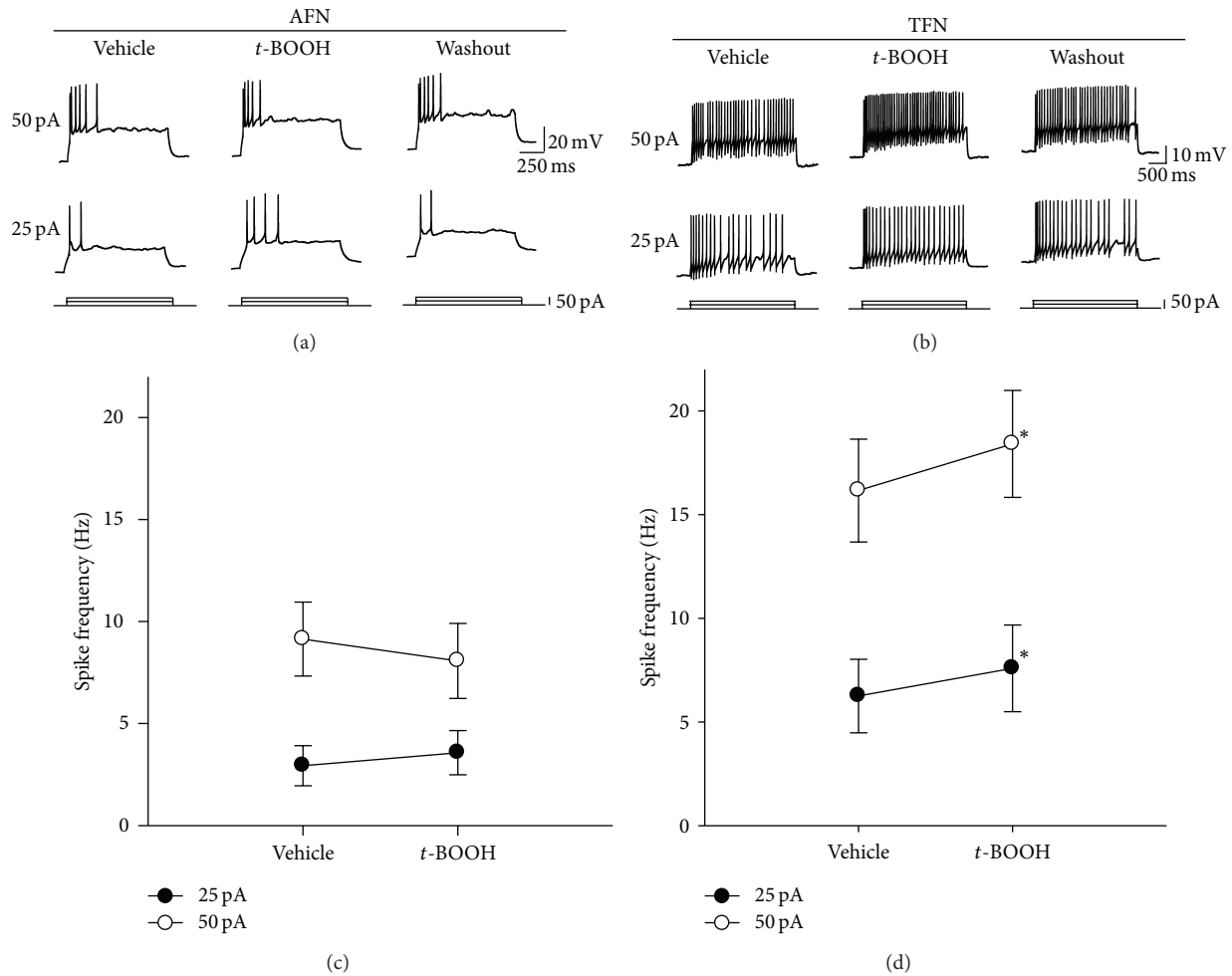


FIGURE 4: Effects of *t*-BOOH on the excitability of SG neurons in spinal cord slices. (a) Recordings of action potentials generated in an AFN. Action potentials were evoked by direct intracellular injections of current pulses (25 or 50 pA). (b) Changes in the frequency of action potential in a TFN. After *t*-BOOH treatment, the frequency of action potentials increased, compared to that observed with the vehicle treatment. (c) Average action potential firing rate measured by step current pulses after *t*-BOOH treatment in AFNs ($n = 14$). The data are mean with standard errors of the mean. (d) Average action potential firing rate measured by step current pulses after *t*-BOOH treatment in TFNs ($n = 12$). Asterisks indicate values that are significantly different from those for the vehicle control as determined by a paired *t*-test ($P < 0.05$).

current pulses of 25 and 50 pA, respectively (Figures 4(b) and 4(d)), indicating that *t*-BOOH increased the excitability of TFNs but not AFNs.

4. Discussion

This study showed that intrathecal administration of ROS donors *t*-BOOH (an OH^\bullet donor) and NaOCl (an OCl^- donor) but not H_2O_2 induced mechanical hyperalgesia of the hind paw in a dose-dependent manner in rats. Increased responses of WDR neurons to mechanical stimuli were also seen after application of *t*-BOOH to the spinal cord. In whole-cell patch clamp recordings of spinal dorsal horn neurons, application of *t*-BOOH depolarized membrane potential and increased the frequency of action potential evoked by injection of a current. These results suggest that increases in the superoxide intermediates OH^\bullet and OCl^- sensitize dorsal

horn neurons and thereby produce hyperalgesia in normal rats.

ROS play a critical role in normal physiological functions and various pathological conditions [2]. The many types of ROS include $\text{O}_2^{\bullet-}$, OH^\bullet , H_2O_2 , OCl^- , NO, and peroxynitrite [2, 3]. These ROS have been linked to pathological conditions, including pain. Recently, many ROS scavengers have been shown to induce analgesic effects for neuropathic and inflammatory pain. In several rat models of pain, tirilazad [22], superoxide dismutase mimetics [5], phenyl-N-*tert*-butylnitron [6, 7], 5,5-dimethyl-1-pyrroline-N-oxide [6], and vitamin E [8] reduced hyperalgesic behaviors, mainly through the action on the spinal cord [6, 8]. Those findings suggest that free radicals in the spinal cord are critically involved in neuropathic and inflammatory pain. However, it is still unclear which types of ROS in the spinal cord are critical for production of pain behaviors.

Superoxide radicals ($O_2^{\bullet-}$), a primary ROS formed in cells, facilitate OH^{\bullet} production by reacting H_2O_2 with intracellular iron (i.e., Fenton reaction). t -BOOH, a donor of OH^{\bullet} , has been used widely in oxidative stress experiments because it easily penetrates the cell membrane, breaks down to produce ROS as a simple chemical reaction, and is further decomposed into OH^{\bullet} by increasing the level of free iron in cells [23–25]. t -BOOH induces spinal long-term potentiation in superficial cord slices, and this long-term potentiation is maintained for 20–30 min after t -BOOH is washed out, suggesting the involvement of OH^{\bullet} [11]. t -BOOH decreases the frequency of inhibitory postsynaptic currents (IPSCs) without affecting the amplitude of IPSCs [26]. The development of hyperalgesia and enhanced sensitivity of spinal WDR neurons after treatment with t -BOOH in our study may have been due to a reduction of inhibitory neurotransmission stemming from an increase of OH^{\bullet} in the spinal cord.

NaOCl, used as a donor of hypochlorite in this study, hydrolyzes to hypochlorous acid (HOCl) in the solution. HOCl can be naturally produced by chloride ions and H_2O_2 in the presence of myeloperoxidase. As microglia, monocytes/macrophages, and neutrophils are a major source for myeloperoxidase [27–29], HOCl can be produced in the nervous tissue. HOCl crosses the plasma membrane, inactivates intracellular enzymes, inhibits mitochondrial respiration, and rapidly oxidizes intracellular glutathione [30–33]. In addition, HOCl can react with a wide range of functional groups, such as thiol, thioether, amino, and heme groups [34, 35]. It can also generate highly reactive singlets and hydroxyl radicals with H_2O_2 and $O_2^{\bullet-}$ [36, 37]. Moreover, HOCl can react with nitrite, the major end-product of nitric oxide, to form highly reactive nitryl chloride [38]. A previous study showed that hypochlorite (OCl^-) activates calcium influx and membrane currents via mediation of TRPA1 (transient receptor potential cation A1) channels, contributing to pain behaviors [39]. In the present study, intrathecal injection of NaOCl decreased mechanical thresholds of hind paws. Therefore, induction of hyperalgesia by intrathecal NaOCl is likely caused by activation of sensory neurons in the spinal dorsal horn or conversion of NaOCl into reactive radicals, such as OH^{\bullet} .

In our *in vivo* extracellular recordings, the evoked responses of WDR neurons in the spinal dorsal horn were greatly enhanced by t -BOOH treatment, with responses eventually returning to baseline levels. Whole-cell patch clamp recordings revealed that treatment with t -BOOH enhanced the excitability of spinal dorsal horn neurons, depolarized the membrane potential of SG neurons, and increased the amplitude and frequency of EPSPs. The EPSP changes in SG neurons began within 2–3 min after application of t -BOOH and were maintained for up to 5–30 min after washout. These findings suggest that increased ROS, particularly OH^{\bullet} , in the spinal cord critically contribute to central sensitization via modulation of excitatory neurotransmission.

The functional roles of H_2O_2 have been studied extensively in various brain regions. In the brain, H_2O_2 influences neuronal excitability by modulating synaptic transmission and the activation of various ion channels. H_2O_2 induces hyperexcitability in thalamic neurons by altering the

balance between excitatory and inhibitory synapses [40]. It also produces hyperexcitability by activating the N-methyl-D-aspartate receptor [41] and by increasing extracellular glutamate [42, 43] in hippocampal or cortical neurons. In addition, H_2O_2 induces membrane depolarization and increases excitability in medium spiny neurons via activation of transient receptor potential channels [44]. In contrast, few studies have examined the role of H_2O_2 in spinal dorsal horn neurons in development of hyperalgesia. One study showed that when injected into the plantar surface of hind paws in mice, H_2O_2 induced thermal or mechanical hyperalgesia in a dose-dependent manner [45]. In another study, Takahashi et al. [46] reported that H_2O_2 increased the frequency of GABAergic miniature inhibitory postsynaptic currents in SG neurons, thereby leading to antihyperalgesia. In the present study, spinal injection of H_2O_2 failed to induce hyperalgesia or pain behaviors. Taken together, these findings suggest that H_2O_2 in spinal dorsal horn neuron may not participate directly in generation of hyperalgesia.

The recorded SG neurons were classified as AFNs or TFNs, based on their intrinsic firing properties evoked by intracellular current injection [19, 20]. AFNs generate short burst of spikes at the beginning of depolarization and most of them are physiologically classified as nociceptive neuron. TFNs exhibit repetitive spike firing and little adaptation during sustained depolarization and majority of them are shown to be wide dynamic range (WDR) or nociceptive neurons [20]. Superfusion of t -BOOH increased the firing frequency of TFNs but not AFNs in our study, indicating that t -BOOH treatment increased the excitability of WDR or nociceptive neurons. In combination with the data from our *in vivo* extracellular recordings showing that intrathecal administration of t -BOOH caused enhanced excitability of WDR neurons in normal rats, the results suggest that ROS, particularly OH^{\bullet} , generate hyperalgesia by acting on TFNs or other WDR neurons.

5. Conclusion

Intrathecal administration of the ROS donors t -BOOH and NaOCl significantly decreased the mechanical thresholds of pain behaviors and increased the responses of WDR neurons in the spinal dorsal horn to mechanical stimuli in normal rats. t -BOOH also increased the membrane excitability of SG neurons in spinal cord slices. Our findings indicate that ROS, particularly OH^{\bullet} , play an important role in the development of pain and the process of central sensitization in the spinal cord. Reducing the levels of ROS in the spinal cord may therefore be an effective way to treat pain.

Conflict of Interests

The authors declare that there is no conflict of interests regarding the publication of this paper.

Authors' Contribution

Hee Young Kim and Inhyung Lee contributed equally to this paper.

Acknowledgments

This work was supported by NIH Grant R01 NS031680 and by Grants 2014R1A2A1A11053104 and 2012R1A5A2A42671316 from the National Research Foundation of Korea. The authors thank The Department of Scientific Publications at MD Anderson Cancer Center for editorial services and English services.

References

- [1] P. Maher and D. Schubert, "Signaling by reactive oxygen species in the nervous system," *Cellular and Molecular Life Sciences*, vol. 57, no. 8-9, pp. 1287-1305, 2000.
- [2] M. Valko, D. Leibfritz, J. Moncol, M. T. D. Cronin, M. Mazur, and J. Telser, "Free radicals and antioxidants in normal physiological functions and human disease," *International Journal of Biochemistry & Cell Biology*, vol. 39, no. 1, pp. 44-84, 2007.
- [3] D. Salvemini, T. M. Doyle, and S. Cuzzocrea, "Superoxide, peroxynitrite and oxidative/nitrative stress in inflammation," *Biochemical Society Transactions*, vol. 34, no. 5, pp. 965-970, 2006.
- [4] M. Antolovich, P. D. Prenzler, E. Patsalides, S. McDonald, and K. Robards, "Methods for testing antioxidant activity," *The Analyst*, vol. 127, no. 1, pp. 183-198, 2002.
- [5] Z.-Q. Wang, F. Porreca, S. Cuzzocrea et al., "A newly identified role for superoxide in inflammatory pain," *Journal of Pharmacology and Experimental Therapeutics*, vol. 309, no. 3, pp. 869-878, 2004.
- [6] H. K. Kim, S. K. Park, J.-L. Zhou et al., "Reactive oxygen species (ROS) play an important role in a rat model of neuropathic pain," *Pain*, vol. 111, no. 1-2, pp. 116-124, 2004.
- [7] I. Lee, H. K. Kim, J. H. Kim, K. Chung, and J. M. Chung, "The role of reactive oxygen species in capsaicin-induced mechanical hyperalgesia and in the activities of dorsal horn neurons," *Pain*, vol. 133, no. 1-3, pp. 9-17, 2007.
- [8] H. K. Kim, J. H. Kim, X. Gao et al., "Analgesic effect of vitamin E is mediated by reducing central sensitization in neuropathic pain," *Pain*, vol. 122, no. 1-2, pp. 53-62, 2006.
- [9] E. S. Schwartz, I. Lee, K. Chung, and J. M. Chung, "Oxidative stress in the spinal cord is an important contributor in capsaicin-induced mechanical secondary hyperalgesia in mice," *Pain*, vol. 138, no. 3, pp. 514-524, 2008.
- [10] E.-S. Park, X. Gao, J. M. Chung, and K. Chung, "Levels of mitochondrial reactive oxygen species increase in rat neuropathic spinal dorsal horn neurons," *Neuroscience Letters*, vol. 391, no. 3, pp. 108-111, 2006.
- [11] K. Y. Lee, K. Chung, and J. M. Chung, "Involvement of reactive oxygen species in long-term potentiation in the spinal cord dorsal horn," *Journal of Neurophysiology*, vol. 103, no. 1, pp. 382-391, 2010.
- [12] E. S. Schwartz, Y. K. Hee, J. Wang et al., "Persistent pain is dependent on spinal mitochondrial antioxidant levels," *The Journal of Neuroscience*, vol. 29, no. 1, pp. 159-168, 2009.
- [13] G. D. Mao and M. J. Poznansky, "Electron spin resonance study on the permeability of superoxide radicals in lipid bilayers and biological membranes," *FEBS Letters*, vol. 305, no. 3, pp. 233-236, 1992.
- [14] A. U. Khan and T. Wilson, "Reactive oxygen species as cellular messengers," *Chemistry & Biology*, vol. 2, no. 7, pp. 437-445, 1995.
- [15] S. R. Chaplan, F. W. Bach, J. W. Pogrel, J. M. Chung, and T. L. Yaksh, "Quantitative assessment of tactile allodynia in the rat paw," *Journal of Neuroscience Methods*, vol. 53, no. 1, pp. 55-63, 1994.
- [16] W. J. Dixon, "Efficient analysis of experimental observations," *Annual Review of Pharmacology and Toxicology*, vol. 20, pp. 441-462, 1980.
- [17] H. I. Lee, A. Park, and S. W. Chun, "Effects of NaOCl on neuronal excitability and intracellular calcium concentration in rat spinal substantia gelatinosa neurons," *International Journal of Oral Biology*, vol. 38, no. 1, pp. 5-12, 2013.
- [18] W. D. Willis Jr. and R. E. Coggeshall, *Sensory Mechanisms of the Spinal Cord: Volume 2: Ascending Sensory Tracts and Their Descending Control*, Springer Science & Business Media, 2004.
- [19] T. J. Grudt and E. R. Perl, "Correlations between neuronal morphology and electro-physiological features in the rodent superficial dorsal horn," *The Journal of Physiology*, vol. 540, no. 1, pp. 189-207, 2002.
- [20] J. A. Lopez-Garcia and A. E. King, "Membrane properties of physiologically classified rat dorsal horn neurons in vitro: correlation with cutaneous sensory afferent input," *The European Journal of Neuroscience*, vol. 6, no. 6, pp. 998-1007, 1994.
- [21] S. F. A. Santos, I. V. Melnick, and B. V. Safronov, "Selective postsynaptic inhibition of tonic-firing neurons in substantia gelatinosa by μ -opioid agonist," *Anesthesiology*, vol. 101, no. 5, pp. 1177-1183, 2004.
- [22] Z. Khalil, T. Liu, and R. D. Helme, "Free radicals contribute to the reduction in peripheral vascular responses and the maintenance of thermal hyperalgesia in rats with chronic constriction injury," *Pain*, vol. 79, no. 1, pp. 31-37, 1999.
- [23] J. D. Adams Jr., B. Wang, L. K. Klaidman, C. P. LeBel, I. N. Odunze, and D. Shah, "New aspects of brain oxidative stress induced by tert-butylhydroperoxide," *Free Radical Biology & Medicine*, vol. 15, no. 2, pp. 195-202, 1993.
- [24] G. Minotti, "tert-butyl hydroperoxide-dependent microsomal release of iron and lipid peroxidation. II. Evidence for the involvement of nonheme, nonferritin iron in lipid peroxidation," *Archives of Biochemistry and Biophysics*, vol. 273, no. 1, pp. 144-147, 1989.
- [25] D. L. Tribble, D. P. Jones, and D. E. Edmondson, "Effect of hypoxia on tert-butylhydroperoxide-induced oxidative injury in hepatocytes," *Molecular Pharmacology*, vol. 34, no. 3, pp. 413-420, 1988.
- [26] J. Yowtak, K. Y. Lee, H. Y. Kim et al., "Reactive oxygen species contribute to neuropathic pain by reducing spinal GABA release," *Pain*, vol. 152, no. 4, pp. 844-852, 2011.
- [27] R. M. Nagra, B. Becher, W. W. Tourtellotte et al., "Immunohistochemical and genetic evidence of myeloperoxidase involvement in multiple sclerosis," *Journal of Neuroimmunology*, vol. 78, no. 1-2, pp. 97-107, 1997.
- [28] A. Daugherty, J. L. Dunn, D. L. Rateri, and J. W. Heinicke, "Myeloperoxidase, a catalyst for lipoprotein oxidation, is expressed in human atherosclerotic lesions," *The Journal of Clinical Investigation*, vol. 94, no. 1, pp. 437-444, 1994.
- [29] W. B. Dunn, J. H. Hardin, and S. S. Spicer, "Ultrastructural localization of myeloperoxidase in human neutrophil and rabbit heterophil and eosinophil leukocytes," *Blood*, vol. 32, no. 6, pp. 935-944, 1968.
- [30] D. W. Eley, J. M. Eley, B. Korecky, and H. Fliss, "Impairment of cardiac contractility and sarcoplasmic reticulum Ca^{2+} ATPase

- activity by hypochlorous acid: reversal by dithiothreitol," *Canadian Journal of Physiology and Pharmacology*, vol. 69, no. 11, pp. 1677–1685, 1991.
- [31] J. M. Pullar, C. C. Winterbourn, and M. C. M. Vissers, "Loss of GSH and thiol enzymes in endothelial cells exposed to sublethal concentrations of hypochlorous acid," *The American Journal of Physiology: Heart and Circulatory Physiology*, vol. 277, no. 4, pp. H1505–H1512, 1999.
- [32] I. U. Schraufstatter, K. Browne, A. Harris et al., "Mechanisms of hypochlorite injury of target cells," *The Journal of Clinical Investigation*, vol. 85, no. 2, pp. 554–562, 1990.
- [33] M. C. M. Vissers and C. C. Winterbourn, "Oxidation of intracellular glutathione after exposure of human red blood cells to hypochlorous acid," *Biochemical Journal*, vol. 307, no. 1, pp. 57–62, 1995.
- [34] J. M. Albrich, C. A. McCarthy, and J. K. Hurst, "Biological reactivity of hypochlorous acid: implications for microbicidal mechanisms of leukocyte myeloperoxidase," *Proceedings of the National Academy of Sciences of the United States of America*, vol. 78, no. 1, pp. 210–214, 1981.
- [35] C. C. Winterbourn, "Comparative reactivities of various biological compounds with myeloperoxidase-hydrogen peroxide-chloride, and similarity of the oxidant to hypochlorite," *Biochimica et Biophysica Acta—General Subjects*, vol. 840, no. 2, pp. 204–210, 1985.
- [36] S. J. Weiss, "Tissue destruction by neutrophils," *The New England Journal of Medicine*, vol. 320, no. 6, pp. 365–376, 1989.
- [37] L. P. Candeias, K. B. Patel, M. R. L. Stratford, and P. Wardman, "Free hydroxyl radicals are formed on reaction between the neutrophil-derived species superoxide anion and hypochlorous acid," *FEBS Letters*, vol. 333, no. 1-2, pp. 151–153, 1993.
- [38] J. P. Eiserich, C. E. Cross, A. Daniel Jones, B. Halliwell, and A. Van der Vliet, "Formation of nitrating and chlorinating species by reaction of nitrite with hypochlorous acid. A novel mechanism for nitric oxide-mediated protein modification," *The Journal of Biological Chemistry*, vol. 271, no. 32, pp. 19199–19208, 1996.
- [39] B. F. Bessac, M. Sivula, C. A. von Hehn, J. Escalera, L. Cohn, and S.-E. Jordt, "TRPA1 is a major oxidant sensor in murine airway sensory neurons," *The Journal of Clinical Investigation*, vol. 118, no. 5, pp. 1899–1910, 2008.
- [40] M. V. Frantseva, J. L. P. Velazquez, and P. L. Carlen, "Changes in membrane and synaptic properties of thalamocortical circuitry caused by hydrogen peroxide," *Journal of Neurophysiology*, vol. 80, no. 3, pp. 1317–1326, 1998.
- [41] M. V. Avshalumov and M. E. Rice, "NMDA receptor activation mediates hydrogen peroxide-induced pathophysiology in rat hippocampal slices," *Journal of Neurophysiology*, vol. 87, no. 6, pp. 2896–2903, 2002.
- [42] P. Saransaari and S. S. Oja, "Release of endogenous glutamate, aspartate, GABA, and taurine from hippocampal slices from adult and developing mice under cell-damaging conditions," *Neurochemical Research*, vol. 23, no. 4, pp. 563–570, 1998.
- [43] F. Mailly, P. Marin, M. Israël, J. Glowinski, and J. Prémont, "Increase in external glutamate and NMDA receptor activation contribute to H_2O_2 -induced neuronal apoptosis," *Journal of Neurochemistry*, vol. 73, no. 3, pp. 1181–1188, 1999.
- [44] L. Bao, M. V. Avshalumov, and M. E. Rice, "Partial mitochondrial inhibition causes striatal dopamine release suppression and medium spiny neuron depolarization via H_2O_2 elevation, not ATP depletion," *The Journal of Neuroscience*, vol. 25, no. 43, pp. 10029–10040, 2005.
- [45] J. E. Keeble, J. V. Bodkin, L. Liang et al., "Hydrogen peroxide is a novel mediator of inflammatory hyperalgesia, acting via transient receptor potential vanilloid 1-dependent and independent mechanisms," *Pain*, vol. 141, no. 1-2, pp. 135–142, 2009.
- [46] A. Takahashi, M. Mikami, and J. Yang, "Hydrogen peroxide increases GABAergic mIPSC through presynaptic release of calcium from IP3 receptor-sensitive stores in spinal cord substantia gelatinosa neurons," *The European Journal of Neuroscience*, vol. 25, no. 3, pp. 705–716, 2007.

Research Article

Modulation of Spinal GABAergic Inhibition and Mechanical Hypersensitivity following Chronic Compression of Dorsal Root Ganglion in the Rat

Moon Chul Lee,¹ Taick Sang Nam,¹ Se Jung Jung,¹ Young S. Gwak,² and Joong Woo Leem¹

¹Department of Physiology, Yonsei University College of Medicine, 50 Yonsei-ro, Seodaemun-gu, Seoul 120-752, Republic of Korea

²Department of Physiology, Daegu Haany University, 136 Shincheondong-ro, Daegu 706-828, Republic of Korea

Correspondence should be addressed to Young S. Gwak; ysgwak@dhu.ac.kr and Joong Woo Leem; jwleem@yuhs.ac

Received 7 January 2015; Accepted 9 April 2015

Academic Editor: Yong Jeong

Copyright © 2015 Moon Chul Lee et al. This is an open access article distributed under the Creative Commons Attribution License, which permits unrestricted use, distribution, and reproduction in any medium, provided the original work is properly cited.

Chronic compression of dorsal root ganglion (CCD) results in neuropathic pain. We investigated the role of spinal GABA in CCD-induced pain using rats with unilateral CCD. A stereological analysis revealed that the proportion of GABA-immunoreactive neurons to total neurons at L4/5 laminae I–III on the injured side decreased in the early phase of CCD (post-CCD week 1) and then returned to the sham-control level in the late phase (post-CCD week 18). In the early phase, the rats showed an increase in both mechanical sensitivity of the hind paw and spinal WDR neuronal excitability on the injured side, and such increase was suppressed by spinally applied muscimol (GABA-A agonist, 5 nmol) and baclofen (GABA-B agonist, 25 nmol), indicating the reduced spinal GABAergic inhibition involved. In the late phase, the CCD-induced increase in mechanical sensitivity and neuronal excitability returned to pre-CCD levels, and such recovered responses were enhanced by spinally applied bicuculline (GABA-A antagonist, 15 nmol) and CGP52432 (GABA-B antagonist, 15 nmol), indicating the regained spinal GABAergic inhibition involved. In conclusion, the alteration of spinal GABAergic inhibition following CCD and leading to a gradual reduction over time of CCD-induced mechanical hypersensitivity is most likely due to changes in GABA content in spinal GABA neurons.

1. Introduction

Neuropathic pain caused by diseases or injury involving the peripheral or central nervous system has characteristic symptoms of spontaneous burning pain, allodynia (non-painful becomes painful), and hyperalgesia (painful becomes increasingly painful) [1]. Clinical reports have indicated that more than 60% of neuropathic pain patients were associated with spinal abnormalities including spinal infections and tumors, as well as structural changes of spinal vertebra, such as spinal disc herniation, spinal stenosis, and intervertebral foramen stenosis [2]. Compression of a spinal nerve induced by structural changes of spinal vertebra leads to radicular or low back pain that originates from the lower back and radiates down to the back of the leg and the foot [3]. In addition, about 40% of chronic low back pain patients are

shown to have neuropathic pain [4]. Thus, it is possible that peripheral neuropathic pain and radicular pain share a common underlying mechanism.

A rat model of radicular pain that has been developed by chronic compression of the dorsal root ganglion (CCD) demonstrates behavioral signs of neuropathic pain such as mechanical allodynia, hyperalgesia, and enhanced excitability of dorsal root ganglion (DRG) neurons [5–7]. The massive impulses that originate from injured DRG neurons to the spinal cord contribute to altered spinal synaptic plasticity or central sensitization known as the neural mechanisms of hyperalgesia and allodynia. One of the speculated aspects of the underlying mechanisms in spinal central sensitization is the decrease of spinal GABAergic inhibition, or spinal GABAergic disinhibition, caused by the impairment of GABAergic inhibition in the spinal cord. Although this spinal

GABAergic disinhibition in neuropathic pain behaviors following peripheral nerve injury has previously been studied, different results are reported. The cell deaths of spinal GABA neurons were observed after injury [8–10]. However, no loss of spinal GABA neurons after injury was detected [11–13]. In addition, an increased GABA level in the spinal dorsal horn was found after injury [14].

The involvement of spinal GABAergic disinhibition in CCD-induced neuropathic pain has not been well studied. The CCD injury model revealed that a gradual recovery of neuropathic pain behavior occurs over time [15]. Thus, one way to verify a spinal GABA involvement in the CCD model is to examine the changes of spinal GABAergic inhibition, which depends on GABA levels and GABA receptor activity, both in the early and later phases following CCD. In the present study, we have investigated first whether the change in the number of GABA neurons as compared with the total neurons in the lumbar spinal dorsal horn does exist following CCD. Second, we have determined the effects of pharmacological activation of spinal GABA receptors on established mechanical hypersensitivity in the early phase, as well as the effects of inhibition of spinal GABA receptors on the reduced hypersensitivity in the later phase.

2. Materials and Methods

2.1. Animals and Surgery for CCD. A total of 83 male rats (Sprague-Dawley, 180–200 g, Korea) were used in this study and housed at an animal facility with autocontrolled temperature, humidity, and light-dark cycles of 12 hours. All experimental procedures were performed according to the NIH and the Institutional Animal Care and Use Committee of Yonsei University College of Medicine. Chronic compression of the fifth lumbar DRG was performed as previously described [5]. Under deep anesthesia (enflurane, induction 5% and maintenance 2% in mixed oxygen gas), the back skin and muscle were incised to expose the lumbar fifth vertebra and intervertebral foramina. To compress the L5 DRG and nerve root, a sterilized stainless steel rod (0.7 mm diameter and 4 mm length) was inserted in the space of the fifth intervertebral foramen. After injury, the musculature and skin were sutured. A sham operation was performed according to the same procedures; however, the stainless steel rod was not inserted. The postsurgical care was performed with food and water *ad libitum*. Animals were allocated into four groups: those that had received CCD injury ($n = 26$) or sham operation ($n = 26$) 18 weeks earlier and those with CCD one week ($n = 26$) or 8 weeks ($n = 5$) earlier. The sham-operated, 1-week, and 18-week post-CCD groups were subjected to studies of pharmacological responses to GABA-related drugs, in which saline-treated controls were used for stereological cell counting and electrophysiological recordings. The 8-week post-CCD group included animals used for stereological cell counting. All experiments were performed by investigators blinded to animal treatments.

2.2. Drugs and Application. The effects of pharmacological activation and inhibition of spinal GABA receptors on

mechanical sensitivity and WDR neuronal activity were examined using drugs including GABA-A receptor agonist muscimol (Tocris Cookson, UK) and antagonist (–)-bicuculline methobromide (Tocris Cookson, UK) as well as GABA-B receptor agonist baclofen (Sigma, Saint Louis, MO, USA) and antagonist CGP52432 (Tocris Cookson, UK). The drugs and doses were selected according to previous studies [16–18]. All drugs were dissolved in 0.9% saline and administered intrathecally using a lumbar puncture for studying mechanical sensitivity changes via behavioral assessment; alternatively, drugs were also applied topically on the spinal cord for examining neuronal activity changes via electrophysiological assessment. For intrathecal administration by lumbar puncture, a 26-gauge needle attached to a Hamilton syringe was inserted into the groove between the T13 and L1 vertebrae and carefully advanced into the intervertebral space, with the angle of the needle at about 10 degrees. Proper placement of the needle in the lumbar subarachnoid space was confirmed at the time of entry by a sudden loss of resistance and a brief twitch of the muscles of the hip and thigh. Each drug in a volume of 10 μ L was administered slowly over a 30-second period. For topical application, drugs (10 μ L) were applied using a Hamilton syringe onto the spinal cord surface near the site where the recording electrode was located. Data were collected at 15 min after drug application, as this time point was empirically determined to be the best for testing during the period of drug efficacy (typically 5–50 min).

2.3. GABA Immunohistochemistry. Under deep anesthesia (urethane, 12.5 mg/kg, i.p.), animals were perfused transcardially with heparinized solution-A (50 mM cacodylate acid and 1% sodium metabisulfite), followed by solution-B (100 mM cacodylate acid, 2.5% glutaraldehyde and 1% sodium metabisulfite). After spinal laminectomy, the L4-L5 spinal cord was dissected out, followed by postfixation for 2 h at room temperature. With the L4-L5 spinal cord blocks, transverse sections (40 μ m thick) were cut using a Vibratome (VT1000M, Leica, Germany). Two consecutive sections were collected every 15 sections into 24-well plates containing solution-C (50 mM Tris and 1% sodium metabisulfite) for GABA and NeuN immunostaining. In brief, free-floating sections were pretreated in 49% solution-C, 50% methanol, and 1% H_2O_2 for 15 min, and then washed in solution-C (3×5 min) and blocked in 98% solution-C and 2% normal goat serum for 3 h. Sections were incubated with anti-GABA (1:100, AB131, Millipore, Billerica, MA, USA) or anti-NeuN (1:400, MAB377, Millipore, Billerica, MA, USA) in a blocking solution for 16 h at 4°C, and then washed in solution-D (50 mM Tris and 145 mM sodium chloride, 3×5 min). Sections were then incubated with biotinylated goat anti-mouse IgG (1:200) for 1 h. After washing in solution-D (3×5 min), sections were incubated with an avidin-biotin peroxidase complex (1:200) for 1 h and washed in solution-D (3×5 min). For visualization, sections were incubated with DAB substrate kit solution (Invitrogen, Frederick, MD, USA) containing DAB and 0.6% H_2O_2 for 5 min, and then followed by dehydration using 80, 90, and 100% ethyl alcohol and

xylylene. Finally, sections were mounted on slides and fixed with permount mounting media (SP15-100 Toluene Solution UN1294, Fisher Scientific, El Paso, Texas, USA) under cover glasses.

2.4. Computer Assisted Stereological Analysis. The total number of GABA- and NeuN-immunoreactive (ir) cells was estimated from the immunostained sections (9–12 sections for each cell type) using Computer Assisted Stereological Toolbox (CAST), consisting of an imaging system (Olympus BX-51, Melville, NY, USA) and software (CAST grid version 2.3.1.5, Olympus, Albertslund, Denmark). For counting cells, a section superimposed by the grid moved in stepwise motion to grid intersections along the step length in both x -axis and y -axis ($92 \times 92 \mu\text{m}$) in laminae I–III so that a particular position of grid intersections was moved to the center of the field of view on a monitor. The section was then viewed under a 100x oil immersion objective on the monitor to set the counting frame, with its size being 20% of the area of the square with a side length of x -steps and y -steps. The thickness of each section was determined before counting proceeded, and counting was performed with the optical dissector through a $20 \mu\text{m}$ depth of a counting frame. Among cells that came into focus within the $20 \mu\text{m}$ height of the optical dissector, only cells inside the counting frame plus those that touched the left and bottom lines of the counting frame were included for cell counts. The estimation of the total number of cells in L4–L5 was performed using this formula: $N = \Sigma Q \times (1/\text{ASF}) \times (1/\text{SSF}) \times (1/\text{TSF})$, where N is the estimated total number of cells, ΣQ is the number of counted cells, ASF is the area sampling fraction (the area of the counting frame/the area of the sampling grid), SSF is the section sampling fraction (the number of sections sampled for analysis/the number of sections obtained for staining), and TSF is the thickness sampling fraction (the thickness of the counting frame/the thickness of the section) [19].

2.5. Behavioral Assessment. Each rat was housed and held 15 min in a transparent acryl box ($8 \times 8 \times 25 \text{ cm}$) on a metal mesh to avoid environmental stress. After accommodation, six applications of the von Frey filament (log unit 3.61–5.46, equivalent to 0.4–26.0 g, North Coast Medical, CA, USA) were applied at the center of the plantar surface of the hind paw; these tests measured paw withdrawal responses through the biting of the filaments, head turning, and changes of body posture. The paw withdrawal thresholds (PWTs) on filament application were determined by the modified up-down testing paradigm [20] using the formula: $\log(50\% \text{ threshold}) = Xf + \kappa\delta$, where Xf is the value of the final von Frey filament (log unit), κ represents the correction factors (from a calibration table), and δ represents the mean differences of log units between stimuli.

2.6. Electrophysiological Assessment. After anesthesia (urethane, 12.5 mg/kg, i.p.), a cannulation was performed for induction and maintenance of skeletal muscular relaxation, with a tracheostomy additionally performed for ventilation. The respiration of each rat was maintained by ventilator

(CWE Inc., Ardmore, PA, USA), and CO_2 levels monitored by CO_2 analyzer (CWE Inc., Ardmore, PA, USA) were held stable at 3.5%–4.5%. The body temperature of the rat was maintained at about 36–37°C with a thermal blanket. A laminectomy at T13–L2 was performed to expose the lumbar enlargement, and the rat was then fixed on a stereotaxic frame, with the exposed spinal cord covered by mineral oil to prevent dryness and electric insults from the environment. The dura matter, arachnoid membranes, and pia matter were removed. For recoding the neuronal activity, wide dynamic range (WDR) neurons in the L4–L5 spinal dorsal horns were chosen. The reason for this choice is due to the important role that the spinal WDR neurons are known to play in signaling sensory-discriminative components of pain [21, 22]. Furthermore, we have previously observed that there exists a correlation between spinal WDR neuronal responses and nociceptive behavior in a spinal cord injury model [17]. To examine the neuronal excitability, a single carbon filament-filled glass microelectrode (2–4 M Ω) was inserted into the dorsal horn (depths of 100–600 μm below the dorsal surface) using a micropositioner (Narishige, Tokyo, Japan). The characterization of WDR neurons was determined according to response patterns to brushing (using a camel-hair brush), pressing (using a large arterial clip, 100 g force, nonpainful), and pinching (using a small arterial clip, 400 g force, painful) stimuli. The single impulses generated from WDR neurons and evoked for 10 sec with each stimulation were amplified (DAM-80, World Precision Instruments, Sarasota, FL, USA), and these amplified signals were fed to an oscilloscope for monitoring as well as to the data acquisition system (CED 1401 plus, Cambridge Electronic Design, Cambridge, UK) for data analysis. The single impulses that were identical in shape and amplitude were collected using a window discriminator (World Precision Instruments, Sarasota, FL, USA), and the collected signals were analyzed with Spike 2 software (Version 5.0, Cambridge Electronic Design, Cambridge, UK). The total number of impulses evoked by each 10 s stimulus was used for data analysis.

2.7. Statistical Analysis. The differences of repeated measurements after a treatment from baseline were analyzed using the Friedman repeated measures ANOVA on ranks followed by Dunnett's test for multiple comparisons. For the comparison of two different groups, the Mann-Whitney rank-sum test for unmatched pairs was used. For the comparison of measurements before and after treatment, the Wilcoxon signed rank test for matched pairs was employed. Differences were considered statistically significant, if $P < 0.05$. Data were expressed as mean \pm SE.

3. Results

3.1. Time Course of Changes in Mechanical Sensitivity of the Hind Paw following CCD. One week after chronic compression of the fifth lumbar DRG (CCD), the paw withdrawal thresholds (PWTs) in the injured side of the hind paw were $2.23 \pm 0.21 \text{ g}$ and showed a significant decrease when compared with values of pre-CCD ($17.83 \pm 0.16 \text{ g}$; $P < 0.05$)

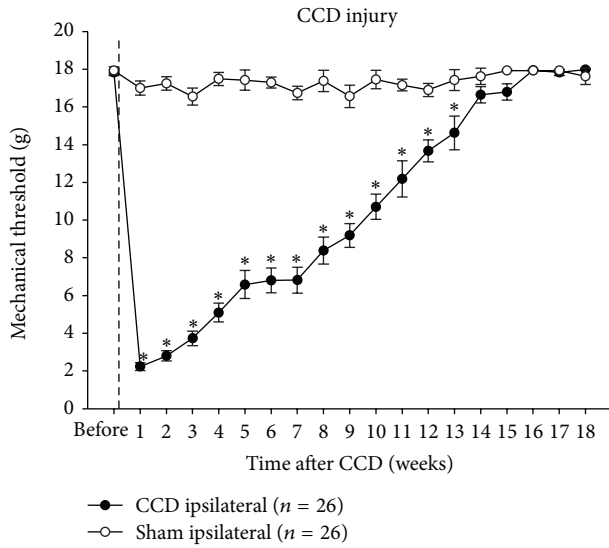


FIGURE 1: Changes in mechanical sensitivity of hind paws after CCD. A unilateral CCD led to mechanical hypersensitivity of the affected hind paw by showing decreased paw withdrawal thresholds. This hypersensitivity gradually returned to the normal level by post-CCD week 14. * $P < 0.05$ when compared with sham-operated rats.

and sham-operated groups (17 ± 0.37 g; $P < 0.05$). The decreased PWTs gradually recovered to the levels of pre-CCD or sham-operated groups after 14 weeks after the injury (Figure 1, $P > 0.05$). On the contralateral side of the hind paw in CCD groups, no significant changes in PWTs were observed (data not shown).

3.2. Changes in GABA-ir Cell Numbers in the Spinal Dorsal Horn following CCD. Figure 2 presents photographic images for GABA-ir and NeuN-ir immunohistochemistry in the lumbar dorsal horn. The square areas cover the lateral portions of laminae I–III on both sides of the spinal cord, shown in Figure 2(a). For 1-week and 8-week post-CCD groups, GABA-ir cells in ipsilateral laminae I–III appeared less dense than those for the sham-operated and 18-week post-CCD groups; however, no density differences in the contralateral laminae were observed among the four groups (Figure 2(b)). NeuN-ir cells on both sides of laminae showed no density differences among four groups. Typical GABA-ir and NeuN-ir cells are seen in insets at the lower right of each image (indicated by arrows).

To illustrate the stereological counting of GABA-ir and NeuN-ir cells, images at six consecutive focal planes from the top to the bottom of the dissector are shown in Figure 3(a). In the examples shown, the dissector for sham-operated group contained 5 GABA-ir and 9 NeuN-ir cells, and the dissector for the 1-week post-CCD group contained 3 GABA-ir and 10 NeuN-ir cells (indicated by arrows). Mean thicknesses of cord sections sampled for stereological counting (10 sections per a rat, five rats per each group) were 26.7, 27.2, 27.6, and 27.3 μ m for sham-operated, 1-week, 8-week, and 18-week post-CCD groups, respectively. The total number of cell counts in L4–L5 dorsal horn laminae I–III of each animal was estimated

according to the formula described in the Materials and Methods section, and mean values for the four experimental groups are presented in Figure 3(b). The total number of GABA-ir cells significantly decreased ($P < 0.05$) on the ipsilateral side to injury for both 1-week ($12,468 \pm 4,667$) and 8-week ($17,357 \pm 4,424$) post-CCD groups, compared with sham-operated groups ($28,159 \pm 2,763$), with no significant differences on the contralateral side among the four groups. For NeuN-positive cells, however, the total numbers did not show significant differences.

3.3. Effects of Activation or Deactivation of Spinal GABA Receptors on Mechanical Sensitivity. In sham-operated animals (Figure 4(a)), an intrathecal (i.t.) administration of bicuculline (15 nmol, $n = 8$) or CGP52432 (15 nmol, $n = 8$) reduced the PWTs maximally at 30 min postdrug (0.92 ± 0.02 g and 5.23 ± 0.98 g, resp.) compared with predrug controls (17.45 ± 0.50 g and 17.98 ± 0.03 g, resp.; $P < 0.05$) as well as with saline-injected controls (17.97 ± 0.02 g; $n = 10$; $P < 0.05$). The reduced PWTs lasted for 150 min. In rats with decreased PWTs on 1 week after CCD (Figure 4(b)), muscimol (i.t., 5 nmol, $n = 8$) or baclofen (i.t., 25 nmol, $n = 8$) reversed the reduced PWTs maximally at 30 min postdrug (17.42 ± 0.37 g and 13.04 ± 2.20 g, resp.) compared with preapplication controls (2.69 ± 0.31 g and 2.66 ± 0.24 g, resp.; $P < 0.05$) as well as with saline-injected controls (3.33 ± 0.54 g; $n = 10$; $P < 0.05$). The reversion lasted for 180 min. In rats with PWTs that had recovered completely to pre-CCD levels on 18 weeks after CCD (Figure 4(c)), bicuculline (i.t., 15 nmol, $n = 8$) or CGP52432 (i.t., 15 nmol, $n = 8$) produced a maximum reduction of PWTs at 30 min postdrug (3.83 ± 2.04 g and 5.91 ± 1.04 g, resp.) compared with predrug controls (17.95 ± 0.23 g and 17.59 ± 0.36 g, resp.; $P < 0.05$) as well as with saline-injected controls (17.64 ± 0.82 g; $n = 10$; $P < 0.05$). The reduced PWTs lasted for 150 min.

3.4. Effects of Activation or Deactivation of Spinal GABA Receptors on Neuronal Excitability. In the sham-operated group (Figures 5(a) and 5(b)), topical application of bicuculline (15 nmol, $n = 6$) significantly increased responses of spinal WDR neurons to brushing, pressing, and pinching stimuli at 15 min postdrug (364 ± 55 , 443 ± 48 , and 562 ± 53 spikes) compared with predrug controls (128 ± 9 , 178 ± 29 , and 262 ± 28 spikes; $P < 0.05$). The application of CGP52432 (15 nmol, $n = 6$) also significantly increased such responses (235 ± 20 , 380 ± 27 , and 517 ± 75 spikes), compared with predrug control (128 ± 16 , 183 ± 14 , and 297 ± 36 spikes; $P < 0.05$). This antagonism of GABA receptors also enhanced WDR neuronal after discharge activity.

In rats on 1 week after CCD (Figures 5(c) and 5(d)), WDR neuronal responses to the three mechanical stimuli were significantly enhanced under predrug conditions (245 ± 30 , 374 ± 50 , and 621 ± 44 spikes for pre-muscimol and 306 ± 35 , 373 ± 93 , and 550 ± 69 spikes for pre-baclofen), compared with those seen in the sham-operated groups (refer to values of predrug controls in Figures 5(a) and 5(b); $P < 0.05$). These enhanced responses were suppressed by topical application of muscimol (121 ± 42 , 135 ± 16 , and 171 ± 27 spikes;

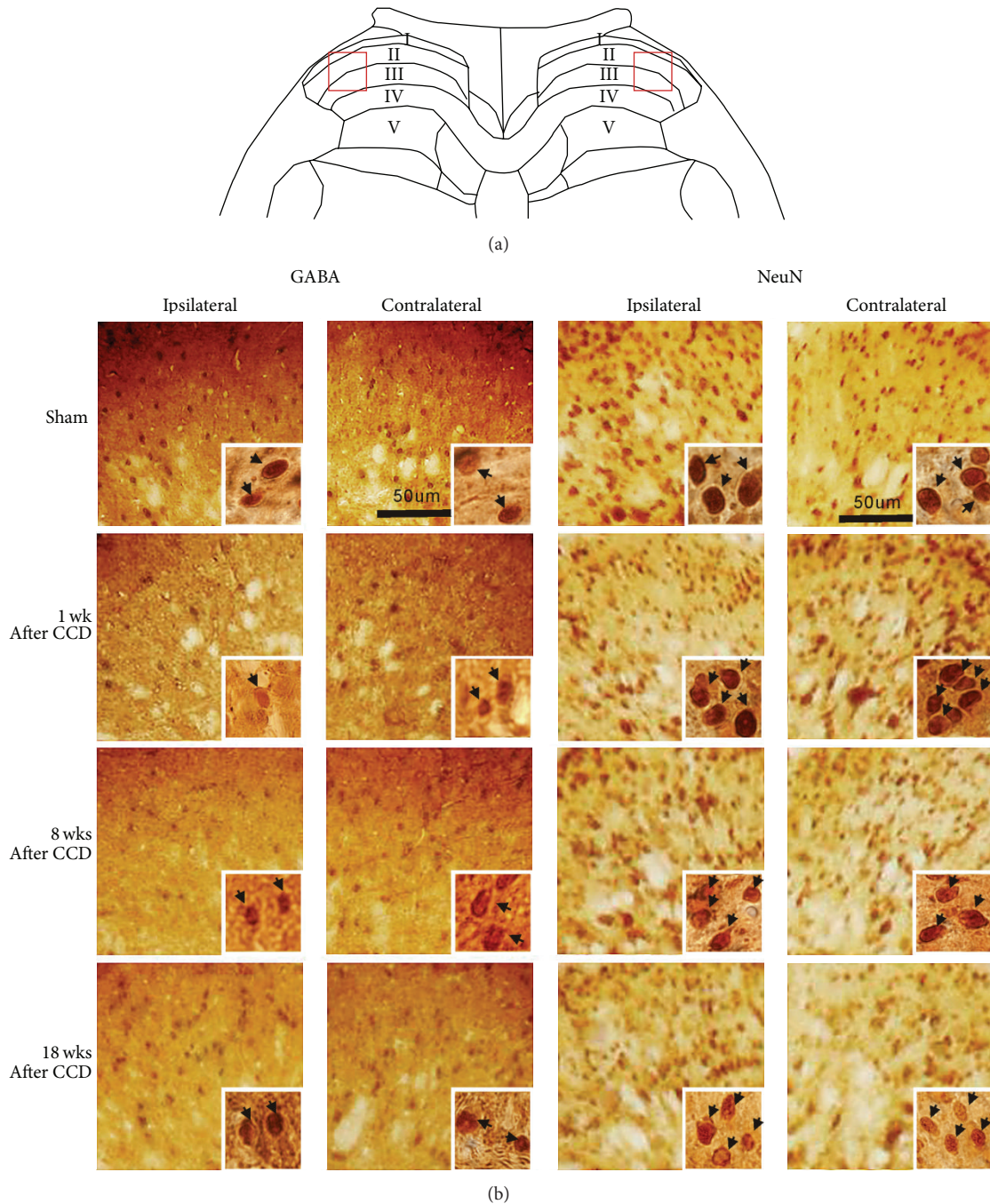


FIGURE 2: Representative images of GABA-ir and NeuN-ir cells in laminae I–III of the spinal dorsal horn. Photomicrographs of the areas of the squares are presented in (a), which cover the lateral portions of laminae I–III, and are shown in (b). The GABA-ir cells in the ipsilateral laminae I–III appear to be distributed less densely for 1-week and 8-week post-CCD groups than for sham-operated and 18-week post-CCD groups, with no density difference in the contralateral laminae among the four groups. The NeuN-ir cells show no differences in density between both sides of the dorsal horn laminae as well as among all four groups. Typical GABA-ir and NeuN-ir cells are seen in insets at the lower right of each image (indicated by arrows).

5 nmol; $n = 6$) and baclofen (109 ± 11 , 132 ± 44 , and 175 ± 46 spikes; 25 nmol; $n = 6$), respectively. The WDR neuronal after discharge activity seen in rats on 1 week after CCD was also suppressed by this activation of GABA receptors.

In rats on 18 weeks after CCD (Figures 5(e) and 5(f)), WDR neuronal responses to the three mechanical stimuli returned to the sham-control levels (refer to values of predrug controls in Figures 5(a) and 5(b)) as seen under predrug conditions (149 ± 7 , 201 ± 14 , and 294 ± 45 spikes for

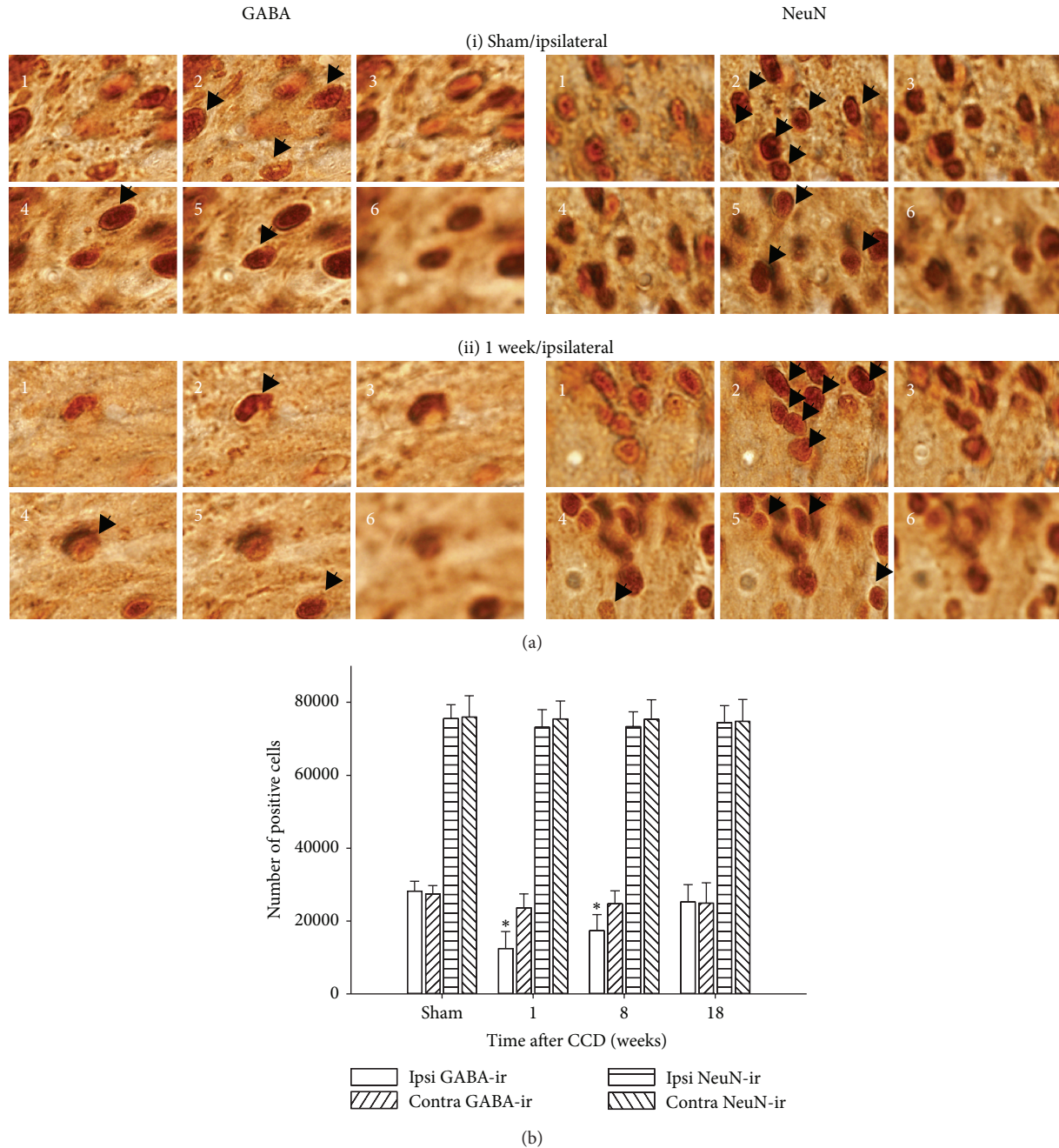


FIGURE 3: Quantitative analysis of GABA-ir and NeuN-ir cells by stereological cell counting. In (a), images used for stereological cell counts are shown, taken at six consecutive focal planes from the top to the bottom of the 20 μ m optical dissector. The dissector contains 5 GABA-ir and 9 NeuN-ir cells for the sham-operated group (i) and 3 GABA-ir and 10 NeuN-ir cells for the 1-week post-CCD group (ii) (indicated by arrows). In (b), the mean numbers of cells estimated by stereological analysis from L4-L5 dorsal horn laminae I–III of individual animals are represented in bar graphs ($n = 5$ rats for each group). The number of GABA-ir cells significantly decreased for both 1-week and 8-week post-CCD groups compared with the sham-operated group, whereas no significant differences in NeuN-ir cell number were seen among all four groups. * $P < 0.05$ when compared with sham-treated control.

prebicuculline and 167 ± 18 , 234 ± 47 , and 286 ± 41 spikes for pre-CGP52432). These recovered responses were enhanced by topical application of bicuculline (304 ± 21 , 494 ± 45 , and 567 ± 47 spikes; 15 nmol; $n = 6$) and CGP52432 (283 ± 29 ,

458 ± 43 , and 524 ± 97 spikes; 15 nmol; $n = 6$), respectively. As seen in the sham-control group, this antagonism of GABA receptors resulted in enhancement of WDR neuronal after discharge activity.

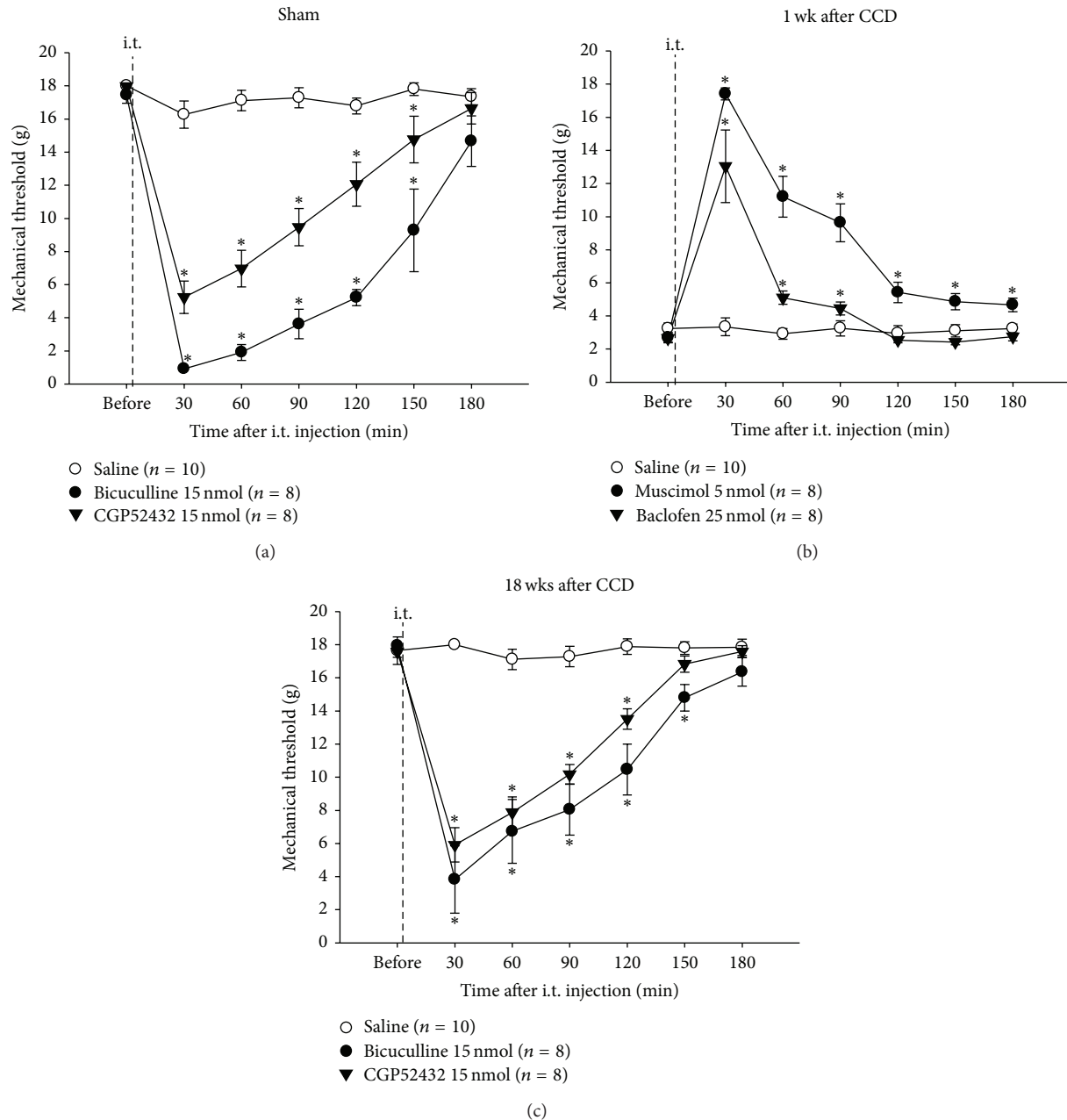


FIGURE 4: The effects of inhibition or activation of spinal GABA receptors on mechanical sensitivity following CCD. In sham-operated rats (a), an intrathecal (i.t.) administration of bicuculline (15 nmol) or CGP52432 (15 nmol) produced a decrease in the paw withdrawal thresholds (PWTs) for at least 150 min. On 1 week after CCD (b), an i.t. administration of muscimol (5 nmol) or baclofen (25 nmol) reversed the decreased PWTs for longer than 90 min. On 18 weeks after CCD (c), bicuculline (15 nmol) or CGP52432 (15 nmol) resulted in the decrease of PWTs for at least 150 min. * $P < 0.05$ when compared with saline-treated control.

4. Discussion

Previous reports have suggested that compression of the fifth lumbar DRG caused neuropathic pain in the injured side of the hind paw [3, 23]. In addition, we and others have reported that decreased spinal GABAergic inhibition, or GABAergic disinhibition, contributed to neuropathic pain, following direct damages to the spinal cord and peripheral nerves, respectively [17, 18, 24]. In the present study, we

suggest that the decrease of spinal GABAergic inhibition without the decrease of neurons contributes to mechanical hypersensitivity at the hind paw and spinal neuronal hyperexcitability in the early phase following CCD.

Numerous studies have been performed to seek the underlying mechanisms of CCD-induced hyperexcitability in the DRG and spinal nociceptive neurons that lead to neuropathic pain. For instance, ectopic spontaneous and evoked activities of CCD neurons were enhanced by activation of

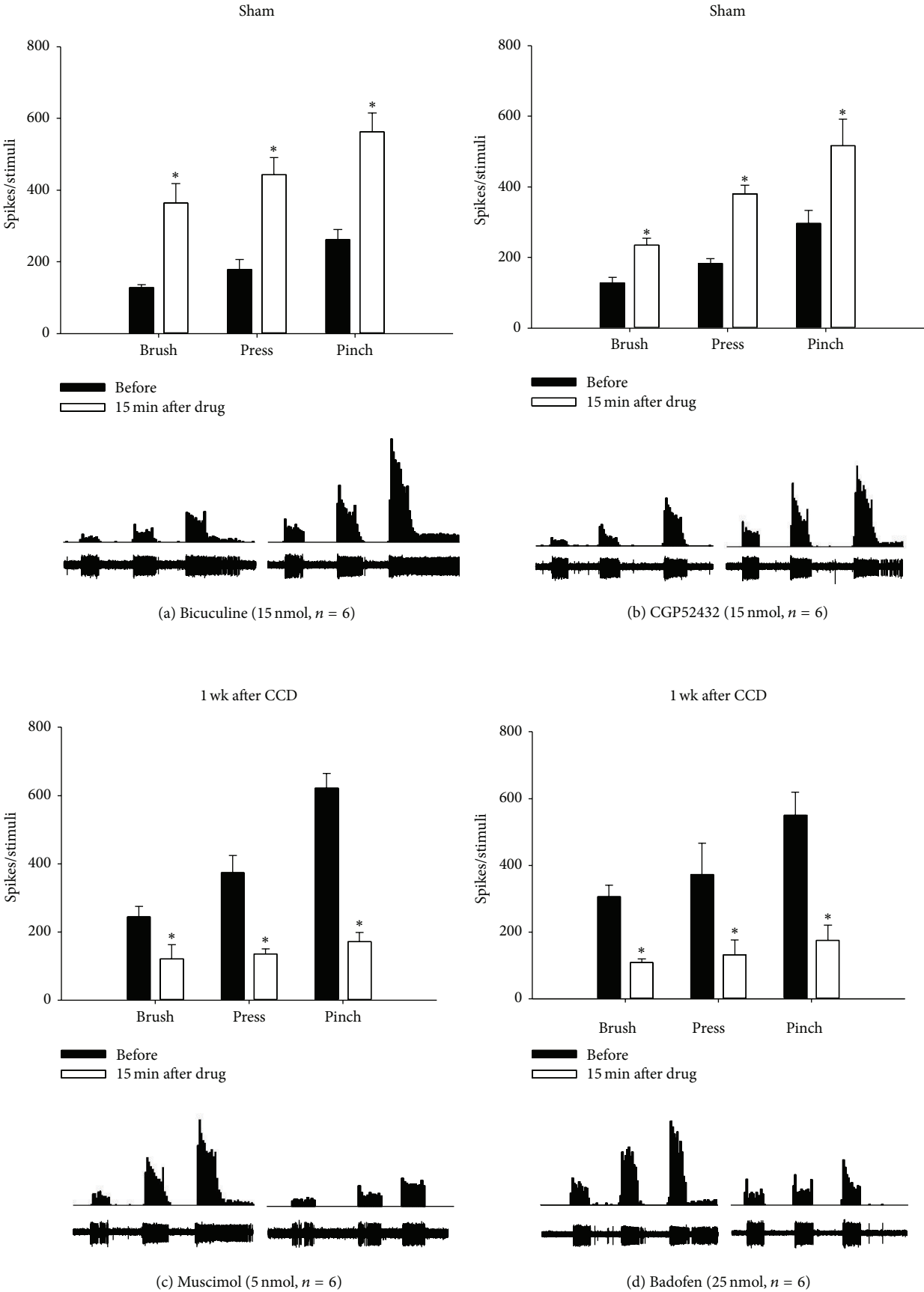


FIGURE 5: Continued.

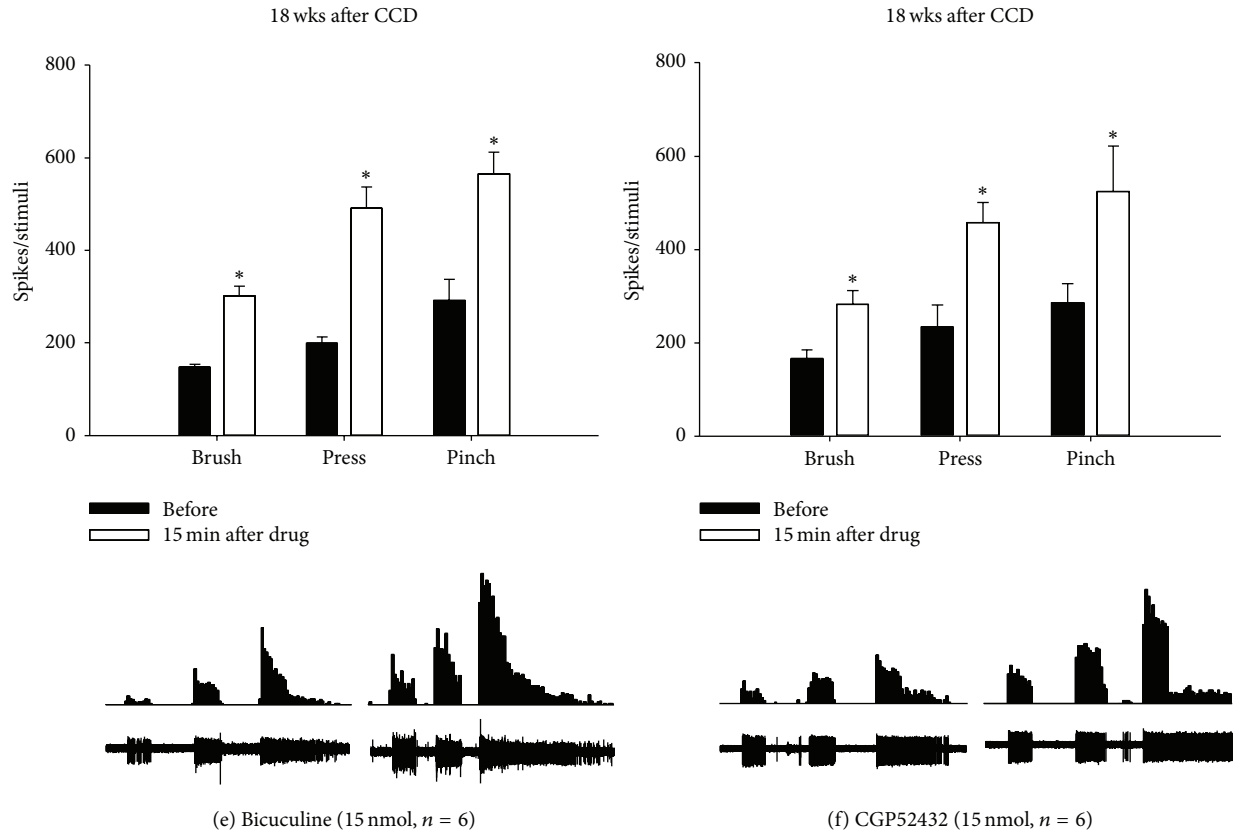


FIGURE 5: The effects of inhibition or activation of spinal GABA receptors on WDR neuronal activity following CCD. In sham-operated animals, topical application of bicuculline ((a), 15 nmol) or CGP52432 ((b), 15 nmol) enhanced the activity of spinal WDR neurons evoked by brushing, pressing, and pinching stimuli. On 1 week after CCD, topical application of muscimol ((c), 5 nmol) or baclofen ((d), 25 nmol) attenuated the enhanced evoked activity of WDR neurons. On 18 weeks after CCD, bicuculline ((e), 15 nmol) or CGP52432 ((f), 15 nmol) led to an increase in evoked activity of WDR neurons. Data were expressed as the mean number of spike discharges generated from a single WDR neuron evoked by three types of 10 s mechanical stimuli. Below each bar graph, examples of extracellular recordings of stimulus-evoked spike discharges from a single WDR neuron (lower rows) and of peristimulus time histograms for visualizing the rate of spike discharges (upper rows) are shown. * $P < 0.05$ when compared with predrug control.

inflammatory mediators via protein kinase A [25, 26], by protease-activated receptor 2 (PAR2) [27, 28], by increased sodium-channel and decreased potassium-channel activity [29], by upregulation of chemokine receptor 2 (CCR2) induced by monocyte chemoattractant protein-1 (MCP-1) [30], and by activation of P2X receptors [31], respectively. However, the implication of spinal GABAergic disinhibition in CCD-induced neuropathic pain has not been well studied.

In previous studies, several possible explanations for spinal GABAergic disinhibition in peripheral nerve injury-induced neuropathic pain have been proposed. The first possibility is a loss of GABA cells after nerve injury. Injury-induced nerve impulses trigger massive releases of glutamate in the spinal dorsal horn, followed by cell excitotoxicity that results in the loss of GABAergic cells, consequently leading to decreased GABAergic inhibitory function [8–10, 32, 33]. However, this hypothesis has been challenged; quantitative analysis has revealed that the number of spinal GABA neurons in rats with peripheral nerve injury is not different from controls [11–13, 34]. In addition, our data showed no changes in the total number of neurons at L4–L5 lumbar dorsal horn

laminae I–III following CCD and suggested no decrease of GABA neurons in rats with CCD. The second proposed explanation is the decrease of GABA synthesis. Studies on peripheral nerve injury models have reported that the level of glutamic acid decarboxylase-65 (GAD-65) decreased in the spinal dorsal horn after peripheral nerve injury [8, 10]. Our data, which demonstrate the decreased proportion of GABA neurons to the total NeuN-ir cells at laminae I–III in the early phase after CCD, agree with a proposal of nerve injury-induced decrease of GABA synthesis, as GABA neurons having an undetectable GABA level may be excluded from the cell count. However, it remains for further studies to evaluate whether CCD causes this decrease of GAD activity. The third possibility is the decreased function of GABA receptors via downregulation or decreased binding affinity without any loss of GABA neurons. In support of this theory, previous studies have demonstrated the decrease of GABA-A receptor mRNA levels in primary afferent terminals after spinal nerve ligation injury [35] as well as the decreased binding affinity of GABA-B receptors in the spinal dorsal horn after sciatic nerve transection injury [36, 37].

However, no loss of spinal GABA-A receptors has been reported in rats with spared nerve injury [34]. Our data indicate that spinal GABA receptor activity remains intact after CCD, since spinal GABA receptor inactivation and activation could influence mechanical sensitivity and neuronal excitability in the early and late phases after CCD. Our data also demonstrate a close correlation between the time-dependent changes of spinal GABA content and mechanical sensitivity following CCD, suggesting an involvement of spinal GABAergic function in CCD-induced neuropathic pain. In the early phase after CCD, spinally applied GABA receptor agonists decreased CCD-induced mechanical hypersensitivity, suggesting a reduction of spinal GABAergic inhibition. After the return of mechanical sensitivity to normal levels in the late phase, spinally applied GABA antagonists regenerated mechanical hypersensitivity, suggesting a regain of spinal GABAergic inhibition. We postulate the feasible mechanisms of time-dependent changes in spinal GABAergic inhibition after CCD as follows. The DRG compression induced by a stainless steel rod insertion into the intervertebral foramen is the primary cause for developing mechanical hypersensitivity of the hind paw. In the early phase after CCD, DRG compression-induced enhancement of sensory input triggers an increase of GABA release in the spinal cord, where the balance between excitation and inhibition is usually maintained. The increased spinal GABA release may lead to the decreased GABA synthesis in spinal GABA neurons, which results in decreased spinal GABAergic inhibition, thus producing mechanical hypersensitivity. In the later phase, however, the increased spinal GABA synthesis may occur so that spinal GABAergic inhibition is regained to reduce the CCD-induced mechanical hypersensitivity.

Since our knowledge of spinal synaptic circuits that include inhibitory (mostly GABAergic/glycinergic) and excitatory (mostly glutamatergic) interneurons is limited, it is difficult to explain why spinal GABAergic neurons are vulnerable to CCD. As proposed in the gate control theory of pain [38], inputs from nociceptive and low-threshold (LT) primary afferents converge onto a dorsal horn projection neuron for pain signal transmission to the brain. In this proposal, the LT input also activates an inhibitory interneuron that produces postsynaptic inhibition of the projection neuron and the presynaptic inhibition of LT input. In addition, the nociceptive input to the projection neuron is disynaptic through an excitatory interneuron. Although the projection neuron responds to both nociceptive and LT inputs, the effectiveness of the LT input is normally reduced by the inhibitory interneuron activity. If this inhibitory action is disrupted, the LT input leads to stronger excitation of the projection neuron, which has been shown in this study. A previous study has revealed a high incidence of spontaneous ectopic discharge that is generated after CCD from large-sized DRG neurons of the injured ganglion [39]. This observation suggests that inhibitory transmission is more affected than excitatory transmission in spinal synaptic circuits following CCD, because of excessive ectopic discharge input from the injured LT afferents. Moreover, GABAergic interneurons outnumber glycinergic interneurons, 35% versus 18% of the total neuronal population, in laminae I–III of the dorsal horn

[40]. Thus, CCD-induced ectopic discharge of LT afferents would lead to a loss for more GABAergic inhibition than glycinergic inhibition.

It has been reported that the restoration of lumbar intervertebral foramen space improves mechanical hypersensitivity and that decompression of the DRG reduces compression-induced decreases of DRG neurons [41]. Thus, it is possible to expect that gradual attenuation of CCD-induced mechanical hypersensitivity is due to the recovery of damaged CCD neurons by the gradual widening of the intervertebral foramen over a period of time after injury. In clinical data, 60% of neuropathic pain patients who had undergone surgery to enlarge narrowed foramina show attenuation of neuropathic pain within a year [42]. Taken together, the recovery of damaged peripheral nerves and subsequent restoration of spinal GABAergic inhibition are critical for the improvement of chronic neuropathic pain following CCD.

5. Conclusions

CCD modulates spinal GABAergic inhibitory function. In the early phase after CCD, spinal GABAergic inhibition is reduced via the decrease of GABA content in GABA neurons, resulting in mechanical hypersensitivity in the hind paw and spinal neuronal hyperexcitability. In the later phase, GABAergic inhibition level is restored to normal via recovery of GABA content, leading to alleviation of such mechanical hypersensitivity and neuronal hyperexcitability. Therefore, the control of spinal GABA levels could be a useful tool for the treatment of neuropathic pain following CCD.

Highlights

- (i) GABA-ir neurons were decreased without changes in total neuron numbers on the CCD injury side in the early phase, whereas there were no changes in GABA-ir neurons in the late phase.
- (ii) Mechanical hypersensitivity and spinal WDR neuronal hyperexcitability developed on the CCD injured side in the early phase, which returned to normal in the late phase.
- (iii) GABA receptor agonists reduced CCD-induced mechanical hypersensitivity and neuronal hyperexcitability in the early phase.
- (iv) GABA receptor antagonists reinduced mechanical hypersensitivity and neuronal hyperexcitability in the late phase.

Conflict of Interests

The authors declare that there is no conflict of interests regarding the publication of this paper.

Authors' Contribution

Moon Chul Lee has seen the original study data, reviewed the analysis of the data, and approved the final paper. Taick Sang Nam has seen the original study data, reviewed the analysis of the data, and approved the final paper. Se Jung Jung has seen the original study data and approved the final paper. Young S. Gwak has seen the original study data, reviewed the analysis of the data, and approved the final paper and the archive author. Joong Woo Leem has seen the original study data, reviewed the analysis of the data, and approved the final paper and the archive author.

Acknowledgment

This work was funded by the Stem Cell Research Center of the 21st Century Frontier Research Program (SC4140) from the Ministry of Science and Technology and from the National Research Foundation (NRF-2014R1A1A4A01004179) of Korea.

References

- [1] C. J. Woolf and R. J. Mannion, "Neuropathic pain: aetiology, symptoms, mechanisms, and management," *The Lancet*, vol. 353, no. 9168, pp. 1959–1964, 1999.
- [2] A. Berger, E. M. Dukes, and G. Oster, "Clinical characteristics and economic costs of patients with painful neuropathic disorders," *Journal of Pain*, vol. 5, no. 3, pp. 143–149, 2004.
- [3] A. W. Tarulli and E. M. Raynor, "Lumbosacral radiculopathy," *Neurologic Clinics*, vol. 25, no. 2, pp. 387–405, 2007.
- [4] R. Freynhagen, R. Baron, T. Tölle et al., "Screening of neuropathic pain components in patients with chronic back pain associated with nerve root compression: a prospective observational pilot study (MIPOPT)," *Current Medical Research and Opinion*, vol. 22, no. 3, pp. 529–537, 2006.
- [5] S.-J. Hu and J.-L. Xing, "An experimental model for chronic compression of dorsal root ganglion produced by intervertebral foramen stenosis in the rat," *Pain*, vol. 77, no. 1, pp. 15–23, 1998.
- [6] Z. Y. Tan, D. F. Donnelly, and R. H. LaMotte, "Effects of a chronic compression of the dorsal root ganglion on voltage-gated Na^+ and K^+ currents in cutaneous afferent neurons," *Journal of Neurophysiology*, vol. 95, no. 2, pp. 1115–1123, 2006.
- [7] J.-M. Zhang, X.-J. Song, and R. H. Lamotte, "Enhanced excitability of sensory neurons in rats with cutaneous hyperalgesia produced by chronic compression of the dorsal root ganglion," *Journal of Neurophysiology*, vol. 82, no. 6, pp. 3359–3366, 1999.
- [8] M. J. Eaton, J. A. Plunkett, S. Karmally, M. A. Martinez, and K. Montanez, "Changes in GAD- and GABA- immunoreactivity in the spinal dorsal horn after peripheral nerve injury and promotion of recovery by lumbar transplant of immortalized serotonergic precursors," *Journal of Chemical Neuroanatomy*, vol. 16, no. 1, pp. 57–72, 1998.
- [9] T. Ibuki, A. T. Hama, X.-T. Wang, G. D. Pappas, and J. Sagen, "Loss of GABA-immunoreactivity in the spinal dorsal horn of rats with peripheral nerve injury and promotion of recovery by adrenal medullary grafts," *Neuroscience*, vol. 76, no. 3, pp. 845–858, 1996.
- [10] K. A. Moore, T. Kohno, L. A. Karchewski, J. Scholz, H. Baba, and C. J. Woolf, "Partial peripheral nerve injury promotes a selective loss of GABAergic inhibition in the superficial dorsal horn of the spinal cord," *Journal of Neuroscience*, vol. 22, no. 15, pp. 6724–6731, 2002.
- [11] S. P. Janssen, M. Truin, M. van Kleef, and E. A. Joosten, "Differential GABAergic disinhibition during the development of painful peripheral neuropathy," *Neuroscience*, vol. 184, pp. 183–194, 2011.
- [12] E. Polgár, D. I. Hughes, J. S. Riddell, D. J. Maxwell, Z. Puskár, and A. J. Todd, "Selective loss of spinal GABAergic or glycinergic neurons is not necessary for development of thermal hyperalgesia in the chronic constriction injury model of neuropathic pain," *Pain*, vol. 104, no. 1–2, pp. 229–239, 2003.
- [13] D. L. Somers and F. R. Clemente, "Dorsal horn synaptosomal content of aspartate, glutamate, glycine and GABA are differentially altered following chronic constriction injury to the rat sciatic nerve," *Neuroscience Letters*, vol. 323, no. 3, pp. 171–174, 2002.
- [14] O. Satoh and K. Omote, "Roles of monoaminergic, glycinergic and GABAergic inhibitory systems in the spinal cord in rats with peripheral mononeuropathy," *Brain Research*, vol. 728, no. 1, pp. 27–36, 1996.
- [15] X.-J. Song, D.-S. Xu, C. Vizcarra, and R. L. Rupert, "Onset and recovery of hyperalgesia and hyperexcitability of sensory neurons following intervertebral foramen volume reduction and restoration," *Journal of Manipulative and Physiological Therapeutics*, vol. 26, no. 7, pp. 426–436, 2003.
- [16] M. Dambrova, L. Zvejniece, E. Liepinsh et al., "Comparative pharmacological activity of optical isomers of phenibut," *European Journal of Pharmacology*, vol. 583, no. 1, pp. 128–134, 2008.
- [17] Y. S. Gwak, H. Y. Tan, T. S. Nam, K. S. Paik, C. E. Hulsebosch, and J. W. Leem, "Activation of spinal GABA receptors attenuates chronic central neuropathic pain after spinal cord injury," *Journal of Neurotrauma*, vol. 23, no. 7, pp. 1111–1124, 2006.
- [18] J. H. Hwang and T. L. Yaksh, "The effect of spinal GABA receptor agonists on tactile allodynia in a surgically-induced neuropathic pain model in the rat," *Pain*, vol. 70, no. 1, pp. 15–22, 1997.
- [19] M. J. West, L. Slomianka, and H. J. G. Gundersen, "Unbiased stereological estimation of the total number of neurons in the subdivisions of the rat hippocampus using the optical fractionator," *Anatomical Record*, vol. 231, no. 4, pp. 482–497, 1991.
- [20] S. R. Chaplan, F. W. Bach, J. W. Pogrel, J. M. Chung, and T. L. Yaksh, "Quantitative assessment of tactile allodynia in the rat paw," *Journal of Neuroscience Methods*, vol. 53, no. 1, pp. 55–63, 1994.
- [21] R. Dubner, D. R. Kenshalo Jr., W. Maixner, M. C. Bushnell, and J.-L. Oliveras, "The correlation of monkey medullary dorsal horn neuronal activity and the perceived intensity of noxious heat stimuli," *Journal of Neurophysiology*, vol. 62, no. 2, pp. 450–457, 1989.
- [22] W. Maixner, R. Dubner, M. C. Bushnell, D. R. Kenshalo Jr., and J. L. Oliveras, "Wide-dynamic-range dorsal horn neurons participate in the encoding process by which monkeys perceive the intensity of noxious heat stimuli," *Brain Research*, vol. 374, no. 2, pp. 385–388, 1986.
- [23] M. Sekiguchi, Y. Sekiguchi, S.-I. Konno, H. Kobayashi, Y. Homma, and S.-I. Kikuchi, "Comparison of neuropathic pain and neuronal apoptosis following nerve root or spinal nerve compression," *European Spine Journal*, vol. 18, no. 12, pp. 1978–1985, 2009.

- [24] L. S. Sorkin, S. Puig, and D. L. Jones, "Spinal bicuculline produces hypersensitivity of dorsal horn neurons: effects of excitatory amino acid antagonists," *Pain*, vol. 77, no. 2, pp. 181–190, 1998.
- [25] S.-J. Hu, X.-J. Song, K. W. Greenquist, J.-M. Zhang, and R. H. LaMotte, "Protein kinase A modulates spontaneous activity in chronically compressed dorsal root ganglion neurons in the rat," *Pain*, vol. 94, no. 1, pp. 39–46, 2001.
- [26] C. Ma, K. W. Greenquist, and R. H. LaMotte, "Inflammatory mediators enhance the excitability of chronically compressed dorsal root ganglion neurons," *Journal of Neurophysiology*, vol. 95, no. 4, pp. 2098–2107, 2006.
- [27] Z.-J. Huang, H.-C. Li, A. A. Cowan, S. Liu, Y.-K. Zhang, and X.-J. Song, "Chronic compression or acute dissociation of dorsal root ganglion induces cAMP-dependent neuronal hyperexcitability through activation of PAR2," *Pain*, vol. 153, no. 7, pp. 1426–1437, 2012.
- [28] X.-J. Song, Z.-B. Wang, Q. Gan, and E. T. Walters, "cAMP and cGMP contribute to sensory neuron hyperexcitability and hyperalgesia in rats with dorsal root ganglia compression," *Journal of Neurophysiology*, vol. 95, no. 1, pp. 479–492, 2006.
- [29] N. Fan, P. Sikand, D. F. Donnelly, C. Ma, and R. H. LaMotte, "Increased Na⁺ and K⁺ currents in small mouse dorsal root ganglion neurons after ganglion compression," *Journal of Neurophysiology*, vol. 106, no. 1, pp. 211–218, 2011.
- [30] F. A. White, J. Sun, S. M. Waters et al., "Excitatory monocyte chemoattractant protein-1 signaling is up-regulated in sensory neurons after chronic compression of the dorsal root ganglion," *Proceedings of the National Academy of Sciences of the United States of America*, vol. 102, no. 39, pp. 14092–14097, 2005.
- [31] Z. Xiang, Y. Xiong, N. Yan et al., "Functional up-regulation of P2X3 receptors in the chronically compressed dorsal root ganglion," *Pain*, vol. 140, no. 1, pp. 23–34, 2008.
- [32] R. E. Coggeshall, H. A. Lekan, F. A. White, and C. J. Woolf, "A-fiber sensory input induces neuronal cell death in the dorsal horn of the adult rat spinal cord," *Journal of Comparative Neurology*, vol. 435, no. 3, pp. 276–282, 2001.
- [33] T. Sugimoto, G. J. Bennett, and K. C. Kajander, "Transsynaptic degeneration in the superficial dorsal horn after sciatic nerve injury: effects of a chronic constriction injury, transection, and strychnine," *Pain*, vol. 42, no. 2, pp. 205–213, 1990.
- [34] E. Polgár and A. J. Todd, "Tactile allodynia can occur in the spared nerve injury model in the rat without selective loss of GABA or GABA_A receptors from synapses in laminae I-II of the ipsilateral spinal dorsal horn," *Neuroscience*, vol. 156, no. 1, pp. 193–202, 2008.
- [35] T. Fukuoka, A. Tokunaga, E. Kondo, K. Miki, T. Tachibana, and K. Noguchi, "Change in mRNAs for neuropeptides and the GABA(A) receptor in dorsal root ganglion neurons in a rat experimental neuropathic pain model," *Pain*, vol. 78, no. 1, pp. 13–26, 1998.
- [36] J. M. Castro-Lopes, M. Malcangio, B. H. Pan, and N. G. Bowery, "Complex changes of GABAA and GABAB receptor binding in the spinal cord dorsal horn following peripheral inflammation or neurectomy," *Brain Research*, vol. 679, no. 2, pp. 289–297, 1995.
- [37] M. P. Engle, M. A. Merrill, B. Marquez de Prado, and D. L. Hammond, "Spinal nerve ligation decreases γ -aminobutyric acid B receptors on specific populations of immunohistochemically identified neurons in L5 dorsal root ganglion of the rat," *Journal of Comparative Neurology*, vol. 520, no. 8, pp. 1663–1677, 2012.
- [38] R. Melzack and P. D. Wall, "Pain mechanisms: a new theory," *Science*, vol. 150, no. 3699, pp. 971–979, 1965.
- [39] X.-J. Song, S.-J. Hu, K. W. Greenquist, J.-M. Zhang, and R. H. LaMotte, "Mechanical and thermal hyperalgesia and ectopic neuronal discharge after chronic compression of dorsal root ganglia," *Journal of Neurophysiology*, vol. 82, no. 6, pp. 3347–3358, 1999.
- [40] A. J. Todd and A. C. Sullivan, "Light microscope study of the coexistence of GABA-like and glycine-like immunoreactivities in the spinal cord of the rat," *Journal of Comparative Neurology*, vol. 296, no. 3, pp. 496–505, 1990.
- [41] Z.-Y. Tang, B. Shu, X.-J. Cui et al., "Changes of cervical dorsal root ganglia induced by compression injury and decompression procedure: a novel rat model of cervical radiculoneuropathy," *Journal of Neurotrauma*, vol. 26, no. 2, pp. 289–295, 2009.
- [42] R. Chou, A. Qaseem, V. Snow et al., "Diagnosis and treatment of low back pain: a joint clinical practice guideline from the American College of Physicians and the American Pain Society," *Annals of Internal Medicine*, vol. 147, no. 7, pp. 478–491, 2007.

Research Article

PKA Inhibitor H89 (N-[2-p-bromocinnamylamino-ethyl]-5-isoquinolinesulfonamide) Attenuates Synaptic Dysfunction and Neuronal Cell Death following Ischemic Injury

Juhyun Song,¹ So Yeong Cheon,^{1,2} Won Taek Lee,¹ Kyung Ah Park,¹ and Jong Eun Lee^{1,2}

¹Department of Anatomy, Yonsei University College of Medicine, Seoul 120-752, Republic of Korea

²BK21 Plus Project for Medical Sciences and Brain Research Institute, Yonsei University College of Medicine, Seoul 120-752, Republic of Korea

Correspondence should be addressed to Jong Eun Lee; jelee@yuhs.ac

Received 8 January 2015; Revised 27 February 2015; Accepted 17 March 2015

Academic Editor: Young W. Yoon

Copyright © 2015 Juhyun Song et al. This is an open access article distributed under the Creative Commons Attribution License, which permits unrestricted use, distribution, and reproduction in any medium, provided the original work is properly cited.

The cyclic AMP-dependent protein kinase (PKA), which activates prosurvival signaling proteins, has been implicated in the expression of long-term potentiation and hippocampal long-term memory. It has come to light that H89 commonly known as the PKA inhibitor have diverse roles in the nervous system that are unrelated to its role as a PKA inhibitor. We have investigated the role of H89 in ischemic and reperfusion injury. First, we examined the expression of postsynaptic density protein 95 (PSD95), microtubule-associated protein 2 (MAP2), and synaptophysin in mouse brain after middle cerebral artery occlusion injury. Next, we examined the role of H89 pretreatment on the expression of brain-derived neurotrophic factor (BDNF), PSD95, MAP2, and the apoptosis regulators Bcl2 and cleaved caspase-3 in cultured neuroblastoma cells exposed to hypoxia and reperfusion injury. In addition, we investigated the alteration of AKT activation in H89 pretreated neuroblastoma cells under hypoxia and reperfusion injury. The data suggest that H89 may contribute to brain recovery after ischemic stroke by regulating neuronal death and proteins related to synaptic plasticity.

1. Introduction

Protein kinase A (PKA) [1] acts to phosphorylate other proteins, regulating them in a reversible manner. When cyclic adenosine monophosphate (cAMP) binds to the subunits of PKA, they undergo a conformational change that promotes phosphorylation [2]. PKA is implicated also in neural health. It stimulates neurite outgrowth in neurons and neuronal cell lines [3, 4] and promotes axon regeneration in vivo [5, 6]. cAMP/PKA signaling affects long-term synaptic plasticity and long-term memory [7].

Many studies that evaluate the role of PKA, which include smooth muscle cells [8, 9], neuronal tissue [10, 11], and epithelial cells [12, 13], have relied on the isoquinoline derivative N-[2-p-bromocinnamylamino-ethyl]-5-isoquinolinesulfonamide (H89), an inhibitor of PKA. H89 has an inhibition constant (K_i) of 0.05 mM in its inhibition of PKA [14, 15]. However, effects of H89 that are unrelated

to its inhibition have been observed. In a kinase study, at a concentration of 10 μ M, H89 inhibited the activity of the protein kinases Rho-associated kinase- (ROCK-) II, MSK1 and the ribosomal protein S6 kinase β -1 (S6K1) far more potently than it inhibited PKA itself [16]. In addition, H89 10 μ M maintains the neurite outgrowth of neuroblastoma cells [17]. There are several reports that H89 reduced Ca^{2+} uptake into the sarcoplasmic reticulum by attenuating the Ca^{2+} -ATPase's [18] affinity for calcium [19]. At 20 μ M, H89 prevented the glucose-induced increase in cytosolic calcium in pancreatic islets and attenuated the release of calcium in a differentiated β -cell line. In a study of expression of myelin basic protein in oligodendrocytes, H89 is involved in the phosphorylation of extracellular-signal-regulated kinase 1 and 2 (ERK 1 and 2) phosphorylation in response to insulin-like growth factor-1 [20] and it lowered potassium current through voltage-gated channels in rat myocytes [21].

Of particular interest is the H89 inhibition of S6K1, noted above. S6K1 is a downstream target of the mammalian target of rapamycin (mTOR) protein, which regulates the autophagy pathway [22] and is a mechanism target for regulation of cell size [23]. Several researchers have questioned the role of PKA in autophagy, since the studies rely at least in part on the selectivity of H89, which they consider uncertain [24, 25]. The second issue involves the action of H89 itself. Clearly, it has physiological effects unrelated to PKA. We have elected to examine those effects and chose to focus on H89's role in neural health, especially ischemic stroke.

Cerebral ischemia leads to neuronal death and synaptic dysfunction, resulting in cognitive decline [26–29]. Understanding the pathogenesis after ischemic stroke should inform medical care and maximize recovery. In the present study, we investigated the role of H89 in many aspects of nervous system function. Specifically, we examined its role in the expression of brain-derived neurotrophic factor (BDNF) in the development of neurites to axons [30–32], learning and memory [33], synaptic plasticity [34], the expression of B-cell lymphoma 2 (Bcl2) [35, 36] as it relates to neuronal death, the expression of synaptophysin [37], postsynaptic density protein 95 (PSD-95) [38, 39] as it relates to synaptic plasticity, and the expression of microtubule-associated protein 2 (MAP2). The latter interacts with actin filaments, shown to be necessary for neurite outgrowth [40–43] in a middle cerebral artery occlusion (MCAO) animal model and in an *in vitro* study. In present study, we suggest that H89 may confer protection from brain damage following cerebral ischemia.

2. Materials and Methods

2.1. Animal Model. Male C57BL/6 mice (Orient, GyeongGi-Do, Korea) that were eight-to-twelve weeks old were used in this study. Hypoxia followed by reperfusion (H/R) was imposed by subjecting mice to transient focal cerebral ischemia by intraluminal middle cerebral artery blockade with a nylon suture, as previously described [44]. After 60 min of MCAO, blood flow was restored by withdrawing the suture and regional cerebral blood flow was monitored with a laser Doppler flow meter (Transonic Systems, Inc., Ithaca, NY, USA). All animal procedures and experiments were performed in accordance with the Guide to the Care and Use of Laboratory Animals and were approved by the Association for Assessment and Accreditation of Laboratory Animal Care. All procedures were done at room temperature unless indicated otherwise. We used 5 rats in each group for study. Each measurement included 3 repeats per animal.

2.2. Immunohistochemistry. Frozen brain sections were cut into 5 μm sections and mounted on clean glass slides (Thermo Scientific, Waltham, MA, USA), air-dried, and fixed in cold acetone for 10 min at -20°C . The slides were washed in Tris-buffered saline (TBS; 20 mM Tris (pH 7.2), 150 mM NaCl), incubated with 0.3% H_2O_2 in methanol to quench endogenous peroxidase activity, and washed three times with distilled water, and the sections were blocked with 10% normal rabbit serum. Additional frozen brain sections (20 μm) were fixed in ice-cold acetone for 20 min. To block

nonspecific labeling, sections were incubated in 5% bovine serum albumin (BSA; Sigma-Aldrich, St. Louis, MO, USA) in 0.1% phosphate-buffered saline (PBS) for 30 min before addition of primary and secondary antibodies. Primary antibodies for PSD-95 (1:100, Millipore, Massachusetts, MA, USA), synaptophysin (1:100, Millipore, Massachusetts, MA, USA), and MAP2 (1:100, Abcam, Cambridge, MA, USA) were applied to the samples for 24 h at 4°C ; then the samples were incubated with the appropriate fluorescence secondary antibody (1:100, Invitrogen, Carlsbad, CA, USA) for 90 min, washed three times for 10 min in PBS with Tween-20 (PBST), and incubated with rhodamine-conjugated sheep anti-rabbit or fluorescein isothiocyanate- (FITC-) conjugated sheep anti-mouse secondary antibody (both diluted to 1:200 with 5% BSA fraction V in 0.1% PBST) for 2 h in the dark. This was followed by three washes in PBS and incubation in 1 $\mu\text{g}/\text{mL}$ 4',6-diamidino-2-phenylindole (DAPI; Sigma-Aldrich, St. Louis, MO, USA) for counterstaining. Tissues were then visualized under a confocal microscope (Zeiss LSM 700, Carl Zeiss, Thornwood, NY, USA).

2.3. Cell Culture. Neuro2A (N2A) cells purchased from ATCC biotechnology (ATCC, Manassas, VA, USA) were derived from mouse neuroblastoma. The cells exhibited properties of neuronal stem cells and were capable of differentiating into neuron-like cells in the presence of retinoic acid (RA). Undifferentiated N2A cells were cultured in Dulbecco's modified eagle medium (DMEM) supplemented with 10% fetal bovine serum (FBS; Gibco, Grand Island, NY, USA) and 100 $\mu\text{g}/\text{mL}$ penicillin-streptomycin (Gibco, Grand Island, NY, USA). N2A cells were passaged at least twice and then plated at 5×10^4 cells/mL in DMEM supplemented with 10% FBS for 24 h, after which the medium was changed to DMEM supplemented with 2% FBS and 20 μM RA for differentiation. Cultures were maintained in a humidified atmosphere of 5% CO_2 at 37°C . The medium was changed every two days [45].

2.4. Hypoxia and Reperfusion (H/R) and H89 Treatment. Confluent cells were transferred to an anaerobic chamber (Forma Scientific, OH, USA, O_2 tension = 0.1%). They were washed three times with PBS and the culture medium was replaced with deoxygenated, glucose-free balanced salt solution and incubated for 4 h. Following H/R injury, cells were incubated for 18 h under normal growth conditions [46]. H89 (10 μM , Sigma-Aldrich, St. Louis, MO, USA) was treated in the N2A cells at 2 h before H/R injury. In present study, we used the 10 μM concentration of H89, considering previous researches regarding other functions except from PKA inhibitor [17–19, 47, 48].

2.5. Neurite Length Measurement. To determine the length of their neurites, the cells were fixed for 20 min in 3.7% formaldehyde. Neurite formation was defined as an outgrowth from the cell body that was longer than the diameter of the cell body. N2A cells in three randomly selected fields (30–100 cells per field) were measured using ImageJ software (ImageJ, Madison, WI, USA) [49]. At least 30 cells per treatment were scored [50].

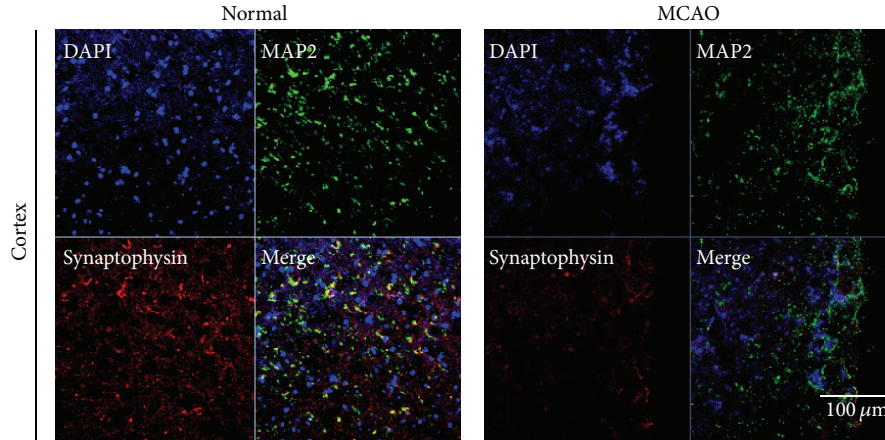


FIGURE 1: Immunofluorescence image for confirmation reduced synaptophysin expression in MCAO mouse brain. Immunofluorescence images showed that synaptophysin-positive cells (red) were decreased as expressed in MCAO mouse cortex. In addition, immunofluorescence images showed that MAP2- (considered as the neuron specific microtubule protein) positive cells (green) were strongly decreased in MCAO mouse cortex compared to the normal group. We used 5 rats in each groups for study. Each measurement included 3 repeats per animal. Scale bar = 100 μ m, synaptophysin: red, MAP2: green, 4', 6-diamidino-2-phenylindole (DAPI): blue, normal: normal control group, and MCAO: reperfusion 24 hr after MCAO injury.

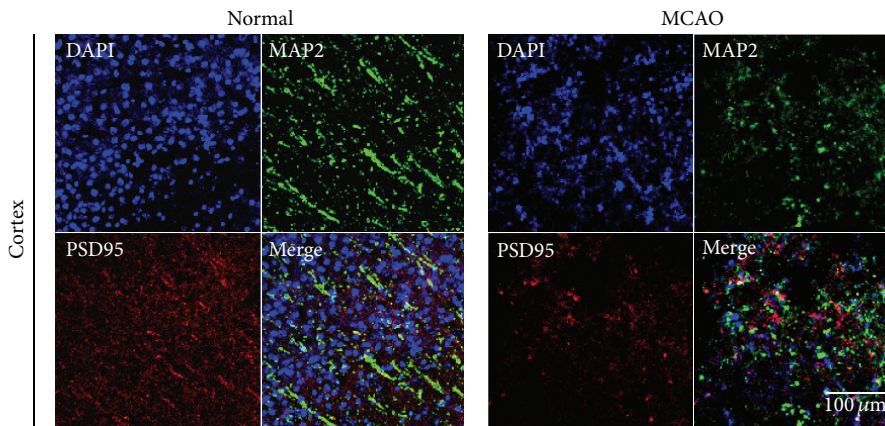


FIGURE 2: Immunofluorescence image for confirmation reduced PSD-95 expression in MCAO mouse brain. Immunofluorescence images showed that PSD-95- (as the post synaptic density protein) positive cells (red) were decreased as expressed in MCAO mouse cortex. Postsynaptic proteins were hardly observed in MCAO mouse brain cortex, whereas the normal cortex was observed evidently. We used 5 rats in each groups for study. Each measurement included 3 repeats per animal. Scale bar = 100 μ m, PSD-95: red, MAP2: green, 4', 6-diamidino-2-phenylindole (DAPI): blue, normal: normal control group, and MCAO: reperfusion 24 hr after MCAO injury.

2.6. Reverse Transcription PCR (RT-PCR). To examine the expression of BDNF, Bcl2, and MAP2 in N2A cells after H/R injury, RT-PCR was performed. Briefly, samples were lysed with TRIzol reagent (Invitrogen, Carlsbad, CA, USA) and total RNA was extracted according to the manufacturer's protocol. Complementary DNA synthesis from mRNA and sample normalization was performed. PCR was performed using the following thermal cycling conditions: 10 min at 95°C, 35 cycles of denaturing at 95°C for 15 sec, annealing for 30 sec at 70°C, elongation at 72°C for 30 sec, final extension for 10 min at 72°C, and maintenance at 4°C. PCR was performed using the following primers (5' to 3'); BDNF (F): AGT GAT GAC CAT CCT TTT CCT TAC, (R): CCT CAA ATG TGT CAT CCA AGG A, Bcl2 (F): AAG CTG TCA CAG AGG GGC TA, (R):

CAG GCT GGA AGG AGA AGA TG, MAP2 (F): TGA AGA ATG GCA GAT GAA C, (R): AGA AGG AGG CAG ATT AGC, GAPDH (F): GGCATGGACTGTGGTCATGAG, (R): TGCACCACCAACTGCTTAGC. PCR products were electrophoresed in 1.5% agarose gels and stained with ethidium bromide.

2.7. Western Blot Analysis. After H/R injury, cells were washed rapidly with ice-cold PBS, scraped, and collected. Cell pellets were lysed with ice-cold RIPA buffer (Sigma-Aldrich, St. Louis, MO, USA). The lysates were centrifuged at 13,200 rpm for 1 h at 4°C to produce whole-cell extracts. Protein was quantified with the bicinchoninic acid (BCA) method (Pierce biotechnology, Rockford, IL, USA). Protein (20 μ g) was separated on a 10% SDS-polyacrylamide (PAGE)

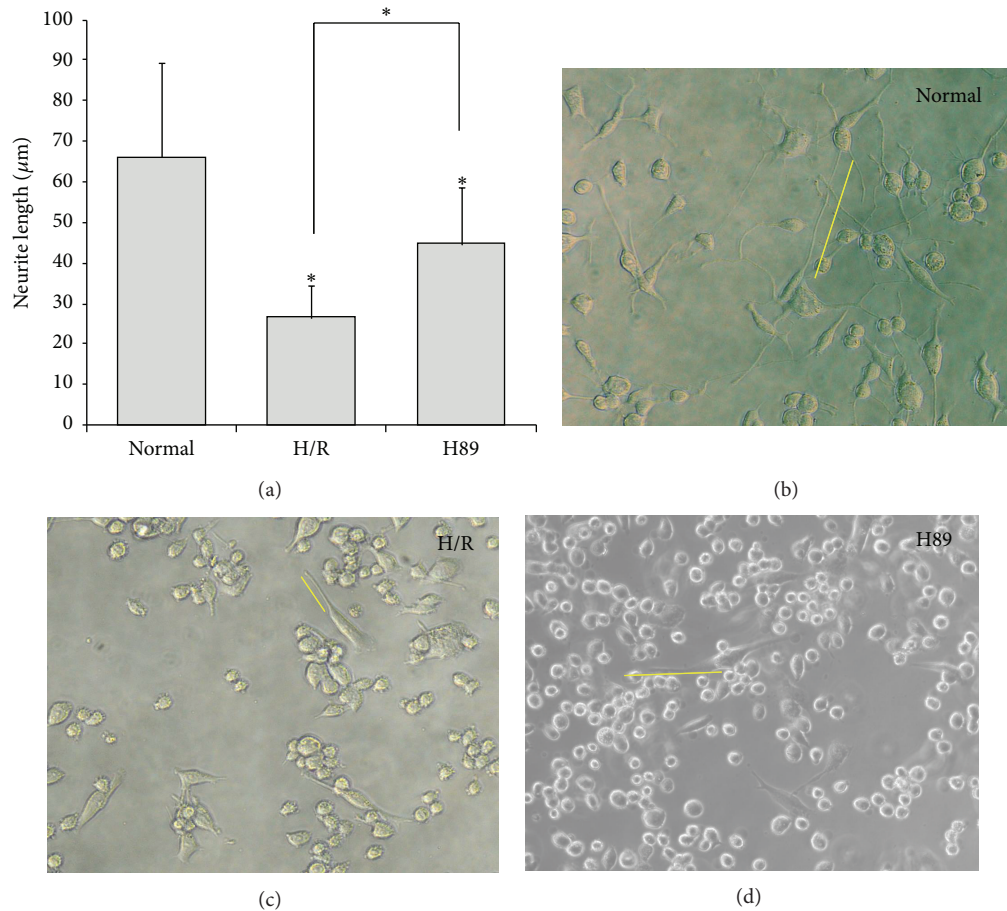


FIGURE 3: The measurement of neurite outgrowth in Neuro2A cells. (a) The graph of neurite outgrowth length (μm) in all groups. The neurite length significantly decreases in N2A cells against hypoxia reperfusion injury. Data are expressed as mean \pm S.E.M. Significant intergroup differences were determined by one-way analysis of variance (ANOVA) followed by Bonferroni post hoc multiple-comparison test. Differences were considered significant at $*P < 0.05$. (b) The image using bright field microscope in the normal group shows well developed neurite of N2A cells. (c) The image using bright field microscope in hypoxia reperfusion group shows shorter neurite outgrowth of N2A cells than the normal group. (d) The image using bright field microscope in H89 group shows well developed neurite of N2A cells compared to the hypoxia reperfusion group. Each experiment included 3 repeats per condition. H89 protected N2A cells against the neurite damage under H/R injury. Normal: the normal control group, H/R: 4 hr hypoxia and 18 hr reperfusion injury group, and H89: 2 hr PKA inhibitor H89 treatment group before 4 hr hypoxia and 18 hr reperfusion injury.

gel and transferred onto a polyvinylidene difluoride (PVDF) membrane. After blocking with 5% BSA (in TBS/Tween [TBS-T]) for 1 h, immunoblots were incubated overnight at 4°C with primary antibodies specific for Bcl2 (1:2000, Millipore, Massachusetts, MA, USA), cleaved caspase-3 (1:2000, Santa Cruz, Santa Cruz, CA, USA), PSD-95 (1:2000, Millipore, Massachusetts, MA, USA), AKT (1:2000, Cell signaling, Danvers, MA, USA), p-AKT (1:2000, Cell signaling, Danvers, MA, USA), or β -actin (1:2000, Santa Cruz, Santa Cruz, CA, USA). Next, blots were incubated with horseradish peroxidase- (HRP-) linked anti-mouse and anti-rabbit IgG antibodies purchased from Abcam (Abcam, Cambridge, MA, USA) for 1 h. Enhanced chemiluminescence was performed by electrochemiluminescence (ECL: Pierce Biotechnology, Rockford, IL, USA) [51].

2.8. Immunocytochemistry. The expression of BDNF, cleaved caspase-3, Bcl2, and PSD-95 in N2A cells was confirmed by

immunocytochemistry. Cells in all experimental groups were washed three times with PBS, fixed with 4% paraformaldehyde for 3 h, and then washed with PBS. N2A cells were permeabilized with 0.025% Triton X-100 and blocked for 1 h with dilution buffer (Invitrogen, Carlsbad, CA, USA). The following primary antibodies: anti-rabbit BDNF (1:500, Abcam, Cambridge, MA, USA), anti-rabbit cleaved caspase-3 (1:500, Santa Cruz, Santa Cruz, CA, USA), anti-rabbit PSD-95 (1:500, Millipore, Massachusetts, MA, USA), anti-mouse Bcl2 (1:500, Millipore, Massachusetts, MA, USA) were prepared in dilution buffer, added to samples, and incubated for 3 h. Primary antibody was then removed and cells were washed three times for 3 min each with PBS. Later, samples were incubated with FITC-conjugated goat, anti-rabbit (1:200, Jackson ImmunoResearch, PA, USA), or rhodamine-conjugated donkey, anti-mouse secondary antibodies (1:500, Millipore, Massachusetts, MA, USA) for 2 h. Cells were washed again three times for 3 min each with PBS and stained

with 1 $\mu\text{g}/\text{mL}$ DAPI (1:100, Sigma-Aldrich, St. Louis, MO, USA) for 10 min at room temperature. Fixed samples were imaged using a Zeiss LSM 700 confocal microscope (Carl Zeiss, Thornwood, NY, USA).

2.9. Statistical Analysis. Statistical analyses were carried out using SPSS 18.0 software (IBM Corp., Armonk, NY, USA). Data are expressed as mean \pm S.E.M. Significant intergroup differences were determined by one-way analysis of variance (ANOVA) followed by Bonferroni post hoc multiple-comparison test. Each experiment included four replicates per treatment. Differences were considered significant at $P < 0.05$ (*) or $P < 0.001$ (**).

3. Results

3.1. MCAO Mouse Brain Exhibited Neuronal Death and Synaptic Plasticity Damage. We performed immunohistochemistry of the brain of H/R injured and control mice, using antibodies to synaptophysin (Figure 1), PSD-95 (Figure 2), and MAP2 (Figures 1 and 2). The former two were used as markers of synaptic plasticity; the latter is considered to be a neuronal microtubule protein marker. The immunoreactivity of all three proteins was less in the H/R injured group than in the control group. These results indicate that cerebral ischemia suppresses the expression of synaptophysin, PSD-95, and MAP2 in ischemic brain and that synaptic neuronal microtubule proteins were damaged by ischemic injury.

3.2. H/R Injury in Neuro2A Cells Inhibited, and H89 Pretreatment Restored, Neurite Outgrowth. Neurite outgrowth of Neuro2A cells was assessed by measuring neurite length with ImageJ software (Figure 3). The average length of normal N2A cells was approximately 65 μm , whereas neurites of cells subjected to H/R injury were approximately 26 μm long (Figure 3(a)). Neurites from cells that had been pretreated with H89 before H/R injury were, on average, approximately 45 μm , or almost twice that of the injured cells that were not pretreated (Figure 3(a)). Bright-field images showed the neurite length in all groups (Figures 3(b), 3(c), and 3(d)). The yellow line in all images permits easy comparison of neurite lengths.

We also performed RT-PCR (Figure 4) to assess MAP2, a protein essential to neurite growth [41, 42]. The mRNA level of MAP2 in H/R injured N2A cells was reduced considerably compared to the control group (Figure 4). We conclude that H/R injury leads to reduction of neurite outgrowth, which can be alleviated by H89 pretreatment. Thus, H89 may ameliorate the effects of H/R injury.

3.3. Cell Survival Was Increased in H89 Pretreated Neuro2A Cells after H/R Injury. To confirm whether or not H89 is involved in the neuronal cell death during H/R injury, we conducted the immunocytochemistry (Figures 5(a) and 5(b)), western blot analysis (Figures 5(c) and 5(d)), and RT-PCR (Figure 7(b)) using cleaved caspase-3 (as a marker of mitochondrial cell death) and Bcl2 (as a marker of anti-apoptosis) antibodies. H/R injured N2A cells were observed: the reduced Bcl2 immunoreactivity (Figure 5(b)),

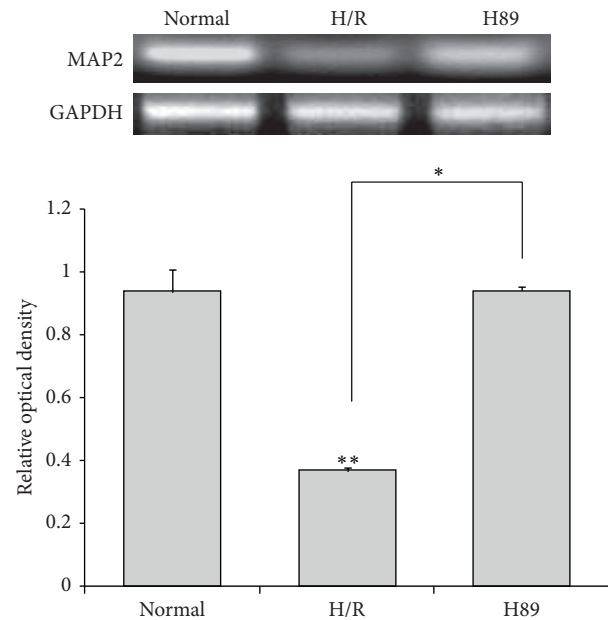


FIGURE 4: The measurement of MAP2 mRNA level in Neuro2A cells after PKA inhibitor treatment. MAP2 mRNA levels were measured by using RT-PCR. The H89 group showed higher mRNA levels of MAP2 compared to the hypoxia reperfusion injury group. Data were expressed as mean \pm S.E.M, and each experiment included 3 repeats per condition. GAPDH was used as a control. Differences were considered significant at * $P < 0.05$ and ** $P < 0.001$. Normal: the normal control group, H/R: 4 hr hypoxia and 18 hr reperfusion injury group, and H89: 2 hr PKA inhibitor H89 treatment group before 4 hr hypoxia and 18 hr reperfusion injury.

the decreased Bcl2 mRNA level (Figure 7(b)), the attenuated Bcl2 protein level (Figure 5(d)), the increased cleaved caspase-3 immunoreactivity (Figure 5(a)), and the increased cleaved caspase-3 protein level (Figure 5(c)). H89 pretreatment before H/R injury group showed the increased Bcl2 expression (Figures 5(b), 5(d), and 7(b)) and the reduced cleaved caspase-3 expression (Figures 5(a) and 5(c)) compared with the H/R group. These results indicated that the cell death in N2A cells was attenuated by H89 pretreatment in spite of hypoxia and reperfusion injury. Thus, we suggest that H89 may contribute to the neuronal cell survival pathway under hypoxia and reperfusion injury.

3.4. The Increase of BDNF Expression in Neuro2A Cells Pretreated with H89 in Hypoxia Reperfusion Injury. We performed immunocytochemistry analysis (Figure 6) and RT-PCR (Figure 7(a)) using BDNF as the representative of neurotrophic factors in N2A cells to examine whether there was the alteration of neurotrophic factor expression in H89 pretreated N2A cells under hypoxia and reperfusion injury. We observed evidently lesser immunoreactivity of BDNF (Figure 6) in the H/R injured N2A cells compared to the normal control group. However, BDNF- (Figure 6) positive cells were obviously more expressed in H89 pretreated N2A cells than the H/R injury group. In addition, the BDNF mRNA level in N2A cells was higher in H89 pretreated N2A

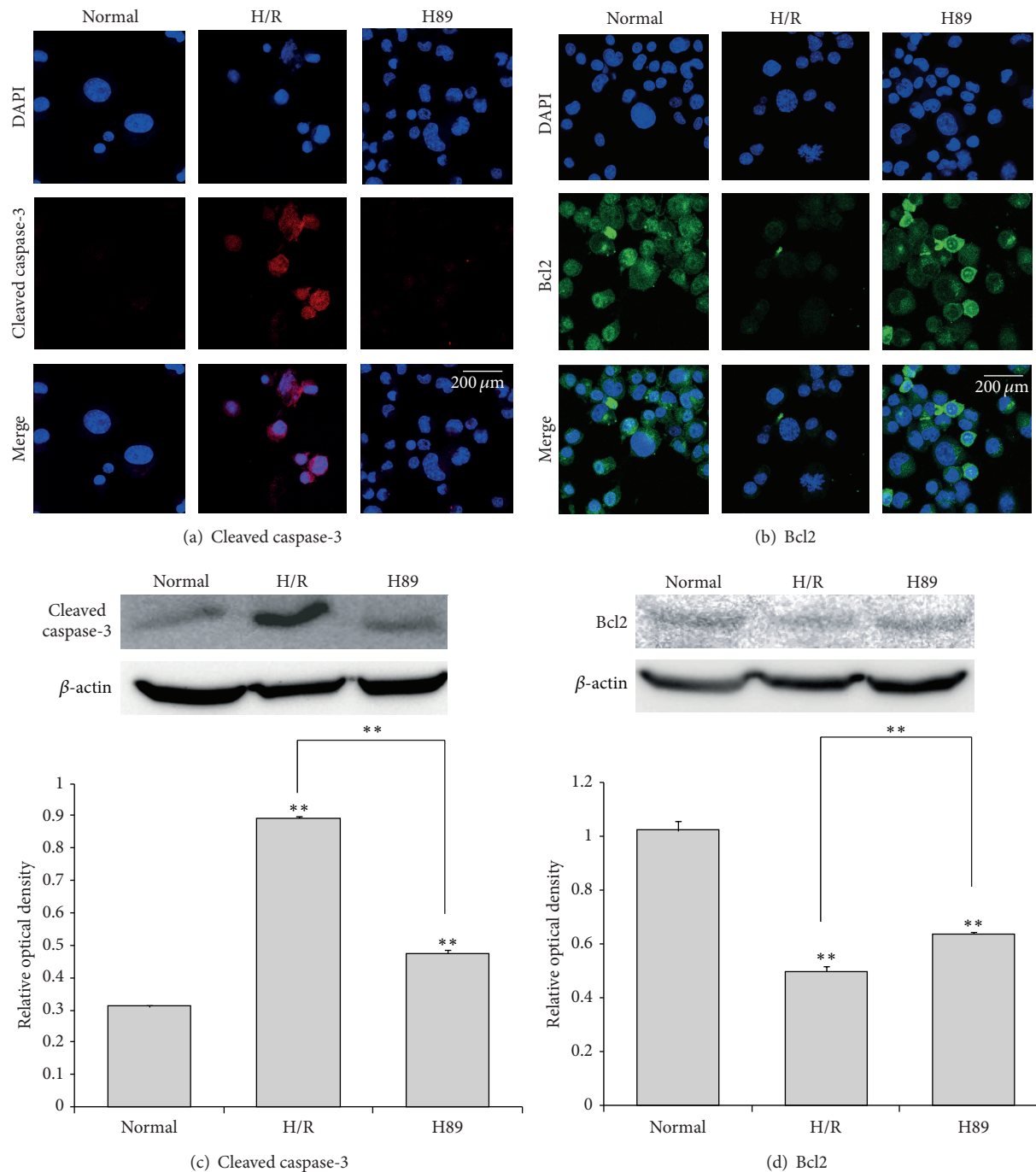


FIGURE 5: The measurement of cleaved caspase-3 and Bcl2 expression in Neuro2A cells after H/R-induced injury. (a) The level of cleaved caspase-3 was evaluated by immunocytochemistry. This image shows that the expression of cleaved caspase-3 in the H/R group was strongly increased compared to the normal group. Cleaved caspase-3 expression was attenuated in H89 pretreatment treatment group under H/R-induced injury. (b) The level of Bcl2 was evaluated by immunocytochemistry. This image shows that the expression of Bcl2 in the H/R group was increased compared to the normal group. PKA inhibitor H89 pretreatment preserved the expression of Bcl2 in spite of hypoxia reperfusion injury. (c) Western blotting experiments showed that the relative protein expression of cleaved caspase-3 evidently attenuated in the H89 group compared to the hypoxia reperfusion group. (d) Western blotting experiments showed that the relative protein expression of Bcl2 slightly increased in the H89 group compared to the hypoxia reperfusion group. Data were expressed as mean \pm S.E.M, and each experiment included 4 repeats per condition. Differences were considered significant $**P < 0.001$. Scale bar: 200 μm , cleaved caspase-3: red, Bcl2: green, 4',6-diamidino-2-phenylindole (DAPI): blue, normal: the normal control group, H/R: 4 hr hypoxia and 18 hr reperfusion injury group, and H89: 2 hr PKA inhibitor H89 treatment group before 4 hr hypoxia and 18 hr reperfusion injury.

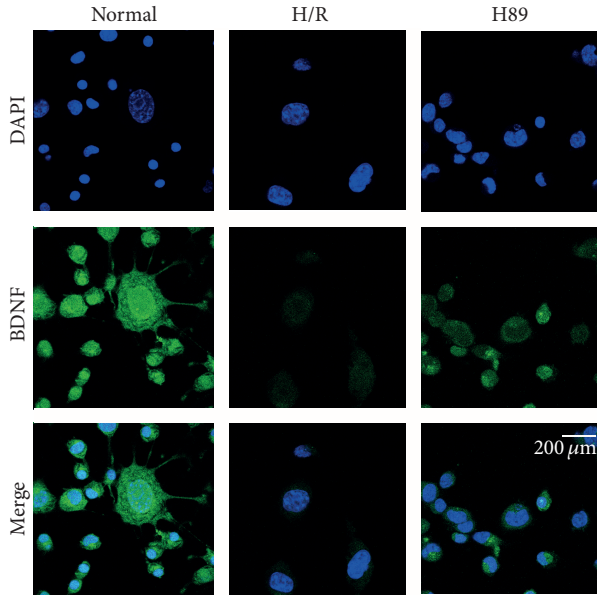


FIGURE 6: The measurement of BDNF expression in Neuro2A cells after H/R-induced injury. The level of BDNF was evaluated by immunocytochemistry. This image shows that the expression of BDNF in the H/R group was reduced compared to the normal group. H89 pretreatment increased the expression of BDNF in N2A cells in spite of hypoxia reperfusion injury. Scale bar: 200 μ m, BDNF: green, 4',6-diamidino-2-phenylindole (DAPI): blue, normal: the normal control group, H/R: 4 hr hypoxia and 18 hr reperfusion injury group, and H89: 2 hr PKA inhibitor H89 treatment group before 4 hr hypoxia and 18 hr reperfusion injury.

cells than the H/R injury group. These results showed that hypoxia and reperfusion stress suppresses the expression of BDNF in N2A cells, whereas H89 pretreatment H/R injured N2A cells considerably did not reduced the expression of BDNF against H/R injury. Based on these consequences, our results suggest that neurotrophic factor BDNF's expression was not reduced by H89 pretreatment despite ischemic injury. Thus, H89 may contribute to the expression of BDNF in N2A cells following hypoxia and reperfusion stress.

3.5. The Preservation of PSD-95 Expression in Neuro2A Cells Pretreated with H89 during Hypoxia Reperfusion Injury. We performed immunocytochemistry analysis (Figure 8(a)) and western blot analysis (Figure 8(b)) using PSD-95 antibody in N2A cells to investigate whether there was the alteration of synaptic plasticity related proteins in H89 pretreated N2A cells under hypoxia and reperfusion injury. In addition, we confirmed evidently decreased immunoreactivity of PSD-95 (Figure 8(a)) in the H/R injured N2A cells compared to the normal control group. On the other hand, the immunoreactivity of PSD-95 was more increased in H89 pretreated N2A cells than the H/R injury group (Figure 8(a)). Moreover, the protein level of PSD-95 (Figure 8(b)) in N2A cells was slightly higher in H89 pretreated N2A cells than the H/R injury group. These results indicated that hypoxia and reperfusion stress reduced the expression of PSD-95 in N2A cells, whereas H89 pretreatment H/R injured N2A cells considerably did not

reduce expression of PSD-95 against H/R injury compared to H/R injured N2A cells. It is possible to extrapolate these results to suggest that the H/R injury reduced the expression of PSD-95. Data tend to support the conclusion that H89 may alleviate the synaptic plasticity damage of N2A cells against ischemic stress.

3.6. The Measurement of Phosphorylation AKT Protein Level in H89 Pretreated Neuro2A Cells against Hypoxia Reperfusion Injury. We performed western blot analysis (Figure 9) using AKT and phosphorylation-AKT (p-AKT) antibody in N2A cells to investigate the change of AKT phosphorylation in H89 pretreated N2A cells under hypoxia and reperfusion injury. The protein level of phosphorylation-AKT (Figure 9) was evidently increased in H89 pretreated H/R injured N2A cells than the H/R injury group. This result shows that H89 considerably promotes the activation of AKT signaling in N2A cells against H/R injury. Our data supports the hypothesis that H89 may boost the phosphorylation of AKT in N2A cells to survive the cells against ischemic stress.

4. Discussion

In cerebral ischemia, the reduction of synaptic dysfunction and neuronal cell loss are important issues and are implicated in severe pathogenesis such as memory impairment following ischemic stroke [26–29, 52, 53]. In the search for a solution, many researchers study the molecules and the signal pathways that lead to reduced synaptic plasticity and cell death [54–56]; an example of one is PKA signaling [3–7]. H89, known as the molecule commonly used to inhibit PKA action, recently has been reported to have a variety of functions unrelated to its effect on PKA inhibition [16, 18, 21, 57]. H89 affects ROCK II and, through that effect, cell morphology [48] and neurite extension [58, 59]. The data presented here indicate that H89 promotes neurite outgrowth and protects it after hypoxia stress. MAP2 (known as the neuron specific cytoskeletal protein) is present during all stages of neuromorphogenesis [60] and is necessary for neurite initiation [60–62]. Our MAP2 expression data support the contention that H89 may also support neurite outgrowth through MAP2. We speculate that the maintenance of neurite outgrowth after ischemic stroke is central to the role of H89. Several studies have demonstrated that H89 induces autophagy in cells independent of PKA signaling [24, 25] and increases cell survival after inflammation [54, 63]. In the present study, we observed reduced expression of cleaved caspase-3 and increased expression of Bcl2 following pretreatment with H89, supporting the conclusion that H89 protects against hypoxia injury, specifically, that it increases neuronal cell survival rate after ischemic stroke. Neurotrophic molecules regulate synaptic plasticity of the nervous system [64–66]. Specifically, many researches demonstrated that BDNF accelerates the axogenesis [30–32], promotes poststroke plasticity in an in vivo study [32, 67–71], and contributes to healthy brain function, notably, neuronal survival and maintenance, neurogenesis, modulation of dendritic branching and dendritic spine morphology [72, 73],

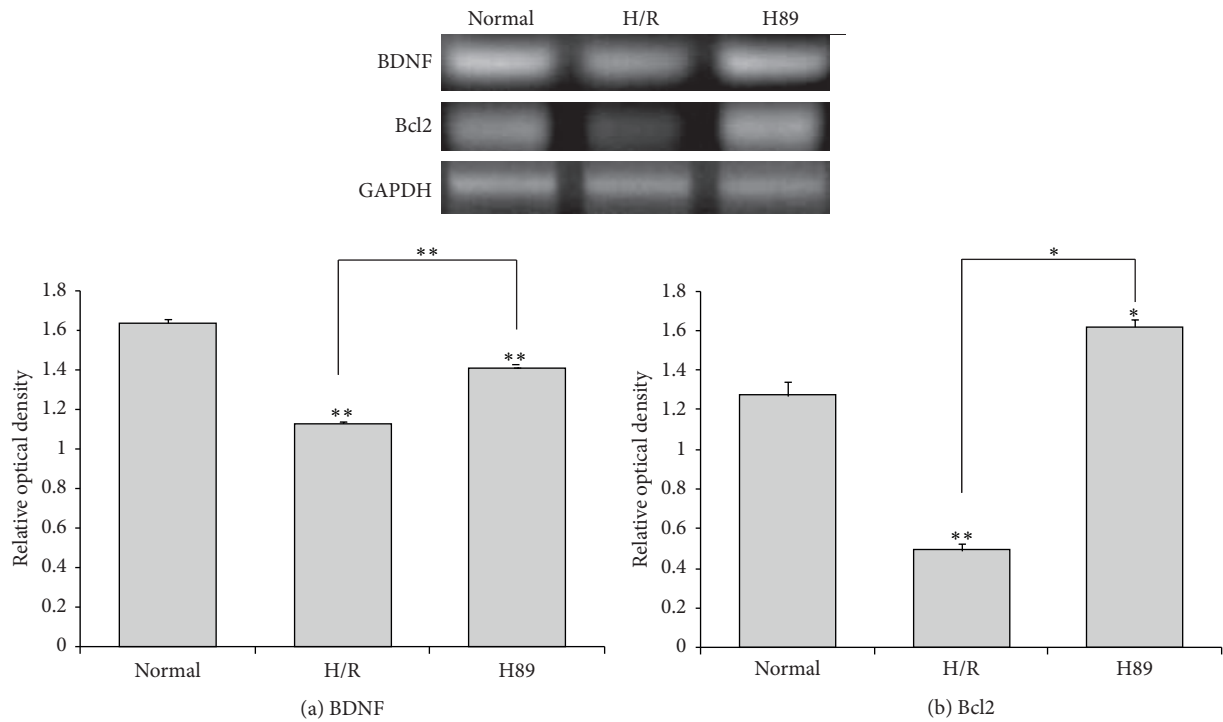


FIGURE 7: The measurement of BDNF and Bcl2 mRNA level in Neuro2A cells after H/R-induced injury. (a) BDNF and (b) Bcl2 mRNA levels were measured by using RT-PCR. The H89 pretreatment group showed higher mRNA levels of (a) BDNF and (b) Bcl2 compared to the hypoxia reperfusion injury group. Data were expressed as mean \pm S.E.M, and each experiment included 3 repeats per condition. GAPDH was used as a control. Differences were considered significant at * $P < 0.05$ and ** $P < 0.001$. Normal: the normal control group, H/R: 4 hr hypoxia and 18 hr reperfusion injury group, H89: 2 hr PKA inhibitor H89 treatment group before 4 hr hypoxia and 18 hr reperfusion injury.

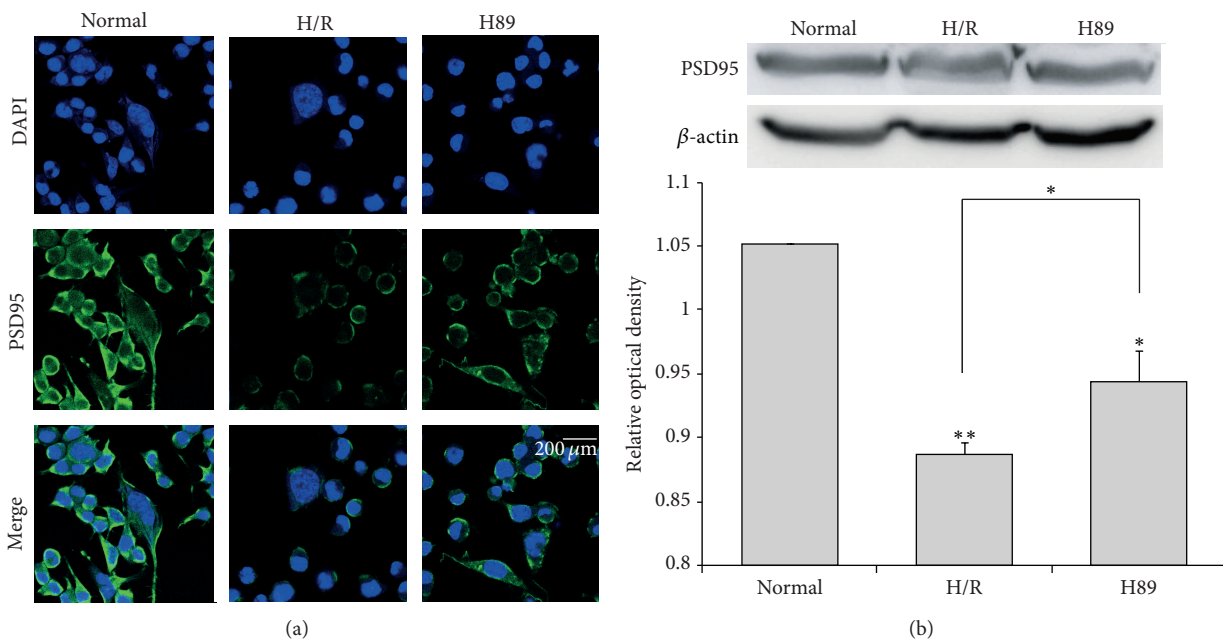


FIGURE 8: The measurement of PSD-95 expression in Neuro2A cells after H/R-induced injury. The level of PSD-95 was evaluated by immunocytochemistry. This image shows that the expression of PSD-95 in the H/R group was decreased compared to the normal group. PKA inhibitor H89 pretreatment increased the expression of PSD-95 in spite of hypoxia reperfusion injury. (b) Western blotting experiments showed that the relative protein expression of PSD-95 slightly increased in the H89 group compared to the hypoxia reperfusion group. β -actin was used as an internal control. Data were expressed as mean \pm S.E.M, and each experiment included 4 repeats per condition. Differences were considered significant at * $P < 0.05$ and ** $P < 0.001$. Scale bar: 200 μ m, PSD-95: green, 4', 6-diamidino-2-phenylindole (DAPI): blue, normal: the normal control group, H/R: 4 hr hypoxia and 18 hr reperfusion injury group, and H89: 2 hr PKA inhibitor H89 treatment group before 4 hr hypoxia and 18 hr reperfusion injury.

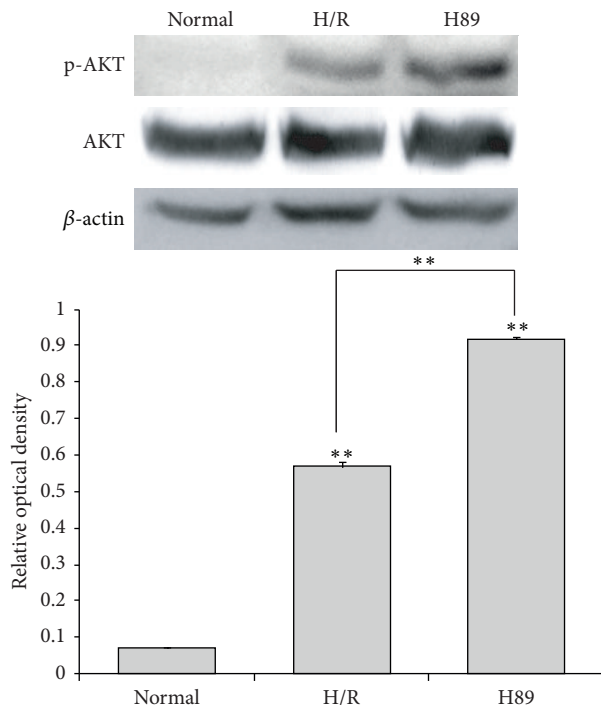


FIGURE 9: The measurement of AKT phosphorylation in Neuro2A cell against H/R injury. Western blotting experiments showed that the relative protein level of phosphorylation-AKT (p-AKT)/AKT significantly was increased in the H89 pretreatment group compared to the hypoxia and reperfusion group. β -actin was used as an internal control. Data were expressed as mean \pm S.E.M, and each experiment included 4 repeats per condition. Differences were considered significant at $**P < 0.001$. Normal: the normal control group, H/R: 4 hr hypoxia and 18 hr reperfusion injury group, H89: 2 hr PKA inhibitor H89 treatment group before 4 hr hypoxia and 18 hr reperfusion injury, and p-AKT: phosphorylation-AKT.

and development of neuronal connections required for learning and memory [74–76]. BDNF, through phosphorylation of its TrkB receptor, activates a neuron-specific protein, controls the actin cytoskeleton in dendritic spines [77] and their regression [78, 79], and promotes the actin polymerization [80]. Inhibition of BDNF synthesis results in smaller spine heads and impairs long-term potentiation of synaptic transmission [81, 82]. Moreover, BDNF signaling plays a crucial role in the development of synapses by controlling the transport of PSD-95, which is the major scaffolding protein at mature glutamate synapses [83, 84]. PSD-95 itself and its interaction with BDNF signaling have been implicated in diverse brain diseases [85–87]. When localized in postsynaptic terminals, PSD-95 has an important role in postsynaptic function and plasticity [88–90]. The loss of PSD-95 results in severe cognitive decline due to loss of neurons and synaptic disruption [91–93]. In addition, synaptophysin as a marker of the pre-synaptic nerve terminal density is essential for vesicle fusion and the release of neurotransmitter [94]. The reduction of synaptophysin has been reported to reduce synaptic plasticity in the brain [95, 96]. Our results suggest that H89 may enhance synaptic plasticity by promoting

the BDNF expression in neuronal cells under ischemic brain injury. Also H89 may be involved in neurite outgrowth by regulating the preservation of synaptic proteins, such as PSD-95 and synaptophysin, following ischemic brain damage. AKT which is activated by phosphatidylinositol 3-kinase activity [97] has known to promote a cellular protection after ischemic injury in the brain [98]. Moreover, AKT has been reported that it mediates anti-apoptosis signalings in ischemic stroke studies [99, 100]. Some study indicated that H89 markedly enhances the phosphorylation of AKT [101]. Considering our results, we assume that H89 may contribute to the survival of neuronal cells against ischemic injury through the activation of AKT. In present study, although learning and memory were not assessed in the animal model used here and we have some limitations to identify the specific molecular mechanism by H89, we propose that H89 may ameliorate the pathophysiology following ischemic stroke by reducing neuronal cell death and involving synaptic plasticity.

Conflict of Interests

The authors declare that they have no conflict of interests regarding the publication of this paper.

Acknowledgment

This research was supported by the Basic Science Research Program through the National Research Foundation of Korea (NRF) funded by the Ministry of Education, Science, and Technology (NRF-2014R1A2A2A01006556).

References

- [1] D. A. Walsh, J. P. Perkins, and E. G. Krebs, "An adenosine 3',5'-monophosphate-dependant protein kinase from rabbit skeletal muscle," *The Journal of Biological Chemistry*, vol. 243, no. 13, pp. 3763–3765, 1968.
- [2] V. F. Castellucci, E. R. Kandel, and J. H. Schwartz, "Intracellular injection of the catalytic subunit of cyclic AMP-dependent protein kinase simulates facilitation of transmitter release underlying behavioral sensitization in *Aplysia*," *Proceedings of the National Academy of Sciences of the United States of America*, vol. 77, no. 12, pp. 7492–7496, 1980.
- [3] M. Brunelli, V. Castellucci, and E. R. Kandel, "Synaptic facilitation and behavioral sensitization in *Aplysia*: possible role of serotonin and cyclic AMP," *Science*, vol. 194, no. 4270, pp. 1178–1181, 1976.
- [4] E. R. Kandel, "The molecular biology of memory storage: a dialog between genes and synapses," *Bioscience Reports*, vol. 21, no. 5, pp. 565–611, 2001.
- [5] R. E. Rydel and L. A. Greene, "cAMP analogs promote survival and neurite outgrowth in cultures of rat sympathetic and sensory neurons independently of nerve growth factor," *Proceedings of the National Academy of Sciences of the United States of America*, vol. 85, no. 4, pp. 1257–1261, 1988.
- [6] J. Qiu, D. Cai, H. Dai et al., "Spinal axon regeneration induced by elevation of cyclic AMP," *Neuron*, vol. 34, no. 6, pp. 895–903, 2002.

- [7] B. D. Burrell and C. L. Sahley, "Learning in simple systems," *Current Opinion in Neurobiology*, vol. 11, no. 6, pp. 757–764, 2001.
- [8] A. Ferro, M. Coash, T. Yamamoto, J. Rob, Y. Ji, and L. Queen, "Nitric oxide-dependent beta2-adrenergic dilatation of rat aorta is mediated through activation of both protein kinase A and Akt," *British Journal of Pharmacology*, vol. 143, no. 3, pp. 397–403, 2004.
- [9] A. Sobolewski, K. B. Jourdan, P. D. Upton, L. Long, and N. W. Morrell, "Mechanism of cicaprost-induced desensitization in rat pulmonary artery smooth muscle cells involves a PKA-mediated inhibition of adenylyl cyclase," *American Journal of Physiology—Lung Cellular and Molecular Physiology*, vol. 287, no. 2, pp. L352–L359, 2004.
- [10] K. Kaneishi, Y. Sakuma, H. Kobayashi, and M. Kato, "3',5'-cyclic adenosine monophosphate augments intracellular Ca^{2+} concentration and gonadotropin-releasing hormone (GnRH) release in immortalized GnRH neurons in an Na^{+} -dependent manner," *Endocrinology*, vol. 143, no. 11, pp. 4210–4217, 2002.
- [11] S. H. Kim, S. J. Won, X. O. Mao, K. Jin, and D. A. Greenberg, "Involvement of protein kinase A in cannabinoid receptor-mediated protection from oxidative neuronal injury," *Journal of Pharmacology and Experimental Therapeutics*, vol. 313, no. 1, pp. 88–94, 2005.
- [12] K. Burvall, L. Palmberg, and K. Larsson, "Expression of TNF α and its receptors R1 and R2 in human alveolar epithelial cells exposed to organic dust and the effects of 8-bromo-cAMP and protein kinase A modulation," *Inflammation Research*, vol. 54, no. 7, pp. 281–288, 2005.
- [13] A. C. Skinn and W. K. MacNaughton, "Nitric oxide inhibits cAMP-dependent CFTR trafficking in intestinal epithelial cells," *The American Journal of Physiology—Gastrointestinal and Liver Physiology*, vol. 289, no. 4, pp. G739–G744, 2005.
- [14] T. Chijiwa, A. Mishima, M. Hagiwara et al., "Inhibition of forskolin-induced neurite outgrowth and protein phosphorylation by a newly synthesized selective inhibitor of cyclic AMP-dependent protein kinase, N-[2-(pBromocinnamylamino)ethyl]-5-isoquinolinesulfonamide (H-89), of PC12 pheochromocytoma cells," *The Journal of Biological Chemistry*, vol. 265, no. 9, pp. 5267–5272, 1990.
- [15] H. Hidaka, M. Inagaki, S. Kawamoto, and Y. Sasaki, "Isoquinolinesulfonamides, novel and potent inhibitors of cyclic nucleotide dependent protein kinase and protein kinase C," *Biochemistry*, vol. 23, no. 21, pp. 5036–5041, 1984.
- [16] S. P. Davies, H. Reddy, M. Caivano, and P. Cohen, "Specificity and mechanism of action of some commonly used protein kinase inhibitors," *Biochemical Journal*, vol. 351, part 1, pp. 95–105, 2000.
- [17] D. W. Singleton, C. L. Lu, R. Colella, and F. J. Roisen, "Promotion of neurite outgrowth by protein kinase inhibitors and ganglioside GM1 in neuroblastoma cells involves MAP kinase ERK1/2," *International Journal of Developmental Neuroscience*, vol. 18, no. 8, pp. 797–805, 2000.
- [18] M. Hussain, G. A. Drago, M. Bhogal, J. Colyer, and C. H. Orchard, "Effects of the protein kinase A inhibitor H-89 on Ca^{2+} regulation in isolated ferret ventricular myocytes," *Pflügers Archiv*, vol. 437, no. 4, pp. 529–537, 1999.
- [19] P. Lahouratate, J. Guibert, J.-C. Camelin, and I. Bertrand, "Specific inhibition of cardiac and skeletal muscle sarcoplasmic reticulum Ca^{2+} pumps by H-89," *Biochemical Pharmacology*, vol. 54, no. 9, pp. 991–998, 1997.
- [20] N. Palacios, F. Sánchez-Franco, M. Fernández, I. Sánchez, G. Villuendas, and L. Cacicedo, "Opposite effects of two PKA inhibitors on cAMP inhibition of IGF-I-induced oligodendrocyte development: a problem of unspecificity?" *Brain Research*, vol. 1178, no. 1, pp. 1–11, 2007.
- [21] C. Pearman, W. Kent, N. Bracken, and M. Hussain, "H-89 inhibits transient outward and inward rectifier potassium currents in isolated rat ventricular myocytes," *British Journal of Pharmacology*, vol. 148, no. 8, pp. 1091–1098, 2006.
- [22] S. H. Um, D. D'Alessio, and G. Thomas, "Nutrient overload, insulin resistance, and ribosomal protein S6 kinase 1, S6K1," *Cell Metabolism*, vol. 3, no. 6, pp. 393–402, 2006.
- [23] I. Ruvinsky and O. Meyuhas, "Ribosomal protein S6 phosphorylation: from protein synthesis to cell size," *Trends in Biochemical Sciences*, vol. 31, no. 6, pp. 342–348, 2006.
- [24] A. Lochner and J. A. Moolman, "The many faces of H89: a review," *Cardiovascular Drug Reviews*, vol. 24, no. 3–4, pp. 261–274, 2006.
- [25] A. J. Murray, "Pharmacological PKA inhibition: all may not be what it seems," *Science Signaling*, vol. 1, no. 22, article re4, 2008.
- [26] N. Khatri and H.-Y. Man, "Synaptic activity and bioenergy homeostasis: implications in brain trauma and neurodegenerative diseases," *Frontiers in Neurology*, vol. 4, article 199, 2013.
- [27] J. T. Neumann, C. H. Cohan, K. R. Dave, C. B. Wright, and M. A. Perez-Pinzon, "Global cerebral ischemia: synaptic and cognitive dysfunction," *Current Drug Targets*, vol. 14, no. 1, pp. 20–35, 2013.
- [28] J. Hofmeijer, A. T. B. Mulder, A. C. Farinha, M. J. A. M. van Putten, and J. le Feber, "Mild hypoxia affects synaptic connectivity in cultured neuronal networks," *Brain Research*, vol. 1557, pp. 180–189, 2014.
- [29] W. Li, R. Huang, R. A. Shetty et al., "Transient focal cerebral ischemia induces long-term cognitive function deficit in an experimental ischemic stroke model," *Neurobiology of Disease*, vol. 59, pp. 18–25, 2013.
- [30] M. P. Mattson and J. Partin, "Evidence for mitochondrial control of neuronal polarity," *Journal of Neuroscience Research*, vol. 56, no. 1, pp. 8–20, 1999.
- [31] M. P. Mattson, "Pathways towards and away from Alzheimer's disease," *Nature*, vol. 430, no. 7000, pp. 631–639, 2004.
- [32] R. H. Lipsky and A. M. Marini, "Brain-derived neurotrophic factor in neuronal survival and behavior-related plasticity," *Annals of the New York Academy of Sciences*, vol. 1122, pp. 130–143, 2007.
- [33] B. Lu, K. H. Wang, and A. Nose, "Molecular mechanisms underlying neural circuit formation," *Current Opinion in Neurobiology*, vol. 19, no. 2, pp. 162–167, 2009.
- [34] J. Burkhalter, H. Fiumelli, I. Allaman, J.-Y. Chatton, and J.-L. Martin, "Brain-derived neurotrophic factor stimulates energy metabolism in developing cortical neurons," *The Journal of Neuroscience*, vol. 23, no. 23, pp. 8212–8220, 2003.
- [35] M. P. Kashyap, A. K. Singh, D. K. Yadav et al., "4-Hydroxy-trans-2-nonenal (4-HNE) induces neuronal SH-SY5Y cell death via hampering ATP binding at kinase domain of Akt1," *Archives of Toxicology*, vol. 89, no. 1–2, pp. 243–258, 2014.
- [36] G. B. Chiarotto, L. Drummond, G. Cavarretto, A. L. Bombeiro, and A. L. R. de Oliveira, "Neuroprotective effect of tempol (4 hydroxy-tempo) on neuronal death induced by sciatic nerve transection in neonatal rats," *Brain Research Bulletin*, vol. 106, pp. 1–8, 2014.

- [37] S. W. Scheff, D. A. Price, M. A. Ansari et al., "Synaptic change in the posterior cingulate gyrus in the progression of Alzheimer's disease," *Journal of Alzheimer's Disease*, vol. 43, no. 3, pp. 1073–1090, 2015.
- [38] R. Sultana, W. A. Banks, and D. A. Butterfield, "Decreased levels of PSD95 and two associated proteins and increased levels of BCL2 and caspase 3 in hippocampus from subjects with amnesic mild cognitive impairment: insights into their potential roles for loss of synapses and memory, accumulation of A β , and neurodegeneration in a prodromal stage of Alzheimer's disease," *Journal of Neuroscience Research*, vol. 88, no. 3, pp. 469–477, 2010.
- [39] Q. Li, H. F. Zhao, Z. F. Zhang et al., "Long-term green tea catechin administration prevents spatial learning and memory impairment in senescence-accelerated mouse prone-8 mice by decreasing Abeta1-42 oligomers and upregulating synaptic plasticity-related proteins in the hippocampus," *Neuroscience*, vol. 163, no. 3, pp. 741–749, 2009.
- [40] H. Kim, L. I. Binder, and J. L. Rosenbaum, "The periodic association of MAP2 with brain microtubules in vitro," *The Journal of Cell Biology*, vol. 80, no. 2, pp. 266–276, 1979.
- [41] S. C. Selden and T. D. Pollard, "Phosphorylation of microtubule-associated proteins regulates their interaction with actin filaments," *The Journal of Biological Chemistry*, vol. 258, no. 11, pp. 7064–7071, 1983.
- [42] S. C. Selden and T. D. Pollard, "Interaction of actin filaments with microtubules is mediated by microtubule-associated proteins and regulated by phosphorylation," *Annals of the New York Academy of Sciences*, vol. 466, pp. 803–812, 1986.
- [43] R. F. Sattilaro, "Interaction of microtubule-associated protein 2 with actin filaments," *Biochemistry*, vol. 25, no. 8, pp. 2003–2009, 1986.
- [44] A. W. Unterberg, J. Stover, B. Kress, and K. L. Kiening, "Edema and brain trauma," *Neuroscience*, vol. 129, no. 4, pp. 1021–1029, 2004.
- [45] Y. Nakamura, N. Nakamichi, T. Takarada, K. Ogita, and Y. Yoneda, "Transferrin receptor-1 suppresses neurite outgrowth in neuroblastoma Neuro2A cells," *Neurochemistry International*, vol. 60, no. 5, pp. 448–457, 2012.
- [46] Z. Y. Mei, C. M. Chin, J. C. Yoon et al., "Agmatine inhibits matrix metalloproteinase-9 via endothelial nitric oxide synthase in cerebral endothelial cells," *Neurological Research*, vol. 29, no. 7, pp. 749–754, 2007.
- [47] M. Wieprecht, T. Wieder, and C. C. Geilen, "N-[2-bromocinnamyl(amino)ethyl]-5-isoquinolinesulphonamide (H-89) inhibits incorporation of choline into phosphatidylcholine via inhibition of choline kinase and has no effect on the phosphorylation of CTP:phosphocholine cytidyltransferase," *Biochemical Journal*, vol. 297, part 1, pp. 241–247, 1994.
- [48] J. Leemhuis, S. Boutillier, G. Schmidt, and D. K. Meyer, "The protein kinase A inhibitor H89 acts on cell morphology by inhibiting Rho kinase," *The Journal of Pharmacology & Experimental Therapeutics*, vol. 300, no. 3, pp. 1000–1007, 2002.
- [49] T. Watanabe, Y. Yasutaka, T. Nishioku et al., "Atorvastatin stimulates neuroblastoma cells to induce neurite outgrowth by increasing cellular prion protein expression," *Neuroscience Letters*, vol. 531, no. 2, pp. 114–119, 2012.
- [50] K. Yuasa, T. Nagame, M. Dohi et al., "cGMP-dependent protein kinase I is involved in neurite outgrowth via a Rho effector, rohtekin, in Neuro2A neuroblastoma cells," *Biochemical and Biophysical Research Communications*, vol. 421, no. 2, pp. 239–244, 2012.
- [51] H.-J. Jung, Y.-H. Jeon, K. K. Bokara et al., "Agmatine promotes the migration of murine brain endothelial cells via multiple signaling pathways," *Life Sciences*, vol. 92, no. 1, pp. 42–50, 2013.
- [52] M. C. Tjepkema-Cloostermans, R. Hindriks, J. Hofmeijer, and M. J. A. M. van Putten, "Generalized periodic discharges after acute cerebral ischemia: reflection of selective synaptic failure?" *Clinical Neurophysiology*, vol. 125, no. 2, pp. 255–262, 2014.
- [53] Y.-D. Zhao, S.-Y. Cheng, S. Ou, P.-H. Chen, and H.-Z. Ruan, "Functional response of hippocampal CA1 pyramidal cells to neonatal hypoxic-ischemic brain damage," *Neuroscience Letters*, vol. 516, no. 1, pp. 5–8, 2012.
- [54] H. Park, P. Licznarski, K. N. Alavian, M. Shanabrough, and E. A. Jonas, "Bcl-xL is necessary for neurite outgrowth in hippocampal neurons," *Antioxidants & Redox Signaling*, vol. 22, no. 2, pp. 93–108, 2015.
- [55] J. Thundiyil, S. Manzanero, D. Pavlovski et al., "Evidence that the EphA2 receptor exacerbates ischemic brain injury," *PLoS ONE*, vol. 8, no. 1, Article ID e53528, 2013.
- [56] N. G. Bazan, V. L. Marcheselli, and K. Cole-Edwards, "Brain response to injury and neurodegeneration: endogenous neuroprotective signaling," *Annals of the New York Academy of Sciences*, vol. 1053, pp. 137–147, 2005.
- [57] B. Eftekharzadeh, M. Ramin, F. Khodagholi et al., "Inhibition of PKA attenuates memory deficits induced by β -amyloid (1–42), and decreases oxidative stress and NF- κ B transcription factors," *Behavioural Brain Research*, vol. 226, no. 1, pp. 301–308, 2012.
- [58] H. Bito, T. Furuyashiki, H. Ishihara et al., "A critical role for a Rho-associated kinase, p160ROCK, in determining axon outgrowth in mammalian CNS neurons," *Neuron*, vol. 26, no. 2, pp. 431–441, 2000.
- [59] G. Tigyi, D. J. Fischer, Á. Sebök, F. Marshall, D. L. Dyer, and R. Milei, "Lysophosphatidic acid-induced neurite retraction in PC12 cells: neurite-protective effects of cyclic AMP signaling," *Journal of Neurochemistry*, vol. 66, no. 2, pp. 549–558, 1996.
- [60] A. Caceres, G. A. Banker, and L. Binder, "Immunocytochemical localization of tubulin and microtubule-associated protein 2 during the development of hippocampal neurons in culture," *The Journal of Neuroscience*, vol. 6, no. 3, pp. 714–722, 1986.
- [61] R. Bernhardt and A. Matus, "Light and electron microscopic studies of the distribution of microtubule-associated protein 2 in rat brain: a difference between dendritic and axonal cytoskeletons," *Journal of Comparative Neurology*, vol. 226, no. 2, pp. 203–221, 1984.
- [62] A. Caceres, J. Mautino, and K. S. Kosik, "Suppression of MAP2 in cultured cerebellar macroneurons inhibits minor neurite formation," *Neuron*, vol. 9, no. 4, pp. 607–618, 1992.
- [63] L. P. Sousa, A. F. Carmo, B. M. Rezende et al., "Cyclic AMP enhances resolution of allergic pleurisy by promoting inflammatory cell apoptosis via inhibition of PI3K/Akt and NF- κ B," *Biochemical Pharmacology*, vol. 78, no. 4, pp. 396–405, 2009.
- [64] M. P. Mattson, "Neurotransmitters in the regulation of neuronal cytoarchitecture," *Brain Research*, vol. 472, no. 2, pp. 179–212, 1988.
- [65] G. Loers and M. Schachner, "Recognition molecules and neural repair," *Journal of Neurochemistry*, vol. 101, no. 4, pp. 865–882, 2007.
- [66] K. Gottmann, T. Mittmann, and V. Lessmann, "BDNF signaling in the formation, maturation and plasticity of glutamatergic and GABAergic synapses," *Experimental Brain Research*, vol. 199, no. 3–4, pp. 203–234, 2009.
- [67] D. K. Binder and H. E. Scharfman, "Brain-derived neurotrophic factor," *Growth Factors*, vol. 22, no. 3, pp. 123–131, 2004.

- [68] J. Chen, C. Zhang, H. Jiang et al., "Atorvastatin induction of VEGF and BDNF promotes brain plasticity after stroke in mice," *Journal of Cerebral Blood Flow and Metabolism*, vol. 25, no. 2, pp. 281–290, 2005.
- [69] W.-R. Schäbitz, C. Berger, R. Kollmar et al., "Effect of brain-derived neurotrophic factor treatment and forced arm use on functional motor recovery after small cortical ischemia," *Stroke*, vol. 35, no. 4, pp. 992–997, 2004.
- [70] M. W. Kim, M. S. Bang, T. R. Han et al., "Exercise increased BDNF and trkB in the contralateral hemisphere of the ischemic rat brain," *Brain Research*, vol. 1052, no. 1, pp. 16–21, 2005.
- [71] W.-R. Schäbitz, T. Steigleder, C. M. Cooper-Kuhn et al., "Intravenous brain-derived neurotrophic factor enhances poststroke sensorimotor recovery and stimulates neurogenesis," *Stroke*, vol. 38, no. 7, pp. 2165–2172, 2007.
- [72] H. W. Horsch and L. C. Katz, "BDNF release from single cells elicits local dendritic growth in nearby neurons," *Nature Neuroscience*, vol. 5, no. 11, pp. 1177–1184, 2002.
- [73] J.-I. Tanaka, Y. Horiike, M. Matsuzaki, T. Miyazaki, G. C. R. Ellis-Davies, and H. Kasai, "Protein synthesis and neurotrophin-dependent structural plasticity of single dendritic spines," *Science*, vol. 319, no. 5870, pp. 1683–1687, 2008.
- [74] A. K. McAllister, D. C. Lo, and L. C. Katz, "Neurotrophins regulate dendritic growth in developing visual cortex," *Neuron*, vol. 15, no. 4, pp. 791–803, 1995.
- [75] S. L. Patterson, T. Abel, T. A. S. Deuel, K. C. Martin, J. C. Rose, and E. R. Kandel, "Recombinant BDNF rescues deficits in basal synaptic transmission and hippocampal LTP in BDNF knockout mice," *Neuron*, vol. 16, no. 6, pp. 1137–1145, 1996.
- [76] H. W. Horsch, A. Krüttgen, S. D. Portbury, and L. C. Katz, "Destabilization of cortical dendrites and spines by BDNF," *Neuron*, vol. 23, no. 2, pp. 353–364, 1999.
- [77] C. Sala, V. Piëch, N. R. Wilson, M. Passafaro, G. Liu, and M. Sheng, "Regulation of dendritic spine morphology and synaptic function by Shank and Homer," *Neuron*, vol. 31, no. 1, pp. 115–130, 2001.
- [78] M. Bennett, "Positive and negative symptoms in schizophrenia: the NMDA receptor hypofunction hypothesis, neuregulin/ErbB4 and synapse regression," *Australian and New Zealand Journal of Psychiatry*, vol. 43, no. 8, pp. 711–721, 2009.
- [79] B. Xu, K. Zang, N. L. Ruff et al., "Cortical degeneration in the absence of neurotrophin signaling: dendritic retraction and neuronal loss after removal of the receptor TrkB," *Neuron*, vol. 26, no. 1, pp. 233–245, 2000.
- [80] C. R. Bramham and D. G. Wells, "Dendritic mRNA: transport, translation and function," *Nature Reviews Neuroscience*, vol. 8, no. 10, pp. 776–789, 2007.
- [81] J. J. An, K. Gharami, G.-Y. Liao et al., "Distinct role of Long 3' UTR BDNF mRNA in spine morphology and synaptic plasticity in hippocampal neurons," *Cell*, vol. 134, no. 1, pp. 175–187, 2008.
- [82] E. G. Waterhouse and B. Xu, "New insights into the role of brain-derived neurotrophic factor in synaptic plasticity," *Molecular and Cellular Neuroscience*, vol. 42, no. 2, pp. 81–89, 2009.
- [83] A. Yoshii and M. Constantine-Paton, "BDNF induces transport of PSD-95 to dendrites through PI3K-AKT signaling after NMDA receptor activation," *Nature Neuroscience*, vol. 10, no. 6, pp. 702–711, 2007.
- [84] A. Yoshii, Y. Murata, J. Kim, C. Zhang, K. M. Shokat, and M. Constantine-Paton, "TrkB and protein kinase M ζ regulate synaptic localization of PSD-95 in developing cortex," *The Journal of Neuroscience*, vol. 31, no. 33, pp. 11894–11904, 2011.
- [85] N.-P. Tsai, J. R. Wilkerson, W. Guo et al., "Multiple autism-linked genes mediate synapse elimination via proteasomal degradation of a synaptic scaffold PSD-95," *Cell*, vol. 151, no. 7, pp. 1581–1594, 2012.
- [86] C. Cao, M. S. Rioult-Pedotti, P. Migani et al., "Impairment of TrkB-PSD-95 signaling in Angelman syndrome," *PLoS Biology*, vol. 11, no. 2, Article ID e1001478, 2013.
- [87] J. Mukai, A. Dhillia, L. J. Drew et al., "Palmitoylation-dependent neurodevelopmental deficits in a mouse model of 22q11 microdeletion," *Nature Neuroscience*, vol. 11, no. 11, pp. 1302–1310, 2008.
- [88] A. E.-D. El-Husseini, E. Schnell, D. M. Chetkovich, R. A. Nicoll, and D. S. Bredt, "PSD-95 involvement in maturation of excitatory synapses," *Science*, vol. 290, no. 5495, pp. 1364–1368, 2000.
- [89] C. A. Vickers, B. Stephens, J. Bowen, G. W. Arbuthnott, S. G. N. Grant, and C. A. Ingham, "Neurone specific regulation of dendritic spines in vivo by post synaptic density 95 protein (PSD-95)," *Brain Research*, vol. 1090, no. 1, pp. 89–98, 2006.
- [90] K. Radwanska, N. I. Medvedev, G. S. Pereira et al., "Mechanism for long-term memory formation when synaptic strengthening is impaired," *Proceedings of the National Academy of Sciences of the United States of America*, vol. 108, no. 45, pp. 18471–18475, 2011.
- [91] K. Han and E. Kim, "Synaptic adhesion molecules and PSD-95," *Progress in Neurobiology*, vol. 84, no. 3, pp. 263–283, 2008.
- [92] R. D. Terry, E. Masliah, D. P. Salmon et al., "Physical basis of cognitive alterations in Alzheimer's disease: synapse loss is the major correlate of cognitive impairment," *Annals of Neurology*, vol. 30, no. 4, pp. 572–580, 1991.
- [93] S. W. Scheff, D. A. Price, F. A. Schmitt, M. A. Scheff, and E. J. Mufson, "Synaptic loss in the inferior temporal gyrus in mild cognitive impairment and Alzheimer's disease," *Journal of Alzheimer's Disease*, vol. 24, no. 3, pp. 547–557, 2011.
- [94] P. Greengard, F. Valtorta, A. J. Czernik, and F. Benfenati, "Synaptic vesicle phosphoproteins and regulation of synaptic function," *Science*, vol. 259, no. 5096, pp. 780–785, 1993.
- [95] G. M. A. Cunha, P. M. Canas, C. R. Oliveira, and R. A. Cunha, "Increased density and synapto-protective effect of adenosine A2A receptors upon sub-chronic restraint stress," *Neuroscience*, vol. 141, no. 4, pp. 1775–1781, 2006.
- [96] S. Rapp, M. Baader, M. Hu, C. Jennen-Steinmetz, F. A. Henn, and J. Thome, "Differential regulation of synaptic vesicle proteins by antidepressant drugs," *Pharmacogenomics Journal*, vol. 4, no. 2, pp. 110–113, 2004.
- [97] A. Toker and L. C. Cantley, "Signalling through the lipid products of phosphoinositide-3-OH kinase," *Nature*, vol. 387, no. 6634, pp. 673–676, 1997.
- [98] A. Yamaguchi, M. Tamatani, H. Matsuzaki et al., "Akt activation protects hippocampal neurons from apoptosis by inhibiting transcriptional activity of p53," *Journal of Biological Chemistry*, vol. 276, no. 7, pp. 5256–5264, 2001.
- [99] Y. Zhang, T. S. Park, and J. M. Gidday, "Hypoxic preconditioning protects human brain endothelium from ischemic apoptosis by Akt-dependent survivin activation," *American Journal of Physiology—Heart and Circulatory Physiology*, vol. 292, no. 6, pp. H2573–H2581, 2007.
- [100] S. Dimmeler, B. Assmus, C. Hermann, J. Haendeler, and A. M. Zeiher, "Fluid shear stress stimulates phosphorylation of Akt in human endothelial cells: involvement in suppression of apoptosis," *Circulation Research*, vol. 83, no. 3, pp. 334–341, 1998.

- [101] Y. Kato, N. Ozaki, T. Yamada, Y. Miura, and Y. Oiso, “H-89 potentiates adipogenesis in 3T3-L1 cells by activating insulin signaling independently of protein kinase A,” *Life Sciences*, vol. 80, no. 5, pp. 476–483, 2007.

Research Article

Statins Promote Long-Term Recovery after Ischemic Stroke by Reconnecting Noradrenergic Neuronal Circuitry

Kyoung Joo Cho,¹ So Young Cheon,² and Gyung Whan Kim¹

¹Department of Neurology, College of Medicine, Yonsei University, Seoul 120-752, Republic of Korea

²Department of Anesthesiology and Pain, College of Medicine, Yonsei University, Seoul 120-752, Republic of Korea

Correspondence should be addressed to Gyung Whan Kim; gyungkim@yuhs.ac

Received 13 February 2015; Revised 6 April 2015; Accepted 28 April 2015

Academic Editor: Midori A. Yenari

Copyright © 2015 Kyoung Joo Cho et al. This is an open access article distributed under the Creative Commons Attribution License, which permits unrestricted use, distribution, and reproduction in any medium, provided the original work is properly cited.

Inhibitors of HMG-CoA reductase (statins), widely used to lower cholesterol in coronary heart and vascular disease, are effective drugs in reducing the risk of stroke and improving its outcome in the long term. After ischemic stroke, cardiac autonomic dysfunction and psychological problems are common complications related to deficits in the noradrenergic (NA) system. This study investigated the effects of statins on the recovery of NA neuron circuitry and its function after transient focal cerebral ischemia (tFCI). Using the wheat germ agglutinin (WGA) transgene technique combined with the recombinant adenoviral vector system, NA-specific neuronal pathways were labeled, and were identified in the locus coeruleus (LC), where NA neurons originate. NA circuitry in the atorvastatin-treated group recovered faster than in the vehicle-treated group. The damaged NA circuitry was partly reorganized with the gradual recovery of autonomic dysfunction and neurobehavioral deficit. Newly proliferated cells might contribute to reorganizing NA neurons and lead anatomic and functional recovery of NA neurons. Statins may be implicated to play facilitating roles in the recovery of the NA neuron and its function.

1. Introduction

Therapeutic aims after CNS injury are to prevent second complications in acute stage and to enhance functional recovery of the damaged brain in chronic stage. The neurological secondary implications contain urinary disorders, depression, or dementia [1]. Cardiac complications including sudden death are also frequent during recovery phase after stroke [2]. Response to increased serum cardiac enzyme and high blood pressure, plasma noradrenaline (NA) levels are often elevated [3, 4]. Dysfunction of the noradrenergic system is a frequent feature in various neurodegenerative disorders such as Alzheimer's disease and Parkinson's disease, as well as in acute ischemic stroke. At stroke onset, ischemic sites and lesion size may be related to different characteristics of autonomic dysfunction [5]. Malfunction in the noradrenergic system is also implicated in many psychiatric disorders manifesting abnormal social behavior, attention deficit, hyperactivity, anxiety, and depression. Brain ischemia induces pathological synaptic plasticity caused by delayed neuronal death and induces physiological plasticity which leads to structural

reorganization resulting in functional recovery [6, 7]. NA has been reported to regulate neural stem cell and also act as a positive modulator for hippocampal neurogenesis in vitro and in vivo [8]. In adult mice, alteration of noradrenergic system could affect neurogenesis and consequently improve the performing ability to perceptual learning task [9].

Inhibitors of 3-hydroxy-3-methylglutaryl-coenzyme A (HMG-CoA) reductase are widely used for secondary stroke prevention [10]. Statin has been reported to have numerous effects on neuron survival, angiogenesis, and neurogenesis as well as lipid-lowering activity [11, 12]. Along with these therapeutic usage, it was been mainly investigated whether statin treatment, HMG-CoA reductase inhibition, could promote neurological recovery, perilesional, and contralateral neuronal plasticity in the post-acute stroke phase promotes [13]. Administration of rosuvastatin for 30 days after middle cerebral artery occlusion (MCAO) showed the effect on reducing dementia [13]. Similar results were also reported in treatment by simvastatin or atorvastatin [14]. Additionally, statin might be related to reducing risk of dementia [15–17], and it received attention regarding playing

another role in neurodegenerative disease. In Parkinson's disease (PD) animal model, simvastatin treatment showed various neuroprotective effects by interacting with NMDA receptor [18] and also by regulating muscarinic M1/4 receptor [19]. Additionally, mevalonate pathway inhibited the neurites outgrowth by blocking the cell rounding rapidly induced [17].

However, it is extremely poorly reported that statin affects NA system which is deeply affected and altered by cerebral ischemic stroke and closely related to chronic disabilities of physical and emotional type. This current study presented the visualized noradrenergic neuronal circuitry using a genetic tracing method and investigated the effects of statins on the functional recovery after stroke by focusing on NA neuron circuitry and its function. We put the point on the behavioral improvement in chronic stage by statin treatment.

2. Materials and Methods

2.1. Animal Model and Drug Treatment. To obtain focal cerebral ischemia animal model, adult male C57BL/6 mice (23–26 g; Orient Co., Gyeonggi-do, South Korea) were housed in a 12 h light/dark cycle and permitted food and water. These mice were anesthetized by inhalation of isoflurane in N₂O/O₂ (%, 70:30) and subjected to fFCI by MCA occlusion with a surgical nylon suture (5.0, Silkam, B. Braum, PA, USA) for 1 hour. A Laser Doppler flowmeter (Transonic System Inc., New York, USA) probe placed directly on the skull surface over the territory of the MCA (1 mm posterior and 5 mm lateral to bregma) measured regional CBF before and after occlusion and immediately before sacrifice. Blood pressure was monitored by cannulating a femoral artery with Pressure Transducer (Harvard Apparatus, Inc., Holliston, MA, USA). All procedures were approved by the animal care committee at Yonsei University medical college. Statin (atorvastatin) was dissolved to concentration of 1 mg/mL in 5% methanol (methanol 10 μ L in saline 20 mL). The prepared statin solution was treated with intraperitoneal injection with 10 mg/kg from 1 day after MCAO.

2.2. MRI Analysis and Infarct Size Measurement. To obtain consecutive brain damage images, we performed MRI scans of mice. For MRI analysis, mice were put on a horizontal bore (400 mm) after anesthetizing with isoflurane by 4.7 Tesla MR scanner (Brucker Biospin, Billerica, MA, USA). Images were obtained using a T2-weighted fast spin echo sequence. Diffusion images were also acquired. Temperature was maintained and respiration was monitored throughout the entire scan. Mice recovered quickly following the scan with a 100% survival rate. Among the obtained MR images, 4 cuts were used in infarct size measurement and were combined. Each damage region was measured by ImageJ and represented by relative value with area of contralateral side versus damaged area of ipsilateral side.

2.3. Recombinant Adenoviral Construction and Viral Infection. The procedure for generation of recombinant adenoviruses was described and performed previously [20, 21]. The PRS-WGA adenovirus was friendly gifted from Dr. Huh, Kyung Hee University. A gene cassette containing the WGA gene

downstream of the PRS2x8 promoter was inserted into the pAdTrack plasmid and finally into the pAdEasy1. Recombinant adenoviral DNA was cut with *PacI* and transfected into HEK293 cells using Lipofectamine (Invitrogen, CA, USA). Viruses were harvested 5 days after transfection from the transfected HEK293 cells and amplified on dishes. The viral particles were purified by cesium chloride density gradient ultracentrifugation, dialyzed, and tittered.

Animals were anesthetized and placed in a stereotaxic instrument. After incision of the skin, a small burr hole was made directly at LC (5.4 mm posterior, 1.0 mm lateral, and 3.8 mm deep to bregma) and the viral vector was unilaterally injected into the LC of ischemic hemisphere using a Hamilton syringe (Hamilton Co., Nevada, USA). A single injection of 0.2–0.3 μ L of the concentrated adenovirus suspension (about 2×10^{13} cfu/mL) was used in this study. The scalp was then sutured, and then the mouse was returned to standard housing. After 2 days of virus injection, mice were perfused with 4% formaldehyde and the brains were removed for histological analysis.

2.4. Immunohistochemistry. Fixed mouse brains were sectioned with a cryostat to obtain 40 μ m sections, respectively. The sections were pretreated for 20 min with 1% H₂O₂ in PBS containing 0.3% Triton X-100 for inactivation of endogenous peroxidase activity and permeabilization of cells. The sections were then incubated for 30 min with 5% normal rabbit serum in PBS to block nonspecific protein-binding sites and incubated with anti-WGA polyclonal antibody (1:2000, Vector Laboratory, CA, USA) and anti-BrdU monoclonal antibody (1:200, AbD Serotec, UK) in PBS containing 0.3% Triton X-100 with 2% normal rabbit serum overnight at 4°C and for 2 hours at room temperature. After washing, the sections were incubated with biotin-labeled anti-goat IgG (1:200, Vector Laboratory) followed by Vectastain ABC elite kit (Vector Laboratory), TSA kit (Perkin Elmer, Boston, USA), and Vectastain ABC elite kit again. Signals were visualized with Ni²⁺-intensified diaminobenzidine/peroxide reaction kit (Vector Laboratory). Specimens were observed with a microscope and computerized digital camera system (Olympus, Tokyo, Japan: Provis) and an image analysis system and program (Adobe Photoshop, San Jose, CA).

2.5. BrdU Labeling and Tissue Processing. Cell proliferation was measured by the incorporation of the thymidine analogue 5'-bromo-2-deoxyuridine (BrdU) that is incorporated into the DNA of dividing cells in immunohistochemically detectable quantities during the S phase of cell division. After MCAO, the animals were twice injected intraperitoneally with BrdU (Roche) (50 mg/kg at a concentration of 10 mg/mL in 0.9% NaCl) at 24 hours and 1 hour before sacrifice. For immunohistochemical detection of incorporated BrdU, double-stranded DNA was denatured to a single-stranded form suitable for immunohistochemical detection on sections. Sections were incubated in 50% formamide in standard sodium citrate at 65°C for 2 hours and treated further with 2 M HCl at 35°C for 30 min. After being rinsed for 10 min at room temperature in 0.1 M boric acid, the sections were washed with PBS and then incubated with 0.03% H₂O₂ in

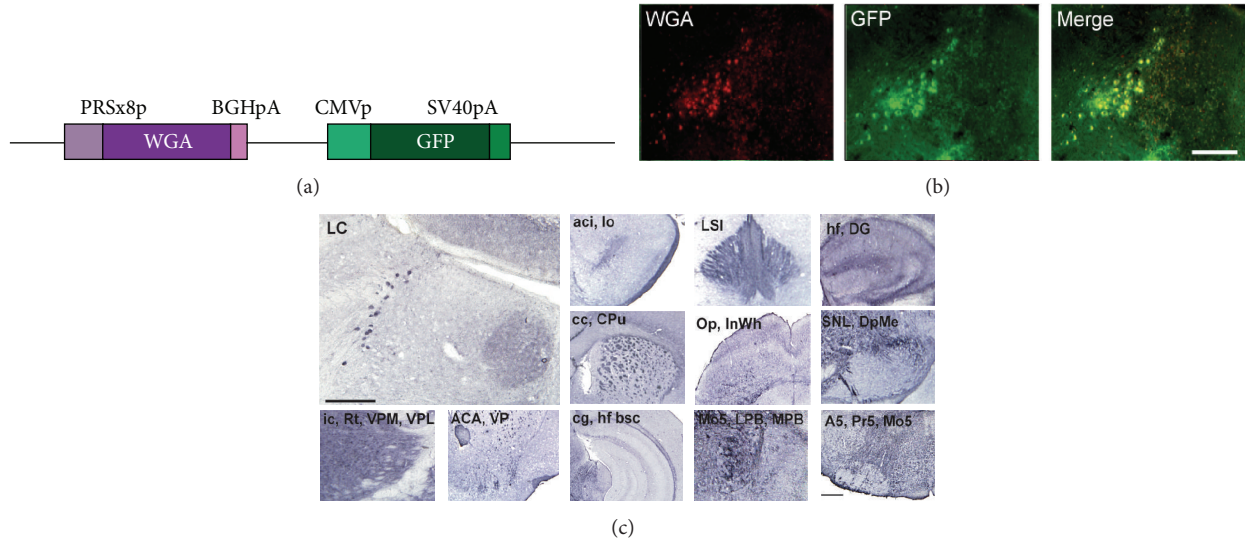


FIGURE 1: Expression of WGA and GFP in LC, detecting PRS-WGA adenovirus. (a) Schematic diagram representing the structure of the transgene. (b) WGA immunoreactivity in the noninjured mouse brain. After 2 days of PRS-WGA adenovirus injection in the LC, LC-originated WGA protein was detected in NA neurons and other areas. Scale bars = 500 μ m.

methanol for 5 min. The sections were incubated with a primary antibody against BrdU (1:1,000, Roche Diagnostics) at room temperature for 30 minutes, washed with PBS, and reacted with a FITC-conjugated secondary antibody (1:200, Jackson ImmunoResearch, PA, USA) for 30 min at room temperature. After washing, stained tissue samples were mounted using Vectashield mounting medium (Vector Lab, Burlingame, CA, USA).

2.6. Behavioral Assessment-Light/Dark Transition Test and Resident-Aggression-Intruder Test

2.6.1. Light/Dark Transition Test. The test is based on the aversive nature of mice to light and on their spontaneous exploratory behavior in new environments [22]. The apparatus for the test consisted of a dark chamber and a bright chamber. There are gates to pass between two chambers and mice are allowed to move freely between the two chambers. The test is performed in the bright illuminated chamber and the number of entries into the dark chamber evaluated for 5 min. Besides the number of transitions, latent time in dark chamber was evaluated.

2.6.2. Resident-Aggression-Intruder Test. Mice were habituated in the same cage for at least over 1 week. Aggression level was assessed with three sessions at three-day interval. Evaluating items were duration of aggressive behavior and the number of aggression. Duration of aggression indicates the sum of time that determine resident animal the duration to show active move action toward intruder, social exploration, lateral threat, or clinch attack. Latency to attack was expressed by measuring the time between the introduction of the intruder and the first clinch attack.

2.7. Data Analysis. The data were expressed as mean \pm S.D. The statistical comparisons were performed by unpaired *t*-test and one-way ANOVA (StatView, SAS Institute, Inc., Cary, NC, USA). The significance between the groups was assigned at **p* < 0.05 and ***p* < 0.001.

3. Results

3.1. Adenovirus-Mediated NA Neuron Expressing WGA in the Locus Coeruleus (LC). Adenoviral construct used in this study contains the wheat germ agglutinin (WGA) gene under control of the eight copies of PRS promoter and the green fluorescent protein (GFP) gene under the control of the cytomegalovirus (CMV) promoter, which makes it possible to detect viral delivery to the target sites (Figure 1(a)). After injection of the PRS-WGA adenovirus to the LC, localization of GFP expression and WGA protein was examined on adjacent coronal sections. Colocalization of GFP and WGA demonstrates that WGA protein was synthesized in NA neurons of the LC in our previous report [21]. In sagittal sections of noninjured brain, intense WGA immunoreactivity was detected in the pontine reticular nucleus, motor and sensory trigeminal nucleus, thalamic nucleus, lateral hypothalamic area, deep mesencephalic nucleus, superior colliculus, caudate putamen, corpus callosum, anterior commissure, and olfactory bulb (Figure 1(b)). WGA immunoreactivity was also observed in the parabrachial nucleus, A5 NA cells, substantia nigra, lateral habenular nucleus, hippocampus, optic tract, and piriform cortex in coronal sections (Figure 1(b)). In adenovirus infected mice there was no evidence of cell loss or tissue damage due to the viral infection in LC. All of the experimental animals that recovered after the infection remained healthy until being sacrificed without exhibiting any behavioral abnormalities.

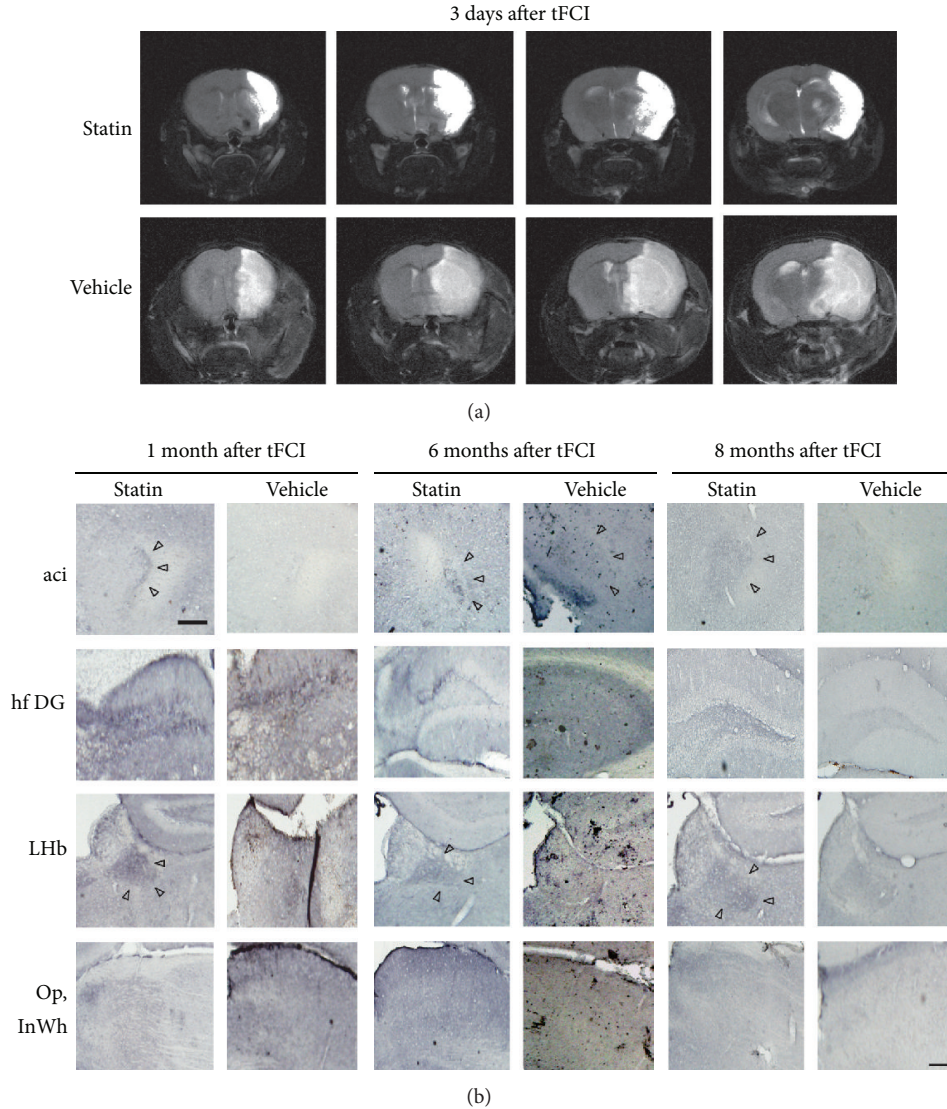


FIGURE 2: Immunoreactivity of WGA in the tFCI mouse brain. WGA immunoreactivity at 30, 180, and 240 days after tFCI in the vehicle- and atorvastatin-treated groups showed that NA circuitry in the atorvastatin-treated group recovered faster than in the vehicle-treated group at 180 days. aci: anterior commissure, intrabulbar part; hf DG: hippocampal fissure and dentate gyrus; LHb: lateral habenular nucleus; Op: optic nerve layer of the superior colliculus; InWh: intermediate gray layer of the superior colliculus. Scale bar = 500 μ m.

3.2. Transsynaptic Transfer of WGA in Noradrenergic Neurons of Vehicle-Treated and Statin-Treated Mice after MCA Occlusion. After transient focal cerebral ischemia (tFCI), WGA immunoreactivity showed the transsynaptic pattern of NA neurons according to day in each vehicle-treated or statin-treated mouse (Figure 2). NA circuits containing thalamic area, lateral hypothalamic area, cortex, and hippocampus were destroyed with severe infarction (data not shown). Although a large infarction was formed in the MCA territory, mice that survived slowly and gradually recovered the damaged area in the long-term stage (Figure 2(a)). When statin was given for a long period, the convalescence periods were faster than the vehicle-treated mice (Figure 2(b)). Whereas WGA immunoreactivity was not detected in some region such as superior colliculus from 1 month to 8 months

in vehicle-treated mice after tFCI, a very strong WGA immunoreactivity was observed in the statin-treated mice in the intrabulbar part of the anterior commissure (aci) and lateral habenular nucleus (LHb). These features indicated that damaged NA circuits were partly reorganized over time in the area of previous lesion.

3.3. Ischemic Brain Damage and Convalescent Process after MCAO in Vehicle- or Statin-Treated Mice. Physiological data and regional cerebral blood flow (rCBF) were measured. There were no statistically significant differences in rCBF during ischemic condition between the group before occlusion and the group after reperfusion (10 min before occlusion, $100 \pm 0\%$; 10 min after occlusion, 23.1 ± 5.3 ; 10 min after reperfusion, 96.2 ± 3.7 ; mean \pm S.D. of each value; $n = 9$, each

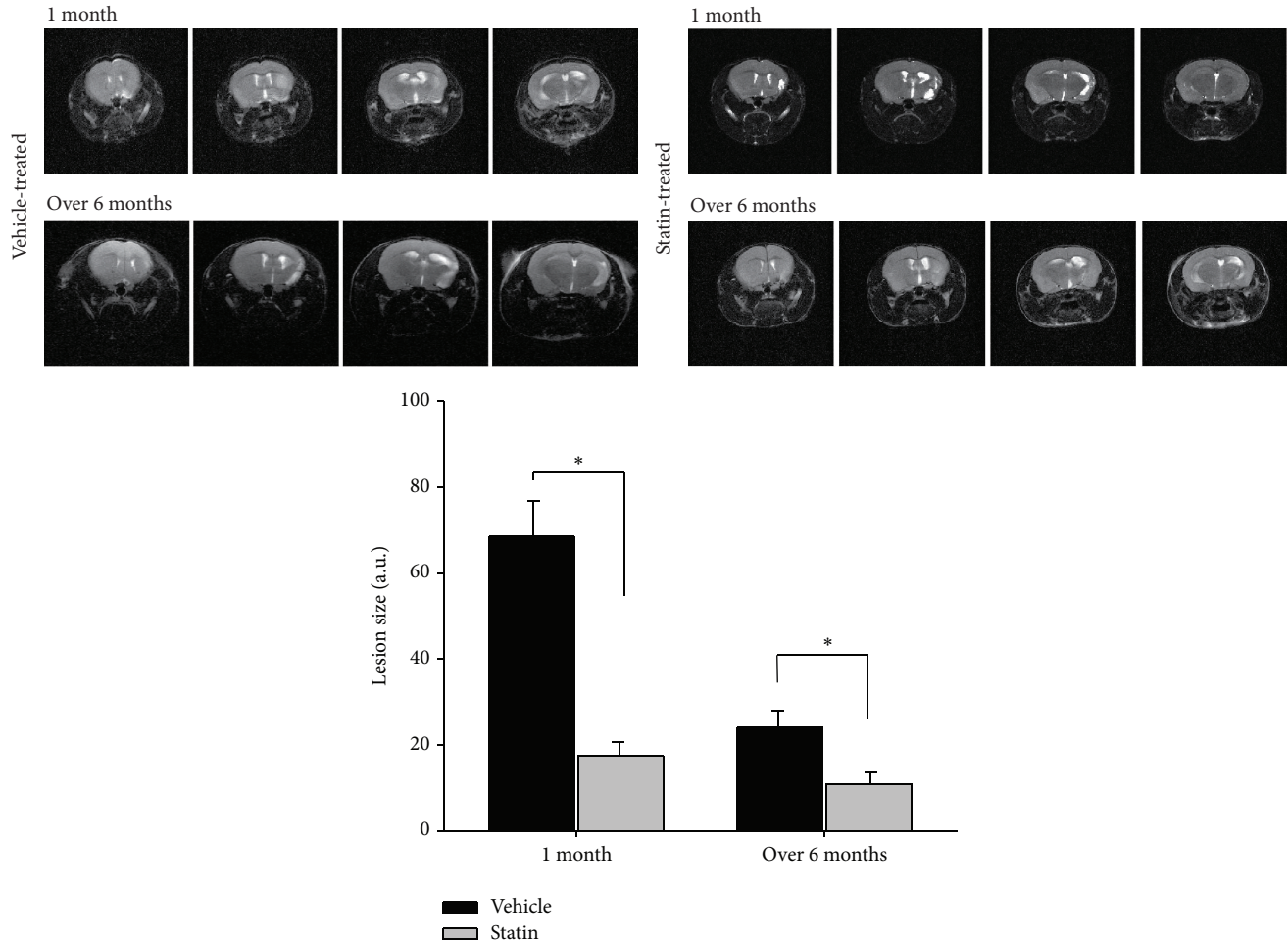


FIGURE 3: Ischemic brain damage and convalescent processes shown by magnetic resonance imaging (MRI) after MCAO.

group). Presented in the magnetic resonance images (MRI), the infarcted area after reperfusion from MCAO was gradually reduced, and significantly statin-treated mice showed smaller infarct area than vehicle-treated mice (Figure 3). After a longer period, the damaged brain region was naturally ameliorated even in the vehicle-treated mice, but the recovery showed earlier in statin-treated mice than vehicle-treated mice. The differences in the recovery time determined the behavioral improvement and related to NA neuron circuitry, as shown in the result of the behavior test (Figure 5).

3.4. Neurogenesis after Ischemic Injury in Normal and Vehicle- or Atorvastatin-Treated Mice. In postischemic brain injury, neuronal cells derived from neural precursor cells are newly born and the cells can be detected by bromodeoxyuridine (BrdU). The BrdU-immunopositive cells were observed in the postischemic cortex, striatum, and subventricular zone (SVZ) on the ipsilateral side of the ischemic infarct at 1 month and 6 months (Figures 4(a) and 4(b)). The BrdU-positive cells were more frequently observed in the ipsilateral side of the statin-treated mice than in the contralateral side. Especially at 1 month after tFCI, many BrdU- and NeuN-immunopositive cells were detected in the lesioned cortex

and striatum at the direct site to ischemic damage by MCAO (Figure 4(c)). It could be implicated that newborn cells have arisen from the SVZ and migrated into striatum and even into cortical area. Moreover, the proliferation of neural cells is promoted by long-term statin treatment. At 6 months and 8 months after fFCI, the incidence of BrdU-positive cells in the ipsilateral striatum and cortex was significantly diminished compared to that of 1 month after fFCI (data not shown). The BrdU-positive cells were not detected in either striatum or cortex, but a few BrdU-positive cells were detected in SVZ and corpus callosum.

3.5. Neurological Outcome and Physiological Parameters according to NA Circuitry. The mean arterial blood pressure (MABP) slightly increased until 4 months after fFCI and then gradually returned to the initial level at 8 months (Figure 5(a)). In contrast, statin treatment for a long period sustained the constant MABP level overall duration after tFCI. The body temperature and weight governed by NA system were also monitored according to month, but they just slightly oscillated with no significant changes. To evaluate the NA system alteration after tFCI and effects of statin on the NA system after tFCI, mice performed the light/dark

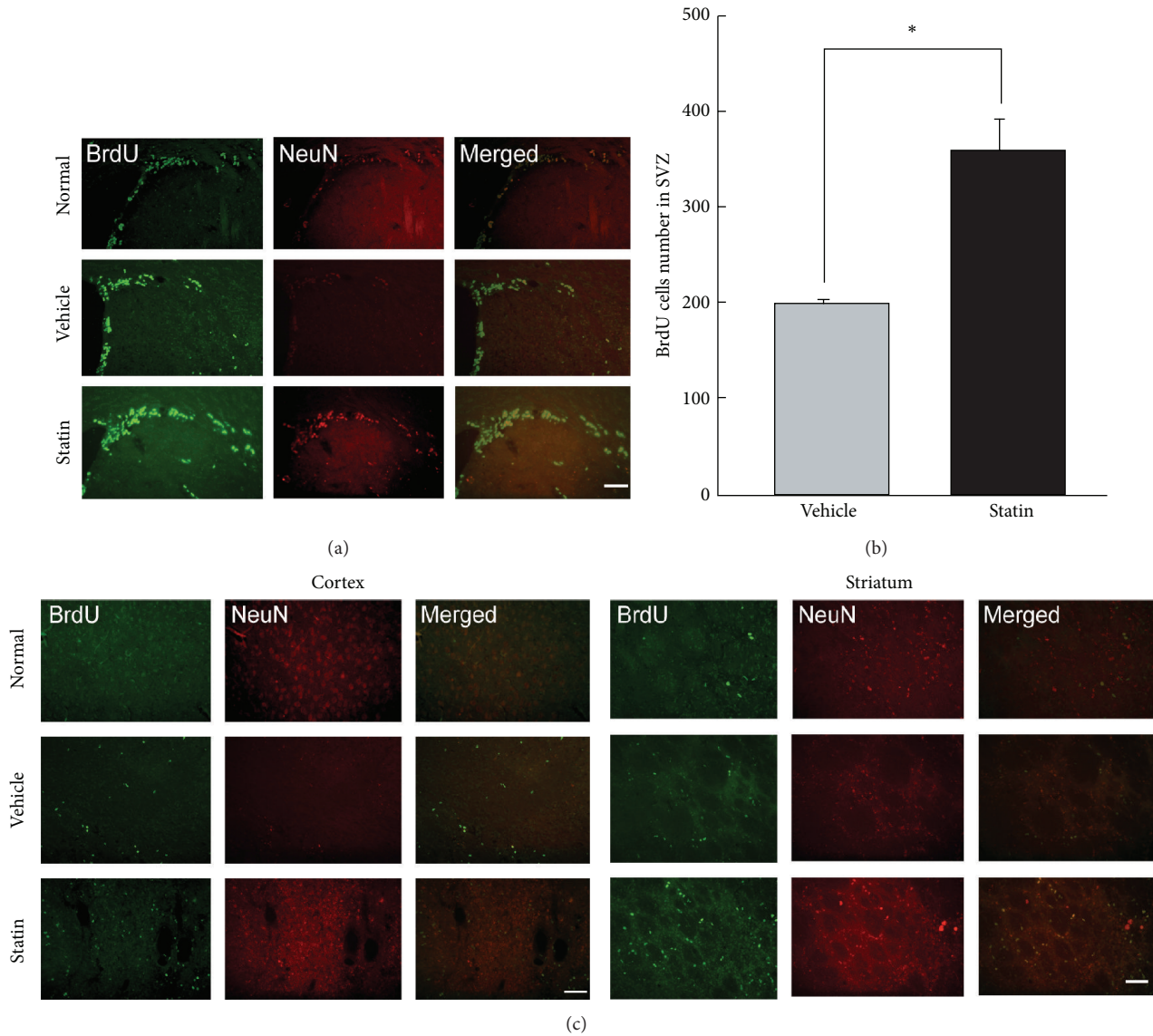


FIGURE 4: Neurogenesis after ischemic injury in normal and vehicle- or atorvastatin-treated group. (a) Cell proliferation in SVZ of the ischemic hemisphere is identified by BrdU (green) and NeuN (red) immunoreactivity. Many BrdU-positive cells are shown in the SVZ of both groups, with increased BrdU-positive cells in the striatum of the atorvastatin-treated group. (b) A quantitative graph representing the number of BrdU-positive cells, which is increased in the atorvastatin-treated group compared with the vehicle-treated group in the SVZ. (c) The migration of the proliferated cells is identified in the cortex and striatum each stained with BrdU (green) and NeuN (red). Scale bars = 20 μ m.

transition test and aggression-intruder test. In the light/dark transition test, the number entering into the bright chamber from the dark chamber was convalescent at 6 months onward (Figure 5(b)). However, the duration of time spent in the light chamber for vehicle-treated mice was longer, over two times the normal, until 6 months and then it got back to normal at 8 months. Whereas the vehicle-treated mice had a fluctuation, the statin-treated mice were stable from the initial to final stage. The duration of aggression swung in the vehicle-treated mice; however, the duration in statin-treated mice did not vacillate (Figure 5(c)). The tendency to show aggression to new intruder was slightly higher in statin-treated mice than vehicle-treated mice in later stages (i.e., at

8 months). In general, statin-treated mice presented peaceful condition without upset through the observed duration.

4. Discussion

This study demonstrated that the NA neurons were transsynaptically labeled by the WGA-expressing adenoviral vector. By simply injecting the virus into the unilateral LC, the NA neural pathways were clearly visualized with great accuracy and high reproducibility from the LC to its projection areas of interest. The current study shows the following: (1) Transsynaptic tracing visualized NA circuitry during long-term recovery after ischemic damage and it is promoted

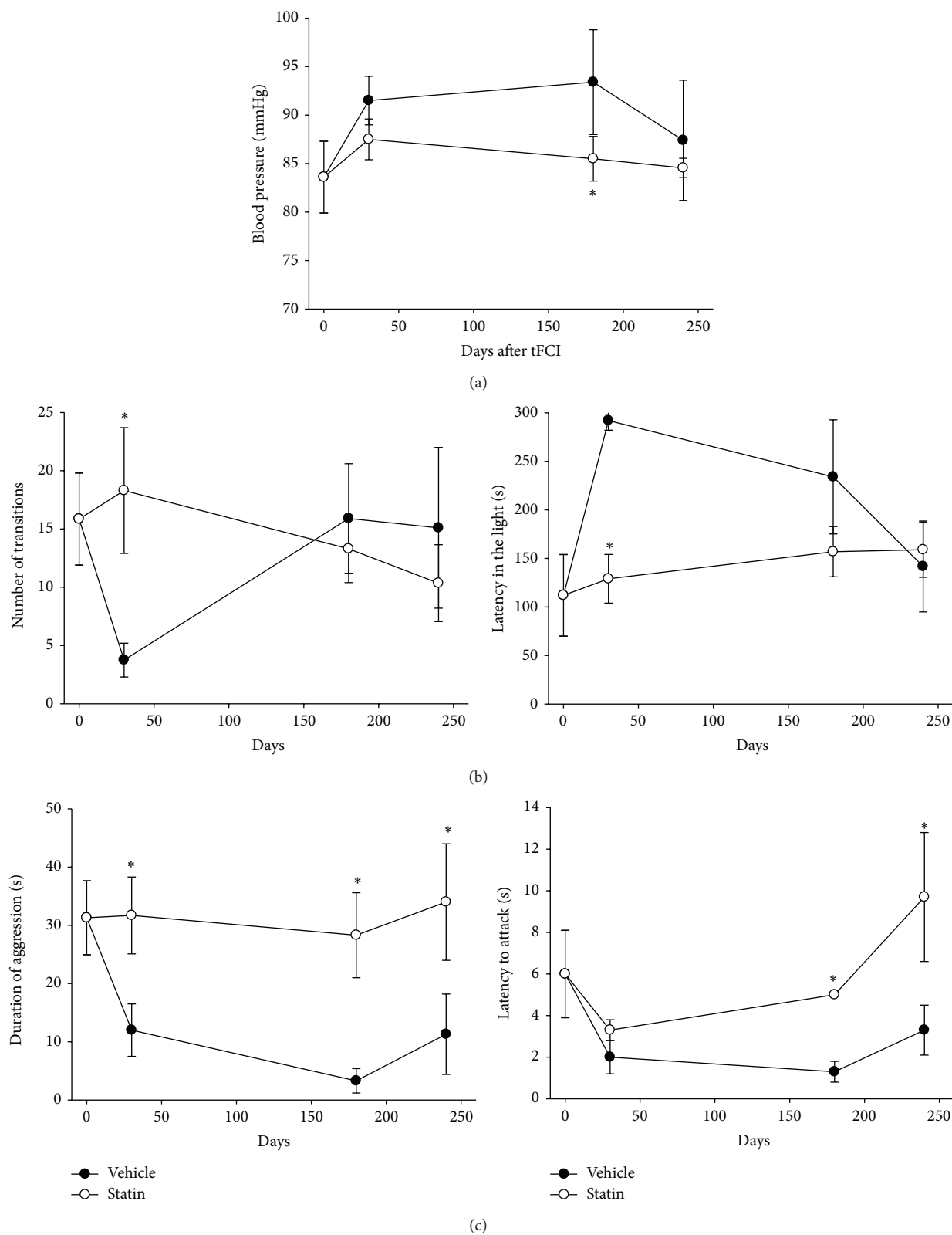


FIGURE 5: Physiological recovery and behavioral tests relating to the NA circuitry. (a) Profiles of blood pressure in vehicle-treated or atorvastatin-treated mice after tFCl. (b) Effects of atorvastatin on behavioral parameters in the light/dark test. The light/dark test was performed at 30, 180, and 240 days after tFCl in mice. The effect on mouse behavior in the light/dark test was determined by p -test. Data presented are the mean value \pm S.E.M., * $p < 0.05$ relative to the vehicle group. (c) Effects of atorvastatin on behavioral parameters in the aggression-intruder test in mice. Aggression-intruder test was performed at 30, 180, and 240 days after tFCl in mice. The effect on mouse behavior in the aggression-intruder test was determined by p -test. Data presented are mean value \pm S.E.M., * $p < 0.05$ relative to the vehicle group.

by statin. (2) Eventually statin ameliorated the damaged behavioral function of NAergic neuron during long-term recovery period after stroke injury.

The WGA protein injection method had been used to visualize optic pathways in monkeys [23], olfactory systems in rodents [24], common afferent projections to the LC in rat [25], and connections of the A5 noradrenergic cell group in rat [26]. A genetic strategy employing cDNA for WGA as a transgene under the control of specific promoter elements was introduced in neural tracing study [27]. The present method successfully and reliably detected strong transsynaptically transferred WGA protein, which might be related to efficient infection of the adenovirus to the NA neurons, as well as the promoter elements (PRS promoter) being used for robust expression of WGA. PRS has previously been shown to be an NA-specific *cis* element binding to paired-like homeodomain factor Phox2a/Phox2b [28]. It has been confirmed that increasing copies of PRS cause synergistic activation of reporter gene expression, reaching maximal efficacy at eight copies [20], which is in agreement with successful visualization of the NA system in a mouse brain with a recombinant adenoviral vector expressing WGA under the control of PRS promoter elements in this study (Figure 1). NA is the neurotransmitter being implicated in many of these disorders and has been found to affect social behavior in both humans and animals [29, 30]. Therefore, investigating alterations of the NA systems in stroke may provide clues to the understanding of its symptomology, clinical courses, and adequate management. NA alteration may help to modulate the pathologically altered motor system in stroke patients, which resulted in upregulated coupling of damaged motor areas and consequently improved motor function [15]. Actually d-Amphetamine has a role in multiple brain transmitter systems, improved functional recovery after stroke, and its effect has been attributed to its noradrenergic systems [31]. Intense WGA immunoreactivity was initially detected in the most contralateral side and the ipsilateral nonlesioned areas, such as the thalamic nucleus, lateral habenular nucleus, and amygdala. These findings suggest that compensatory reinforcement of undamaged contralateral NA circuits occurred shortly after the onset of tFCI and then evolved into subsequent reorganization of NA circuitries in severely damaged area. Moreover, this process can be promoted by statin treatment. When NA synaptic activity increased pharmacologically, symptoms derived by cortical damage were recovered [32]. Synaptic activity also represents the functional recovery after a stroke in human. After focal cortical damage, circuitry reorganization is related to functional recovery, which takes place at the primary cortical level [33]. Therefore, investigating alterations of NA systems in stroke may provide clues to understand its symptomology, clinical courses, and adequate management. It has been known that an acute stroke induced by MCAO induced cellular proliferation or neurogenesis in the ipsilateral SVZ and that a large number of immature neurons migrate from the SVZ to ipsilateral infarcted areas at 2 weeks following insults [34, 35]. Statins are well-known drug to reduce cholesterol level. There are some reports that chronic statin treatment promotes endogenous neuronal cell proliferation,

neurogenesis, and new synapse formation, as well as protecting the neuron from cell death in acute stage [12, 14]. In a long-term stage, we assume that statins are involved in facilitating long-term recovery after stroke by reconnecting the NA circuit using the newly proliferated cells in SVZ or subgranular zone (SGZ). BrdU immunohistochemistry, a thymidine analogue, was used at 1 month and 6 months after tFCI (Figure 4). It was also known that brain insults such as cerebral ischemia, causing neuronal death, are accompanied by increased neurogenesis in the SGZ and SVZ [36, 37]. BrdU-positive cells were observed in cortical and striatal lesions, and increased numbers of BrdU-positive cells were observed in SVZ and corpus callosum, which is consistent with the process of initial neuronal proliferation in SVZ and the subsequent migration into the ischemic lesions as a repair mechanism.

To assess the relationship of the remodeling process with functional recovery in the NA system, the alteration of blood pressure was measured starting 1 month after tFCI (Figure 5). Blood pressure and behavior change following acute ischemic stroke were related with the anatomical reorganization from 6-months after tFCI. Besides blood pressure [38, 39], dysfunction of the NA system has been widely known to be associated with body temperature [40, 41], body weight [42], and anxiety [29, 43]. Previous experiments indicate that blood pressure is significantly higher in mice having insular infarction [38, 39]. The insular cortex is directly connected with central nucleus of the amygdala and the posterior lateral hypothalamus [44, 45] belonging to NA system. Our results indicated that altered physiological dysfunction by acute ischemic stroke injury gradually recovered with the reorganization of damaged processes in the mature NA systems in those structures. The behavioral test using the light/dark test and the aggression-intruder test showed a significant difference between vehicle-treated mice and statin-treated mice (Figure 5). For longer period of up to 8 months after stroke attack, statin improved the malfunctioning anxiety and aggression from an earlier period. Vehicle-treated mice had altered anxiety-like behavior in a time-dependent manner following tFCI, as displayed by a significant increase in the time spent in the light chamber. In contrast to the fluctuating pattern related to the NA system in vehicle-treated mice, statin-treated mice were stable. Increase in NA signaling is associated with higher anxiety and decreased NA signaling with lower anxiety [46, 47]. It has been reported that oxidative stress in the CNS is related to anxiety [48, 49], and aggressive behavior is linked to oxidative stress, which is one of the main pathologies of ischemic stroke [50]. Our results also presented that after initial dysfunction of NA activities, gradual recovery followed along with reorganization of NA circuits in the infarcted structures.

5. Conclusion

Taken together, the present study visualized the NA circuitry of mice by tracing with the PRS-WGA adenoviral system after tFCI for a long duration. Our result showed the reorganization of damaged NA circuit after tFCI. In a chronic stage after stroke, statins were involved in long-term recovery of the NA

circuitry and promoted the neurons to be proliferated and migrate to the infarcted area. Statins could ameliorate the NA-related malfunction after stroke in a chronic period.

Conflict of Interests

The authors declare that there is no conflict of interests regarding the publication of this paper.

Authors' Contribution

Kyoung Joo Cho and So Young Cheon equally contributed to this work.

References

- [1] A. Członkowska and M. Leśniak, "Pharmacotherapy in stroke rehabilitation," *Expert Opinion on Pharmacotherapy*, vol. 10, no. 8, pp. 1249–1259, 2009.
- [2] F. L. Silver, J. W. Norris, A. J. Lewis, and V. C. Hachinski, "Early mortality following stroke: a prospective review," *Stroke*, vol. 15, no. 3, pp. 492–496, 1984.
- [3] M. G. Myers, J. W. Norris, V. C. Hachinski, and M. J. Sole, "Plasma norepinephrine in stroke," *Stroke*, vol. 12, no. 2, pp. 200–204, 1981.
- [4] S. L. Tokgözoğlu, M. K. Batur, M. A. Topçuoğlu, O. Saribas, S. Kes, and A. Oto, "Effects of stroke localization on cardiac autonomic balance and sudden death," *Stroke*, vol. 30, no. 7, pp. 1307–1311, 1999.
- [5] D. Sander, K. Winbeck, J. Klingelhöfer, T. Etgen, and B. Conrad, "Prognostic relevance of pathological sympathetic activation after acute thromboembolic stroke," *Neurology*, vol. 57, no. 5, pp. 833–838, 2001.
- [6] M. Hallett, "Plasticity of the human motor cortex and recovery from stroke," *Brain Research Reviews*, vol. 36, no. 2-3, pp. 169–174, 2001.
- [7] M. Rijntjes and C. Weiller, "Recovery of motor and language abilities after stroke: the contribution of functional imaging," *Progress in Neurobiology*, vol. 66, no. 2, pp. 109–122, 2002.
- [8] V. Meneghini, B. Cuccurazzu, V. Bortolotto et al., "The noradrenergic component in tapentadol action counteracts μ -opioid receptor-mediated adverse effects on adult neurogenesis," *Molecular Pharmacology*, vol. 85, no. 5, pp. 658–670, 2014.
- [9] M. M. Moreno, K. Bath, N. Kuczewski, J. Sacquet, A. Didier, and N. Mandaïron, "Action of the noradrenergic system on adult-born cells is required for olfactory learning in mice," *The Journal of Neuroscience*, vol. 32, no. 11, pp. 3748–3758, 2012.
- [10] J. Chen, Z. G. Zhang, Y. Li et al., "Statins induce angiogenesis, neurogenesis, and synaptogenesis after stroke," *Annals of Neurology*, vol. 53, no. 6, pp. 743–751, 2003.
- [11] Z. Zheng and B. Chen, "Effects of Pravastatin on neuroprotection and neurogenesis after cerebral ischemia in rats," *Neuroscience Bulletin*, vol. 23, no. 4, pp. 189–197, 2007.
- [12] M. Rodriguez-Yanez, J. Agulla, R. Rodriguez-Gonzalez, T. Sobrino, and J. Castillo, "Statins and stroke," *Therapeutic Advances in Cardiovascular Disease*, vol. 2, no. 3, pp. 157–166, 2008.
- [13] E. Kilic, R. Reitmeir, A. Kilic et al., "HMG-CoA reductase inhibition promotes neurological recovery, peri-lesional tissue remodeling, and contralateral pyramidal tract plasticity after focal cerebral ischemia," *Frontiers in Cellular Neuroscience*, vol. 8, article 422, 2014.
- [14] K. Karki, R. A. Knight, Y. Han et al., "Simvastatin and atorvastatin improve neurological outcome after experimental intracerebral hemorrhage," *Stroke*, vol. 40, no. 10, pp. 3384–3389, 2009.
- [15] Q. Wang, J. Yan, X. Chen et al., "Statins: multiple neuroprotective mechanisms in neurodegenerative diseases," *Experimental Neurology*, vol. 230, no. 1, pp. 27–34, 2011.
- [16] Y.-Q. Xu, L. Long, J.-Q. Yan et al., "Simvastatin induces neuroprotection in 6-OHDA-Lesioned PC12 via the PI3K/AKT/Caspase 3 pathway and anti-inflammatory responses," *CNS Neuroscience and Therapeutics*, vol. 19, no. 3, pp. 170–177, 2013.
- [17] M. Hughes, V. Snetkov, R.-S. Rose, S. Trousil, J. E. Mermoud, and C. Dingwall, "Neurite-like structures induced by mevalonate pathway blockade are due to the stability of cell adhesion foci and are enhanced by the presence of APP," *Journal of Neurochemistry*, vol. 114, no. 3, pp. 832–842, 2010.
- [18] J. Yan, Y. Xu, C. Zhu et al., "Simvastatin prevents dopaminergic neurodegeneration in experimental parkinsonian models: the association with anti-inflammatory responses," *PLoS ONE*, vol. 6, no. 6, Article ID e20945, 2011.
- [19] Q. Wang, X. Wei, H. Gao et al., "Simvastatin reverses the down-regulation of M1/4 receptor binding in 6-hydroxydopamine-induced parkinsonian rats: the association with improvements in long-term memory," *Neuroscience*, vol. 267, pp. 57–66, 2014.
- [20] D.-Y. Hwang, W. A. Carlezon Jr., O. Isacson, and K.-S. Kim, "A high-efficiency synthetic promoter that drives transgene expression selectively in noradrenergic neurons," *Human Gene Therapy*, vol. 12, no. 14, pp. 1731–1740, 2001.
- [21] H. J. Kim, H. W. Kim, B. I. Lee et al., "Tracing of noradrenergic neuronal circuitry and functional recovery after permanent focal cerebral ischemia in mice," *Neurocritical Care Journal*, vol. 1, no. 1, pp. 31–42, 2008.
- [22] M. Bourin and M. Hascoët, "The mouse light/dark box test," *European Journal of Pharmacology*, vol. 463, no. 1–3, pp. 55–65, 2003.
- [23] S. K. Itaya and G. W. van Hoesen, "WGA-HRP as a transneuronal marker in the visual pathways of monkey and rat," *Brain Research*, vol. 236, no. 1, pp. 199–204, 1982.
- [24] S. K. Itaya, "Anterograde transsynaptic transport of WGA-HRP in rat olfactory pathways," *Brain Research*, vol. 409, no. 2, pp. 205–214, 1987.
- [25] H. S. Lee, M.-A. Kim, and B. D. Waterhouse, "Retrograde double-labeling study of common afferent projections to the dorsal raphe and the nucleus of the locus coeruleus in the rat," *Journal of Comparative Neurology*, vol. 481, no. 2, pp. 179–193, 2005.
- [26] C. E. Byrum and P. G. Guyenet, "Afferent and efferent connections of the A5 noradrenergic cell group in the rat," *Journal of Comparative Neurology*, vol. 261, no. 4, pp. 529–542, 1987.
- [27] Y. Hanno, M. Nakahira, K.-I. Jishage, T. Noda, and Y. Yoshihara, "Tracking mouse visual pathways with WGA transgene," *European Journal of Neuroscience*, vol. 18, no. 10, pp. 2910–2914, 2003.
- [28] C. Yang, H.-S. Kim, H. Seo, C.-H. Kim, J.-F. Brunet, and K.-S. Kim, "Paired-like homeodomain proteins, Phox2a and Phox2b, are responsible for noradrenergic cell-specific transcription of the dopamine β -hydroxylase gene," *Journal of Neurochemistry*, vol. 71, no. 5, pp. 1813–1826, 1998.
- [29] M. D. Marino, B. N. Bourdolat-Parks, L. Cameron Liles, and D. Weinshenker, "Genetic reduction of noradrenergic function alters social memory and reduces aggression in mice," *Behavioural Brain Research*, vol. 161, no. 2, pp. 197–203, 2005.

- [30] M. S. Marcin and C. B. Nemeroff, "The neurobiology of social anxiety disorder: the relevance of fear and anxiety," *Acta Psychiatrica Scandinavica, Supplement*, vol. 108, no. 417, pp. 51–64, 2003.
- [31] C. Breitenstein, A. Flöel, C. Korsukewitz, S. Wailke, S. Bushuven, and S. Knecht, "A shift of paradigm: from noradrenergic to dopaminergic modulation of learning?" *Journal of the Neurological Sciences*, vol. 248, no. 1-2, pp. 42–47, 2006.
- [32] D. M. Feeney, M. P. Weisend, and A. E. Kline, "Noradrenergic pharmacotherapy, intracerebral infusion and adrenal transplantation promote functional recovery after cortical damage," *Journal of Neural Transplantation and Plasticity*, vol. 4, no. 3, pp. 199–213, 1993.
- [33] N. S. Ward and L. G. Cohen, "Mechanisms underlying recovery of motor function after stroke," *Archives of Neurology*, vol. 61, no. 12, pp. 1844–1848, 2004.
- [34] A. Arvidsson, T. Collin, D. Kirik, Z. Kokaia, and O. Lindvall, "Neuronal replacement from endogenous precursors in the adult brain after stroke," *Nature Medicine*, vol. 8, no. 9, pp. 963–970, 2002.
- [35] Z. Kokaia and O. Lindvall, "Neurogenesis after ischaemic brain insults," *Current Opinion in Neurobiology*, vol. 13, no. 1, pp. 127–132, 2003.
- [36] W. Jiang, W. Gu, T. Brännström, R. Rosqvist, and P. Wester, "Cortical neurogenesis in adult rats after transient middle cerebral artery occlusion," *Stroke*, vol. 32, no. 5, pp. 1201–1207, 2001.
- [37] K. Jin, M. Minami, J. Q. Lan et al., "Neurogenesis in dentate subgranular zone and rostral subventricular zone after focal cerebral ischemia in the rat," *Proceedings of the National Academy of Sciences of the United States of America*, vol. 98, no. 8, pp. 4710–4715, 2001.
- [38] S. Meyer, M. Strittmatter, C. Fischer, T. Georg, and B. Schmitz, "Lateralization in autonomic dysfunction in ischemic stroke involving the insular cortex," *NeuroReport*, vol. 15, no. 2, pp. 357–361, 2004.
- [39] K. E. Smith, V. C. Hachinski, C. J. Gibson, and J. Ciriello, "Changes in plasma catecholamine levels after insula damage in experimental stroke," *Brain Research*, vol. 375, no. 1, pp. 182–185, 1986.
- [40] D. Corbett and J. Thornhill, "Temperature modulation (hypothermic and hyperthermic conditions) and its influence on histological and behavioral outcomes following cerebral ischemia," *Brain Pathology*, vol. 10, no. 1, pp. 145–152, 2000.
- [41] L. Y. Moy, D. S. Albers, and P. K. Sonsalla, "Lowering ambient or core body temperature elevates striatal MPP+ levels and enhances toxicity to dopamine neurons in MPTP-treated mice," *Brain Research*, vol. 790, no. 1-2, pp. 264–269, 1998.
- [42] B. M. King, "The rise, fall, and resurrection of the ventromedial hypothalamus in the regulation of feeding behavior and body weight," *Physiology and Behavior*, vol. 87, no. 2, pp. 221–244, 2006.
- [43] J. Pandaranandaka, S. Poonyachoti, and S. Kalandakanond-Thongsong, "Anxiolytic property of estrogen related to the changes of the monoamine levels in various brain regions of ovariectomized rats," *Physiology and Behavior*, vol. 87, no. 4, pp. 828–835, 2006.
- [44] E. J. Mufson, M.-M. Mesulam, and D. N. Pandya, "Insular interconnections with the amygdala in the rhesus monkey," *Neuroscience*, vol. 6, no. 7, pp. 1231–1248, 1981.
- [45] C. B. Saper, "Convergence of autonomic and limbic connections in the insular cortex of the rat," *Journal of Comparative Neurology*, vol. 210, no. 2, pp. 163–173, 1982.
- [46] M. Cecchi, H. Khoshbouei, and D. A. Morilak, "Modulatory effects of norepinephrine, acting on alpha1 receptors in the central nucleus of the amygdala, on behavioral and neuroendocrine responses to acute immobilization stress," *Neuropharmacology*, vol. 43, no. 7, pp. 1139–1147, 2002.
- [47] M. D. S. Lapid, Y. Mateo, S. Durkin, T. Parker, and C. A. Marsden, "Effects of central noradrenaline depletion by the selective neurotoxin DSP-4 on the behaviour of the isolated rat in the elevated plus maze and water maze," *Psychopharmacology*, vol. 155, no. 3, pp. 251–259, 2001.
- [48] H. Rammal, J. Bouayed, C. Younos, and R. Soulimani, "Evidence that oxidative stress is linked to anxiety-related behaviour in mice," *Brain, Behavior, and Immunity*, vol. 22, no. 8, pp. 1156–1159, 2008.
- [49] H. Rammal, J. Bouayed, C. Younos, and R. Soulimani, "The impact of high anxiety level on the oxidative status of mouse peripheral blood lymphocytes, granulocytes and monocytes," *European Journal of Pharmacology*, vol. 589, no. 1-3, pp. 173–175, 2008.
- [50] H. Rammal, J. Bouayed, and R. Soulimani, "A direct relationship between aggressive behavior in the resident/intruder test and cell oxidative status in adult male mice," *European Journal of Pharmacology*, vol. 627, no. 1-3, pp. 173–176, 2010.